ESO ASTROPHYSICS SYMPOSIA

European Southern Observatory

S. Hubrig
M. Petr-Gotzens
A. Tokovinin
Editors

MULTIPLE STARS ACROSS THE H-R DIAGRAM

Springer

ESO ASTROPHYSICS SYMPOSIA
European Southern Observatory

Series Editor: Bruno Leibundgut

S. Hubrig   M. Petr-Gotzens   A. Tokovinin (Eds.)

Multiple Stars Across the H-R Diagram

Proceedings of the ESO Workshop
held in Garching, Germany,
12-15 July 2005

Springer

Volume Editors

Swetlana Hubrig
European Southern Observatory
3107 Alonso de Cordova
Santiago, Vitacura
Chile

Andrei Tokovinin
Inter-American Observatory
Cerro Tololo (CTIO)
La Serena
Chile

Monika Petr-Gotzens
European Southern Observatory
Karl-Schwarschild-Str. 2
85748 Garching
Germany

Series Editor

Bruno Leibundgut
European Southern Observatory
Karl-Schwarzschild-Str. 2
85748 Garching
Germany

Library of Congress Control Number: 2007936287

ISBN 978-3-540-74744-4 Springer Berlin Heidelberg New York

Springer is a part of Springer Science+Business Media
springer.com

Cover design: WMXDesign, Heidelberg
Typesetting: by the authors
Production: Integra Software Services Pvt. Ltd., Puducherry, India

Printed on acid-free paper 55/3180/Integra 5 4 3 2 1 0

Preface

The ESO workshop “Multiple Stars across the H-R Diagram” was held in Garching on 12–15, July 2005. The topics included observations of multiple stars from ground and space, dynamical and stellar evolution in multiple systems, effects of the environment on multiplicity, formation and early evolution of multiple stars, and special components of multiple stars (chemically peculiar stars, blue stragglers, brown dwarfs, etc.).

Stars show a marked tendency to be in systems of different multiplicity, ranging from simple binaries and triples to globular clusters with $N \approx 10^7$. Modern observations give a frequency of binary and multiple stars in the Galactic field of up to 70%, and between 5% and 20% of these systems are at least triple. There is evidence that the degree of multiplicity increases with primary mass. Many known multiple systems are too wide to have significant physical interaction between their components. However, tidal and N-body dynamical interactions are important even in relatively wide systems and probably lead to the shrinkage of inner orbits. This sets the stage for spectacular evolutionary processes such as Roche-lobe overflow, mergers, supernovae, formation of special components, etc. Only recently did we realize that some of these processes require at least three stars.

The formation of multiple systems remains a difficult and challenging part of astrophysics, although it has been addressed at the Workshop only briefly. Instead, we concentrated on the subsequent stages, more precisely, on how the components, evolution may affect multiple systems and whether there is a difference in comparison to binary stars. The growing information on triple and higher-multiplicity systems with a variety of characteristics has been used to examine critically the assumptions underlying stellar evolutionary models.

The purpose of this meeting was to bring together teams interested in studies of X-ray, UV, visual, near-IR and far-IR properties of stars of all types which are members of multiple systems, and covering stars of high, intermediate and low mass, thus combining specialists with complementary expertise. The Workshop was well timed, since major developments happened in this field of research during recent years due to the availability of large-aperture telescopes equipped with highly sophisticated instruments for multi-wavelength observations, modern interferometers (VLTI, Keck interferometer, CHARA array, etc.) and new satellites such as Chandra, Fuse and the Spitzer Space Telescope. The combination of results from satellites and ground-based facilities resulted in vivid interaction between the experts of all stellar type. The current state of observational and theoretical knowledge has been reviewed, and priorities for future studies have been discussed, so as to provide the necessary input for further progress in the understanding of the genesis of multiple stars, their structure and their role for the study of stellar evolution.

Altogether, 47 people from 16 countries attended this meeting, showing that it was fulfilling a real need. Indeed, the reader will realize that significant progress has been made in the last years, especially in the studies of dynamical evolution in multiple stars, the effects of the environment on multiple system parameters, stellar evolution within multiple stars, multiplicity of massive stars, pre-Main-Sequence multiple systems of intermediate mass, multiplicity of low-mass stars from embedded protostars to open clusters, and brown dwarfs and planets in multiples. We look forward to the future progress which will be presented in a few special sessions at the IAU Symposium 240 "Binary Stars as Critical Tools and Tests in Contemporary Astrophysics" during the XXVI-th IAU General Assembly in Prague this year.

We are grateful to all participants for stimulating presentations and discussions. We thank the local organizing committee chaired by Monika Petr-Gotzens and the European Southern Observatory which fully sponsored this conference.

Santiago and La Serena, Chile
May 2006

Swetlana Hubrig
Andrei Tokovinin

Contents

Evolutionary Processes in Multiple Systems
P.P. Eggleton and L. Kisseleva-Eggleton 1

Dynamics and Stability of Triple Stars
Seppo Mikkola 11

Multiple Stars: Physics vs. Dynamics
R. Zhuchkov, V. Orlov and A. Rubinov 21

Gliese 225.2: An Old (Stable?) Quadruplet
V. Orlov, A. Tokovinin, O. Kiyaeva, M. Sterzik, A. Rubinov and R. Zhuchkov 31

Multiple Stars: Designation, Catalogues, Statistics
A. Tokovinin 37

Radial-velocity Studies of Certain Multiple Systems
R.F. Griffin 43

Spectral Disentangling Applied to Triple Systems: RV Crt
H. Hensberge, L.P.R. Vaz, K.B.V. Torres and T. Armond 47

Evidence for Rapid Variability in the Multiple System 68 u Her
K. Uytterhoeven, P. Koubský, P. Harmanec, J.H. Telting, S. Yang, M.T. Richards and I. Ilyin 53

DG Leo: A Triple System with a Surprising Variety of Physical Phenomena
P. Lampens, Y. Frémat, H. Hensberge, V. Tamazian, J.A. Docobo and Y. Balega 59

A Spectroscopic Study of HD 208905
Pavel Koubský, Simone Daflon, Petr Hadrava, Katia Cunha, Jiří Kubát, Dana Korčáková, Petr Škoda, Miroslav Šlechta, Viktor Votruba, Verne V. Smith and Dimitri Bizyaev 67

The Suspected Binarity of the Nearby Flare Star Gl 424
V.S. Tamazian, J.A. Docobo and Y.Y. Balega 71

The Ecology of Dense Star Clusters with Binaries
Simon F. Portegies Zwart 75

The Formation of Multiple Stars
Eduardo J. Delgado-Donate and Cathie J. Clarke 87

Population of Dynamically Formed Triples in Dense Stellar Systems
Natalia Ivanova 101

Interferometric Studies of Multiple Stars
Christian A. Hummel 107

Interferometric Orbits of New Hipparcos Binaries
I.I. Balega, Y.Y. Balega, K.-H. Hofmann, E.V. Malogolovets, D. Schertl, Z.U. Shkhagosheva and G. Weigelt 113

New Facts about δ Velorum: Fewer but Larger Components
A. Kellerer, M.G. Petr-Gotzens, P. Kervella and V. Coudé du Foresto . 119

Speckle Interferometry of Two Low-mass Triple Systems in the Solar Neighbourhood
E.V. Malogolovets, Y.Y. Balega, K.-H. Hofmann, D.A. Rastegaev and G. Weigelt 125

Tertiary Companions to Close Spectroscopic Binaries
A. Tokovinin, S. Thomas, M. Sterzik and S. Udry 129

Spectroscopic Subcomponents in Visual Double Stars: The Most Probable Values of their Physical and Orbital Parameters. Application to the System WDS 14404+2159
José A. Docobo and Manuel Andrade 137

Multiple Stars in the Field
Brian D. Mason and William I. Hartkopf 141

Multiplicity of Chemically Peculiar Stars
Swetlana Hubrig, Nancy Ageorges and Markus Schöller 155

Multiplicity of Contact Binary Stars
T. Pribulla and S.M. Rucinski 163

Extrasolar Planets in Double and Multiple Stellar Systems
A. Eggenberger, S. Udry, M. Mayor, G. Chauvin, B. Markus, J.-L. Beuzit, A.-M. Lagrange, T. Mazeh, S. Zucker and D. Ségransan . 169

Homogeneous Comparison of Directly Detected Planet Candidates: GQ Lup, 2M1207, AB Pic
Ralph Neuhäuser 183

Searching for Planets Around Stars in Wide Binaries
Silvano Desidera, Raffaele Gratton, Riccardo Claudi, Mauro Barbieri, Giovanni Bonannno, Mariangela Bonavita, Rosario Cosentino, Michael Endl, Sara Lucatello, Aldo F. Martinez Fiorenzano, Francesco Marzari and Salvo Scuderi 193

Multiplicity at the Very Low Mass End of the H-R Diagram
H. Bouy, E.L. Martín, W. Brandner and J. Bouvier 199

Spectroscopic Companions of Very Young Brown Dwarfs
Viki Joergens 211

The Observed Multiplicity of Low-mass Stars: From Embedded Protostars to Open Clusters
Gaspard Duchêne and Jérôme Bouvier 219

High-order Multiplicity of PMS Stars: Results from a VLT/NACO Survey
S. Correia, H. Zinnecker, Th. Ratzka and M.F. Sterzik 233

Accretion onto Binary YSOs Through Gap from Their Circum-binary Disk
Tomoyuki Hanawa, Yasuhiro Ochi and Koichi Ando 239

The Nearest Pre-Main Sequence Multiple Stars
C.A. Grady 245

A Study of the Young Quadruple System AO Vel with a ZAMS Eclipsing BpSi Primary and PMS Companions
J.F. González, S. Hubrig, N. Nesvacil and P. North 259

Multiplicity of Massive Stars
Hans Zinnecker 265

The Triple System θ^1 Orionis A in the Heart of the Orion Trapezium Cluster
Monika G. Petr-Gotzens and Maria Massi 281

The Primordial Binary Population in OB Associations
Thijs Kouwenhoven 289

Multiplicity of Early-type Stars in the Field: Progress Report
N. Huélamo, G. Chauvin, C. Foellmi, M. Hartung, X. Haubois, V. Ivanov, C. Melo, D. Nürnberger and M. Sterzik 295

Search for Low-mass Companions to X-ray Emitting A-type Stars
B. Stelzer, G. Micela, N. Huélamo and M. Hünsch 299

List of Participants

Andrade, Manuel
Astronomical Observatory R.M. Aller (Spain)
oandrade@usc.es

Balega, Yuri
Special Astrophysical Observatory (Russia)
balega@sao.ru

Bouy, Hervé
Instituto de Astrofísica de Canarias (Spain)
bouy@iac.es

Brandeker, Alexis
University of Toronto (Canada)
brandeker@astro.utoronto.ca

Correia, Serge
Astrophysikalisches Institut Potsdam (Germany)
scorreia@aip.de

Coudé du Foresto, Vincent
Observatoire de Paris-Meudon – LESIA (France)
vincent.foresto@obspm.fr

Delgado-Donate, Eduardo
Stockholm Observatory (Sweden)
edelgado@astro.su.se

Desidera, Silvano
Osservatorio Astronomico di Padova (Italy)
desidera@pd.astro.it

Duchene, Gaspard
Observatoire de Grenoble (France)
Gaspard.Duchene@obs.ujf-grenoble.fr

Eggenberger, Anne
Geneva Observatory (Switzerland)
anne.eggenberger@obs.unige.ch

Esposito, Massimiliano
Università degli Studi di Salerno (Italy)
mesposito@sa.infn.it

Grady, Carol
NASA – GSFC (USA)
cgrady@echelle.gsfc.nasa.gov

Griffin, Roger
Cambridge University (UK)
rfg@ast.cam.ac.uk

Hanawa, Tomoyuki
Chiba University (Japan)
hanawa@cfs.chiba-u.ac.jp

Hensberge, Herman
Royal Observatory, Brussels (Belgium)
herman.hensberge@oma.be

Hubrig, Swetlana
ESO (Chile)
shubrig@eso.org

Huelamo, Nuria
ESO (Chile)
nhuelamo@eso.org

Hummel, Christian
ESO (Chile)
chummel@eso.org

Ivanova, Natalia
Northwestern University (USA)
nata@northwestern.edu

Joergens, Viki
Leiden Observatory (The Netherlands)
viki@strw.leidenuniv.nl

Kellerer, Aglaé
ESO, Garching (Germany)
akellere@eso.org

Kisseleva-Eggleton, Ludmila
California State University Maritime Academy (USA)
lkisseleva@csum.edu

Koubsky, Pavel
Astronomical Institute, Ondrejov (Czech Republic)
koubsky@sunstel.asu.cas.cz

Kouwenhoven, Thijs
University of Amsterdam (The Netherlands)
kouwenho@science.uva.nl

Lampens, Patricia
Royal Observatory, Brussels (Belgium)
Patricia.Lampens@oma.be

Malogolovets, Eugene
Special Astrophysical Observatory (Russia)
evmag@sao.ru

Mason, Brian
US Naval Observatory, Washington (USA)
bdm@usno.navy.mil

Mikkola, Seppo
Turku University Observatory (Finland)
mikkola@utu.fi

Neuhäuser, Ralph
AIU Jena (Germany)
rne@astro.uni-jena.de

Orlov, Victor
Sobolev Astronomical Institute, St. Petersburg (Russia)
vor@astro.spbu.ru

Petr-Gotzens, Monika
ESO, Garching (Germany)
mpetr@eso.org

Pinzon Estrada, Giovanni
AIU Jena (Germany)
gpinzon@astro.uni-jena.de

Portegies Zwart, Simon
University of Amsterdam (The Netherlands)
spz@science.uva.nl

Pribulla, Theodor
Astronomical Institute, Slovak Academy of Sciences (Slovakia)
pribulla@auriga.ta3.sk

Stelzer, Beate
Osservatorio Astronomico di Palermo (Italy)
stelzer@astropa.unipa.it

Sterzik, Michael
ESO (Chile)
msterzik@eso.org

Tamazian, Vakhtang
Astronomical Observatory R.M. Aller (Spain)
oatamaz@usc.es

Tokovinin, Andrei
CTIO, La Serena (Chile)
atokovinin@ctio.noao.edu

van Kerkwijk, Marten
University of Toronto (Canada)
mhvk@astro.utoronto.ca

Zinnecker, Hans
Astrophysikalisches Institut Potsdam (Germany)
hzinnecker@aip.de

Evolutionary Processes in Multiple Systems

P.P. Eggleton[1] and L. Kisseleva-Eggleton[2]

[1] Lawrence Livermore National Laboratory, Livermore, CA 94550
ppe@igpp.ucllnl.org
[2] California State University Maritime Academy, Vallejo, CA 94590-8181
lkisseleva@csum.edu

Summary. There are several ways in which triple stars can evolve in somewhat unusual ways. We discuss two: situations where Case A Roche-lobe overflow, followed by a merger, can produce anomalous wide binaries such as γ Per; and Kozai cycles in triples with non-parallel orbits, which can produce merged rapidly-rotating stars like (we suggest) AB Dor, and which can also lead to the delayed ejection of one component of a multiple, as may have been observed in T Tau in 1998.

1 Introduction

We identify two classes of triple system that are likely to be of particular interest regarding their evolutionary history, past or future. These are
(a) those in which the *outer* orbit has a period less than $\sim$ 30 yr, because evolution in such systems might bring about Roche-lobe overflow (RLOF) in *both* orbits, presumably at different times
(b) those in which the outer orbit, which might be of much longer period than in (a), is highly inclined ($\eta > \sin^{-1}\sqrt{2/5} \sim 39°$) to the inner orbit, because in such systems Kozai cycles (in combination with tidal friction) can severely modify the inner orbit.

These two classes can overlap substantially. For instance β Per has an outer orbit of less than two years, and a mutual inclination $\eta \sim 100°$ [9].

The statistics of these classes are not well known, but we can make some reasonable estimates. Binary systems constitute probably $\sim$ 50% of stellar systems, and triple or higher-multiple systems may be $\sim$ 10% in addition, leaving perhaps 40% single, but with wide error bars on each percentage. By 'system' in this context we mean single and binary stars as well as multiples. Among the 60 systems nearer than $\sim$ 5.5 pc (61 including the Sun), about 20 are binary (including three with massive planets) and 8 are triple, but the census of multiples continues to increase slowly, e.g. [11]. Nearby stars are usually of low mass, and massive stars appear to be even more likely to be binary or multiple.

Something like 4540 systems have a (combined) Hipparcos magnitude $Hp < 6.0$. About 3050 are currently not known to be other than single, about 1130 double, and the rest (about 360) appear to be higher multiples. Of the last group, about 40 fall in category (a) above. This is only about 1%, but it is likely that this is a *severe* underestimate. If we restrict ourselves to the much smaller sample of about 450 systems brighter than $Hp = 4.0$, singles, doubles and higher multiples are about 240, 140 and 70. These proportions of binaries and multiples are substantially higher, and suggest that there is a considerable degree of incompleteness regarding the larger sample. Eleven of the smaller sample fall in category (a), i.e. about 2.5%. Thus it is reasonable to suppose that even 2.5% is only a lower limit, at best.

The sample of ~ 4500 bright stars is of course not very representative of stars as a whole; for example it lacks M dwarfs (except as low-mass companions), and M dwarfs are much the greater part of stars as a whole. But the sample is fairly representative of those stars in the Galaxy which are massive enough to undergo significant evolution in a Hubble time.

The statistics of mutual inclinations are harder to come by, because even if the inclinations to the line-of-sight of both orbits (in a triple) are known, the mutual inclination is somewhat indeterminate (see Sterzik & Tokovinin 2002 [17]). The mutual inclination of $100°$ in β Per, referred to above, was the result of VLBI astrometry, which has been applied so far to only a handful of systems ([12]).

From a theoretical point of view, one might arrive at either of two fairly contradictory conclusions regarding the distribution of inclinations. On the one hand, successive fragmentation of a proto-stellar gas cloud might be seen to imply that typically multiple systems would have roughly coplanar orbits. On the other hand, dynamical interactions between systems while they are still in the fairly small confines of a star-forming region might randomise the relative orientations in multiples, before they get scattered out into the general Galactic environment where such interactions would become rare. Randomisation might imply that the mean inclination is $\sim 60°$, which is more than enough to put systems in category (b) above. For the purposes of the present article, we will attach more weight to the second possibility.

Muterspraugh et al (2005) [12] list six systems with unambiguously known mutual inclinations, including Algol; the results are marginally inconsistent with randomisation, but two exceed the Kozai limit ($39°$) considerably, two by small amounts, and two are below it. Our subjective impression is that the distribution is totally inconsistent with the hypothesis of near-coplanarity.

2 Multiples with Two Periods Less than 30 Years

In a triple where the outer period is sufficiently short we can anticipate two distinct episodes of RLOF. Which occurs first probably depends most on which of the three components is the most massive. We [2] have already discussed some of the wealth of possibilities that might arise. Consequently we discuss here only one possibility, since it has ramifications beyond what was perceived in 1996.

Suppose that the most massive component is in the close pair. RLOF has a quite high probability of producing a merger. Nelson & Eggleton [13] considered a large sample of theoretical models undergoing RLOF in Case A. If the initial mass ratio was fairly large ($\gtrsim 1.5-2$), evolution into contact was almost certain. And evolution into contact was also almost certain if the initial period was short – even by the standards of Case A. Although evolution once contact is established is uncertain, the most likely outcome seems to be a merger. The net result is that the system changes from triple to binary. In many cases it will be difficult to know that a particular observed binary is a merged former triple, rather than a system that has always been binary. But in some cases it may be fairly evident, because the binary might have some remarkable properties.

R. E. M. Griffin (1996, private communication) has drawn attention to the fact that several 'ζ Aur' systems have components that seem to violate what we would expect from simple binary evolution. She refers to the problem as 'oversized secondaries'. These binaries consist typically of a G/K giant or supergiant paired with a B/A main sequence (MS) star, in a fairly wide orbit, sufficiently wide that no RLOF is to be expected (yet). If in such a system the mass ratio is greater than about 1.2 (giant/dwarf) we would expect the dwarf to be rather little evolved, since rate of evolution is very sensitive to mass. Yet several ζ Aur systems have quite highly evolved secondaries, at least to the extent that the B/A dwarf is near the upper edge of the MS band rather than the lower edge.

A good example of an oversized secondary is γ Per [15]. The observed parameters are (G8III + A3V, $2.5+1.86\ M_\odot$, $21+4\ R_\odot$, 5350 d, $e=.79$). The mass ratio is about 1.34, and yet the radius of the A dwarf is more than 2.5 times what we expect for an unevolved star of its mass. It is *very* difficult to account for these parameters with conventional evolution. We suspect that the G8III component was once a close binary, with parameters guessed as ($1.9+0.6\ M_\odot, 1-10$ d). This would allow it to reach RLOF when the A dwarf was close to or slightly beyond the end of its MS life, and the RLOF, whether in Case A or Case B, would be likely to end up (fairly quickly) with a merger because of the rather large mass ratio. The merger remnant would either already be a red giant (in Case B) or else would very quickly become one (in Case A).

A system somewhat similar to our suggested initial system is β Cap, with parameters (B8V + ?; 8.68 d) + K0II-III; 3.76 yr and (3.3 + 0.9) + 3.7 $M_\odot$ [3]. This is actually part of a sextuple system, but the other three components are rather far away. The close pair is single-lined, so that there is an element of guesswork in the masses. The masses are a little on the large side to produce γ Per, and the two highest masses would have to be interchanged, but it is gratifying that even in the small number of triples that are of comparable brightness to γ Per there is one at least with parameters not grossly different from what we require.

We might expect the G giant in γ Per to be rapidly rotating as a result of its merger, and unfortunately it is not. However rapidly rotating G/K giants are likely to be very active, through dynamo activity, and can be expected to spin down to normal speeds quite quickly. We therefore feel that this is not a major problem for our theoretical interpretation.

How prevalent is the problem of oversized secondaries? Among the ~ 4500 bright stars, we identify about 15 ζ Aur systems which have been sufficiently analysed for a reasonably reliable estimate of the masses and radii. There are many more which have not yet been sufficiently analysed. Of these 15, 4 [16] have secondaries which we judge to be substantially oversized: γ Per, δ Sge, QS Vul (HR 7741) and ζ Aur itself. The remaining 11 agree reasonably well with the theoretical expectation that the size of the the secondary relative to the ZAMS radius appropriate to its mass should correlate in a particular way with the mass ratio: anticorrelate, if we define the mass ratio as giant/dwarf.

Although 4 out of 15 may seem an awkwardly large proportion, we suggest that a selection effect may render these systems particularly conspicuous. Secondaries that are oversized will also tend to be overluminous: if the A star in γ Per had the 'right' size for its mass, it would be about 5 times less luminous, and in that case it might be barely measurable at all. It will be necessary to do a population synthesis that takes account of the distribution of *triple*-star parameters, and that also takes account of selection effects, in order to see whether our proposed solution can work. We (X. Dearborn and P.P.Eggleton) are currently undertaking such a study.

A former triple might show up in other ways. V471 Tau is a well-known white dwarf/red dwarf binary in the Hyades. Its period is short (0.5 d), and the system is likely to be a remnant of common-envelope evolution in an earlier (and wider) red giant/red dwarf pair. The white dwarf is hot and luminous, and so is expected to be 'young'. It should therefore be less massive than the other white dwarfs in the Hyades, which are cooler, fainter and therefore 'older'. But in fact it is the most massive (O'Brien et al 2001 [14]). These authors have suggested that the white dwarf was a blue straggler previously, and that the blue straggler was the merged remnant of a previous *close* binary, a sub-component of the previous *wide* binary.

3 Multiples with Highly Inclined Orbits

In the discussion of the previous Section it was taken for granted that the orbital periods for the two binaries that make up a triple do not change in time, except in response to RLOF. However in systems with highly inclined orbits the eccentricity in the shorter-period subsystem will fluctuate substantially, due to the Kozai effect [8] of the third star; and tidal friction, which will operate most strongly when the eccentricity is temporarily at a maximum, may lead the inner orbit to shrink, perhaps by a considerable factor.

If the outer orbit of a triple is inclined at more than 39° to the inner, some parameters of the inner orbit, in particular the eccentricity and angular momentum but *not* the period or semimajor axis, are forced to cycle between two values. The larger value of eccentricity can be quite close to unity and is given by

$$1 - \frac{1-e_{\rm min}^2}{1-e_{\rm max}^2}\cos^2\eta \;=\; \frac{2(e_{\rm max}^2 - e_{\rm min}^2)}{5e_{\rm max}^2}, \tag{1}$$

where η is the angle between the two orbits and $e_{\rm min}$ is the minimum eccentricity. The maximum is unity if the orbits are exactly perpendicular. An analysis of the Kozai mechanism, in the quadrupole approximation, was given by Kiseleva et al. [7].

Table 1 gives some values for $e_{\rm max}$ as a function of η and $e_{\rm min}$. *If* the mutual inclination of the two orbits is random, as we hypothesised in the Introduction, then the cumulative probability of η is given in Col.2. The median inclination should be 60°, and this is quite enough to drive the eccentricity, at the peak of the cycle, to 0.764, even if the orbit is circular to start with. Further, 17% will have an inclination of over 80° and then the peak eccentricity is in excess of 0.974. Thus it is by no means improbable that the periastron separation may decrease by a factor of 40 in the course of a Kozai cycle.

Table 1. Limits of Kozai Cycles

η	prob.	$e_{\rm min}$	$e_{\rm max}$	$e_{\rm min}$	$e_{\rm max}$	$e_{\rm min}$	$e_{\rm max}$
0	.000	0	0	.3	.3	.5	.5
10	.015	0	0	.3	.309	.5	.510
20	.060	0	0	.3	.341	.5	.543
30	.124	0	0	.3	.407	.5	.600
40	.224	0	.149	.3	.521	.5	.679
50	.357	0	.558	.3	.669	.5	.772
60	.500	0	.764	.3	.808	.5	.863
70	.658	0	.897	.3	.914	.5	.937
80	.826	0	.974	.3	.978	.5	.984
90	1.00	0	1.00	.3	1.00	.5	1.00

It is noteworthy that the amplitude of the eccentricity fluctuation depends only on the inclination and eccentricity. It does not depend on the period of either orbit, for example. However the cycle time $P_{\rm K}$ depends on the periods in a very simple way:

$$P_{\rm K} \;\sim\; \frac{M_1+M_2+M_3}{M_3}\,\frac{3P_{\rm out}^2}{2\pi P_{\rm in}}\,(1-e_{\rm out}^2)^{3/2}. \tag{2}$$

This is much the same period as for precession and apsidal motion. Even a brown dwarf, or a major planet, might cause a Kozai cycle of large amplitude, with a period of $\lesssim 10$ Myr if the outer period is $\lesssim 100$ yr.

Three physical processes may, however serve to reduce the maximum eccentricity that is predicted by Table 1. They are (a) general relativity (GR), (b) quadrupolar distortion, due to rotation, in each of the inner pair, and (c) quadrupolar distortion of each star by the other in the inner pair. All three of these processes produce apsidal motion, and if this is comparable to the apsidal motion produced by the third body then they interfere with the Kozai cycle. The eccentricity still cycles (because all these processes are time-reversible) but over a range which may be much more limited.

In a particular case, we took all three masses to be equal (and solar), and $P_{\rm in} = 10$ d, $P_{\rm out} = 10$ yr. We started with both orbits circular, and with a mutual inclination of 80°. Introducing each of processes (a) – (c) in turn, the peak eccentricity was successively reduced, the biggest reduction being for mutual distortion (c); and when all three perturbations are included together the peak is reduced from 0.974 to 0.78. Thus the periastron separation is reduced by a factor of 4.5 rather than 40, but this is still enough to give tidal friction a good chance to operate on a reasonably short timescale; whereas in a 10 d near-circular orbit it would be very slow (several Gyr). Since tidal friction depends mainly on periastron separation, we can say that the *effective* period is as short as $10/4.5^{1.5} \sim 1$ d, and this is indeed the actual period which tends to be reached after several Kozai cycles, each taking $\sim 4 \times 10^3$ yrs.

If we attempted detailed modeling we would have to take into account the fact that it would be difficult for such a binary to dissipate as much orbital energy as is necessary in only a few Kyr. What we expect happens is that the orbital energy, being released by friction inside each star, will tend to expand the stars, increase their quadrupole moments, and so cause the eccentricity cycle to peak at a less extreme value still, so that the process is somewhat self-limiting. It will take many more Kozai cycles, but still the process can only stop when the orbit is circularised at much the same terminal period.

Figure 1 illustrates the region in $(P_{\rm in}, P_{\rm out})$ space where Kozai cycles and tidal friction are important. The whole of the shaded area is where Kozai cycles can occur. The lower boundary is caused by the fact that very close triples are dynamically unstable. The upper boundary is where processes (a), (b) and/or (c) prevent the Kozai cycles. The darkly shaded area is where tidal friction can shrink and circularise the orbit on a timescale of ~ 1 Gyr. This figure assumed a mutual inclination of 80°. The combined effect of Kozai cycles and tidal friction (KCTF) should be to move a system from its initial point within the darly shaded area horizontally towards the left-hand boundary, where it should ultimately settle.

We might note that if KCTF does reduce the inner orbit to a shorter-period circular orbit, it also modifies the mutual inclination towards the Kozai limit (39°, or 141° for retrograde orbits). In the six systems listed by [12],

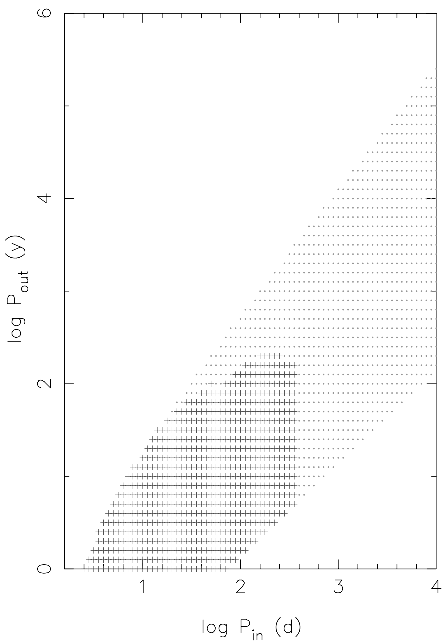

Fig. 1. The entire shaded area is where Kozai cycles, starting from $e = 0.01$ and $\eta = 80°$, are able to increase e to above 0.5 cyclically. The darkly shaded area is where the timescale of tidal friction at the peak of eccentricity is enough to reduce the eccentricity on a timescale of $\lesssim 1$ Gyr. The three masses were all 1 $M_\odot$

two are within a few degrees of this limit, and may be the remnants of this process, having started with more perpendicular orbits.

Since the final $P_{\rm in}$ may be only a few days, or even less than a day if we consider M dwarfs rather than G dwarfs, it is possible for further shrinkage to take place by the mechanism of magnetic braking. Fairly low-mass (F/G/K/M) dwarfs are known to show anomalously strong activity (flares, spots etc.) when they are rapidly rotating, i.e. with periods under $\sim 5-10$ d. Usually this activity causes them to spin more slowly, by magnetic braking, and thus the activity is self-limiting. But in a close binary tidal friction can prevent the star from spinning down below the orbital period. The angular momentum is drained from the orbit rather than the stellar spin, and this causes the orbit and star to spin *up* rather than down. The process can therefore run away, although the 'runaway' is likely to be on a timescale of Myrs rather than days or years.

AB Dor is an unusually rapidly rotating K dwarf ($P_{\rm rot} \sim 0.5$ d). One might attribute its rapid rotation to youth. However (i) it is not in, or even particularly close to, any star-forming region, and (ii) Zuckerman et al. [19] identify it is a member of a rather loose moving group aged about 50 Myr. Its $V \sin i$ is 80 km/s, against an average of 11 km/s for 11 other K dwarfs in the group. We suggest that AB Dor is the result of a recent merger of the two components of a former close binary, perhaps of two early-M dwarfs, or a K dwarf and an L/T dwarf. There is a third (well, currently second) body, an object on the borderline of red/brown dwarfs, in an 11.75 yr, $0.032''$ orbit [1, 5]. In fact there is also a further companion, AB Dor B, an M4e dwarf at $9.1''$, which Close et al. [1] find also to be double ($0.07''$). The $9.1''$ separation corresponds to a likely period of $10^3 - 10^4$ yr.

Perhaps the KCTF mechanism worked within the 11.75 yr orbit, on a primordial sub-binary that no longer exists, to produce an unusually close binary, and then the magnetic breaking mechanism shrank this binary to RLOF. We hypothesise a rather severe mass ratio, which makes it likely that RLOF will lead to a rapid merger, with the formation of a single rapidly-rotating star as observed. Probably the merger would be accompanied by rather substantial but temporary mass ejection. We imagine that this merger might have taken place only 1 or 2 Myr ago, so that the merger remnant is still rapidly rotating.

A very different possible outcome of Kozai cycling may be illustrated by another young system, the prototype young star T Tau. Loinard et al. [10] and Furlan et al. [4] suggested that a remarkable event occurred there in about 1998: one component of the multiple system was ejected from a bound orbit into an unbound orbit. This picture has been questioned more recently (Tamazian [18], Johnston et al. [6]), but until the picture settles down we shall follow the analysis of Furlan et al.

Furlan et al. followed the motion of 3 components that are part of the overall quadruple system. T Tau N is the most conspicuous and longest-known component. T Tau S, $0.73''$ to the south, apparently consists of three components, two of them infrared sources (Sa, Sb) and one a radio source (Sc). As shown in Furlan et al.'s Fig. 3, Sc appeared to move round Sa in part of an elliptical orbit, over about 15 years, before passing close to Sb and then moving off at a tangent to one side. A possible interpretation is that Sa and Sb are in a somewhat wide orbit, with a period of decades, and that Sa and Sc were in a tighter orbit, with a period of ~ 20 yr, that was rendered unstable when a periastron of the larger orbit roughly coincided with an apastron of the smaller orbit.

It may seem odd that the system should take a Megayear or so to become unstable, when it might have been expected to become unstable in only a few decades. But this could be a natural consequence of Kozai cycling. The NS orbit is likely to be of order $10^3 - 10^4$ yr, and if well inclined to the (Sab +Sc) orbit might induce the latter to Kozai-cycle on a timescale of $10^5 - 10^6$ yr. This might cause the smallest orbit (Sa + Sb) to become unstable at a periastron of the intermediate orbit when its eccentricity was maximal. Thus it is not impossible that the breakup was considerably delayed, and only occurred recently.

4 Summary

Evolutionary effects within triple-star, or former triple-star, systems can take place which can produce effects that would be hard to understand in terms of conventional binary-star evolution.

5 Acknowledgments

This work was performed under the auspices of the U.S. Department of Energy, National Nuclear Security Administration by the University of California, Lawrence Livermore National Laboratory under contract No. W-7405-Eng-48. L.K.-E. is grateful to the AAS and the California Maritime Academy for assistance with travel.

References

1. L. M. Close, R. Lenzen, J. C. Guirado et al.: Nature, **433**, 286 (2005)
2. P. P. Eggleton & L. Kiseleva: In: *Evolutionary Processes in Binary Stars*, eds. R. A. M. J. Wijers, M. B. Davies, & C. A. Tout, p. 345 (1996)
3. D. S. Evans & F. C. Fekel: ApJ, **228**, 497 (1979)
4. E. Furlan, W. J. Forrest, D. M. Watson et al.: ApJ, **596**, L87 (2003)
5. J. C. Guirado, J. E. Reynolds, J.-F. Lestrade et al.: ApJ, **490**, 835 (1997)
6. K. J. Johnston, A. L. Fey, R. A. Gaume et al.: AJ, **128**, 822 (2004)
7. L. G. Kiseleva, P. P. Eggleton, & S. Mikkola: MN, **300**, 292 (1998)
8. Y. Kozai: AJ, **67**, 591 (1962)
9. J.-F. Lestrade, R. B. Phillips, M. W. Hodges, & R. A. Preston: ApJ, **410**, 808 (1993)
10. L. Loinard, L. F. Rodríguez, & M. I. Rodríguez: ApJ, **587**, L47 (2003)
11. M. J. McCaughrean, L. M. Close, R.-D. Scholz, R. et al.: A&A **413**, 1029 (2004)
12. M.W. Muterspaugh, B. F. Lane, M. Konacki et al.: A&A, in print (2005), astro-ph/0509855
13. C. A. Nelson & P. P Eggleton: ApJ, **552**, 664 (2001)
14. M. S. O'Brien, H.E. Bond, & E.M. Sion: ApJ, **563**, 971 (2001)
15. D. Pourbaix: A&A, **348**, 127 (1999)
16. K.-P. Schröder, O. R. Pols, & P. P. Eggleton: MN, **285**, 696 (1997)
17. M. F. Sterzik, A. A. Tokovinin: A&A, **384**, 1030 (2002)
18. V. S. Tamazian: AJ, **127**, 2378 (2004)
19. B. Zuckerman, I. Song, & M. S. Bessell: ApJ, **613**, L35 (2004)

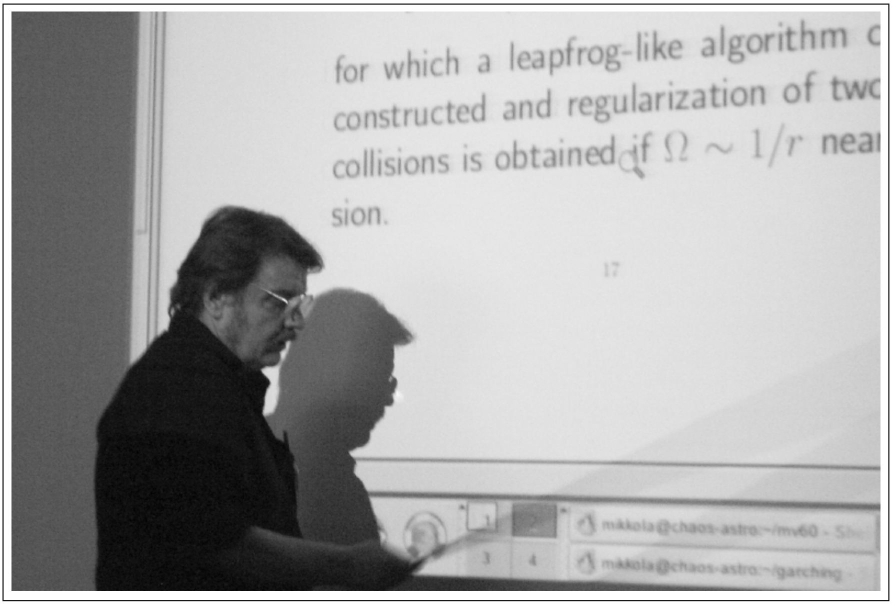

Seppo Mikkola

Dynamics and Stability of Triple Stars

Seppo Mikkola[1]

Tuorla Observatory, University of Turku, 21500 Piikkiö, Finland
seppo.mikkola@utu.fi

Summary. The dynamics of triple stars and methods for computing the motions are briefly reviewed: The topics include the statistical properties of unstable triples, stability limits in hierarchical systems and numerical methods to compute the evolution and the largest Lyapunov exponent of a triple star model.

1 Introduction

Evolution of (point-mass) three-body systems is qualitatively similar in future and past: the system disrupts (*unstable*) ejecting one of the stars, in both direction of time, or it stays bounded (*stable*) forever.

Consequently any encounter of a binary and a single star, however complicated, eventually leads to ejection of one of the stars leaving behind a binary.

Known stable triple systems are hierarchical. An interesting case is high mutual inclination with strong eccentricity variation (Kozai-resonance). Other cases include: the 'figure-8' (quasi-)periodic system, some nearly rectilinear orbits and co-orbital solutions.

The astrophysically most interesting cases are:

1. Systems of three stars that break up after some dynamical evolution. These may be found in star forming regions.
2. Scattering of single stars off close binaries. These events are important in the dynamics of star clusters.
3. Stable hierarchical systems. Numerous such triple stars are known in the galactic field.

Discussions of the astrophysical applications of the three-body dynamics has been provided e.g. by Valtonen and collaborators [32–34].

2 Disruption of Triple Systems and Scattering off Binaries

2.1 Cross-Sections and Thermal Distributions

An important phenomenon in stellar dynamics is the scattering of single stars off binaries which has been extensively studied by Hut and collaborators [10–16, 19].

In that process energy flows from the binaries to single stars thus heating the stellar system. In dense systems this prevents the (total) core collapse.

From the numerical experiments an approximate summary for the relative energy exchange (Δ) cross-section σ can be expressed as

$$\frac{d\sigma}{d\Delta} \approx 2\pi A \left(\frac{V_c}{V}\right)^2 \Delta^{-0.5}(1+\Delta)^{-4}, \tag{1}$$

where the coefficient $A \approx 21$ for equal masses, V is the incoming speed of the third star while V_c is the critical value at which the total energy is zero.

The first comprehensive treatment of three-body scattering was given by Heggie [9]. An important result was that hard binaries get harder and soft ones typically disrupt. Here the boundary between a hard and a soft can be defined in terms of the binding energy of the binary: if the binding energy is larger than a typical kinetic energy of a single star, the binary is hard. Otherwise soft.

As a result of the scattering process the final binding energy (B) distribution of binaries is expected to be [9, 35]

$$f(B) \propto B^{-4.5}, \tag{2}$$

while the square of eccentricity is usually nearly uniformly distributed. For the eccentricity this can be written

$$f(e) = 2e. \tag{3}$$

High eccentricities are thus expected to be common in binaries that have experienced three-body encounters.

These results are valid in the 'thermal equilibrium' in which each event is balanced by an equally probable inverse one [9]. Valtonen and Karttunen [36] recently used phase space volume arguments to arrive at similar results.

2.2 Probability of Escape

The probability of escape of a given star from a strongly interacting triple system depends on the mass

$$P_{esc}(m_k) \approx m_k^{-n} / \sum_\nu m_\nu^{-n}, \tag{4}$$

with a value of $n \approx 2$ applicable in typical triple interactions. This result can be derived from phase-space volume-integrals (in agreement with numerical experiments), and it explains e.g. the fact that the mass ratio distribution varies with the spectral class [35].

However, if considered in more detail, the escape probability exponent n depends significantly on the angular momentum of the system. More precisely, one may write

$$n \approx 3/(1+\lambda/3), \tag{5}$$

where λ is the dimensionless scale-independent parameter

$$\lambda = -c^2 E\langle m\rangle\langle m_i m_j\rangle^{-3} G^{-2}, \tag{6}$$

in which the angular brackets indicate the mean mass and the mean mass product respectively and G is the gravitational constant [22].

One notes that another form of the above equation is

$$P_{ij} = (m_i m_j)^n / \sum_{\alpha\beta} (m_\alpha m_\beta)^n, \tag{7}$$

where P_{ij} is the probability that the pair $m_i m_j$ is the surviving binary. This form has the advantage that one may apply it to more complicated systems. For 4-body systems in which a common outcome is one binary and two independent stars, the value $n \approx 2$ has been obtained in case of low angular momentum [24]. Again, smaller values for n may be expected for larger angular momentum.

2.3 Chaos or Not?

The three-body motions typically change significantly if the the initial conditions are changed a little. This, however, does not always mean that the motions are actually chaotic, but that the phase space is very complicated and is divided into areas of different behavior. The (hyper) surfaces which divide the phase space are associated with orbits leading to a parabolic disruption of the system or a triple collision.

Figure 1 illustrates one aspect of the outcome of triple scattering: The impact parameter was changed in small intervals, the system was integrated to final disruption and the semi-major axis (over the maximum possible value) was plotted in the figure. One notes regions of regular behavior (U-shaped portions of the curve) as well as regions of high sensitivity. However, those chaotic looking sections are actually filled with very narrow U-shaped curves. At the points where $a/a_{max} = 1$ the third star escapes with (asymptotically) parabolic speed (=0 at infinity). Such an orbit is, however, infinitely sensitive to initial conditions because, on one side, there is a hyperbolic escape and, on the other side, a long ejection without escape (yet). One may thus say that we see here dense systems of singular surfaces of parabolic disruption

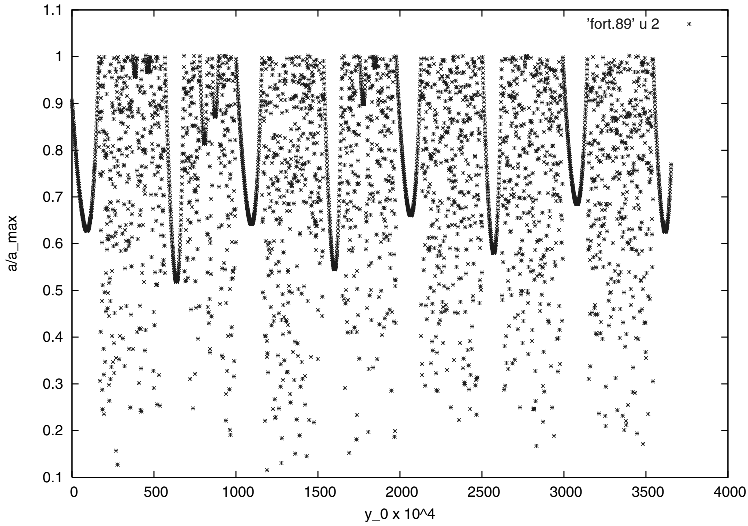

Fig. 1. $z = a/a_{max}$ as function of impact parameter ($\times 10^4$). The value $z = 1$ corresponds to parabolic disruption

[25]. However, near the parabolic escape orbit, in the side where there is no disruption but long ejections, there is a fractal-like structure, as shown by Boyd and McMillan [4].

3 Long Lasting Stability

As far as is known, all observed stable triple stars are hierarchical systems, although theoretically other types of stable systems exist. In this section, first the stability conditions for hierarchical triples are discussed and then some more "exotic" systems are considered.

3.1 Hierarchical Triples

The stability of hierarchical triple stars is largely determined by the pericenter distance of the outer orbit. There are many studies of this in the literature e.g. by Harrington [7], Bailyn [3], Kiseleva and Eggleton [6], Mardling and Aarseth [1, 21]. Those authors give various estimates for the ratio of the pericentre distance R_{peri} of the outer orbit to the semi-major axis a_{in} of the inner orbit:

$$\left(\frac{R_{peri}}{a_{in}}\right)_{\text{Harrington}} = 3.5\left[1 + 0.7\ln\left(\frac{2}{3} + \frac{2}{3}\frac{m_3}{m_1 + m_2}\right)\right] \tag{8}$$

$$\left(\frac{R_{peri}}{a_{in}}\right)_{\text{Bailyn}} = \frac{2.65+e_{in}}{3.5}\left(1+\frac{m_3}{m_1+m_2}\right)^{\frac{1}{3}}\left(\frac{R_{peri}}{a_{in}}\right)_{\text{Harrington}} \tag{9}$$

$$\left(\frac{R_{peri}}{a_{in}}\right)_{\text{Egg-Kise}} = (1+e_{in})\left(1+\frac{3.7}{Q_3}-\frac{2.2}{1+Q_3}+\frac{1.4}{Q_2}\,\frac{Q_3-1}{Q_3+1}\right) \tag{10}$$

$$\left(\frac{R_{peri}}{a_{in}}\right)_{\text{MardlingAarseth}} = 2.8\left[\left(1+\frac{m_3}{m_1+m_2}\right)\frac{1+e_{out}}{\sqrt{1-e_{out}}}\right]^{\frac{2}{5}}. \tag{11}$$

Here $Q_2 = [max(m1/m2, m2/m1)]^{\frac{1}{3}}$, $Q_3 = (\frac{m_1+m_2}{m_3})^{\frac{1}{3}}$ in the Eggleton-Kiseleva criterion. The masses m_1, m_2 are the components of the inner binary and m_3 is the outer body and the indices *in* and *out* refer to the inner and outer orbits. The Eggleton-Kiseleva criterion is for circular orbits only (i.e. both inner and outer are assumed circles initially) while the other expressions are supposed to be useful more generally. However, as we can see, these expressions depend in a different way on masses and orbital elements. They typically give values for $(\frac{R_{peri}}{a_{in}})$ in the range from 3 to 4, although larger values occur in extreme cases. By numerical experiments it is not difficult to find examples in contradiction with the values obtained from these estimates. Thus none of the published estimates is sufficiently accurate for deeming the stability of a triple system with certainty. In practice, especially for cases in the mentioned range, it is better to determine the stability by numerical integration.

Figure 2 illustrates the motion of a stable triple (but near instability boundary). In Fig. 3 the variational equation solutions for this triple and for a close unstable one are plotted. One can see that the instability becomes quickly evident from the behavior of the variation.

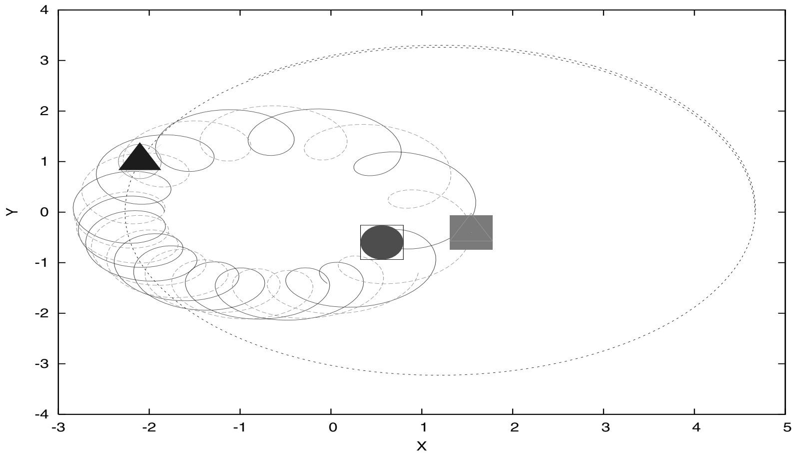

Fig. 2. Motion of a hierarchical stable triple in centre-of-mass coordinates. The big dots describe the positions of the particles at a selected moment

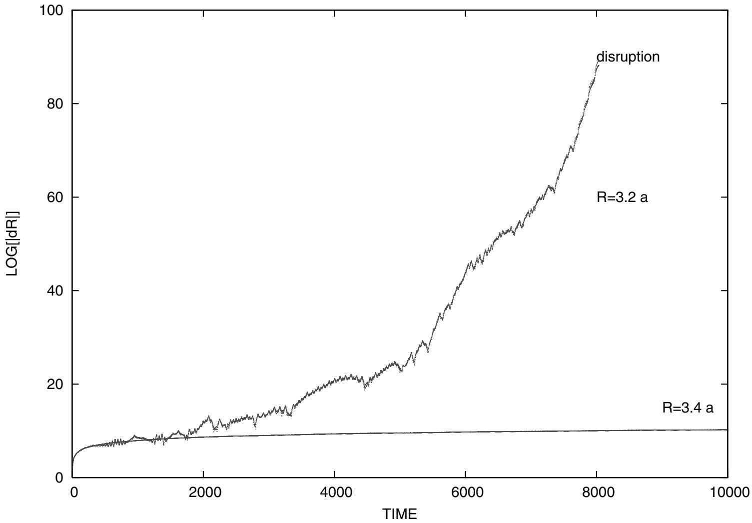

Fig. 3. Evolution of $\ln(|dR|)$ for two hierarchical three-body orbits $[R_{out} = 3.2a_{in}$ and $R_{out} = 3.4a_{in}]$. Masses $= 1,\ a = 5$

3.2 Kozai Resonance

If the mutual inclination in a triple system is high enough, the system undergoes strong periodic variations in the inner eccentricity and the mutual inclination, known as the Kozai resonance [17, 18]. Especially if the orbits are perpendicular, the inner eccentricity should reach the value $e = 1$! This may thus restrict the existing triples to those having small mutual orbital inclinations (or near 180 degrees). On the other hand, the Kozai resonance is sensitively affected by other effects, such as oblateness of the bodies. Otherwise the existence of the moons of Uranus, or the triple system Algol, would not be possible.

3.3 Non-hierarchical Triples

Recently Montgomery [20] discovered an interesting special stable triple orbit in which all the three bodies move along an figure-8 trajectory with one third phase difference. This orbit is illustrated in Fig. 4. Since the periodic orbit is stable, one can expect stable motions in the neighborhood of the basic solution.

Other such cases can be found in the neighborhood of other stable periodic orbits such as the Broucke orbit [5], the rectilinear Schubart orbit [26,31], the co-orbital Lagrangian solutions and the Copenhagen problem. In some cases some of the masses of the bodies must be small (Lagrangian and Copenhagen problems). These special orbits, although very interesting for a theoretician, are less important in astrophysics.

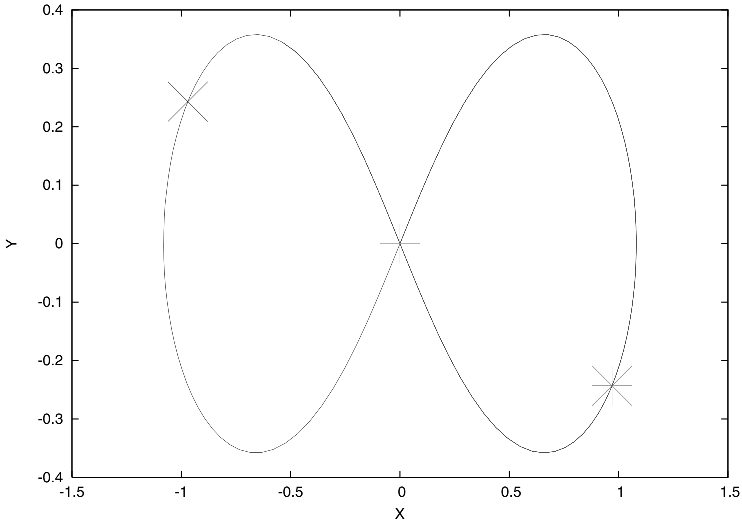

Fig. 4. The figure-8 (stable, periodic) solution

4 Numerical Methods for Triple Stars

Classical numerical methods can be used to compute the motions of triple stars if close approaches do not occur. Typically, however, regularized methods are more accurate even when the interactions are not particularly strong. Today there are several alternative methods available that utilize the Kustaanheimo-Stiefel (KS) transformation. These include the method of Aarseth and Zare [2], the global regularization of Heggie [8, 23], and more recent ones like the logarithmic Hamiltonian method [27, 30]. Details can be found e.g. in the book by Aarseth [1].

4.1 A Regular Symplectic Three-Body Algorithm

Here we consider in more detail only one method which has the advantage that it is simple enough to allow straightforward differentiation of the algorithm thus making it possible to obtain easily the largest Liapunov exponent (i.e. determination of system stability). This method is based on the logarithmic Hamiltonian formalism [27, 30].

Let $\mathbf{r}_1, \mathbf{r}_2, \mathbf{r}_3$ be the position vectors of the bodies m_1, m_2, and m_3 and let us introduce the difference vectors

$$\mathbf{d}_1 = \mathbf{r}_3 - \mathbf{r}_2,\ \mathbf{d}_2 = \mathbf{r}_1 - \mathbf{r}_3,\ \mathbf{d}_3 = \mathbf{r}_2 - \mathbf{r}_1. \tag{12}$$

Then the equations of motion can be written (in units in which the gravitational constant is one)

$$\dot{\mathbf{w}}_k = \mathbf{A}_k(\mathbf{d}) = -M\frac{\mathbf{d}_k}{d_k^3} + m_k \sum_{j=1}^{3} \frac{\mathbf{d}_j}{d_j^3} \tag{13}$$

$$\dot{\mathbf{d}}_k = \mathbf{w}_k, \tag{14}$$

where thus $\mathbf{w}$'s are the derivatives of the relative vectors $\mathbf{d}_k$ and $M = m_1 + m_2 + m_3$ is the total mass. The kinetic energy (in the centre-of-mass system) is

$$T = \frac{1}{2M}(m_1 m_2 \mathbf{w}_3^2 + m_1 m_3 \mathbf{w}_2^2 + m_2 m_3 \mathbf{w}_1^2) \tag{15}$$

and the potential energy

$$U = \frac{m_1 m_2}{d_3} + \frac{m_1 m_3}{d_2} + \frac{m_2 m_3}{d_3}. \tag{16}$$

Using the constant total energy $E = T - U$, which is evaluated only once at the beginning, one may now write new time-transformed equations of motion (which now include also an equation for the time t)

$$\mathbf{w}' = \mathbf{A}(\mathbf{d})/U \tag{17}$$

$$\mathbf{d}' = \mathbf{w}/(T - E) \tag{18}$$

$$t' = 1/(T - E), \tag{19}$$

where the equality $U = T - E$ is used to make the derivatives of $\mathbf{w} = (\mathbf{w}_1, \mathbf{w}_2, \mathbf{w}_3)$ depend only on the coordinates $\mathbf{d} = (\mathbf{d}_1, \mathbf{d}_2, \mathbf{d}_3)$ and the derivatives of $\mathbf{d}$ to depend only on $\mathbf{w}$.

Thus the simple leapfrog algorithm is possible. Since in this case the leapfrog is exact for two-body motion [27, 30], we have an algorithm that is regular in two-body collisions (algorithmic regularization) even if the differential equations are singular.

Defining the two 'subroutines' $\mathbf{X}(s)$ and $\mathbf{V}(s)$ (where s is a step size),

$$\mathbf{X}(s): \qquad \delta t = s/[T(\mathbf{w}) - E]; \quad \mathbf{d} \to \mathbf{d} + \delta t\, \mathbf{w}; \quad t \to t + \delta t \tag{20}$$

$$\mathbf{V}(s): \qquad \widetilde{\delta t} = s/U(\mathbf{d}); \qquad \mathbf{w} \to \mathbf{w} + \widetilde{\delta t}\, \mathbf{A}(\mathbf{d}), \tag{21}$$

one can symbolize one step of the leapfrog algorithm as

$$\mathbf{X}(h/2)\mathbf{V}(h)\mathbf{X}(h/2)$$

or, if several steps are taken between outputs,

$$\mathbf{X}(h/2)\mathbf{V}(h)\mathbf{X}(h)\mathbf{V}(h).....\mathbf{X}(h)\mathbf{V}(h)\mathbf{X}(h/2)$$

i.e. the half-steps are taken only in the beginning and at the end (output).

This algorithm is simple to program, not singular in collision and can be used also for a soft potential model in which $1/r$ is replaced by $1/\sqrt{r^2+\epsilon^2}$. The method is also symplectic and an improvement of accuracy over the Yoshida's higher-order leapfrogs [37] or the extrapolation method [29] is possible.

Due to the structure of the leapfrog, this method exactly conserves the angular momentum, as well as the geometric integrals $\sum_k \mathbf{d}_k = 0$ and $\sum_k \mathbf{w}_k = 0$. One could also integrate only two of the relative vectors $\mathbf{d}_k$ and obtain the third one from the geometric integrals. However, in practice this hardly saves any computational effort. Instead, one may occasionally use the geometric integrals to remove any round-off effect by computing the largest side from the sum of the two others, and applying the same for the corresponding velocities.

An additional important feature of this algorithm is that it is very easy to differentiate so as to obtain the tangent map [28] and thus the maximum Lyapunov exponent. What one does in practice is that the code is first written and then differentiated line by line. Thus one obtains the exact differentials of the algorithm, essentially without considering the variational equations.

5 Conclusion

The scattering of single stars off binaries and the disruption of triple systems are rather well understood, especially in the statistical sense.

However, the stability of hierarchical triple stars still lacks a reliable theoretical estimate. Thus, to determine the stability properties of any triple system model, a check by numerical integration, preferably with a computation of the largest Lyapunov exponent, is recommended.

References

1. S. Aarseth: *Gravitational N-Body Simulations* (Cambridge Univ. Press, Cambridge, 2003)
2. S.J. Aarseth, K. Zare: Cel. Mech., **10**, 185 (1974)
3. C.D. Bailyn: *Ph.D. Thesis* (Yale University, 1987).
4. P.T. Boyd, S.L.W. McMillan: Phys. Rev. **A46**, 6277 (1992)
5. E. Davoust, R. Broucke: A&A **112**, 305 (1982)
6. P. Eggleton, L. Kiseleva: ApJ, **455**, 640 (1995)
7. R.S. Harrington: Cel. Mech. **6**, 322 (1972)
8. D.C. Heggie: Cel. Mech., **10**, 217 (1974)
9. D.C. Heggie: MNRAS **173**, 729 (1975)
10. D.C. Heggie, P. Hut: ApJS **85**, 347 (1993)
11. D.C. Heggie, P. Hut, S.L.W. McMillan: in IAU Symp. 174 Dynamical Evolution of Star Clusters: Confrontation of Theory and Observations, p. 371 (1996)
12. D.C. Heggie, P. Hut, S.L.W. McMillan: ApJ **467**, 359 (1996)

13. P. Hut, J.N. Bahcall: ApJ **268**, 319 (1983)
14. P. Hut: ApJ **268**, 342 (1983)
15. P. Hut: AJ **88**, 1549 (1983)
16. P. Hut: ApJS **55**, 301 (1984)
17. K.A. Innanen, J.Q. Zheng, S. Mikkola, M.J. Valtonen: AJ **113**, 1915 (1997)
18. H. Kinoshita, H. Nakai: Cel. Mech. and Dyn. Astron. **75**, 125 (1999)
19. S.L.W. McMillan: ApJ **467**, 348 (1996)
20. R. Montgomery, A. Chenciner: Ann. of Math. **152**, 881 (2000)
21. R.A. Mardling, S.J. Aarseth: MNRAS **321**, 398 (2001)
22. S. Mikkola, M.J. Valtonen: MNRAS **223**, 269 (1986)
23. S. Mikkola: MNRAS **215**, 171 (1985)
24. S. Mikkola: In *The Few-Body Problem* (ed. M.Valtonen), p. 261 (Kluwer, Dordrecht, 1988)
25. S. Mikkola: MNRAS **269**, 127 (1994)
26. S. Mikkola, J. Hietarinta: Cel. Mech. and Dyn. Astron. **51**, 379 (1991)
27. S. Mikkola, K. Tanikawa: Cel. Mech. and Dyn. Astron. **74**, 287 (1999)
28. S. Mikkola, K. Innanen: Cel. Mech. and Dyn. Astron. **74**, 59 (1999)
29. W.H. Press, B.P. Flannery, S.A. Teukolsky, W.T. Wetterling: *Numerical Recipes* (Cambridge Univ. Press, Cambridge, 1986).
30. M. Preto, S. Tremaine: AJ **118**, 2532 (1999)
31. J. Schubart: AN **283**, 17 (1956)
32. M.J. Valtonen: Vistas in Astron. **32**, 23 (1988)
33. M. Valtonen, S. Mikkola: ARA&A **29**, 9 (1991)
34. M. Valtonen, S. Mikkola, P. Murdin: *Three-body Problem.* In Encyclopedia of Astronomy and Astrophysics (2000)
35. M. Valtonen: RMxAA **21**, 147 (2004)
36. M. Valtonen, H. Karttunen: *The Three Body Problem* (Cambridge Univ. Press, Cambridge, 2005)
37. H. Yoshida: Phys. Lett. **150**, 262 (1990)

Multiple Stars: Physics vs. Dynamics

R. Zhuchkov[1], V. Orlov[2] and A. Rubinov[2]

[1] Chair of Astronomy, Kazan State University, Kremlevskaya ul. 18, Kazan 420008, Russia zhr@ksu.ru

[2] Sobolev Astronomical Institute, St. Petersburg State University, Universitetskii pr. 28, Staryj Peterhof, St. Petersburg 198504, Russia vor@astro.spbu.ru; rav@astro.spbu.ru

Summary. We review physical and dynamical parameters of multiple stars. Possible scenaria of multiple star formation are discussed: their birth in dense cloud cores and the decay of small stellar groups and clusters. We compare physical and dynamical features of simulated multiple stars formed by these processes with the actual multiple stars. Multiplicity function, their period, eccentricity and mass ratio distributions, hierarchy of the structures are analysed. Also we discuss multiple systems where the apparent ages of the components are different. Such diferences can be explained by poor evolutionary tracks for low-mass stars, by formation of such systems by capture or by merging of components during dynamical evolution of multiple stars.

1 Introduction

Many stars were formed in clusters and small groups [1]. The actual multiple stars can contain an information concerning their formation processes. So the physical properties of components, dynamical stability or instability may reflect some details of their formation and evolution.

The dynamics of a system is related to its actual configuration. Historically, the configurations of multiple stars were separated into two types: trapezia (or non-hierarchical) systems and ϵ Lyrae (or hierarchical) systems. We suggest to introduce an intermediate type — low-hierarchy systems. As one example of such systems we consider the quadruple system HD 40887 (Fig. 1 and these Proceedings).

Note that an apparent configuration on the sky is not the same as the actual configuration in space. This is due to the projection effect. Even the type of a configuration may change.

Systems with strong hierarchy are stable with a high probability. The motions in such systems are almost Keplerian. Trapezium-type systems have a completely different behavior. As a rule, these systems are unstable. The motions of stars have a character of chaotic dance and the evolution is ended by a formation of a stable configuration, binary or hierarchical multiple. The actual trapezia-type stars must be dynamically young.

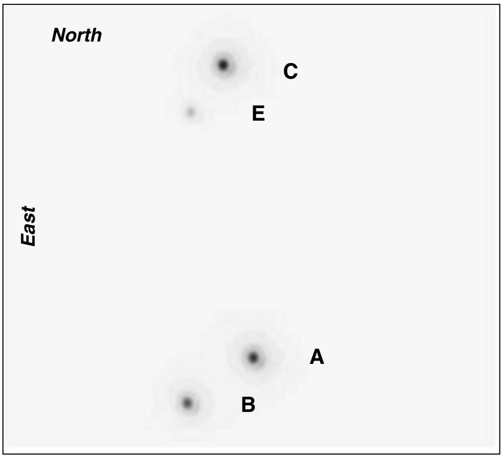

Fig. 1. Apparent configuration of a quadruple system HD 40887

We consider three possible scenaria for multiple system formation:

- escape from unstable non-hierarchical small groups or clusters;
- common formation as a stable or an unstable unit;
- capture in the galactic field or in the field of a common gas-star complex.

Below we consider the first scenario in more detail.

It is interesting to note that recently Goodwin and Kroupa [2] have shown that protostellar cores must typically produce only two or three stars.

2 Statistics of Binaries and Multiples

Let us consider some statistical properties of binary and multiple stars. These properties are used to compare the simulated and observed systems.

One of the important characteristics is the multiplicity function. This is the ratio f_n of the number of the systems with the multiplicity n to the same quantity for the multiplicity $n-1$. The results are given in the Table 1 [3].

This ratio f_n is about 1/4. Only for $n = 3$ it is two times smaller. However, in the nearest solar neighborhood this ratio is $f_3 = 0.20$, i.e. also about 1/4. A very similar result $f_3 = 0.21$ was found for the final states of decay of small non-hierarchical stellar groups. This agreement confirms the hypothesis that many double and stable triple stars were formed initially inside small non-hierarchical stellar groups.

Table 1. Multiplicity function from [3]

n	3	4	5	6	Average 4,5,6
f_n	0.11	0.22	0.20	0.36	0.26
	± 3	± 2	± 4	± 14	± 5

An important information could be deduced from the distributions of orbital elements and mass ratios. We consider such distributions for two samples of binary stars:

1. the binaries where the primary component has the spectral type similar to the solar one (late F or G) [4];
2. spectroscopic binaries where a primary is also of late spectral type (F7 to late K) [5].

Both samples were corrected by the authors for selection effects.

The distributions of the logarithm of the orbital period are shown in Figs. 2 and 3. The first sample shows a unimodal distribution similar to the Gaussian one. The second one shows a rather bimodal distribution. The reason for the difference between the distributions in Figs. 2 and 3 is unclear. The bimodality of the period distribution in Fig. 3 can be explained by two factors: 1) underestimation of selection effects for $P \approx 100^d$ binaries; 2) two different formation mechanisms for close and wide spectroscopic binaries.

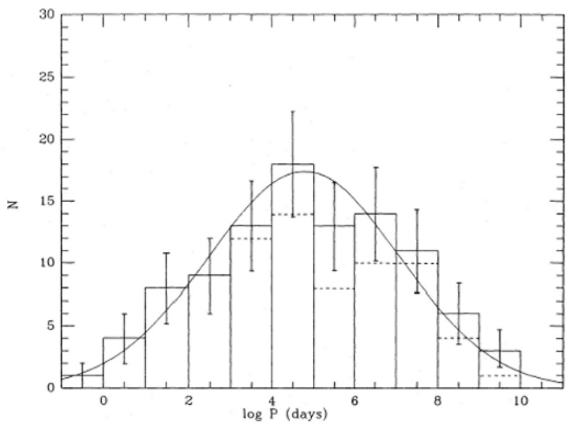

Fig. 2. Period logarithmic distributions according to [4]

The period-eccentricity diagrams for these samples are similar (Figs. 4, 5). There is a general growth of the median eccentricity with period. The circularization of short-period orbits is probably caused by tidal interactions of components.

The mass ratio distributions reflect the initial mass spectrum, but also evolutionary processes in the systems (both dynamical and astrophysical). This distribution seems to be a bimodal or even three-modal (Fig. 6). For the short period orbits, there is a marked population of twins where both components have similar masses. This multimodality could evidence an existence of at least two mechanisms of binary star formation.

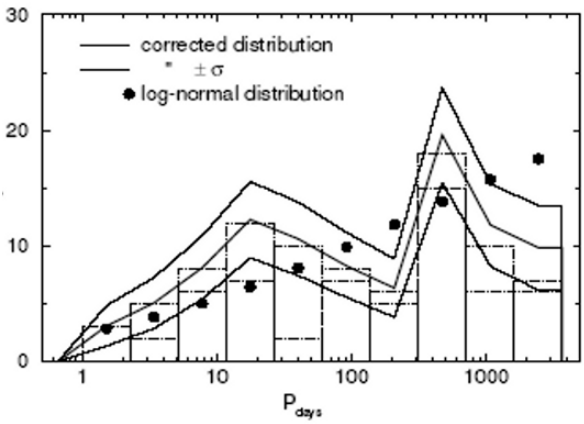

Fig. 3. Period logarithmic distributions according to [5]

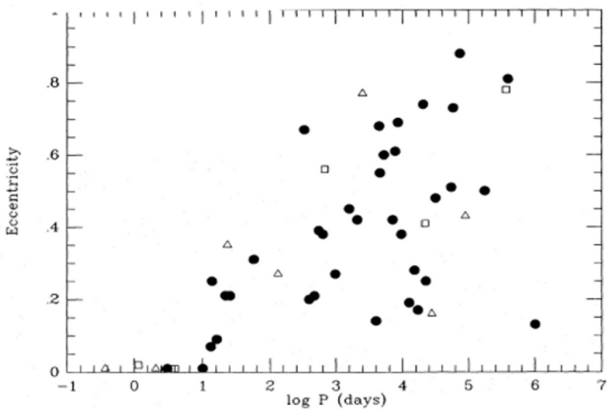

Fig. 4. Period–eccentricity diagram according to [4]

Let us compare observed binaries and multiples with stable final products of a simulated decay of small non-hierarchical groups (Fig. 7).

The eccentricities of escaping and final binaries are distributed according to the Ambartsumian-Heggie law $f(e) = 2e$. The same law is valid for wide binaries in the solar neighborhood according to [3].

The period-eccentricity diagrams of real and simulated binaries are slightly different (Figs. 4, 5, and 8). However, we note that the diagram for simulations is given here only for one value of initial group size $R = 100$ AU. Here close binaries where tidal effects may be essential are absent. At the same time, for long period binaries the period-eccentricity correlation cannot be clearly seen in Fig. 4, 5, and 8.

The mass ratio distributions are also similar (Figs. 6 and 9). The phenomenon of "twins" is clearly seen for escaping binaries, whereas the

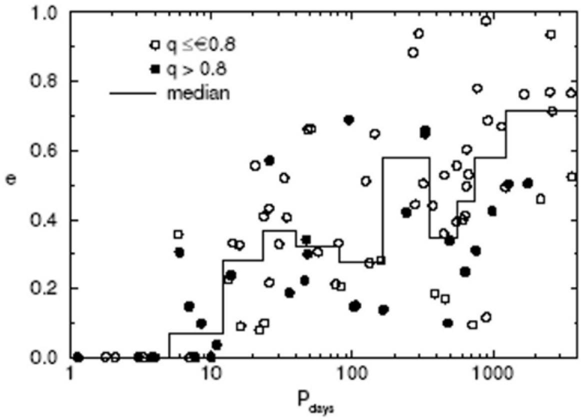

Fig. 5. Period–eccentricity diagram according to [5]

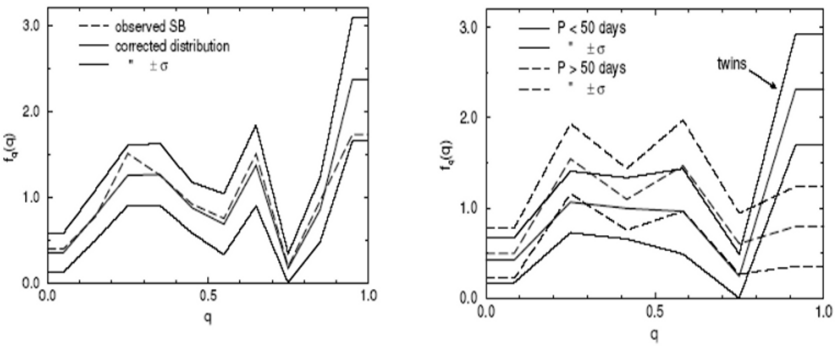

Fig. 6. Mass ratio distribution according to [5]

distribution for the final binaries is approximately flat at $q > 0.2$. The qualitative agreement is observed, although quantitative differences are also evident.

Now we compare observations and simulations of triple stars.

Table 2 contains the mean and median values for the ratio of periods and eccentricities of inner and outer binaries in stable triples — both the final products of simulated small-group dynamical decay and the observed triple stars.

The histograms in Figs. 10 and 11 show the distributions of the period ratio.

The hierarchy degree is high in both samples. The distributions of the period ratio are qualitatively similar — both are unimodal. However, the asymmetries have different signs.

The mean and median eccentricities of inner and outer binaries in the observed triplets are slightly less than in the simulated triples. In inner binaries, the partial circularization could be caused by the tidal interaction

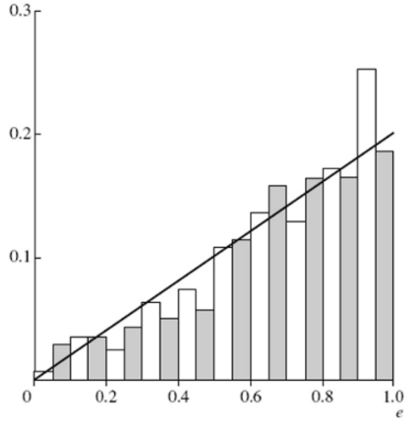

Fig. 7. Eccentricity distributions for final (white columns) and escaping (gray columns) binaries according to [6]. The solid straight line corresponds to the $f(e) = 2e$ law

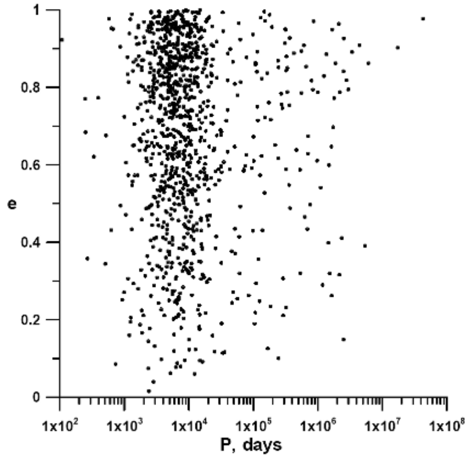

Fig. 8. Period–eccentricity diagram according to numerical simulations [6]

Table 2. Mean and median parameters of stable final triples according to simulations [6] and observations [7]

	$\overline{\frac{P_{in}}{P_{ex}}}$	$(\frac{P_{in}}{P_{ex}})_{\frac{1}{2}}$	$\overline{e}_{in}$	$(e_{in})_{\frac{1}{2}}$	$\overline{e}_{ex}$	$(e_{ex})_{\frac{1}{2}}$	n
observations $P_{in} > 10^d$	0.040 $\pm$0.010	0.013	0.37 $\pm$0.04	0.39	0.38 $\pm$0.04	0.40	38
simulations	0.013 $\pm$0.001	0.011	0.61 $\pm$0.03	0.64	0.51 $\pm$0.02	0.51	80

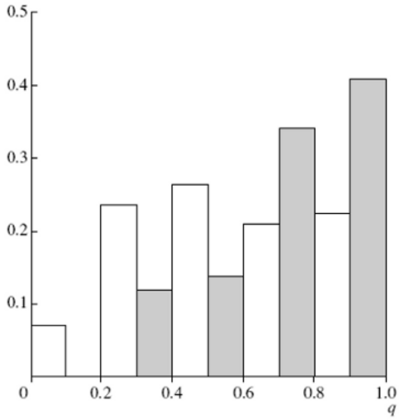

Fig. 9. Mass ratio distribution for final (white columns) and escaping (gray columns) binaries according to [6]

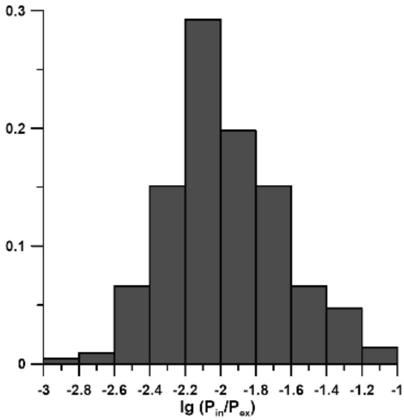

Fig. 10. Period ratio distribution for final stable triples according to [6]

of components. Also we have to bear in mind a bias effect: it is difficult to compute orbits of very eccentric binaries.

Another interesting parameter of hierarchical triples is the angle between the orbital angular momenta of inner and outer binaries. It characterizes the mutual inclination between their orbital planes. Figure 12 shows the cumulative distributions of this angle for simulated triplets and triple stars from the Multiple Star Catalogue, according to Sterzik and Tokovinin [8].

There is a slight difference between observations and simulations for the angles greater than 90° (retrograde motions). This difference may be indicative of some resonance effects, like the Kozai-Lidov effect.

Thus, we have the qualitative agreement between the data for observed and simulated binaries and triples. This agreement can be considered as an

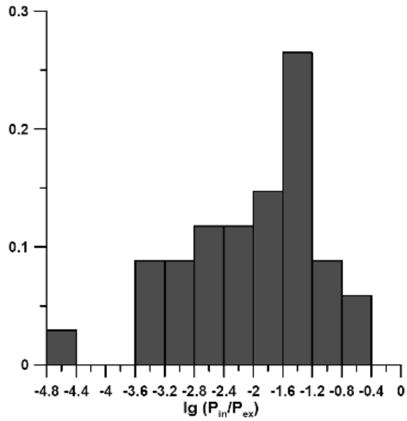

Fig. 11. Period ratio distribution for observed triples according to [7]

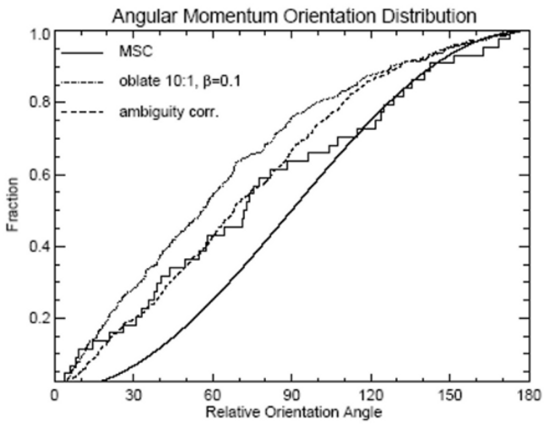

Fig. 12. Cumulative distributions of the angle between the orbital angular momenta of inner and outer binaries for stable triples simulated in small group decay and the observed triples according to [8]

additional argument in favour of the hypothesis that the majority of these systems might be formed by the decay process of small non-hierarchical stellar groups.

3 Stability of Low-hierarchy Multiples

A more interesting question is the dynamical stability of observed multiple stars. In order to study this problem, we have compiled a sample consisting of sixteen triple stars and two quadruple stars (for details see [9] and [10]). The close binaries were considered as a single component.

Two methods of stability study were used: 1) several well-known stability criteria for triple systems and 2) numerical simulations of past and future evolution for all systems during one million years (sometimes ten million years).

The input data on orbital elements and masses have some uncertainties. In order to check the effect of these errors, we have made the Monte Carlo simulations — orbital elements and masses were varied using independent Gaussian distributions, where the mean values were taken as the observed values and the dispersions are the same as root mean square errors. One thousand runs were considered for each system.

Two populations of multiple stars were found: probably stable and probably unstable. The gap between these two populations is rather wide. For "stable" systems, we estimate the decay probability $P_d < 0.1$. A non-zero value of P_d could be explained by too big orbital parameter errors taken into consideration. At the same time, for "unstable" systems we found $P_d > 0.9$ during time interval 1 Myr (more than $10^3 \cdot P_{ex}$). We may suppose that the remaining systems will decay at a longer time. Here we give the list of probably unstable systems: HD 40887 (Gliese 225.2) — quadruple, HD 76644 (ι Uma = ADS 7114) — quadruple, HD 136176 (ADS 9578) — triple, HD 150680 (ADS 10157) — astrometric triple, HD 222326 (ADS 16904) — triple. Among them there are two quadruplets and three triplets.

Possible explanations of apparently unstable systems are:

1. Errors of observations and interpretation.
2. Physical youth of components.
3. Some additional effects are responsible for the physical stability of the system (mass loss etc.).
4. Some additional effects led to the formation of the unstable system (merging etc.).
5. Temporary capture via encounter of a binary (multiple) system and a single (multiple) star.
6. Stability loss via an encounter of a stable multiple star with a massive object (molecular cloud, black hole etc.).
7. Product of dissipation of a stellar group or a cluster.

We believe that the first point is not the only possibility. We have roughly estimated the expected number of unstable systems within 200 pc from the Sun due to the last three mechanisms. The expected number of unstable systems within this sphere for the scenarios 5–7 is about $1 \div 10$ ($P_{ex} < 10^3$ yr). This is not negligible.

As for our probably unstable systems, we can say that each object from the list has the problems concerning its multiplicity or/and orbital parameters. So, our conclusions about their instability are preliminary, and additional studies are extremely welcome.

4 Discussion and Conclusions

Multiple stars could be considered as an astrophysical laboratory. Mostly, the components of the same multiple system have the same age. Therefore we can compare the evolutionary status of the stars of the same age, but with different masses.

One possible scenario of the origin of single, binary, and stable multiple stars due to a decay of small non-hierarchical groups was suggested by Larson [1]. Our statistical comparative analysis of simulated and observed systems has confirmed this point of view.

One new interesting result has been found by Goodwin and Kroupa [2]. They show that most stars were produced in binary or triple systems.

However, sometimes the components of multiple stars could have different ages, as derived from the evolutionary tracks. Four examples of such systems were found by Popper [11]. Here the low-mass components have larger ages. The most plausible explanation of this fact is the unreliability of the used evolutionary stellar models for low-mass stars. However, we cannot reject a hypothesis that some of these systems were formed by capture, and the age differences are real.

Our conclusions are:

1. One can separate multiple stars into high-hierarchical, low-hierarchical, and non-hierarchical.
2. High-hierarchical systems are long-term stable.
3. Non-hierarchical systems usually disrupt.
4. Low-hierarchy systems may be either stable or unstable.
5. A few scenarios of their instability are suggested.

This study was partially supported by RFBR grant N 05-02-17744-a.

References

1. R.B. Larson: Implications of binary properties for theories of star formation. In: *The Formation of Binary Stars, Proceedings of IAU Symp. 200*, ed by H. Zinnecker, R.D. Mathieu (ASP, San Francisco, 2001) p 93
2. S.P. Goodwin, P. Kroupa: A&A **439**, 565 (2005)
3. A.A. Tokovinin: Statistics of multiple stars: some clues to formation mechanisms. In: *The Formation of Binary Stars, Proceedings of IAU Symp. 200*, ed by H. Zinnecker, R.D. Mathieu (ASP, San Francisco, 2001) p 84
4. A. Duquennoy, M. Mayor: A&A **248**, 485 (1991)
5. J.-L. Halbwachs, M. Mayor, S. Udry, F. Arenou: Rev. Mex. Astron. Astrofis. (Ser. Conf.) **21**, 20 (2004)
6. A.V. Rubinov, A.V. Petrova, V.V. Orlov: Astron. Rep. **46**, 942 (2002)
7. V.V. Orlov, A.V. Petrova: Astron. Lett. **26**, 250 (2000)
8. M.F. Sterzik, A.A. Tokovinin: A&A **384**, 1030 (2002)
9. V.V. Orlov, R.Ya. Zhuchkov: Astron. Rep. **49**, 201 (2005)
10. R.Ya. Zhuchkov, V.V. Orlov: Astron. Rep. **49**, 274 (2005)
11. D.M. Popper: AJ **114**, 1195 (1997)

Gliese 225.2: An Old (Stable?) Quadruplet

V. Orlov[1], A. Tokovinin[2], O. Kiyaeva[3], M. Sterzik[4], A. Rubinov[1] and R. Zhuchkov[5]

[1] Sobolev Astronomical Institute, St. Petersburg State University, Universitetskii pr. 28, Staryj Peterhof, St. Petersburg 198504, Russia `vor@astro.spbu.ru; rav@astro.spbu.ru`,

[2] Cerro Tololo Inter-American Observatory, Casilla 603, La Serena, Chile `atokovinin@ctio.noao.edu`,

[3] Central Astronomical Observatory at Pulkovo, Pulkovskoe sh. 65/1, St. Petersburg 196140 Russia `kiyaeva@gao.spb.ru`,

[4] European Southern Observatory, Casilla 19001, Santiago 19, Chile `msterzik@eso.org`,

[5] Chair of Astronomy, Kazan State University, Kremlevskaya ul. 18, Kazan 420008, Russia `zhr@ksu.ru`

Summary. We discovered with adaptive optics a new component E in the nearby multiple system Gliese 225.2, making it quadruple. We derive a preliminary 24-yr astrometric orbit of this new sub-system C,E and a slightly improved orbit of the 68-yr pair A,B. The orientations of the A,B and C,E orbits indicate that they may be close to coplanarity. The 390-yr orbit of AB,CE computed by Baize (1980) was premature, the period is much longer. Large space velocities indicate that Gliese 225.2 belongs to the thick galactic disk and is not young. This quadruple system survived for a long time and should be dynamically stable.

1 Introduction

The multiple system HD 40887 = HIP 28442 = Gliese 225.2 has been known since long time. The wide sub-system A,C has been discovered by J. Herschel and is designated as HJ 3823. The closer pair A,B has been discovered by Hussey in 1911 and is named as HU 1399. This object, despite its brightness and proximity to the Sun, has received very little attention of observers. The location on the Southern sky has certainly contributed to this circumstance.

We are interested in this system because both the wide pair AB,C and the inner system A,B have computed visual orbits. The periods of pairs A,B and AB,C (68 and 390 yr, respectively) are such that the system does not satisfy any dynamical stability criterion. Is it really unstable?

A 12.8^m visual companion D at $20''$ from AB,C is listed in the WDS catalog under the name of B 2595. Rapid relative motion of this companion indicates that it is optical, hence it will not be discussed further.

2 Observations

High spatial resolution images of this object have been obtained using the NAOS-Conica adaptive optics system mounted at the VLT on November 9, 2004. The object was observed as a calibrator star for the program 74.C-0074(A). To our surprise, in addition to the three known visual components A, B, C we saw the fourth star E close to C (Fig. 1). Images in the narrow band around 2.12 μm and in wide photometric bands J, H, Ks, L' were taken. The new component is clearly seen in all images.

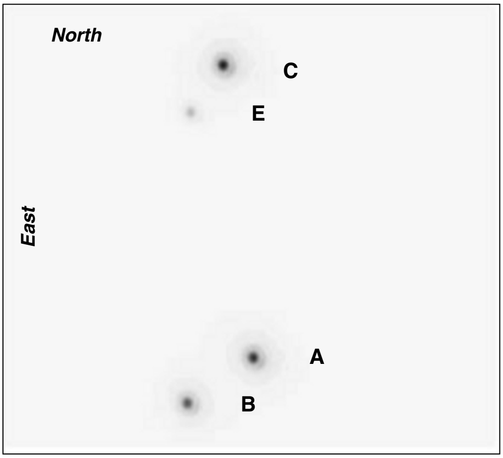

Fig. 1. Narrow-band image of HD 40887 at 2.12 μm. The components are marked by capital letters

3 The Orbits of Subsystems

The orbital elements of the system A,B were computed by Söderhjelm [1]. In order to re-analyze critically the orbits, we asked all archival observations from the WDS database. Those were kindly provided by Gary Wycoff from USNO. Adding the new 2004.86 measurement, we re-computed the orbit by applying differential corrections to the elements using the program ORBIT [2]. The result is similar to the Söderhjelm's one (Table 1). The systematic character of residuals (Fig. 2) indicates that this orbit is probably not quite satisfactory. However, no better result could be achieved.

Let us consider the orbit of AB,C. The angular separations of A,B and A,C are comparable. Thus, before computing the orbit of AB,C we must remove the motion of A in the A,B orbit. The "waves" caused by this motion

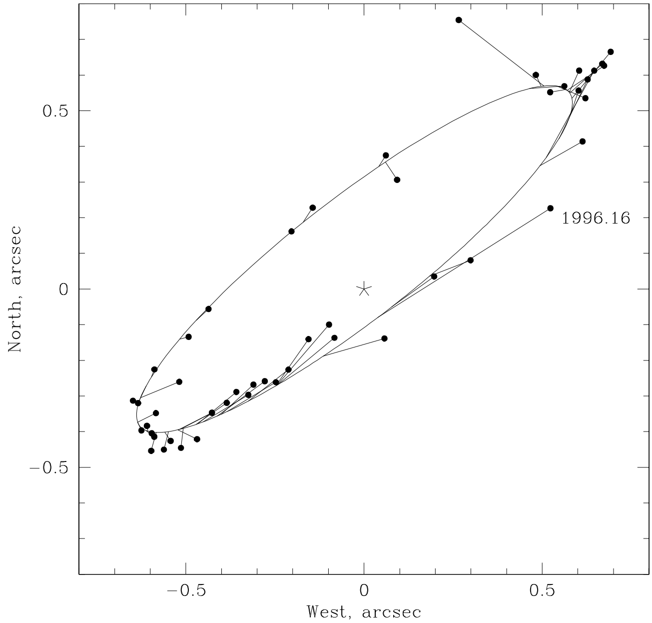

Fig. 2. The visual orbit of the A,B sub-system. The A-component is marked by the star at the coordinate origin, the measured positions of the B-component are joined to ephemeris locations

are apparent in the plots of raw data. We subtracted this correction and analyzed the motion of C around the center-of-mass AB.

The two very first measurements made by J. Herschel in 1835.48 and 1836.86 are very discordant in separation (3.3 and 4.84 arcsec, respectively). It seems evident now that the second measurement was more correct. However, Baize [3] averaged those two critical points. Moreover, he did not subtract the reflex motion of A around AB, the orbit of A,B was not known at the time. Thus, the 390-yr orbit computed for AB,C by Baize is incorrect and contradicts modern observations (see Fig. 3). Using the Baize's orbit led Orlov and Zhuchkov [4] to the conclusion that the triple system AB,C is dynamically unstable.

Table 1. The orbits of A,B

Element	P, yr	T	e	$a,''$	Ω, °	ω, °	i, °
Söderhjelm, 1999	68.0	1998.0	0.45	0.9	125	279	103
This work	67.70	1996.805	0.513	0.912	127.54	275.69	100.38

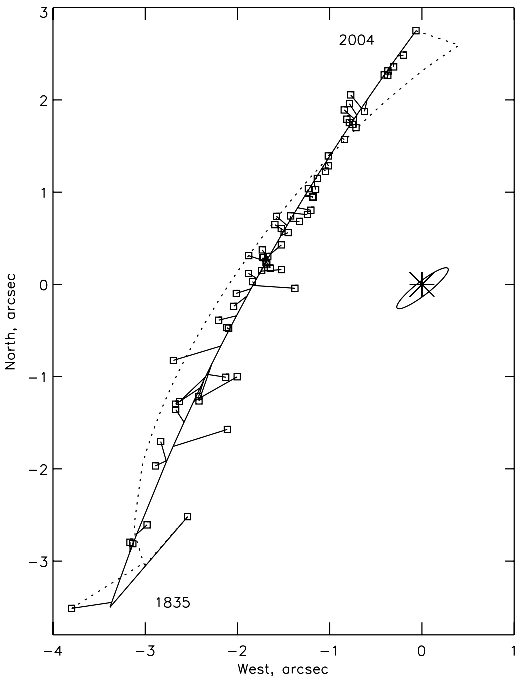

Fig. 3. The apparent motion of AB,C. The observations are plotted as squares, the orbit of Baize [3] as dotted line (connected to two first and one last observations). The solid line shows the quadratic ephemeris. The center of mass AB is marked by a large star at coordinate origin. The small ellipse shows the motion of A around AB

The apparent motion of AB,C is almost rectilinear. The systematic “waves” in the residuals can be explained by the motion of C in the C,E orbit. We fitted these data to a preliminary astrometric orbit (see Table 2).

Table 2. Preliminary astrometric orbit of C,E

	P, yr	T	e	$a,''$	$\Omega,^\circ$	$\omega,^\circ$	$i,^\circ$
Element	23.7	1980.4	0.17	0.120	132	171	124
Error	0.5	1.1	0.04	0.004	10	22	13

4 Discussion

We discovered a new component E in the system and derived its preliminary astrometric orbit. Interestingly, the inclinations and position angles of nodes of A,B and C,E indicate that these pairs may be close to coplanarity. Unfortunately, no radial velocity data is available to determine the acsending nodes of both orbits without ambiguity.

Our study has shown that the visual orbit of the outer sub-system AB,C was premature. The observed motion shows only slight curvature and corresponds to a large, yet unknown orbital period. The fact that AB and CE are seen close to each other may be explained by projection.

Large proper motion and large radial velocity (+102 km/s) indicate that Gl 225.2 belongs to the thick Galactic disk and is not young. Its space velocity module is about 110 km/s. The absence of detectable X-ray radiation also suggests that these stars have no active chromospheres and are old. This quadruple system thus survived for a long time and should be dynamically stable.

This study was partially supported by RFBR grant N 05-02-17744-a.

References

1. S. Söderhjelm: A&A **341**, 121 (1999)
2. A. Tokovinin: Speckle Spectroscopic Studies of Late-Type Stars. In: *Complementary Approaches to Double and Multiple Star Research, IAU Coll. 135*, ed by H.A. McAlister, W.I. Hartkopf (ASP, San Francisco, 1992) p 573
3. P. Baize: Inf. Circ. IAU Comm. 26. **80** (1980)
4. V.V. Orlov, R.Ya. Zhuchkov: Astron. Rep. **49**, 201 (2005)

Multiple Stars: Designation, Catalogues, Statistics

A. Tokovinin

Cerro Tololo Inter-American Observatory, Casilla 603, La Serena, Chile
atokovinin@ctio.noao.edu

Summary. Discussion of the designation of multiple-star components leads to a conclusion that, apart from components, we need to designate systems and centers-of-mass. The hierarchy is coded then by simple links to parent. This system is adopted in the multiple star catalogue, now available on-line. A short review of multiple-star statistics is given: the frequency of different multiplicities in the field, periods of spectroscopic sub-systems, relative orbit orientation, empirical stability criterion, and period-period diagram with its possible connection to formation of multiple stars.

1 Designation of Multiple Stars

Actual designations of binary and multiple stars are historical, non-systematic and confusing. Future space missions like GAIA, ongoing searches for planets, and other large projects will greatly increase the number of known multiple stars and components, making it urgent to develop a coherent and unambiguous designation scheme. Recognizing this need, IAU formed a special group that held its meetings in 2000 and 2003. As a result, IAU adopted the designation system developed for the Washington Multiple Star Catalogue (WMC) [5], an extension of the current designations in the Washington Double Star Catalogue (WDS) [7]. Old WDS designations will not change (to avoid further confusion), new component names will be constructed hierarchically as sequences of letters and numbers, e.g. Ab2. The designations reflect the hierarchical structure of multiple systems, but only to a certain extent. Future discoveries of components at outer or intermediate levels of hierarchy and the constraint of fixed designations will inevitably lead to situations where names do not reflect the true hierarchy, which has then to be coded separately.

In the future, many components of multiple systems will be resolved into sub-systems, so that A will become Aa and Ab, for example. Nevertheless, current designations of these components (or rather *super-components*, as they contain more than one star) will not become obsolete, because past and future measurements of these entities as a whole will still refer to the super-component names such as “A” in our example. It turns out that the concept of super-components is crucial to the whole problem. Once each

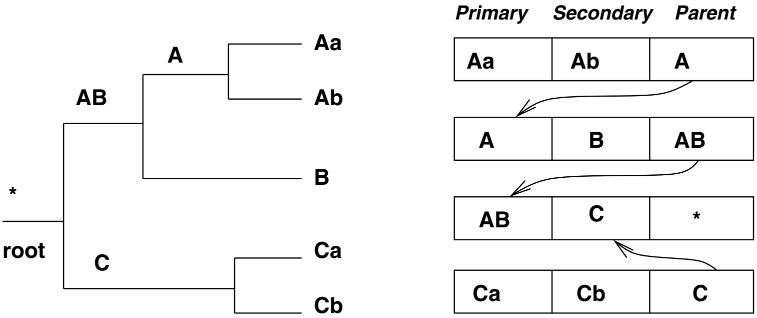

Fig. 1. Hierarchical structure of a quintuple system and its coding by reference to parent. Given the components designations and references to parent (right), the hierarchical tree (left) can be constructed automatically

super-component has its own designation, unique within each multiple system, we can code hierarchies by simple reference to parent (Fig. 1).

The WMC designation system extended to normal components and super-components is thus logical and flexible, permitting to accommodate new discoveries. Its application is not free of ambiguity, however, so that a common center (or clearing house) will still be required. The WMC itself will hopefully play this role.

2 Multiple-Star Catalogues

Although multiple stars are quite common, this fact is not reflected in the catalogues. A researcher wishing to study large samples of multiple stars has to compile his own lists or use the lists published by others, e.g. [2, 4]. It is equally possible to extract multiple stars from binary catalogues. The current 9-th catalogue of spectroscopic binary orbits, SB9[1] [9], contains multiplicity notes and visual-component designations. Many visual multiples are listed in the WDS [7], but the physical relation between their components has not been studied systematically, many are simple line-of-sight projections (optical).

The Multiple Star Catalogue (MSC) [11] is an attempt to create and maintain a list of *physical* systems with 3 or more components. The MSC is essentially complete for "historical" multiple systems known before 1996, with the exception of visual multiples (only a fraction of WDS multiples have been checked for physical relation). The completeness of the MSC (1024 systems as of July 2005) is less evident with respect to new discoveries. An on-line interface to the MSC became available recently[2]. The MSC contains estimates of component masses and orbital parameters, essential for statistical studies, e.g. [16]. Several observing programs have used the MSC to create

[1] `http://sb9.astro.ulb.be`
[2] `http:/www.ctio.noao.edu/~atokovin/stars/`

their samples. The new designation system is now implemented in the MSC and the hierarchical trees like that in Fig. 1 are displayed on-line.

3 Statistics of Multiple Stars

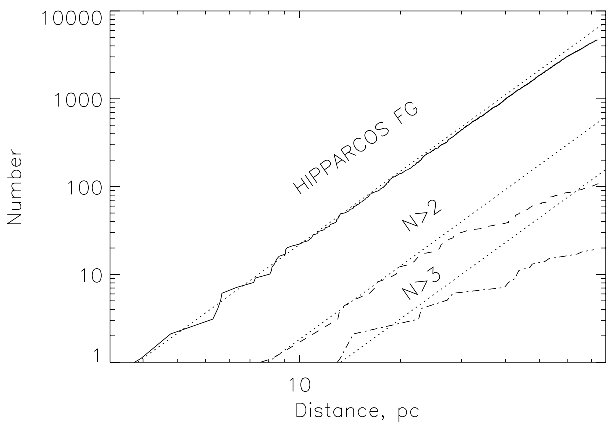

Fig. 2. Completeness of the multiplicity knowledge: number of stars and systems of spectral types F and G ($0.5 < B - V < 0.8$) within given distance. Full line: objects in the HIPPARCOS catalogue follow reasonably well the expected cubic law (dotted line). Dashed line: F- and G-type dwarfs with 3 or more companions from MSC also follow the cubic law, but only up to a distance of 30 pc (1/12th of all stars have 3 or more components). At 50 pc, the estimated completeness is only 40%. Dash-dot: quadruples and higher multiplicities, still very incomplete

Frequency of multiple stars. The values of multiplicity fraction given in the literature are often confusing because of different definitions of this parameter. Let n_k be the fraction of systems with exactly k components, and a_k – the fraction of systems containing at least k components (i.e. counting higher multiplicities as well). Evidently, $n_k = a_k - a_{k+1}$. Batten [1] defines the multiplicity ratio $f_k = a_k/a_{k-1}$ and argues that $f_k \sim 0.25$ for $k \geq 3$. This estimate has been confirmed with a larger sample from the MSC [12]. It follows immediately that $n_k = a_k(1 - f_{k+1})$.

Duquennoy & Mayor [3] (DM91) count all binary pairings, irrespectively of their hierarchy. A *companion star fraction* $CSF = n_2 + 2n_3 + 3n_4 + ... = 0.62$ can be inferred from their Fig. 7. From Fig. 2, we estimate $a_3 \approx 1/12$ (a higher estimate $a_3 = 0.2 - 0.25$ has been given in [14]). Assuming $f_k = 0.25$, we calculate n_3, n_4, n_5, etc., and evaluate the contribution to the CSF from pairings in multiple stars as $2n_3 + 3n_4 + 4n_5 + ... = 0.26$. Hence, the fraction of pure binaries in the DM91 sample should be $n_2 = 0.62 - 0.26 = 0.36$, the fraction of systems that are at least binary is $a_2 = n_2 + a_3 = 0.44$, and the fraction of higher hierarchies with respect to binaries is $f_3 = a_3/a_2 = 0.19$. A smaller number $f_3 = 0.11 \pm 0.04$ (or $a_3 = 0.05$) was derived directly from the DM91 data [12].

Short-period sub-systems and Kozai cycles. Spectroscopic binaries in the field seem to have a period distribution that smoothly rises toward longer periods in the range from 1 to 1000 d, according to several independent studies [3]. In contrast, the distribution of periods of spectroscopic sub-systems in multiple stars shows a maximum at periods below 7 d [15]. This "feature" is too sharp to be explained by selection effects, and the transition period is suspiciously similar to the cutoff period of tidal circularization. Dissipative Kozai cycles are the most likely mechanism that shortens periods of many (but not all) sub-systems below 7 d.

Relative orientation of orbits has been studied by Sterzik & Tokovinin [10]. Only in 22 cases the *visual* orbits of both outer and inner sub-systems are known. This extremely small sample has small ratios of outer-to-inner periods $P_{\mathrm{out}}/P_{\mathrm{in}}$ because at long P_{out} the time coverage of existing visual data (about 200 yr) is still too short (in fact, many long-period orbits are uncertain or wrong), while orbits with short P_{in} are difficult to get for the lack of spatial resolution. The true ascending nodes of visual orbits are, generally, not identified, further complicating data interpretation. The advent of adaptive optics and long-baseline interferometry holds great promise in extending this sample significantly, mostly by resolving the inner (spectroscopic) sub-systems in visual binaries with known outer orbits, e.g. [8].

Despite current observational limitations, it is already clear that the inner and outer orbits are neither coplanar nor completely random. The directions of their orbital angular momenta are weakly correlated. Such correlation could be explained by dynamical decay of small stellar groups [10]. However, alternative explanations are possible, too. It will be extremely important to extend the studies of relative orbit orientation to larger samples and to start probing the orientations in different sub-groups.

Empirical stability criterion. Multiple systems where both inner and outer orbits are known offer rich possibilities for joint analysis of their orbital parameters, e.g. checking the dynamical stability. Theoretical and numerical formulations of the stability criterion in the three-body problem have been offered by many authors and lead to similar results. I take the latest work of Mardling & Aarseth [6] (MA02) as representative and compare their stability criterion with 120 real systems from the MSC (Fig. 3). Some systems are, apparently, unstable. However, I can ignore both unreliable outer orbits with periods over 300 yr and inner periods shorter than 10d (likely affected by Kozai cycles), plotted as crosses in Fig. 3. The remaining systems (diamonds) nicely fall in the stability zone.

When outer orbits are nearly circular, the match between the data and the MA02 criterion is impressive: all systems indeed have $P_{\mathrm{out}}/P_{\mathrm{in}} > 4.7$.

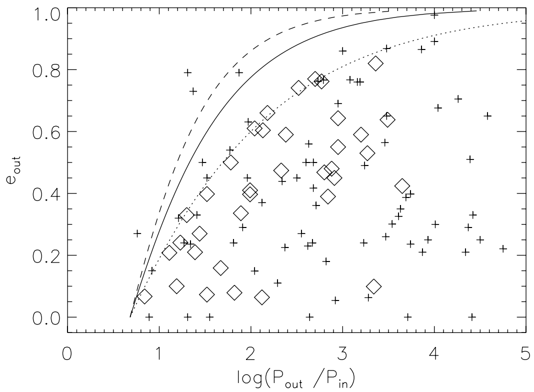

Fig. 3. Comparison of dynamical stability criteria with orbital parameters of the real systems: eccentricity of the outer orbit $e_{\rm out}$ (vertical axis) versus period ratio $P_{\rm out}/P_{\rm in}$ (horizontal axis). The full line depicts the dynamical stability criterion of MA02, the dashed line is its modification proposed in [10], the dotted line is the empirical criterion

However, eccentric outer orbits deviate from the theoretical criterion in a systematic way. The *empirical stability criterion* [14] can be described by the relation $P_{\rm out}(1-e_{\rm out})^3/P_{\rm in} > 5$, whereas all theoretical criteria lead to a similar relation with $(1-e_{\rm out})^{2/3}$ instead of cube. The reason of this discrepancy remains a mystery.

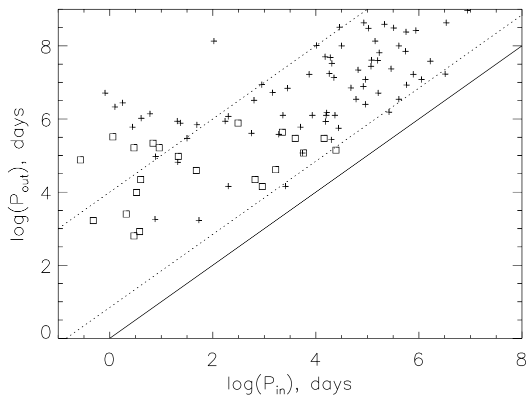

Fig. 4. Periods of inner (horizontal axis) and outer (vertical axis) sub-systems in a sample of nearby late-type multiples from the MSC. Systems where both periods are known from orbital solutions are plotted as squares, in the remaining systems (crosses) at least one period is estimated from the separation. The full line corresponds to equal periods, the dashed lines depict period ratios of 5 and 10 000

Period-period diagram. What is a typical period ratio $P_{\rm out}/P_{\rm in}$ at adjacent hierarchical levels? Fekel [4] found it to be large, around 2000. In the MSC, we encounter all possible ratios allowed by the dynamical stability, i.e. greater than 5. However, systems at intermediate hierarchical levels often remain undiscovered, leading to wrongly estimated period ratios. By restricting the sample to nearby (within 50 pc) late-type stars, we reduce these errors and begin to see the true distribution of period ratios (Fig. 4).

The $P_{\rm out} - P_{\rm in}$ diagram reveals some features of multiple-star formation and evolution. Interestingly, period ratios larger than 10 000 are found only when $P_{\rm in} < 30$d, i.e. where inner periods were likely shortened by some dissipative mechanism like Kozai cycles with tides. The only exception to this rule (the point at the top) is Capella, a pair of giants on a 100-d circular orbit in a quadruple system. It is very likely that all multiple stars have been formed with the period ratio $P_{\rm out}/P_{\rm in} < 10\,000$. Some inner periods were then shortened by tidal or other dissipative processes. In this perspective, Capella had a rather eccentric initial orbit with a period of few tens of years which has been shortened and circularized when its components became giants.

4 Conclusions

Cataloguing of multiple systems, however boring it might seem, offers interesting insights into formation and evolution of stars. New powerful observing techniques (adaptive optics, interferometry, precise radial velocities) should now be applied to large stellar samples in order to "fix" the multiplicity statistics in the solar neighborhood and beyond.

References

1. A.H. Batten: *Binary and multiple systems of stars* (Pergamon, Oxford 1973)
2. J.R. Donnison, D.F. Mikulskis: MNRAS **272**, 1 (1995)
3. A. Duquennoy, M. Mayor: A&A **248**, 485 (1991) [DM91]
4. F.C. Fekel: ApJ **246**, 879 (1981)
5. W.I. Hartkopf, B.D. Mason: Addressing confusion in double star nomenclature: The Washington Multiplicity Catalog. In: *The formation and evolution of binary and multiple stars*, ed. C. Scarfe, C. Allen. Rev. Mex. Astron. Astrof. Conf. Ser., vol. 21, pp 83–90 (2004)
6. R.A. Mardling, S.J. Aarseth: MNRAS **321**, 398 (2002) [MA02]
7. B.D. Mason, G.L. Wycoff, W.I., Hartkopf et al: AJ **122**, 3466 (2001)
8. M.W. Muterspaugh, B.F. Lane, M. Konacki et al.: A&A, in print (2005), astro-ph/0509855
9. D. Pourbaix, A.A. Tokovinin, A.H. Batten et al.: A&A **424**, 727 (2004)
10. M.F. Sterzik, A.A. Tokovinin: A&A **384**, 1030 (2002)
11. A. Tokovinin: A&AS **124**, 75 (1997) [MSC]
12. A. Tokovinin: Statistics of multiple stars: Some clues to formation mechanisms. In: *The formation of binary stars*, ASP Conf. Ser., vol. 84, ed. by H. Zinnecker, R.D. Mathieu (ASP, San Francisco 2001) pp 84–92
13. A. Tokovinin: Designation of multiple-star components. In: *Trans. of the IAU*, ed. O. Engvold, vol. 25B, in print (2005)
14. A. Tokovinin: Statistics of multiple stars. In: *The formation and evolution of binary and multiple stars*, ed. C. Scarfe, C. Allen. Rev. Mex. Astron. Astrof. Conf. Ser., vol. 21, pp 7–14 (2004)
15. A.A. Tokovinin, M.G. Smekhov: A&A **382**, 118 (2002)
16. M.J. Valtonen: A&A **334**, 169 (1998)

Radial-velocity Studies of Certain Multiple Systems

R.F. Griffin

Cambridge University Observatories (England)

Summary. Continued (and continuing) observations are progressively elucidating the outer orbits in a number of spectroscopic triple systems whose inner orbits are already documented.

The speaker has effectively full-time use of the 36-inch reflector on the Cambridge site. It is used with a radial-velocity spectrometer patterned after Mayor's 'Coravel'. The principal programme of observations is the monitoring of the radial velocities of a number of stars whose velocities have been found to change. They include a small proportion of systems that are more complicated than simple doubles, quite apart from the association of additional visual components with an appreciable proportion of the spectroscopic binaries.

Certain triple systems whose orbits have already featured in the speaker's long-running series of papers in *The Observatory* have been retained on the observing programme, with a view to documenting at least a part of the 'outer' (long-period) orbit. They include HD 7426 (Paper 80), HR 965 (Paper 88), HR 2879 B (Paper 119), 24 Aqr (Paper 128), and V455 Aur (Paper 160).

In the 17 years since the 1600-day inner orbit of HD 7426 was described [1], the γ-velocity continued to rise, but the rise now appears to have levelled off. It is possible to fit a plausible outer orbit to the graph of the variation of the γ-velocity, but only by fixing the period; 20,000 days is a suitable value at which to fix it, but the observations so far cover only about 12,000 days, and there is still a lot of uncertainty in the true length of the outer period. A beneficial side-effect of the continuing observations is that the inner orbit, which was indistinguishable from a circle in the original publication, is now seen to have a definite eccentricity of about 0.07, five times its standard deviation.

The existence of a downward drift in the γ-velocity of HR 965, a discovery that came as a surprise to the author when he went to write up the short-period (1100-day) orbit [2], has been fully confirmed, but has now levelled out. Radial-velocity measurements in the literature, ante-dating those measured by the speaker, allow the outer period to be estimated at 16,000 days (44 years). The eccentricity of the inner orbit, which in the published paper was attributed a value of 0.06 ± 0.03, of very marginal significance, currently appears to be 0.03 ± 0.01, so it is still somewhat marginal. Part of the difficulty in obtaining an accurate eccentricity for the inner orbit arises from the period being extremely close to the exact value of three years (it is six days short), which conspires with the location of the star in the sky, only 5 degrees from the north celestial pole, to limit the phase coverage that can be obtained with the Cambridge instrument.

HR 2879 B underwent a dramatic periastron passage in its outer orbit ($e \sim 0.66$) about five years ago; the outer period is now quite well estimated at close to 10,000 days (27 years). The mass ratio between the components in the outer orbit, one of which is the well documented 27-day double, is now determined to be very close to the anticipated value of two to one — the larger but comparatively ill-determined ratio that was implied by the published observations [3] has given place to a much more acceptable figure.

24 Aqr continues to follow accurately the course laid out for it, on the basis of a minor adjustment to the visual orbit, in the published paper [4]. Each year it is possible to obtain radial-velocity traces in which the two observable components are infinitesimally better separated than they have been previously; eventually there should come a time, near the periastron passage, when they can be seen completely separated, thereby enabling their individual profiles to be accurately ascertained and all previous observations to be reduced with increased precision and confidence. Unfortunately the periastron passage is still about fifteen years away.

V455 Aur (HD 45191), which exhibited such a major change of γ-velocity between the two seasons' observations reported in the published paper [5], has scarcely changed at all since then. Evidently the outer orbit is of much longer period than seemed likely at first, and must have a high eccentricity.

Among other multiple systems under current observation, one particularly interesting one is HD 117078, which proves to be quadruple. Two components are visible in radial-velocity traces, but their velocities vary in different periods, about 6 and 204 days, and demonstrate that the system consists of two single-lined binaries. The γ-velocities have varied considerably, in anti-phase with one another as would be expected, and enough of the outer orbit has been seen to enable its period to be estimated, seemingly quite well, at about 13,000 days or 36 years.

A final example of a system that exhibits two periods of radial-velocity variation is enigmatic. It is 32 Cyg, one of the best-known ζ Aur binaries, whose orbital period has long been accurately established from the eclipse cycle of 1147 days. During the last two cycles the radial velocities, systematically measured once a month, have shown a very distinct subsidiary variation with a period of about two years and a peak-to-peak amplitude of about 1 km s^{-1}. It seems most unlikely that the system could include a component with a 2-year period when the known orbit is of 3 years. Possibly the 2-year variation represents azimuthal differences of spectrum or surface brightness in the K-supergiant primary; the period is close to the pseudo-synchronous one.

References

1. Griffin, R.F., 1988, Observatory, 108, 90
2. Griffin, R.F., 1989, Observatory, 109, 180
3. Griffin, R.F., 1994, Observatory, 114, 268
4. Griffin, R.F., Carquillat, J.-M., Ginestet, N, & Udry, S., 1996, Observatory, 116, 162
5. Griffin, R.F., 2001, Observatory, 121, 315

Spectral Disentangling Applied to Triple Systems: RV Crt*

H. Hensberge[1], L.P.R. Vaz[2], K.B.V. Torres[2] and T. Armond[2]

[1] Royal Observatory of Belgium, Ringlaan 3, B-1180 Brussels, Belgium
herman.hensberge@oma.be

[2] Universidade Federal de Minas Gerais, DF-ICEx, C.P. 702,
30.123-970 Belo Horizonte, MG, Brazil lpv@fisica.ufmg.br

Summary. The eclipsing triple system RV Crt shows a composite spectrum dominated by the sharp-lined late-F type spectrum of the tertiary. The spectral lines of the close binary are considerably broadened, since both components rotate synchronously with the orbit. The Doppler shifts and the component spectra are successfully recovered by application of the spectral disentangling technique. The cooler, less massive component of the close binary is larger than the hotter one. The hotter component of the close binary is very similar to the tertiary. The system is probably still on its way to the zero-age main sequence.

1 Introduction

Spectral disentangling is a powerful analysis method for composite spectra, solving self-consistently for N time-independent component spectra and their time-dependent (orbital) Doppler shifts $\Delta\lambda(t_j)$. The relative contribution ℓ_n of each component may depend on time:

$$S_{obs}(t_j) = \sum_{n=1}^{\mathrm{N}_{comp}} \ell_n(t_j) S_n\left(\lambda; \Delta\lambda(t_j)\right) \qquad (1)$$

The numerical solution was first formulated in velocity space (logarithm of wavelength) by [6] and soon thereafter by [3] using the Fourier components of the spectra. These methods solve for the contribution of each component to the composite spectra. In the case of time-dependent relative contributions $\ell_n(t_j)$, the normalized intrinsic component spectra are reconstructed straightforwardly. Without relative light variability, a unique normalization depends on external information. The most favourable case in the latter situation occurs when all components have at least one very deep absorption line (e.g. Ca II K in cool stars, see [2], [1]), since the requirement that absorption lines should have non-negative flux in any of the components is then sufficient to derive accurate ℓ_n. Recent reviews on applications to observed and artificial data are published in [4]. Note that several numerical codes are available

*Based on observations obtained at the European Southern Observatory (ESO), La Silla, Chile to interested users: the Fourier analysis code KOREL maintained by Hadrava (`www.asu.cas.cz/~had/korel.html`), that also deals with hierarchical orbits; and a Fourier analysis code for two (fdbinary) and three components (fd3, preliminary version, `sail.zpf.fer.hr/fdbinary/fd3`) and a spectral separation code (known orbit) in velocity space (`sail.zpf.fer.hr/cres`) maintained by Ilijić.

2 Data

Forty-one high-resolution spectra obtained with the FEROS spectrograph at the 2.2 m ESO telescope, covering adequately the wavelength interval 390–880 nm with a pixel size of 2.7 km s^{-1}, are analysed. The 20 min exposures, one of which is obtained during the 25 min totality in the primary eclipse, have a signal-to-noise ratio above 100 (Fig. 1). They cover well all orbital phases at which the line profiles (averaged over the visible stellar disks) are not affected by partial eclipses.

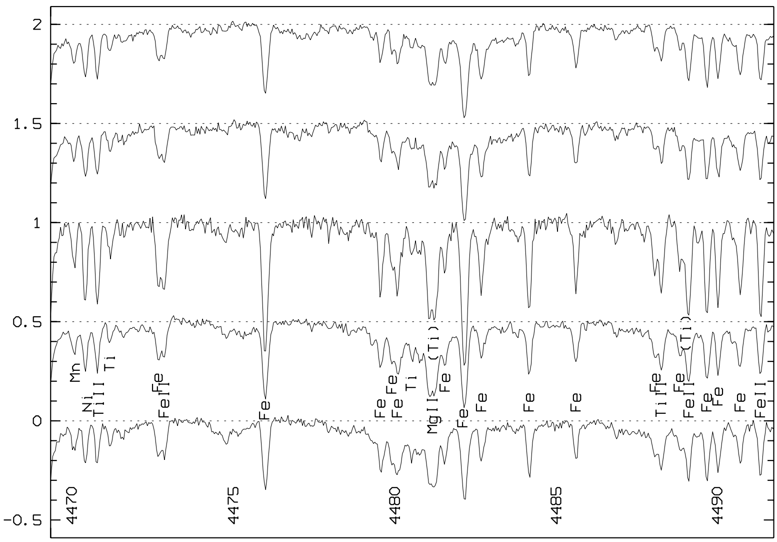

Fig. 1. Detail of the observed spectrum of RV Crt at orbital phases 0.75, 0.875, 0.00, 0.125 and 0.25 respectively (top to bottom). Vertical shifts in relative intensity are applied for clarity. The sharp-lined third component dominates the composite spectrum. Note its stronger, less diluted lines in primary mid-eclipse. The primary is easiest seen near Fe I $\lambda\,4476$, red-shifted in the upper spectra and blue-shifted in the lower ones, and in the moving, broad underlying absorption around $\lambda\,4481$

The orbital period of 1.17050239 d ($\pm 2.1\,10^{-7}$ d) is accurately known from Strömgren *uvby* photometry obtained with the Danish SAT telescope at ESO in 61 nights from 1987 to 1989.

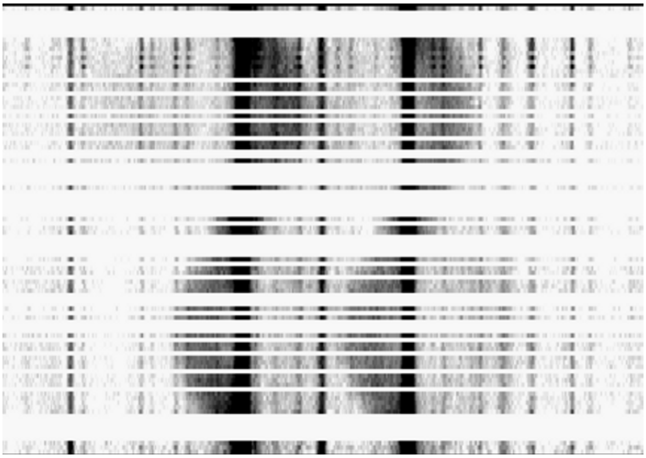

Fig. 2. Visibility of the close binary components in the Na I D lines ($\lambda\lambda$ 5890–5896 Å). Black indicates strong absorption. Orbital phase varies along the vertical axis. Even in these strong lines the contribution of the secondary is only marginally visible (red-shifted in the lower part of the figure, blue-shifted in the upper part)

We use the KOREL code. The Fourier analysis technique requires the selection of wavelength regions with edges in (quasi)-continuum. Each region should also contain a significantly time-dependent contribution from the close binary component(s) (Fig. 2). We selected 25 regions, with either 512 (3 regions), 1024 (5 regions), 2048 (6 regions) or 4096 (11 regions) spectral bins. Some regions overlap with others. KOREL has been adapted at UFMG to deal at once with all these unequal-length regions. The relative light contributions in each wavelength region were fixed making use of the changes of line strengths in primary mid-eclipse, the light curves, and the light ratios predicted by the associated Wilson-Devinney analysis.

3 Component Spectra

Examples of disentangled component spectra are shown in Fig. 3. The spectrum of the primary mimics the tertiary broadened to the rotation velocity required for synchronization with the orbit. This similarity is a strong indication that the disentangling process is performed properly. The primary and the tertiary contribute equally to the system light near λ 4000, and their light

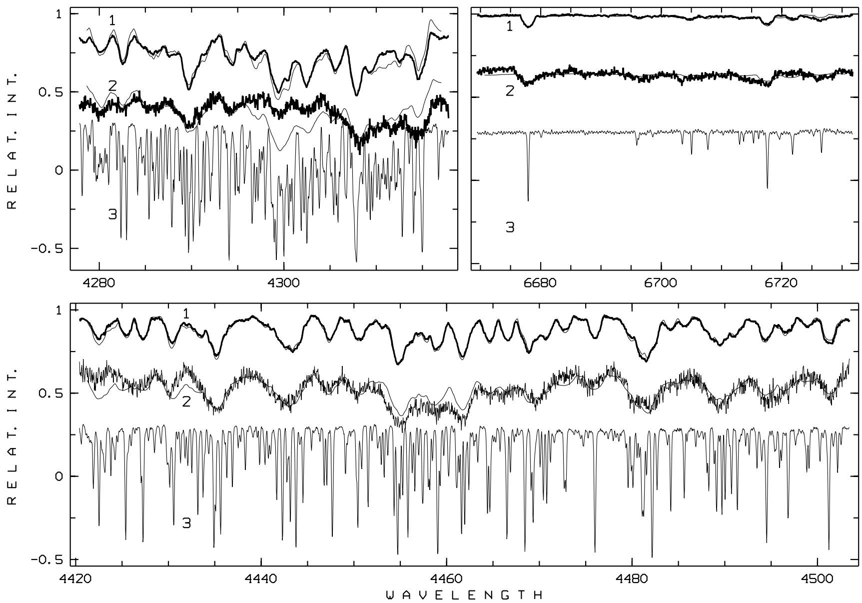

Fig. 3. Disentangled intrinsic component spectra in selected spectral regions. The close-binary component spectra (thick line) are compared to rotationally broadened versions (thin lines) of the tertiary spectrum, assuming rotation synchronous with the orbital period. Note the similarity between primary and tertiary. Shifts in relative intensity are applied to the spectra of the secondary (-0.35) and tertiary component (-0.7)

ratio depends only slightly on wavelength, e.g. the tertiary is 10% brighter at $\lambda\,5500$. The line widths in the spectrum of the secondary are also in line with synchronization with the orbit. The noise in its intrinsic spectrum is a direct consequence of its faintness, its light contribution (out of eclipse) varying roughly from 4% at $\lambda\,4000$ to 16% of the total system light at $\lambda\,8800$. The different line strengths in the spectrum of the secondary are qualitatively in accordance with its lower stellar temperature ($T_{\rm eff} \approx 4\,200$ K, while primary and tertiary have $T_{\rm eff} \approx 6\,600$ K); but the lack of absorption near 4300 Å might signal a weak G-band of CH (Fig. 3). The possible presence of spectral peculiarities shows how useful is the reconstruction of component spectra without a priori assumptions about spectral features.

4 Fundamental Stellar Parameters

Consistent radial velocities are derived from different subsets of regions. In combination with the analysis of the light curves (Figs. 4, 5), they indicate that the secondary (0.41 $M_\odot$, 1.51 $R_\odot$) is less massive, but significantly larger than the primary (0.76 $M_\odot$, 1.13 $R_\odot$). The less massive star is the largest and most over-luminous component, confirming that both stars may be contracting to the main sequence [5].

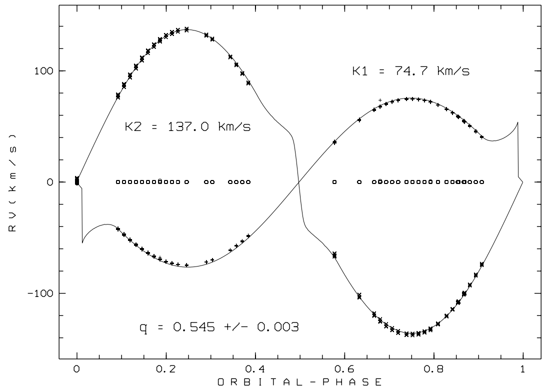

Fig. 4. Radial velocities derived from the subsets of regions with 1024, 2048 and 4096 data points respectively compared to the radial velocity curves computed from the preliminary Wilson-Devinney solution

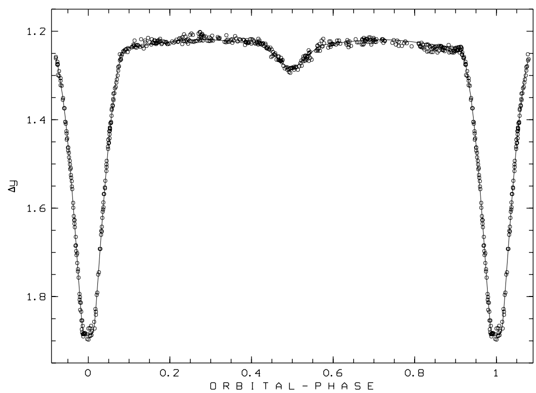

Fig. 5. Differential light-curve in Strömgren y with the Wilson-Devinney solution used in Fig. 4. In both cases low-level systematics in the residuals suggest the need for further refinements

5 Future Work

The present level of disentangling is adequate to derive the orbit and characterize the component spectra. In particular, an accurate mass ratio of the components of the close binary was derived in contrast to earlier attempt using cross-correlation techniques. Nevertheless, minor bias is apparent in the component spectra. An alternative spectral separation, in velocity space, may clarify the role of several effects introducing possibly bias in the component spectra, especially in the fainter one:

- lack of continuum at the edges of the selected regions;
- masking of telluric lines, interstellar lines (presently only done in the Na I lines) and detector blemishes;
- small bias in the input spectra due to imperfect data reduction.

Indeed, Fourier and velocity space disentangling react different to these issues.

A detailed analysis of the component spectra will provide accurate temperatures and the chemical composition of the atmospheres. Combination of the light curves with spectroscopic temperatures and radial velocities leads to final orbital and stellar parameters, which will be confronted with stellar evolution theory.

Acknowledgments

We are indebted to P. Hadrava for making the KOREL code available. Financial support provided by the Belgian Science Policy (IAP P5/36), and by the Brazilian Agencies CNPq, CAPES and FAPEMIG is acknowledged.

References

1. Y. Frémat, P. Lampens & H. Hensberge: MNRAS **356**, 545 (2005)
2. R.E. Griffin: AJ **123**, 988 (2002)
3. P. Hadrava: A&AS **114**, 393 (1995)
4. R.W. Hilditch, H. Hensberge & K. Pavlovski (eds.): *Spectroscopically and Spatially Resolving the Components of Close Binary Stars*, ASP Conf. Ser. **318** (2004)
5. A.C. Machado: MSc Dissertation, DF-ICEx-UFMG (1997)
6. K.P. Simon & E. Sturm: A&A **281**, 286 (1994)

Evidence for Rapid Variability in the Multiple System 68 u Her

K. Uytterhoeven[1], P. Koubský[1], P. Harmanec[1,2], J.H. Telting[3], S. Yang[4], M.T. Richards[5] and I. Ilyin[6]

[1] Astronomical Institute Academy of Sciences, Fričova 298, CZ-251 65 Ondřejov, Czech Republic (katrienu,koubsky)@sunstel.asu.cas.cz
[2] Astronomical Institute Charles University, V Holešovičkách 2, CZ-181 00 Praha 8, Czech Republic hec@sunstel.asu.cas.cz
[3] Nordic Optical Telescope, Apartado de Correos 474, E-38700 Santa Cruz de La Palma, Spain jht@not.iac.es
[4] Dept.of Physics and Astronomy, University of Victoria, P.O. Box 3055, Victoria, B.C. V8W 3P6, Canada yang@uvastro.phys.uvic.ca
[5] Penn State University, 525 Davey Laboratory, University Park, PA 16802, U.S.A mrichards@astro.psu.edu
[6] Astrophysical Institute Potsdam, An der Sternwarte 16,D-14 482 Potsdam, Germany ilyin@aip.de

1 The Project 68 u Her

The eclipsing binary 68 u Herculis (HD 156 633, HR 6431, $\alpha_{2000} = 17^{\mathrm{h}}\,17^{\mathrm{m}}\,19\overset{\mathrm{s}}{.}6$, $\delta_{2000} = +33^\circ\,06'\,00''$, $m_V = 4.8$) is a well studied target on the Northern sky. Over the last century several photometric and spectroscopic campaigns have been undertaken to improve our understanding and the description of this binary system. 68 u Her is a semi-detached system whereby the secondary fills its Roche-lobe and whereby the components revolve in a circular orbit with a seemingly stable period of about $P_{\mathrm{orb}} = 2\overset{\mathrm{d}}{.}051026$ days, e.g. [1–3]. The spectral types of the components of the SB2 system are B2IV (primary) and B8 or B9 (secondary) [3].

Variations in the light-curves and line-asymmetries have been reported. These are interpreted by some authors as an effect of the presence of interstellar matter [4], while others [3,5] explain them in terms of intrinsic variations, given that the primary is located in the instability strip of the β Cephei variables. The intrinsic variability has not yet been studied in detail.

We present the preliminary results of the analysis of a large dataset of spectroscopic observations of 68 u Her which have been gathered over the last 10 years using 5 different telescopes at 4 different observatories. Two different observing strategies were followed. The first is a long-term (1994-2005) monitoring of the target to study the binary system carefully with the aim to solve open questions such as uncertainties concerning the circularity of the orbit and the presence of apsidal motion. Secondly, in the framework of a systematic study of line-profile variable early-type B stars in close binary systems with the aim to study tidal effects on the pulsational behavior, time-series of high-resolution spectra where obtained during consecutive nights in

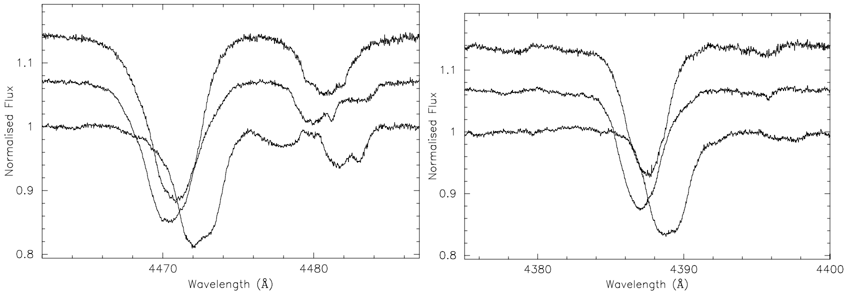

Fig. 1. A randomly chosen set of data for 68 u Her obtained with the SOFIN spectrograph at the NOT telescope. The profiles of the He I 4471.500 Å and Mg II 4481.136 Å lines (left) and the He I 4387.929 Å profiles (right). The spectra are offset for clarity

1996 and 2003. Table 1 gives a logbook of the observations. The spectra of the long-term program are mainly low-resolution spectra ($R < 20000$) centered on the H_α region, while the time-series are échelle spectra with $R \sim 50000$.

Table 1. Journal of the new data of 68 u Her. The last three columns denote the number of available RV measurements of primary and secondary, and the wavelength resolution, respectively

Nr.	Observatory	Telescope/Instrument	HJD interval (−2400000)	♯ RVs comp1	♯ RVs comp2	$\Delta\lambda$ (Å)
1	Ondřejov	2m/Reticon spectr.	49476-51708	34	18	0.25
2	KPNO	0.9m/spectrograph	50130-50604	65	22	0.09
3	DAO	1.22m/spectrograph	50222-50824	44	19	0.15
4	DAO	1.83m/spectrograph	50592-50711	18	12	0.139
5	Ondřejov	2m/CCD spectr.	52303-53464	36	17	0.25
6	ORM	1.56mNOT/SOFIN	52795-52806	175	105	0.02

Ondřejov, Czech Republic; KPNO: Kitt Peak National Observatory, Arizona, US; DAO: Dominion Astrophysical Observatory, Victoria, Canada; ORM: Observatorio del Roque de los Muchachos, La Palma, Spain

2 The Binary System

We selected several absorption lines for the determination of radial velocities (RV) of primary and secondary components. The contribution of the secondary was only prominent enough in the Si II 5055.984 Å, He I 6678.154 Å and Mg II 4481.136 Å lines. Values of the RVs of the secondary could only be derived at phases near elongation, when both profiles were separated. The

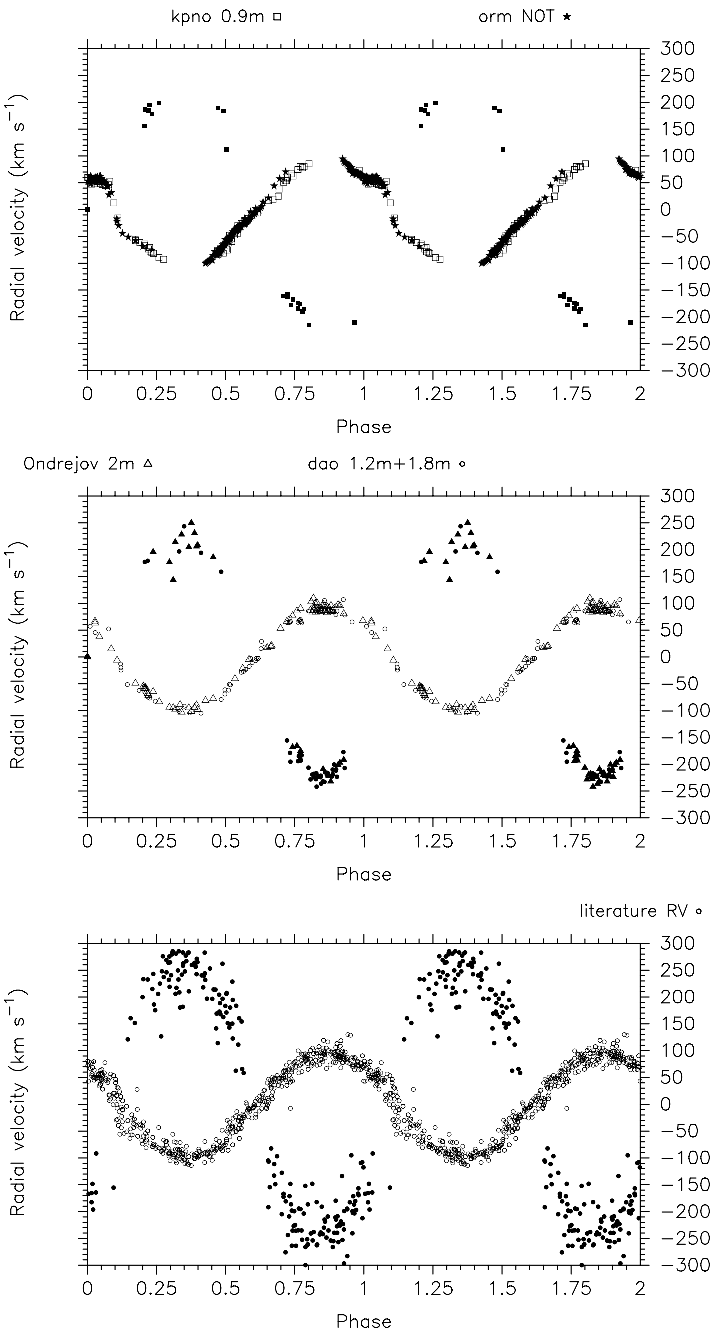

Fig. 2. Phase plots of the RV calculated from the high-resolution KPNO and NOT data (top), from the low-resolution DAO and Ondřejov data (middle) and from the RV found in the literature. ($P_{\rm orb} = 2\overset{\rm d}{.}0510354$ and phase=0 at $T_0 = 2450343.24$)

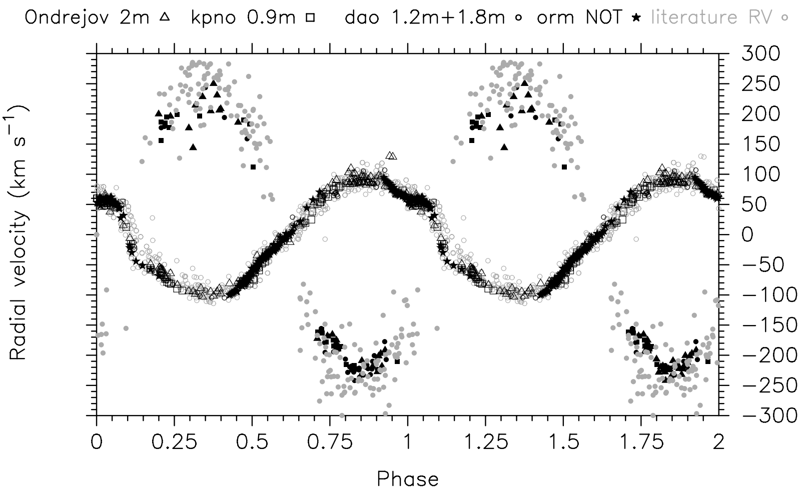

Fig. 3. Phase plot of both the new RV and the RV found in the literature ($P_{\rm orb} = 2\overset{\rm d}{.}0510354$ and phase=0 at $T_0 = 2450343.24$)

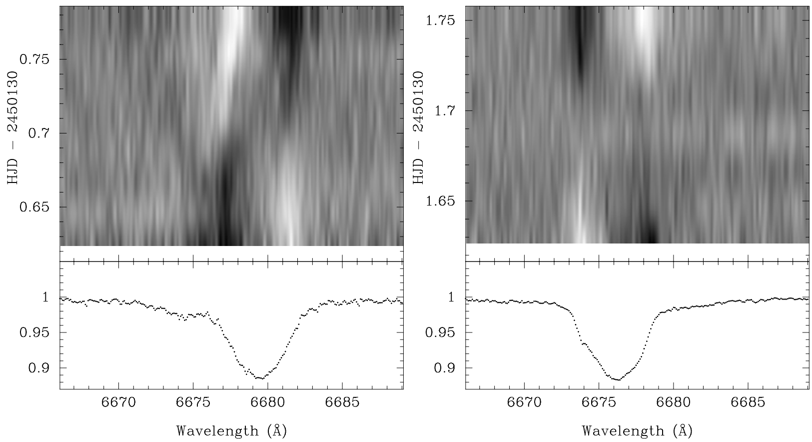

Fig. 4. Gray-scale figures showing the line-profile variability of the He I 6678.154 Å profile of 68 u Her in time during 2 subsequent nights in February 1996 (HJD 2450130 and 2450131). The KPNO spectra are plotted with respect to the nightly average profile, which is given at the bottom of each figure

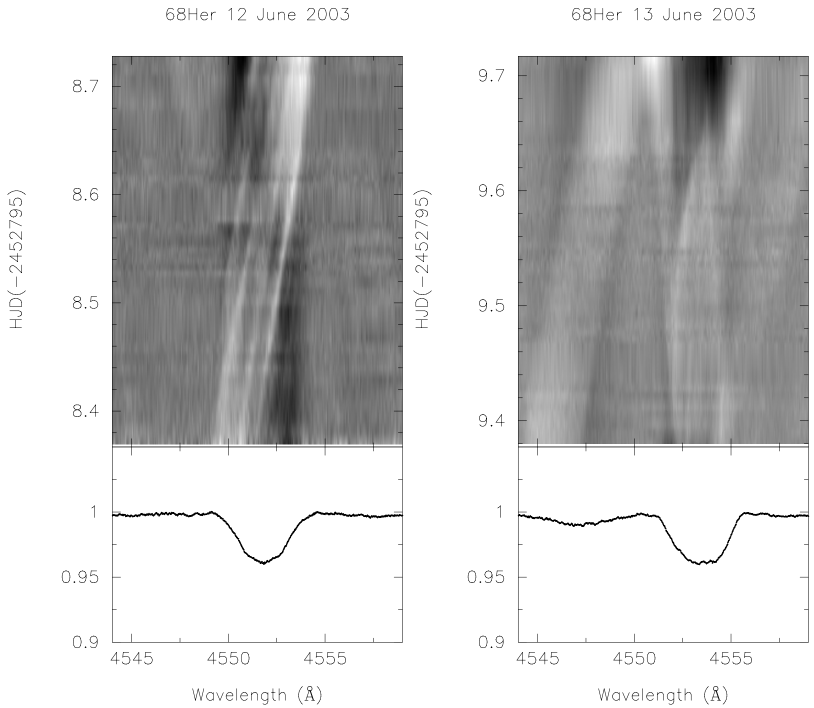

Fig. 5. Similar figure as Fig. 4 but for the SOFIN spectra obtained during two nights in June 2003 (HJD 2452803 and 2452804)

RV were derived from the first normalized velocity moment $\langle v \rangle$, e.g. [6], using variable integration boundaries. A selection of profiles is given in Fig. 1. We present here only the RV calculated from the He lines. We enlarged our sample of RV with the available RV from the literature [3, 4, 7–11]. Most of these older values were obtained from photographic plates.

The analysis of the RV was carried out using the FOTEL code [12]. The results are presented in Figs. 2 and 3. On high resolution spectra the Rossiter effect [13] is clearly visible, while on the old data, mostly from photographic era, it is buried in noise – see Fig. 2 upper and lower panels.

The split of the data into three subsets in time indicates a significant period increase. The rate is small, typical for Algols at the late stages of the mass transfer. The solution with non-zero dP/dt gives a slightly larger r.m.s. error than that for a constant period. However, this might be related to the phases affected by the rotational effect.

All solutions invariably indicate zero eccentricity, a problem that in case of 68 u Her has been discussed for many decades.

3 Rapid Variability

Several time series of spectra of 68 u Her were secured. The preliminary analysis has shown that rapid line-profile variability could be detected only on high resolution spectra. Thus, time series obtained at KPNO and ORM Observatories were analyzed. The results are presented in Fig. 4 and Fig. 5. The black and white bands show a pattern that is typical for non-radial pulsation (NRP) modes. This is the first firm evidence for the pulsations of the primary component of 68 u Her. In order to investigate the NRP further, a detailed line-profile analysis is required.

Acknowledgments

Collection of spectra of this project was started as a part of SEFONO project GAČR 205/96/0162 and later supported from GAČR 2005/03/0788 grant of the Czech Science Foundation. KPNO data were obtained in the framework of National Science Foundation INT-9512791 and Kontakt ES 014 grants. Also the participation of Jiří Krpata, Petr Škoda, Mirek Šlechta and Marek Wolf in data acquisition and reduction is appreciated. We acknowledge the use of the electronic bibliography maintained by NASA/ADS system.

References

1. S. Söderhjelm: A&A **66**, 161 (1978)
2. W.E.C.J. van der Veen: A&A **145**, 380 (1985)
3. R.W. Hilditch: MNRAS **211**, 943 (1984)
4. B.J. Kovachev & M. Reinhardt: AcA **25**, 133 (1975)
5. J.A. Eaton: AcA **28**, 601 (1978)
6. C. Aerts, M. De Pauw, & C. Waelkens: A&A **266**, 294 (1992)
7. R.H. Baker: Publ. of the Allegheny Obs. University of Pittsburgh **1**, 77 (1910)
8. E.B. Frost, S.B. Barrett & O. Struve: ApJ **64**,1 (1926)
9. W.J. Luyten, O. Struve & W.W. Morgan: Publ. Yerkes Obs. **7**, 1 (1939)
10. B. Smith: ApJ **102**, 500 (1945)
11. W.R. Beardsley: Publ. of the Allegheny Obs. University of Pittsburgh **8**, 1 (1969)
12. P. Hadrava: Astrophys. Sp. Sc. **296**, 239 (2005)
13. R.A. Rossiter: ApJ **60**, 15 (1924)

DG Leo: A Triple System with a Surprising Variety of Physical Phenomena

P. Lampens[1], Y. Frémat[1], H. Hensberge[1], V. Tamazian[2], J.A. Docobo[2] and Y. Balega[3]

[1] Royal Observatory of Belgium, Ringlaan 3, Brussel, Belgium
patricia.lampens@oma.be
[2] Observatorio Astronómico Ramón María Aller, Universidade de Santiago de Compostela, Avenida das Ciencias s/n, Santiago de Compostela, Spain
oatamaz@usc.es
[3] Special Astrophysical Observatory, N. Arkhyz, Zelenchukskaya Karachaevo-Cherkesia 369167, Russia balega@sao.ru

Summary. DG Leo consists of three late A-type stars forming a hierarchic and spectroscopic triple system. Although all components have similar age and mass, in-depth spectroscopic analysis showed that the components nevertheless *behave differently with respect to pulsation and to diffusion in their outer atmospheres.* Inclusion of a speckle measure shortly after periastron passage allows to obtain a much improved orbital solution as well as a reliable dynamical parallax and systemic mass. The orbital parameters also suggest a possible coplanar configuration of both pairs. This object therefore represents a first-class opportunity to investigate the link between multiplicity, chemical composition and pulsation in a coeval system.

1 Introduction

As of 2002 one of our goals is to perform an in-depth study of a pulsating star in a binary or a multiple system. Since pulsation is not yet well understood for some classes of variable stars (for example, theory suggests many more modes in δ Scuti stars than are actually observed and the reasons for a particular amplitude or mode are currently unknown), additional constraints based on accurate physical properties can help understand the factors governing the pulsations. Binary and multiple stars with well-characterized components are prime targets as they provide the component's physical properties in an independent and straightforward way. Furthermore, the "common-origin" scenario eliminates some of the factors (distance, environment, overall chemical composition and age) that are otherwise only poorly known.

In the present case study of DG Leo, a δ Scuti component in a triple system, we will demonstrate the potential of a comparative study of the properties between components of "twin" systems. It appeared as a promising target in a review on pulsating stars of type δ Scuti among stellar systems [1]. This hierarchical system consists of three components of spectral type A8/F0 IV-III, all of which are potential candidates for pulsations as well as for spectral peculiarities of type Am [2].

2 Astrophysical Relevance

2.1 The Inner Binary Aa, Ab

The inner pair is a double-lined spectroscopic binary formed by the components Aa and Ab orbiting in a circular orbit with a period of 4.146751 days [3]. Analysis of photometric data obtained during a multi-site, multi-year campaign showed that the most dominant light changes are caused by tidal distortions in the close binary [4]. Tides stretch the components' shapes into ellipsoids, with the long axes aligned along the line connecting the components' centers. Overall, the light curve resembles a double cosine wave [5]. Furthermore, no eclipses were observed [4]. From the absence of eclipses we derived $i_{orb} < 73°$ [3]. Note that this could also be interpreted as $i_{orb} > 107°$ (in good agreement with the orbital inclination of the outer system, see Table 2). This may hint to a coplanar configuration (additionally requiring similar nodes) and also to a common retrograde motion.

The inner pair is circularized. This is a consequence of the very efficient tidal driving during the PMS evolutionary phase of the close binary [6]. We therefore expect a state of spin-orbit synchronization. In the case of full spin-orbit synchronization, there should be no phase lag between e.g. the time of largest visible surface area and the time at which both components cross the nodes of the inner orbit. This is indeed what is observed in Fig. 1. The same conclusion is valid at the conjunction times (90° in orbital phase apart).

The spectral disentangling technique [7] was adopted to study the composite, high S/N spectra acquired with the ELODIE spectrograph at the 1.93-m telescope of the *Observatoire de Haute-Provence* (France). We assumed that the observed spectrum is the combination of three time-independent component spectra that are shifted in wavelength relatively to each other. Using a least-squares method, the code adjusts the variations of the Fourier Transforms of the observed composite spectra with time in order to provide

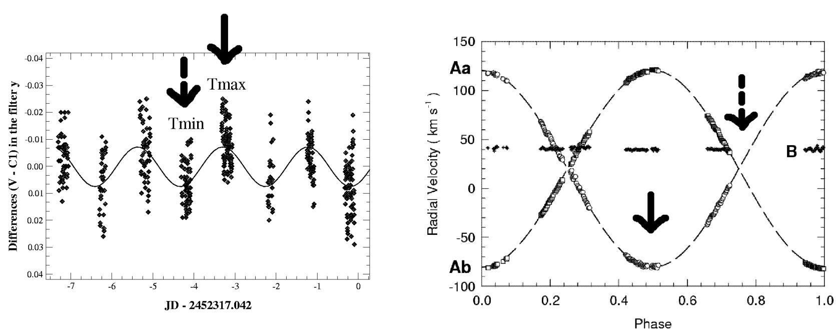

Fig. 1. Ellipsoidal variations (left panel) and radial velocity curves (right panel): arrows indicate the epochs T_{max} and T_{min} corresponding to respectively maximal and minimal flux

the time-averaged spectrum of each component as well as the relative radial velocities at the various epochs (for more details on this technique, see Hensberge, these proceedings). Analysis of the chemical composition of the time-averaged component spectra showed that both components of the inner pair are mild metallic-lined A-type (Am) stars while the time-averaged spectrum of component B didn't present any peculiarity [3].

2.2 The Outer Binary AB

The outer system is a visual binary with components A and B. At the phases of nodal crossing of the inner orbit the lines of all three components are detectable in the spectra. This allowed previous investigators to derive radial velocities for the individual components. Early 2003, significant and abrupt changes in radial velocity, $\mathrm{Vrad}_{Aa,Ab}$ and Vrad_B, were detected when compared to those obtained over the previous decades [8, 9]. The wide binary was also monitored by means of micrometric observations since 1935 and by speckle-interferometric observations since 1976. A complete set of orbital elements was first reported by Frémat et al. [3]: their combined astrometric-spectroscopic analysis revealed an orbital period of the order of 100 yrs and an eccentricity of about 0.9.

Moreover, a recent photometric study allowed the detection and precise determination of at least four pulsation frequencies of type δ Scuti in a narrow range of values, proving that at least one component in the triple system must be a δ Scuti pulsator [4]. Frémat et al. [3], using the disentangled component spectra, reported the existence of line-profile variations in the time-series spectra of the distant and chemically normal companion with time-scales of the same order as the pulsation-related ones found in the photometric study. Their Fig. 10 illustrates the residuals of the time-series KOREL spectra acquired during four consecutive nights.

Table 1 lists the stellar parameters which were determined by fitting synthetic spectra based on Kurucz models (ATLAS9) to the disentangled component spectra. Note the different projected rotation velocity of components Aa and Ab. This can arise because of incomplete synchronization, a difference in radii, a different inclination, as well as by any combination of these factors. In the case of complete spin-orbit synchronization, we expect a synchronous velocity of 36 ± 6 km/s for stellar radii of 3.0 ± 0.2 $R_\odot$.

Table 1. Derived stellar parameters (from [3])

Star	**Aa**	**Ab**	**B**
T_{eff} (K)	7470±220	7390±220	7590±220
V sin i (km s^{-1})	42±2	28±2	31±3
Rel. flux (%)	32±2	31±2	37±2
log g	3.8±0.14	3.8±0.14	3.8±0.12

3 New Orbital Solutions and Dynamical Mass

3.1 The Astrometric and Combined Orbits

The previous orbital solution shows large errors on several orbital elements due to a lack of data at the crucial orbital phase near periastron passage [3]. Furthermore, it fails to predict well the new speckle position obtained at epoch 2004.99 (i.e. after periastron passage) with the 6-m Russian BTA telescope. Using this datum, Docobo & Tamazian [11] derived a new orbit based on all astrometric data known to-date.

Table 2. Orbital elements and system mass

Orbital element	(1) Docobo [13]	(2) Pourbaix [12]
P (yr)	100.8 ± 1.5	113.1 ± 3.4
T	2000.5± 0.2	2000.3 ± 0.3
e	0.867 ± 0.007	0.887 ± 0.008
a ($''$)	0.195 ± 0.004	0.208 ± 0.006
i (°)	104.7 ± 0.5	107.5 ± 0.9
Ω (°)	29.4 ± 0.6	27.9 ± 1.3
ω (°)	335.3 ± 1.0	332.0 ± 4.1
V_0 (km/s)	-	27.0 ± 0.5
$\kappa = \frac{M_B}{M_A+M_B}$	-	0.36 ± 0.05
π_{dyn} ($''$)	-	4.77 ± 0.54
A (A.U.)	-	43.5 ± 6.1
mass A ($M_\odot$)	-	4.1 ± 1.5
mass B ($M_\odot$)	-	2.3 ± 0.7
K1 (km/s)	-	8.5 ± 1.1
K2 (km/s)	-	15.2 ± 1.7
System mass using π_{dyn} ($M_\odot$)	6.8 ± 2.4	6.4 ± 2.2

However, a combined astrometric-spectroscopic analysis leads to an independent determination of both distance and component masses. We therefore recomputed the orbit by combining all astrometric and spectroscopic data and by making use of the code VBSB2 which performs a global exploration of the parameter space followed by a simultaneous least-squares minimization [12].

Both astrometric and combined solutions with their corresponding standard errors are listed in Table 2 and graphically represented in Fig. 2. These solutions fit the observations well and show only tiny differences which is an indication of the remaining uncertainties. Note that the standard errors of many elements have drastically improved with respect to [3], as expected from the addition of a suitably phased speckle observation [10]. The large error on the mass of the visual components is mainly due to the relative error on the dynamical parallax. Since the error in fractional mass is much smaller, and $M_{Aa} = M_{Ab} > 2.1^{+0.2}_{-0.1}\ M_{\odot}$ [3], we conclude that $M_B > 2.0\ M_{\odot}$, which gives a useful lower limit on acceptable pulsation models (see [14]).

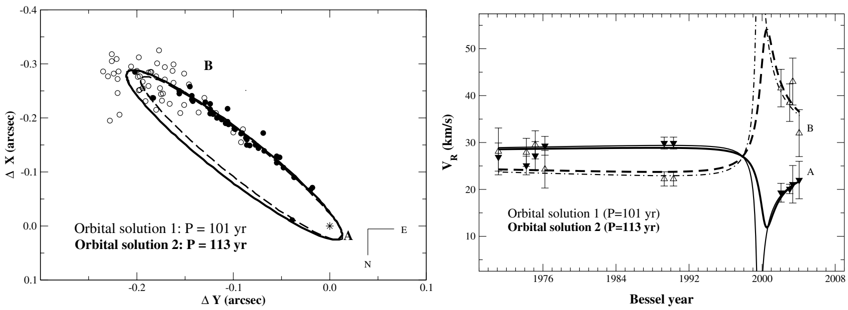

Fig. 2. Orbital solutions 1 (dashed/thin line) and 2 (solid/thick line) corresponding to astrometric (left panel) and spectroscopic (right panel) data

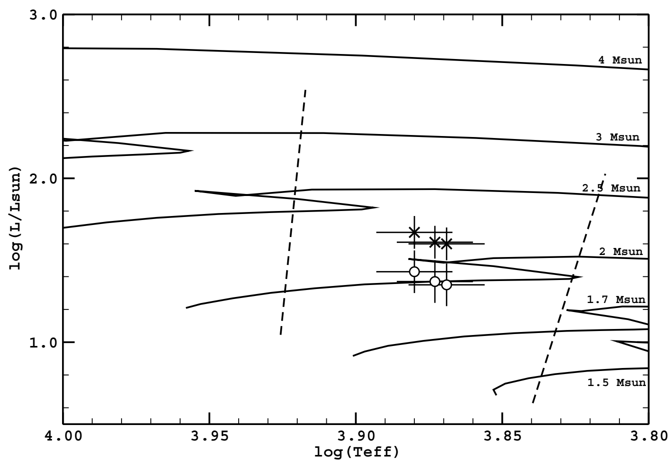

Fig. 3. Location of the components of DG Leo in the HR diagram. X-symbols are based on π_{dyn}. Blue lines denote the edges of the lower Cepheid instability strip. Allowed masses on theoretical evolutionary tracks correspond to a mass $> 2.0\ M_{\odot}$.

3.2 Dynamical Mass and Components' Location in the HR Diagram

The value of the dynamical parallax, though requiring further improvement, is consistent with a systemic mass of about 6 $M_\odot$ (Table 2), as expected from the derived component's physical properties. This also removes the marginal inconsistency that exists if the Hipparcos parallax (π_{Hip}=6.34 ± 0.94 mas [15]) is used (leading to a systemic mass of about 3 $M_\odot$). The difference between both values is at the 1.5 σ-level. Fig. 3 shows the location of DG Leo's components in the HR diagram using both parallaxes. We stress that the position inferred on the basis of π_{Hip} is only just compatible with the lowest acceptable limit for the component masses. For these various reasons we currently adopt a distance of 210 ± 24 pc, corresponding to the dynamical parallax reported in Table 2.

4 Conclusions

Significant progress on the long (resp. short)-period orbit of the wide (resp. close) binary can be achieved provided new speckle (resp. VLTI) data are obtained in a few years from now. As the angular separation of the wide pair is rapidly increasing from 0.05 in 2006 to 0.10″ in 2010, a 3 or 4-m telescope will soon be sufficient. The precise determination of both orbits will provide accurate masses for three A-type stars (including a chemically normal δ Scuti pulsator and 2 mild Am stars which do not seem to pulsate). This remarkable system will thus allow to gain new insights on the link between multiplicity, chemical composition (diffusion) and pulsation in this intriguing region of the HR diagram.

Acknowledgements

The authors thank Dr. Mason for supplying the astrometric data of DG Leo from the Washington Double Star Catalog of Observations and Dr. Pourbaix for providing the VBSB2 code. Financial support by the Belgian Science Policy is gratefully acknowledged (IAP P5/36).

References

1. Lampens, P. & Boffin, H. 2000, In: *Delta Scuti and Related Stars: A Reference Handbook*, ASP Conf. Ser. **210**, eds. M. Breger & M.H. Montgomery, 309
2. Landstreet, J.D. 2004, In: *The A-star puzzle*, Proceedings of IAU Symp. **224**, eds. J., Zverko, J., Žižňowskí, S.J. Adelman & W.W. Weiss, 423

3. Frémat, Y., Lampens, P. & Hensberge, H. 2005, MNRAS **356**, 545
4. Lampens, P., Frémat, Y. et al. 2005, A&A **438**, 201
5. Wilson, R. E. 1994, IAPPP Communications, spring 1994
6. Zahn, J.-P. 1977, A&A **57**, 383
7. Hadrava, P. 1995, AAS **114**, 393
8. Fekel, F. C. & Bopp, B. W. 1977, PASP **89**, 216
9. Rosvick, J. M. & Scarfe, C. D. 1991, PASP **103**, 628
10. Lampens, P. & Frémat, Y. 2005, ASP Conf. Ser. **338**, eds. K. Seidelmann & A. Monet, 276
11. Docobo, J.A. & Tamazian, V. 2005, IAUDS **157**, 1
12. Pourbaix, D. 1998, AAS **131**, 377
13. Docobo, J.A. 1985, Cel. Mech. **36**, 143
14. Grigahcène, A., Suárez, J.C. et al., 2005, In: *Tidal Evolution and Oscillations in Binary Stars*, ASP Conf. Ser. **333**, eds. A. Claret, A. Giménez & J.-P. Zahn
15. ESA 1997, The Hipparcos and Tycho Catalogues ESA-SP 1200

A Spectroscopic Study of HD 208905

Pavel Koubský[1], Simone Daflon[2], Petr Hadrava[1], Katia Cunha[2,3], Jiří Kubát[1], Dana Korčáková[1], Petr Škoda[1], Miroslav Šlechta[1], Viktor Votruba[1], Verne V. Smith[3] and Dimitri Bizyaev[3]

[1] Astronomical Institute AV ČR, 251 65 Ondřejov, Czech Republic
koubsky@sunstel.asu.cas.cz
[2] Observatório Nacional, CEP 20921-400, Rio de Janeiro-RJ, Brazil
[3] National Optical Astronomical Observatory, Tucson, AZ 85726, USA

1 Introduction

HD 208905 (SAO 19758, ADS 15466 AB, CCDM J21573+6118 AB) is a multiple system in the Cep OB2 association, (V=7.0, B1V, $B-V$=0.09, $U-B$=-0.74). The spectrum is composite showing triple absorption profiles. Based on the observed line-strengths, all the three components are believed to be early-type stars. Numerous astrometric measurements, both classical and speckle-interferometrical, can be found in the literature. These data clearly show two components, AB, separated by 300 to 400 mas. On the other hand, only very few RV data were published. Daflon in [1] presented a preliminary study of radial velocities of HD 208905 suggesting variations with a period between 13 and 27 days. Here we report new results of the RV measurements on spectra taken at McDonald, Ondřejov and Palomar Observatories from 1991 till 2005. The first orbital solution for the close pair was obtained. Twenty one spectra were successfully decomposed into three components through the use of the spectral disentangling code KOREL.

2 Spectroscopy

First observations of HD 208905 used in this study were obtained in 1991 when an echelle spectrum was secured with the 60-inch telescope at Palomar Mountain. Observations continued from 1993 till 2003 with the 2.1-m and 2.7-m telescopes at McDonald Observatory. At Ondřejov, observations started in 2003 with the 2.0-m telescope. With one exception, the spectra taken at two American observatories are from echelle spectrographs, while the Ondřejov data were secured with a classical coudé spectrograph, imaging the Hα and He I 6678 Å region on a SITe 2000 x 800-px chip. Altogether 46 spectra were used in this study. They were all measured for radial velocity. As already mentioned in the introduction, HD 208905 shows triple absorption profiles. Therefore, whenever possible, the positions of individual components were determined. The velocities of the strongest component of He I 6678 Å line measured on 21 Ondřejov spectrograms were analyzed with the PDM code [8].

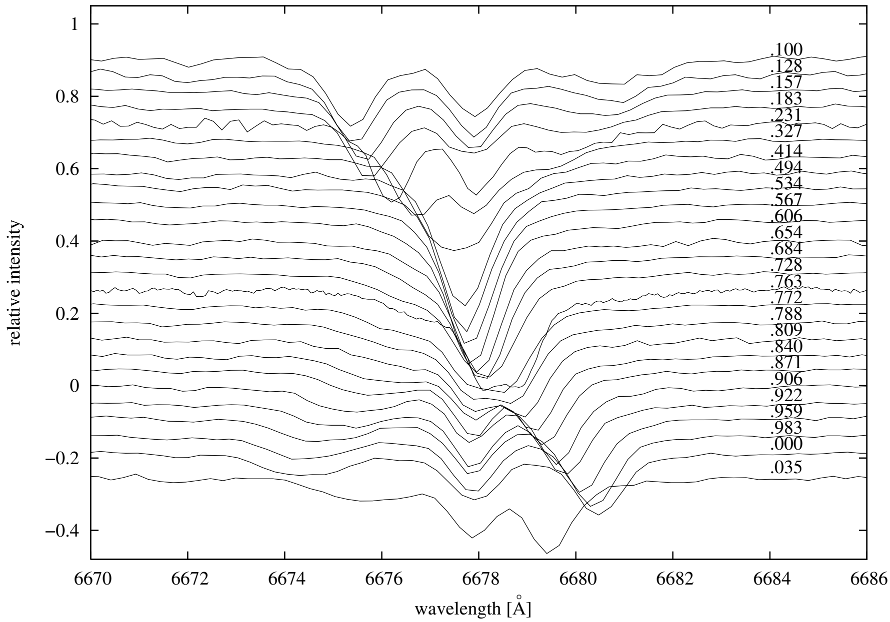

Fig. 1. Montage of helium profiles in the spectrum of HD 208905 folded with the period P=25.6606 days. Phase is shown on the right. Note the abrupt change of the profiles between phases 0.000 (maximum velocity of primary component), 0.035 and 0.100 due to high eccentricity of the orbit

A 25.7-day period was found. In Fig. 1 we show the variation of the He I 6678 Å line with the phase of the period from Table 1. Two components, Aa and Ab, one sharp and the other shallow, clearly move in anti-phase of the 25.7-day period, while the third B, also sharp, has either a constant velocity or is moving very slowly. We therefore decided to determine a preliminary orbital solution for the system A.

Table 1. Orbital elements of HD 208905

P (d)	25.66060 $\pm$0.00027
$T_{\mathrm{periastron}}$ J.D.	48542.73 $\pm$0.10
e	0.684 $\pm$0.013
ω (deg)	84.53 $\pm$1.32
K_1 (km.s^{-1})	114.34 $\pm$2.30
K_2 (km.s^{-1})	140.55 $\pm$2.99
γ (km.s^{-1})	-16.92 $\pm$0.93
rms (km.s^{-1})	7.799
Number of spectra	46

3 Orbital Solution

We combined 16 velocities from Palomar and McDonald spectra (based on metal lines) with 30 velocities obtained at Ondřejov (based on the He I 6678 Å line). Using the code SPEL [5] we derived the orbital solution presented in Table 1.

Fig. 2 shows the corresponding radial velocity curve. It is clear that the velocities in phases, where the component separation is small, cannot be determined very reliably. We tried therefore to decompose the spectra using the KOREL code [4] for spectral disentangling. It was applied to 18 spectra taken at Ondřejov and 3 spectra taken at McDonald and Palomar Observatories. The profiles of individual components in He I 6678 Å line are presented in Fig. 3. The velocity of the third component determined by KOREL varied within few km.s^{-1} during the time span of the observations. It seems that its velocity has been constant or nearly constant over more than 5000 days. This might suggest a very long period for the pair AB. Interestingly enough, this pair has been observed and measured by many observers since 1930's [6]. In modern time, speckle interferometry measurements from 1980 [7] till 1994 [3] give separation of A and B between 400 and 420 mas and a position angle around 170 deg. The only measurement from 1997 [2] states slightly different

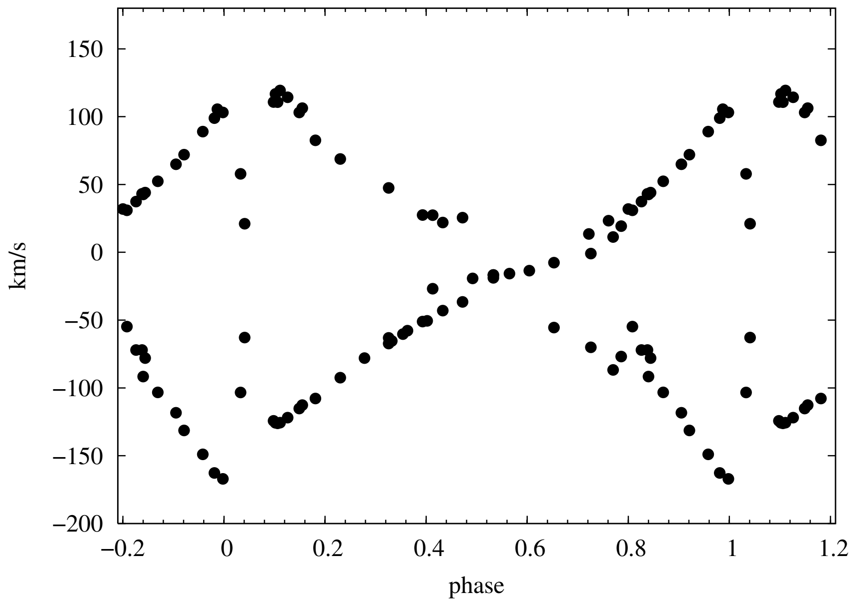

Fig. 2. Radial velocity curve of HD 208905 based on measurements of 46 spectra taken between 1991 and 2005. Velocities are phased with the period and RV max given in Table 1

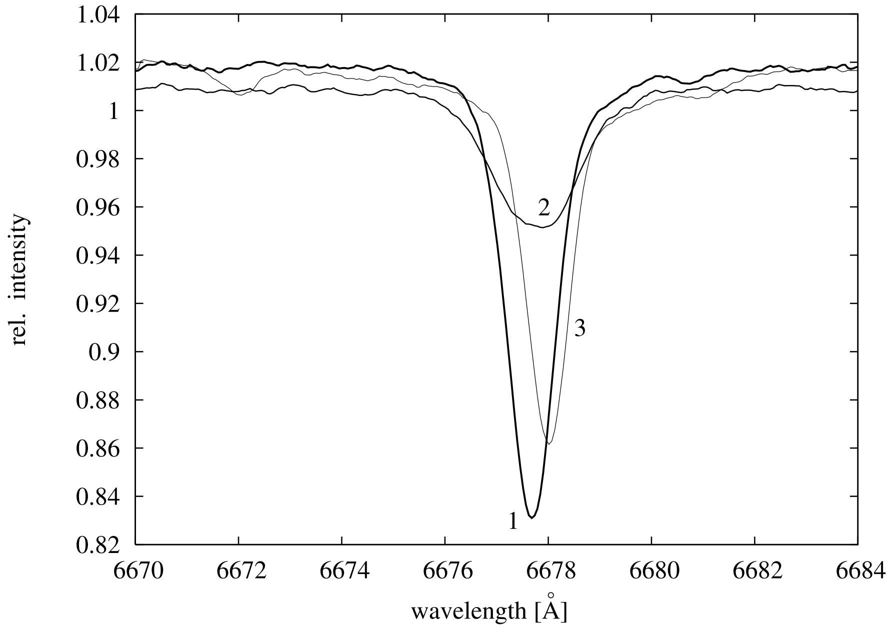

Fig. 3. Disentangled components of He I 6678 Å using KOREL code. The components of the close pair, 1 and 2, show small velocity shift, while the component 3 is shifted by about 15 km.s^{-1}

values (440 mas, 168 deg). One can thus speculate if the pair AB (CCDM J21573+6118) is not a mere coincidental pair.

4 Acknowledgments

Part of the study was supported by a grant GAČR 102/02/1000 of the Czech Science Foundation.

References

1. S. Daflon: Unpublished poster at a binary workshop, Dubrovnik, Croatia, October 20-24 (2003)
2. G.G. Douglas, B.D. Mason, M.E. Germain, C.E. Worley: AJ **118**, 1395 (1999)
3. M.E. Germain, G.G. Douglas, Ch.E. Worley: AJ **117**, 25, (1999)
4. P. Hadrava: Publications Astron. Institute No 91, 15 (2004)
5. J. Horn: PhD Thesis, Ondřejov (1977)
6. G.P. Kuiper: ApJS **6**, 1 (1961)
7. H.A. McAlister, W.I. Hartkopf, J.H. Hendry, B.G. Campbell, F.G. Fekel: ApJS **51**, 309 (1983)
8. R.F. Stellingwerf: ApJ **224**, 953 (1978)

The Suspected Binarity of the Nearby Flare Star Gl 424

V.S. Tamazian[1], J.A. Docobo[1] and Y.Y. Balega[2]

[1] Observatorio Astronómico Ramón María Aller, Avenida das Ciencias s/n, Santiago de Compostela, Spain oatamaz, oadoco@usc.es
[2] Special Astrophysical Observatory, N. Arkhyz, Karachai-Cherkasia 369167, Russia balega@sao.ru

Summary. A suspected $0.''132$ companion to the nearby flare star Gl 424 (=SZ UMa) was observed in the course of our speckle interferometry run with the 6m telescope of the SAO (Russia). The distance and magnitude difference ($\Delta V = 3.^m7$) suggest this companion to be a M 4.5 dwarf with a mass of 0.18 $M_\odot$. Rough estimates for the semi-major axis and the dynamical mass of the system lead to a possible orbital period of about 2.5 years. Should its binarity be confirmed, Gl 424 becomes an excellent target for obtaining an accurate orbit on a short time span.

1 Introduction

Multiplicity is an important parameter in the study of formation and dynamical evolution of stars and stellar systems. The largest part of their astrophysical interest is directly related with the knowledge of the binary (or multiple) character of the star.

The binary fraction is rather well determined for solar like stars [1] but much less constrained for M dwarfs. Investigations of a large sample of M dwarfs show its noticeable scatter from 42% [2] and 35% [3] to 26% [4] which are much less than the 57% obtained by Duquennoy and Mayor [1] for G dwarfs. Such a scatter is partly attributable to the uncertain completeness correction needed to account for the influence of the unresolved systems on the mass and luminosity functions.

The nearby flare stars represent an interesting sample almost exclusively comprising young M dwarfs which exhibit, as a rule, a high level of stellar activity [5]. The catalog of Pettersen [6] (limiting distance 25pc) slightly enlarged by [7] comprises 108 stars (23 visual binaries) whose occurrence in binary and multiple systems is not yet specifically studied in detail. The precise knowledge of their distance coupled with a good quality orbit allow to obtain an accurate dynamical mass estimate for these stars.

With the aim 1) to track the orbital motion in binary systems containing at least one flare star and 2) to search for new close companions, we routinely observe a number of flare stars with the speckle interferometry technique.

Gl 424 is a bright ($V = 9.56$) nearby flare star classified in [8] as M0V. It belongs to the handful of low activity flare stars exhibiting H_α in absorption

[9]. Abundant photometric data regarding this star can be found in [10]. No change in its radial velocity was detected in [11]. Using the Hipparcos parallax $\pi = 109.9$ mas, a distance $d = 9.10$ pc and a luminosity $M_V = 9.77$ are obtained for this star.

2 Observations

The speckle interferometric observations were carried out with the 6m telescope of the Special Astrophysical Observatory (Russia) with the speckle camera and an intensified 1280x1024 pix CCD coupled with a S-25 photocathode. Usually, this system allows to observe binary components as faint as $15.^m0$ in optical wavelengths with a dynamic range of about $4.^m0 - 5.^m0$. The diffraction limited resolution is about 22mas.

The relative position and magnitude difference Δm is derived from the ensemble averaged power spectrum. A double-slit pupil mask and interferometric binaries with slow orbital motion are used for calibration. More details regarding the observation and reduction procedure can be found in [12] and remain essentially unchanged.

Gl 424 was observed on December 28, 2004 and has shown a sign of a close companion at a distance $0.''132$ along the position angle $334.^\circ 0$. The estimated Δm in the red filter centered at 800nm is equal to $3.^m7$ which is close to the detection limit of the speckle camera.

A single previous speckle measurement of Gl 424 was performed at the 3.6m CFHT telescope in 1986 with null detection meaning that the separation at that epoch was less than $0.''04$ [13].

3 Binarity and a Rough Estimate of the Orbital Period

To estimate the probability of a chance projection, we applied criteria described in [14, 15] which lead to 1.8×10^{-6} and 9×10^{-7} respectively. Such a low probabilities indicate that the suspected companion should be physically bound to Gl 424. Hereafter, the primary and secondary components will be referred to as Gl 424A and Gl 424B.

Assuming the same distance for both components and taking into account the magnitude difference $\Delta m = 3.^m7$, we obtain $M_V = 13.^m47$ for Gl 424B. Its spectral type (ST) can be estimated through the relation

$$M_V = 0.101(ST)^2 + 0.596(ST) + 8.96 \quad \text{(Henry et al. 1994 [16])}$$

leading to a M4.5 dwarf.

Evidently, the observational data are insufficient to make any certain suggestion regarding the possible orbital motion. Nevertheless, under assumption

Table 1. Mass, semimajor axis and period estimates

Parameter	Henry et al. 1999	Delfosse et al. 2000
Gl 424A mass ($M_\odot$)	0.404	0.521
Gl 424B mass ($M_\odot$)	0.157	0.184
Mass sum ($M_\odot$)	0.561	0.705
a (AU)	1.513	1.513
P (yr)	2.48	2.21

of a physically bound system, one can make some rough estimates regarding the component's mass, semimajor axis of the orbit and, hence the orbital period – an important datum to be taken into account in future observations.

The mass μ (so designated to distinguish it from the luminosity) can be estimated through empirical relations:

$$\lg(\mu/\mu_\odot) = +0.005239 M_V^2 - 0.2326 M_V + 1.3785 \text{ (Henry et al. 1999 [17])}$$

$$\lg(\mu/\mu_\odot) = 10^{-3}[0.3 + 1.87 M_V + 7.614 M_V^2 - 1.698 M_V^3 + 0.060958 M_V^4]$$
(Delfosse et al. 2000 [18])

As can be seen from results given in the self-instructive Table 1, the mass sum is found within a range 0.56 – 0.70 $M_\odot$.

On the basis of the large samples of binary stars, in [1, 2, 19] several criteria to estimate the semimajor axis a on the basis of the observed angular projected separation ρ'' and parallax π'' were suggested. We followed the relation $a = 1.26\rho''/\pi''$ [2] derived specifically for M dwarfs and yielding $a = 0''.166 = 1.51$ AU for this given case. Then, the mass sum and Kepler's third law lead to an estimate for the orbital period which varies in a rather narrow range 2.2–2.5 yr (see Table 1).

It is worth noting that there are only four more nearby flare stars in visual binary systems with such short periods: HU Del (=AST 2, 1.5yr), V1054 Oph (=KUI 75, 1.7yr), EZ Aqr (=BLA 10, 2.2 yr) and CE Boo (FRT 1A-Ba, 2.4 yr), whereas the next is DT Vir with 14.5 yr.

Thus, should its binarity be confirmed, Gl 424 becomes an excellent target for obtaining an accurate orbit on a short time span. While further observations are feasible even with relatively small telescopes, due to the large magnitude difference between the components a dynamic range of the detecting instrumentation on the order of $5.^m0$ should be an essential requirement.

The increasing number of such systems and a careful comparison of their dynamical and astrophysical properties will provide important clues to many topics concerning the origin, formation and evolution of stars and stellar systems.

References

1. A. Duquennoy, M. Mayor: A&A, **248**, 485 (1991)
2. D. F. Fischer, G. W. Marcy: ApJ, **396**, 178 (1992)
3. I. N. Reid, J. E. Gizis: AJ, **113**, 2246 (1997)
4. Ch. Leinert, T. Henry, A. Glindemann et al: A&A, **325**, 159 (1997)
5. B. R. Pettersen: A&A, **82**, 53 (1980)
6. B. R. Pettersen: MmSAI, **62**, 217 (1991)
7. A. Poveda, C. Allen, M. A. Herrera et al: A&A, **308**, 55 (1996)
8. I. N. Reid, S. L. Hawley, J. E. Gizis: AJ, **110**, 1838 (1995)
9. P. M. Panagi, P. B. Byrne, E. R. Houdebine: A&AS, **90**, 437 (1991)
10. S. K. Leggett: ApJS, **82**, 351 (1992)
11. B. R. Pettersen, R. F. Griffin: Observatory, **100**, 198 (1980)
12. I. I. Balega, Y. Y. Balega, K.-H. Hofmann et al: A&A, **385**, 87 (2002)
13. A. Blazit, D. Bonneau, R. Foy: A&AS, **71**, 57 (1987)
14. J. N. Bahcall, R. M. Soneira: ApJ, **246**, 122 (1981)
15. N. Siegler, L. M. Close, E. E. Mamajek et al: ApJ, **598**, 1265 (2003)
16. T. J. Henry, J. D. Kirkpatrick, D. A. Simons: AJ, **108**, 1437 (1994)
17. T. J. Henry, O. G. Franz, L. H. Wasserman et al: ApJ, **512**, 864 (1999)
18. X. Delfosse, T. Forveille, D. Segransan et al: A&A, **364**, 217 (2000)
19. H. A. Abt, S. G. Levy: ApJS, **30**, 273 (1976)

The Ecology of Dense Star Clusters with Binaries

Simon F. Portegies Zwart

Astronomical Institute 'Anton Pannekoek' and Section Computational Science, University of Amsterdam, Kruislaan 403, 1098SJ Amsterdam, the Netherlands
spz@science.uva.nl

Summary. We study the first 100 Myr of the evolution of isolated star clusters with 117965 single stars and 13107 primordial hard binaries. Our calculations include stellar and binary evolution. The early evolution of these clusters can be characterized by three distinct phases, which we dubbed **A**, **B** and **C**. Here phase **A** lasts for the first ~ 3 Myr and is dominated by two-body relaxation, phase **B** lasts to about 20–100 Myr and is dominated by stellar mass loss, after that phase **C** sets in, which again is dominated by two-body relaxation. The presence of the primordial binaries has little effect on these various stages, nor on the other conclusions we draw here. The mass function of the main-sequence stars in the core becomes as flat as $x = -1.8$ (initial Salpter was $x = -2.35$), and in the outer 10% (by mass) of the cluster the mass function exponent is as steep as $x = -2.6$. Over the lifetime of the star cluster, a large number of stellar-mass black holes and neutron stars are formed. Roughly 50%–70% of the black holes are retained by the clusters, whereas the neutron star retention fraction is about 7%–12%. A relatively large fraction of black holes become members of a binary either with another black hole ($\sim 40\%$) or with another stellar companion ($\sim 50\%$). We conclude that in young (but $\gtrsim 50$ Myr) star clusters the X-ray binaries with a black hole may outnumber those with a neutron star by about a factor of 3.

1 Introduction

The early evolution of dense clusters of stars is of considerable interest, in part to develop a better understanding of the conditions under which star clusters are born, and in part to be able to identify the dynamical state of observable star clusters. The initial conditions of star clusters have been debated actively over the years, but no consensus has been reached either by studying or simulating the formation process of stellar conglomerates or from simulating or observing older systems. The main parameters which characterize a star cluster at birth (and any time later) are the richness, mass function, stellar velocity distribution, etc, all as a function of the three space coordinates.

Part of the problem comes from our static view of the universe, our inability to run simulations backward with time and our lack of understanding of the physics of the star(cluster) formation process. In this paper we take the approach of starting with a pre-selected set of initial conditions, based on observations, and compute the evolution of the star cluster.

2 Simulations

In this study we simulate young, $\leq 100\,\mathrm{Myr}$, star clusters by integrating the equations of motion of all stars and binaries. We use the Starlab environment [15], which acquires it's greatest speed on the GRAPE-6 special purpose computer (GRAvity PipE, [9, 10]). We use the hardware at the university of Tokyo, the MoDeStA[1] platform in Amsterdam and the GRAPE-6 setup at Drexel university for the calculations presented here.

The simulated star clusters are initialized by selecting the number of stars, stellar mass function, binary fraction and their orbital elements and the density profile. For our most concentrated model (simulation #1) we adopt the initial conditions derived by Portegies Zwart et al. [14] to mimic the 7-12 Myr old star cluster MGG-11 in the star-burst galaxy M82, which was observed in detail by McCrady et al [11]. In this paper, however, we extend the evolution of this model to about 100 Myr. Subsequent simulations are performed with larger cluster radius, resulting in longer initial relaxation times. The stellar evolution model adopted is based on [1], and the binaries are evolved with SeBa [16].

We summarize the selection of the initial conditions for simulation #1: first we selected 131072 stars distributed in a King [6] density profile with $W_0 = 12$ and with masses from a Salpeter initial mass function ($x = -2.35$) between $1\,M_\odot$ and $100\,M_\odot$. The total mass of the cluster is then $M \simeq 433000\,M_\odot$. The location in the cluster where the stars are born is not correlated with the stellar mass, i.e. there is no primordial mass segregation. Ten percent of the stars were randomly selected and provided with a companion (secondary) star with a mass between $1\,M_\odot$ and the mass of the selected (primary) star from a flat distribution. The binary parameters were selected as follows: first we chose a random binding energy between $E = 10\,\mathrm{kT}$ (corresponding to a maximum separation of about $1000\,R_\odot$). The maximum binding energy was selected such that the distance at pericenter exceeded four times the radius of the primary star. At the same time we select an orbital eccentricity from the thermal distribution. If the distance between the stars at pericenter is smaller than the sum of the stellar radii we select a new semi-major axis and eccentricity. If necessary, we repeat this step until the binary remains detached. As a result, binaries with short orbital periods are generally less eccentric. We ignored an external tidal field of the Galaxy, but stars are removed from the simulation if they are more than 60 initial half-mass radii away from the density center of the cluster.

For the other simulations #2, #3 and #4, we adopt the same realization of the initial stellar masses, position and velocities (in virial N-body units [5]) but with a different size and time scaling to the stellar evolution, such that the two-body relaxation time (t_{rh}) for simulation #2 is four times that of #1, for simulation #3 we used four times the two-body relaxation time of what was

[1] see `http://modesta.science.uva.nl`

Table 1. Conditions for the four runs performed with 144179 stars (including 10% primordial hard binaries) with a range of cluster radii. Density profiles are taken from King with $W_0 = 12$. The columns give the model name, the initial virial radius and core radius followed by the initial crossing time and half-mass relaxation time. The last column indicates the moment when core collapse happened in these simulations.

Run	$r_{\rm vir}$, pc	$r_{\rm core}$, pc	$t_{\rm ch}$, Myr	$t_{\rm rh}$, Myr	$t_{\rm cc}$ Myr
#1	1.27	0.010	0.032	80	40
#2	3.2	0.026	0.129	320	77
#3	8.1	0.066	0.516	1300	$\gtrsim 100$
#4	20	0.162	2.067	5100	$\gtrsim 100$

used for simulation #2, etc. the initial conditions are summarized in Tab. 1. The binary populations in the various initial realizations therefore have larger maxima to the orbital separation in the clusters with a longer relaxation time, because the adopted maximum binding energy of 10 kT shifts. For the simulations #2, #3 and #4, the maximum orbital separations are about $2000\,R_\odot$, $5000\,R_\odot$ and $10^4\,R_\odot$, respectively.

After initialization we synchronously calculate the evolution of the stars and binaries, and solve the equations of motion for the stars in the cluster. The calculations are continued to an age of about 100 Myr.

During the integration of simulation #2, the energy is conserved on average better than one part in $10^{7.1\pm1.7}$ per crossing time, with a total of $\sim 10^{-4}$ difference between the final and initial energy. For the other runs the energy is conserved at least an order of magnitude better.

Following the paper *Star Cluster Ecology VI* by Portegies Zwart, McMillan & Makino (in preparation, see also [13]), we divide the evolution of star clusters into four distinct phases, each of which is characterized by rather typical parameters. We call them phase **A**, **B**, **C** and phase **Z**. The four phases are classified as follows: phase **A** is an early relaxation dominated phase, followed by phase **B** in which the $\sim 1\%$ (by number) of the most massive stars quickly evolve and lose an appreciable fraction of their mass. Finally, phase **C** starts when stellar evolution slows down and two-body relaxation becomes dominant again. To complete this classification we introduce phase **Z** in which the cluster dissolves due to tidal stripping, but we will not discuss this phase in detail (see [7] for a more analytical approach to phase **Z**).

In Fig. 1 we present the evolution of the core radius, the 5%, 25%, 50% and 75% Lagrangian radii for simulation #2. The three phases of cluster evolution **A**, **B**, and **C** are indicated by the horizontal bar near the bottom

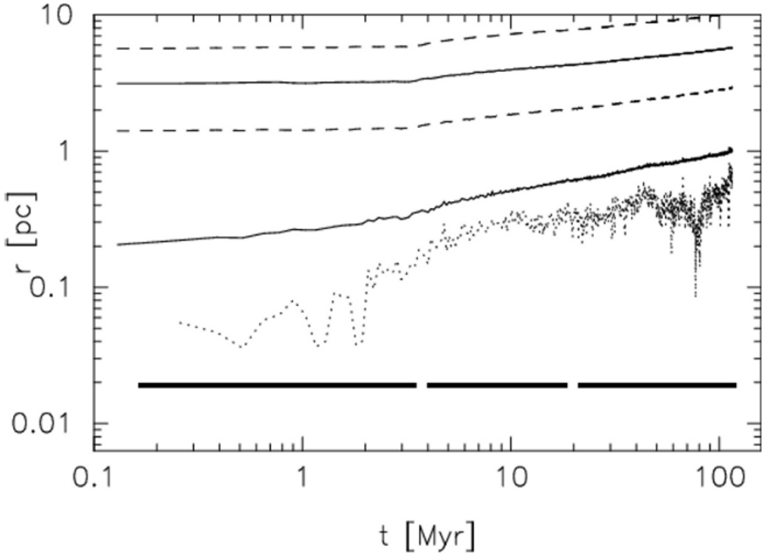

Fig. 1. Evolution of the core radius (dotted curve), 5% Lagrangian radius (lower solid), 25% (lower dashed line), half mass radius (upper solid) and 75% Lagrangian (upper dashed line) radii for the simulation #2. The areas for evolutionary phases **A**, **B**, and **C** are indicated with the three horizontal bars near the bottom of the plot.

of the figure. In phase **A** the cluster expands slowly followed by a more rapid expansion in phase **B**. This latter phase is mainly driven by stellar mass loss. During phase **C** the cluster re-collapses as relaxation processes start to dominate again over stellar mass loss. This leads to a collapse of the cluster core at an age of about 80 Myr.

3 Evolution of the Binding Energies

A seizable fraction of the total potential energy of the simulated star clusters is locked-up in primordial binaries. This energy can be released by dynamical encounters and by stellar evolution.

In Fig. 2 we present the evolution of the energy for simulation #3. The lower dashed line gives the total binding energy in the binaries in dimensionless N-body units [5]. Throughout the evolution of the cluster, this number remains smaller than the total potential energy (lower solid curve in Fig. 2).

The kinetic energy in simulation #3 in the early part ($\lesssim 50$ Myr) is governed by supernova remnants (neutron stars and black holes) which tend to receive high velocity kicks upon formation. Once these objects have escaped the cluster the curve flattens out. It is interesting to note that the cluster is, technically speaking, unbound in this early phase, but it remains bound as

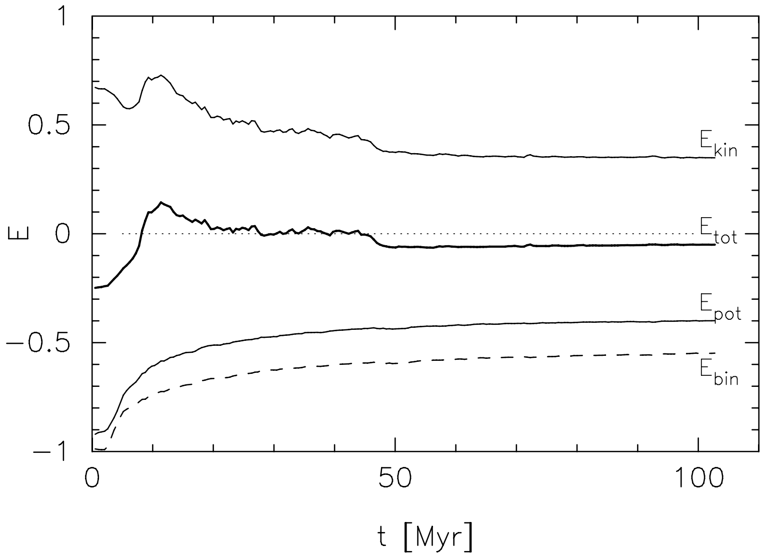

Fig. 2. Evolution of the kinetic, potential and total energy for the simulation #3. The dashed line gives the evolution of the binding energy of the binary population, which was subtracted from the potential and total energies. The dotted line, drawn to guide the eye, indicates regions where the total kinetic energy of the cluster exceeds the potential energy

most of this energy escapes the cluster without heating it effectively. Strictly speaking, this is a bookkeeping problem in the simulation, as one could wonder if a high-velocity neutron star should be counted as a member while it is still within the cluster perimeter but with a velocity exceeding the escape speed.

3.1 Evolution of the Mass Function

All simulations started with a Salpeter ($x = -2.35$) mass function. In due time the mass function changes – in part globally due to stellar evolution and selective evaporation, which is initiated by the dynamical evolution of the cluster. With time, the mass function also starts to vary locally due to mass segregation. It is hard to disentangle all effects and identify the relative importance of each. To qualify and quantify the changes to the global and local mass function we first select those stars which remain on the main sequence during the studied cluster evolution. The turn-off mass at 100 Myr in our stellar evolution model is about $4.63\,M_\odot$ and stars exceeding a mass of $5.54\,M_\odot$ have all turned into remnants. By limiting ourselves to main-sequence stars in this rather small mass range we guarantee that the mass function is not polluted by blue stragglers, giants or stellar remnants. Therefore we measure the mass function exponent for main-sequence stars between $1\,M_\odot$ and $4.5\,M_\odot$.

Throughout the evolution of our clusters, and irrespective of the cluster location, the mass function between $1\,M_\odot$ and $4.5\,M_\odot$ remains accurately represented by a power-law, which is another important motivation to adopt this seemingly arbitrary mass range.

In Fig. 3 we present the evolution of the slope of the cluster mass function between $1\,M_\odot$ and $4.5\,M_\odot$ for simulation #1. The exponent was calculated with a least-squares fit to the binned (100 bins) mass function in the appropriate range. The global mass function is fitted with a power-law to better than in 2%, for the 10% Lagrangian radii the fit is always better than 6%, consistent with the expected variation from the Poissonian noise. The various curves represent the mass function within (or outside) the 50%, 25% and 10% Lagrangian radii, for the dashed, dotted and dash-3-dotted curves respectively.

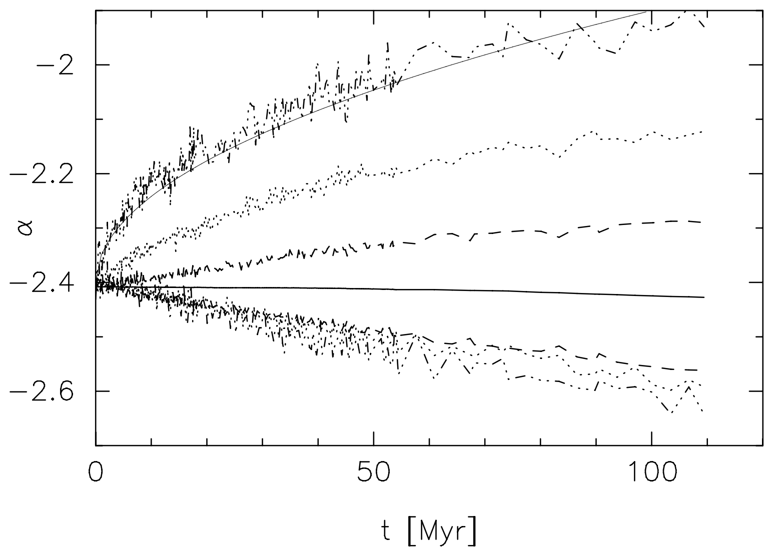

Fig. 3. Evolution of the power-law slope of the mass function of main-sequence stars between $1\,M_\odot$ and $4.5\,M_\odot$ for the run #1. The solid (almost) horizontal curve represents the entire cluster, the curves above (flatter mass function) are for the inner part of the cluster, the lower curves (steeper mass function) are for the outer parts outside the adopted Lagrangian radius. The dashed, dotted and dash-3-dotted curves give the mass function exponent for the stars withing (respectively, outside) the 50%, 25% and 10% Lagrangian radii. The thin solid line through the upper dash-3-dotted curve (mass function within the 10% Lagrangian radius) is calculated with $x \propto \sqrt{t}$ (see text). Note that after 55 Myr we increased the time interval between snapshot outputs from 1 Myr to 5 Myr.

The global mass function (solid curve) in the adopted mass range becomes slightly steeper with time, from $x \simeq -2.41$ at birth to about $x \simeq -2.43$ at an age of 100 Myr, for the simulation #1. The rate of change of the mass function exponent is $\dot{x} \simeq -2.7 \times 10^{-4}$ per Myr, and constant with time after 60 Myr. Similar trends in the global mass function are observed in the other models, though in these cases the changes in x are less regular and more noisy, therefore we decided to show the results for the simulation #1.

The steepening of the main-sequence mass function can be explained by dynamical activity in the cluster center, where relatively high-mass stars tend to be ejected from the cluster more frequently than lower-mass stars. It happens because the latter are not as abundant in the cluster core, and lower-mass stars are less frequently participating in strong dynamical encounters. The change of the global mass function is then mainly driven by strong dynamical encounters in the cluster core and not per se by selective evaporation near the tidal radius. The change in behavior around 60 Myr is caused by the formation of white dwarfs, which tend to compete with the $\sim 1\,M_\odot$ main-sequence stars. Neutron stars are not participating in this competition as the majority of these escape due to the high velocities they receive upon birth.

The mass functions for the outer 10%, 25% and 50% Lagrangian radii become steeper with time, with an exponent of $x \simeq -2.56$ for the outer 50% to $x \simeq -2.64$ for the outer 10% Lagrangian radius in simulation #1. The mass function in the inner parts of the cluster becomes flatter with time. Within the half-mass radius the mass function flattens to $x \simeq -2.3$ in about 100 Myr and for the inner 10% Lagrangian radius the mass function flattens to $x \simeq -1.9$.

The change in the mass function in the inner part of the cluster can be described with

$$x(t) = x(0) + \left(\frac{t}{\tau}\right)^{0.5}. \tag{1}$$

Here $x(0)$ in the initial power-law slope, and τ is a constant. For the inner 10% Lagrangian radius $\tau \sim 400$ Myr; $\tau \sim 1.2$ Gyr; for the inner 25% Lagrangian radius and $\tau \sim 10$ Gyr for the mass function within the half-mass radius. This expression is presented in Fig. 3 as the upper solid curve fitting the mass function in the inner 10% Lagrangian radius.

3.2 Black Hole and Neutron Star Retention

In Fig. 4 we present the stellar content of the simulation #2 for the entire cluster (solid curves) and inside the inner 10% Lagrangian radius (dotted curves). The fraction of main-sequence stars (below the lower solid curve) and binaries (above the top solid curve) gradually decrease with time, whereas the fraction of giants (between the lower and middle solid curve) and stellar remnants (between the middle and top solid curve) increases with time. The figure clarifies that at later age contribution of giants and stellar remnants is considerable, and that in particular the number of compact remnants continue to grow quite rapidly after about 50 Myr. This change in behavior, around 50 Myr, is mainly caused by the formation of white dwarfs, which quickly start to dominate the population of stellar remnants, whereas the fraction of evolved stars (giants) remains roughly constant. Note also that the binary fraction decreases slightly with time.

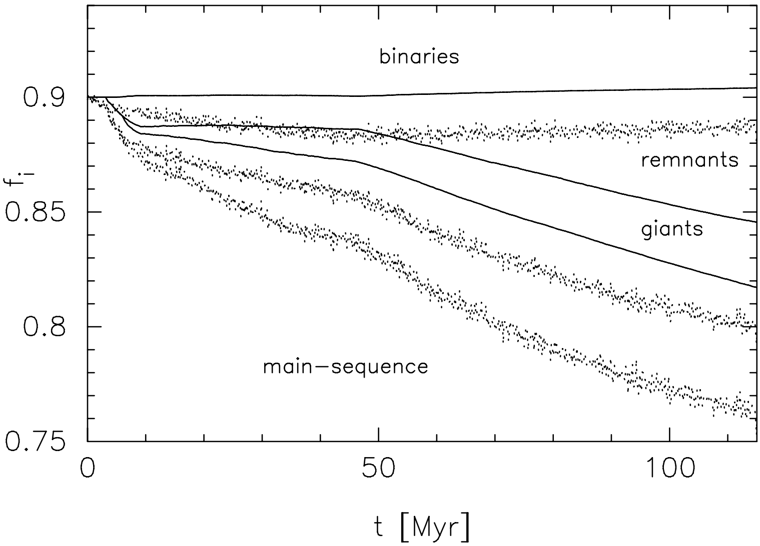

Fig. 4. The stellar content of the simulation #2 as a function of time, for the entire cluster (solid curves) and for the inner 10% Lagrangian radius (dotted curves). The lower lines give the fractional contents of main-sequence stars, followed by the evolved stars (giants) and compact objects (remnants). The top area indicates that the binary fraction reduces only slightly from it initial value of 0.1 throughout the simulation. All fractions add-up to 1

In our simulations, black holes and neutron stars receive kicks upon formation. Neutron star kicks are selected from the Paczynski velocity distribution with a dispersion of $\sigma_{\rm kick} = 300\,{\rm km\ s}^{-1}$ [4], whereas a black hole of mass $m_{\rm bh}$ receives a kick from the same distribution but smaller by a factor of $1.4\,M_\odot/m_{\rm bh}$.

In each run about 1700 black holes were formed in type Ic supernovae, and 6500 neutron stars were formed in type Ib and type II supernovae. Though the initial realizations for the various runs were identical the numbers of supernovae differ slightly from run to run, with more supernovae occurring in the larger (lower-density) clusters. This is mainly caused by selective evaporation of massive stars and by variations in binary evolution. Massive stars are preferentially ejected in strong dynamical encounters, which are more common in the denser clusters. These clusters are also more prone to binary evolution, as the orbital periods are on average shorter.

The retention fraction for black holes varies between 0.48 and 0.71, for neutron stars this fraction is between 0.065 and 0.12. The difference between the lowest and highest retention fractions is about a factor of two. In both cases, more compact objects are retained in the denser clusters. This is a direct consequence of the larger escape speed of the denser clusters, through which fewer black holes and neutron star are able to escape.

A seizable fraction of the compact objects remain in binaries. While initially 10% of the stars were binary members, about 4% of the compact objects are ultimately binary members, which is a rather large fraction considering relatively small ($\lesssim$ 10%) retention fraction.

The majority of the binaries consisting of a compact object with a stellar companion (indicated by $\star$ in Table 2) will turn into X-ray binaries at some moment in time. Such binaries with a black hole outnumber those with a neutron star by about a factor of 2 to 4. Based on these numbers, we conclude that in star clusters which are old enough to have produced most of their black holes and neutron stars, the population of X-ray binaries with a black hole outnumbers those with a neutron star by a factor of 2–4. Such clusters would then be very interesting objects for further X-ray studies. Note, however, that the choice of a lower limit of $1\,M_\odot$ for the initial mass function tends to boost the number of black holes and neutron stars, and the production of black-hole X-ray binaries will be less efficient in star clusters with a lower cut-off to the mass function.

Even though binary black holes are quite common in our simulations, they generally have rather wide orbits. This has the interesting consequences that these binaries will experience Roche-lobe overflow when the stellar companion is a giant, resulting in a rather short but bright X-ray phase. On the other hand, these binaries are not candidates for ground-based gravitational wave detectors. Binaries with two neutron stars have difficulty to survive; none were formed in any of our simulations.

Table 2. Some characteristics of the compact objects at 100 Myr (see text)

Run	$N_{\rm Ic}$	$N_{\rm Ib+II}$	$N_{\rm bh}$	$N_{\rm ns}$	(bh,bh)	(bh,ns)	(ns,ns)	(bh,$\star$)	(ns,$\star$)
#1	1656	6584	1017	585	12	1	0	15	6
#2	1710	6446	1028	553	16	4	0	21	6
#3	1717	6387	834	365	17	2	0	20	3
#4	1728	6735	828	436	11	4	0	16	10

In Fig. 5 we present the number of binaries with at least one compact object (black hole, neutron star or white dwarf) as a function of time. The number of black holes in binaries rises sharply shortly after the start of the simulation with a peak near 8 Myr. This is the moment when the turn-off drops below the minimum mass for forming black holes (at $\sim 20\,M_\odot$), and lower-mass stars form neutron stars. This is also visible in the sharp increase of the number of binaries with a neutron star. The number of black holes in binaries drops rapidly from this moment because many of their companions form neutron stars in a supernova explosion. These newly formed neutron stars receive a much higher asymmetric kick velocity during their formation [8] than black holes [3]. Note here that binary containing a neutron star and a black hole are counted twice, once among the (bh,$\star$) and once for (ns,$\star$).

The solid curves in the bottom panel of Fig. 5 show an interesting depression between about 75 Myr and 80 Myr. It appears that the binaries with a white dwarf located within $2\,r_{\rm core}$ become depleted. This is not really the case, but rather the cluster experiences a phase of core collapse. This may not be so surprising at first, if one imagines that core collapse tend to happen in about 15%–20% of the half-mass relaxation time [12]. For this cluster, the half-mass relaxation time is about 440 Myr and the core collapse is therefore expected at an age of about 65–85 Myr, which is consistent with the moment of core collapse in simulations without primordial binaries.

The moment of core collapse is therefore unaffected by the relatively rich population of hard primordial binaries in these simulations. We conclude that the primordial binary fraction and their distribution in hardness is relatively unimportant for the moment of core collapse. This result is contradicted by other Monte-Carlo simulations which tend to indicate that core collapse is strongly delayed by the presence of a rich binary fraction [2].

White dwarfs start to dominate the population of compact binaries after about 25 Myr, at a turn-off mass of about $10\,M_\odot$. Stars of $\lesssim 8\,M_\odot$ which evolve in isolation, unperturbed from a companion star, turn into white dwarfs, but in a binary system early stripping of the hydrogen envelope may cause a more massive star to become a white dwarf instead of collapsing to a neutron star. The population of compact binaries in clusters older than about 40 Myr is dominated by white dwarfs. But it may take a long while before they also become more common than the primordial main-sequence binaries.

Acknowledgments

I am grateful to Steve McMillan, Jun Makino, Piet Hut and Holger Baumgardt for numerous discussions. I am also grateful to Tokyo University for the use of their GRAPE-6 hardware. This work was supported by NWO (via grant #630.000.001), NOVA, the KNAW and the LKBF. The MoDeStA computer in Amsterdam was used extensively for this work.

a) **b)**

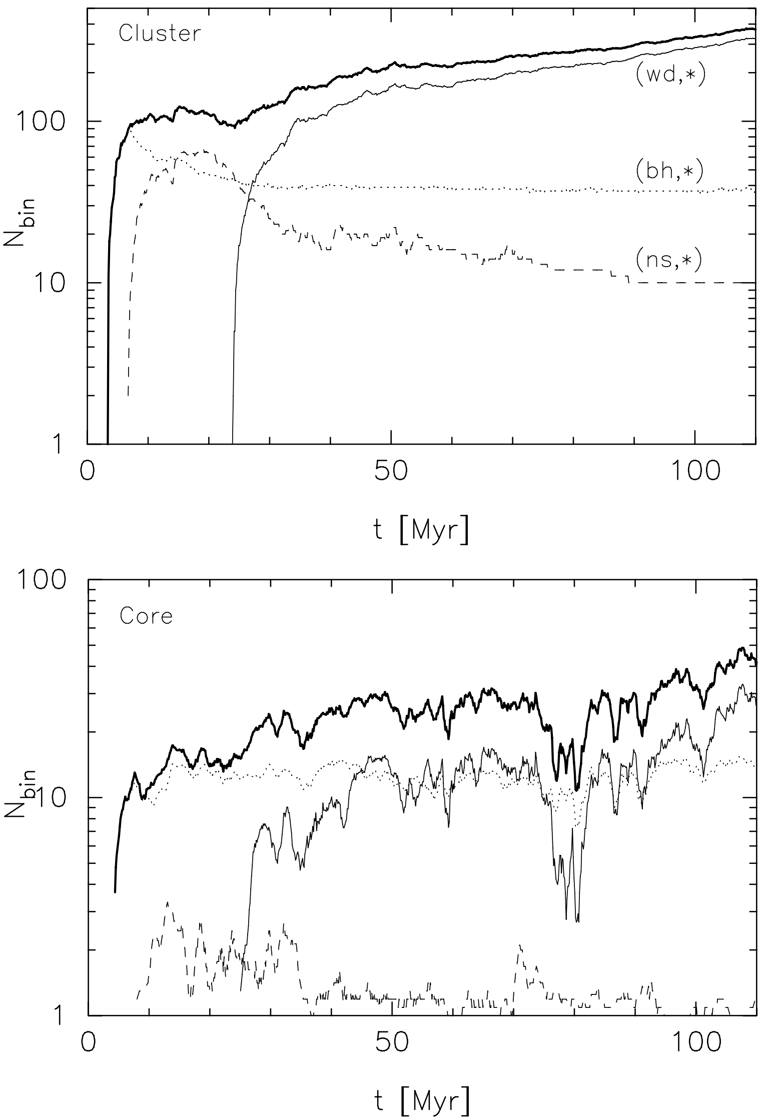

Fig. 5. The number of binaries with a compact object as a function of time for run #2. The top panel (a) gives numbers for the entire cluster, and the bottom panel (b) – within $2r_{\mathrm{core}}$. The top (thick solid) curve gives the total number of binaries with at least one compact object (bh, ns or wd). The thin solid curve gives the number of binaries with one white dwarf, the dashed curve is for neutron stars and the dotted curve for binaries with at least one black hole. Note that binaries with two compact objects are counted twice in this statistics and, as a consequence, the total of thin curves does not add-up to the thick curve.

References

1. P.P. Eggleton, M.J. Fitchett, C.A. Tout: ApJ, **347**, 998 (1989)
2. J. M. Fregeau, M.A. Gürkan, K.J. Joshi, & F. Rasio, ApJ, **593**, 772 (2003)
3. A. Gualandris, M. Colpi, S.F. Portegies Zwart, & A. Possenti, ApJ, **618**, 845 (2005)
4. J.W. Hartman, A&A **322**, 127 (1997)
5. D.C. Heggie, R. Mathieu: in: P. Hut, S. McMillan (eds.), Lecture Not. Phys. **267**, Springer-Verlag, Berlin (1986)
6. I.R. King: AJ, **71**, 64 (1966)
7. H.J.G.L.M. Lamers, M. Gieles, S.F. Portegies Zwart: A&A, **429**, 173 (2005)
8. A. G. Lyne, & D.R. Lorimer, Nature, **369**, 127 (1994)
9. J. Makino, T. Fukushige, M. Koga, K. Namura: PASJ, **55**, 1163 (2003)
10. J. Makino, M. Taiji, T. Ebisuzaki, D. Sugimoto: ApJ, **480**, 432 (1997)
11. N. McCrady, A.M. Gilbert, J.R. Graham: ApJ, **596**, 240 (2003)
12. S.L.W. McMillan, & S.F. Portegies Zwart, ApJ, **596**, 314 (2003)
13. S.F. Portegies Zwart: Book of the Como School of Physics, *Joint Evolution of Black Holes and Galaxies*, Graduate School in Contemporary Relativity and Gravitational Physics (2004)
14. S.F. Portegies Zwart, H. Baumgardt, P. Hut, J. Makino, S.L.W. McMillan: Nature, **428**, 724 (2004)
15. S.F. Portegies Zwart, S.L.W. McMillan, P. Hut, J. Makino: MNRAS, **321**, 199 (2001)
16. S.F. Portegies Zwart, F. Verbunt: A&A, **309**, 179 (1996)

The Formation of Multiple Stars

Eduardo J. Delgado-Donate[1] and Cathie J. Clarke[2]

[1] Stockholm Observatory, AlbaNova University Centre, 106 91 Stockholm, Sweden edelgado@astro.su.se

[2] Institute of Astronomy, University of Cambridge, Madingley Road, Cambridge CB3 0HA, UK cclarke@ast.cam.ac.uk

Summary. We have undertaken a series of SPH hydrodynamic + N-body simulations in order to explore the multiplicity properties of young stars. We find that binary and multiple stars are a natural outcome of collapsing turbulent flows, with a high incidence of $N > 2$ systems, specially among the higher mass objects. We find a positive correlation of multiplicity with primary mass and a companion frequency that decreases with age, during the first few Myr after formation, in accordance with observations. Binary brown dwarfs are rarely formed, in conflict with observational lower limits of 15%. Brown dwarfs as companions are predominantly found orbiting binaries or triples at large distances; thus we reproduce the so-called brown dwarf desert at short separations. The velocity dispersion for singles is found to be slightly larger, on average, than that of multiples. One caveat of these and previous models, namely the paucity of low mass ratio binaries, has been addressed with additional calculations. We tentatively conclude that their formation is intricately related to an appropriate selection of initial conditions and an accurate modelling of disc accretion and fragmentation.

1 Introduction

Most stars are known to be members of binary or even higher-order multiple systems [19, 21]. Among high-mass stars, the multiplicity fraction (MF) is very close to 100%. For lower mass stars, MF is somewhat lower [21, 24], but still high. The multiplicity properties of brown dwarfs are not so well constrained (see different contributions in this volume), but the lowest bound for MF is believed to be 15% [13,35]. Thus, any good star formation theory must be a theory of (at least) binary star formation. Currently we can hope to do more theoretically speaking than produce multiple stars by imposing some multi-armed instability on a collapsing core (see [36], and references therein, for a review of different binary formation mechanisms). Turbulent initial conditions, for example, allow star formation to be triggered in a less predictable way, e.g. [9, 27, 28]. In addition, it has become computationally affordable to study the statistics of star pairing beyond pure N-body integration [16]. These two steps forward have made it possible to perform calculations which both resolve the fragmentation and collapse of molecular clouds and produce a statistically significant number of stellar systems, thus opening the door to a direct comparison with observations [9, 17, 18]. In this paper we review the results from the first hydrodynamic calculations to produce a statistically significant number of *stable* multiple systems in the separation range $1 - 1000$ AU. We will concentrate our attention mostly on those aspects pertaining to the multiplicity properties of low-mass stars, and the formation mechanism of low mass ratio binaries.

2 Episode I: The Gas Menace

For some time, numerical models with predictive power about the multiplicity properties of stars (e.g. multiplicity fractions, mass ratio, semi-major axis distributions) had to rely on pure N-body integration [22, 42, 43]. The masses, location and velocities of the stars were selected at the outset, and subsequently the orbital evolution was calculated. This treatment of multiple star 'formation' was necessary, as the computational expense and complexities involved in the modelling of gas fragmentation, collapse and accretion were too demanding. Even today, N-body models still constitute a useful tool to study the dynamical evolution of star clusters, e.g. [32], or to constrain star formation models, [33], either when the gas content is negligible or because it is the only alternative to study large ensembles of protostars.

However, gas is a fundamental ingredient of the star formation process, not only during the fragmentation and collapse stage, but also during the embedded phase of the life of a star. This is so mainly because large amounts of dense gas accumulate in the form of accretion disks around the protostars and due to the larger scale influence of the gas background where the protostar is embedded. Disks provide a mechanism for the accretion of gas with high angular momentum – which can modify substantially the orbital parameters of a protobinary [2, 6, 39] – and a dissipative medium to alleviate the effect of dynamical encounters with other cluster members [37]. Besides, if sufficiently massive and able to cool efficiently [25, 34], disks can fragment, and in doing so, produce a second generation of objects. The background gas also has important effects, since it accounts for a significant fraction of the gravitational potential of a young cluster and, through the action of gravitational drag, can affect the mass evolution and motion of both single and multiple stars (and hence the binary pairing outcomes, cf. [10, 12, 16].

Early star formation models that included the effect of gas did so to study the formation of binary stars from clouds subject to some kind of specific initial instability (rotation beyond a critical limit, multi-armed spiral density perturbations; see review [41]. These models have been of great importance but a caveat remained: they produce a low number of objects in a more or less predictable fashion. Other models tried to take into account large numbers of stars embedded in a big gas cloud [11], e.g. by utilising point masses with the ability to accrete and interact with the gas and other stars ('sink particles', [5]), but once more, with positions and velocities selected at the outset. These models focused mostly on the study of the resulting initial mass function (IMF). The purely gas dynamical models had to be refined and taken to a larger scale, while the aim of point-masses-in-gas models had to shift to the study of the properties of multiple stars, if star formation models were to match the predictive power of N-body models. The earliest model to take such step was that by Bate and collaborators [9], who applied more general 'turbulent' initial conditions to a relatively large (for theory standards) 50 $M_\odot$ cloud and followed its fragmentation and collapse down to the opacity limit for fragmentation. For higher densities, pressure-supported objects were replaced by 'sink particles' and, thus, the simulation could be followed well beyond the formation of the first object. This calculation showed the power of the combination of more realistic initial conditions and a refined numerical scheme blending gas with N-body dynamics and, beyond any doubt, it meant a great leap forward in star formation studies; but, obviously, it had some shortcomings too. Among them was the high computational expense involved (even to this day) for just one calculation and the fact that the evolution of the cloud could not be followed for as long as it would be desirable in order to ensure that most multiple systems formed have attained stability. Thus, complementary calculations were necessary. We tried to fill this gap by performing simulations of smaller (5 $M_\odot$) clouds (see Section 3), to be run for longer during the gas-dominated stage, and to be followed as an N-body system until the stability of most of the systems could be guaranteed. These models posed a lower computational demand since each of them dealt with a single star forming 'core', and thus most of the gas within was involved in the star formation process and not 'hanging around' in low density regions as in Bate et al. 'multi-core' calculation. It was possible to perform 10 such calculations and, by applying different initial conditions to each of them, study the dependence of the resulting stellar properties on initial conditions. This aspect of the calculations, however, will not be addressed in this review. Rather, we will focus on the properties of the multiple systems.

2.1 Small-N Clusters

To start with, we will review some simple 'small-N cluster' models, which, though simple, give insight into some of the processes that affect multiple star formation in gas-rich calculations. These models were inspired by the work of Bonnell and collaborators [10, 11] who were the first to use 'sink particles' embedded in a uniform gas cloud as a first approach to study the formation of a large ensemble of stars ($N = 100$). Instead, we have considered systems with $N = 5$ protostars. The details of the numerical scheme (SPH) and initial and boundary conditions can be found in [16] (and in a different context in Sect. 3.1 below). It is enough to say that the 'sink particles' start with the same mass (1/20th of the initial cloud mass each) and are randomly positioned in phase space (with virial velocities on the average), the gas is critically Jeans-unstable and initially static and homogeneous, and remains isothermal throughout the calculation. The simulations are run until all the gas is accreted, then the stellar system is integrated as N-body until stability is attained.

2.2 A Dominant Binary

The 'seed' stars grow in mass by accretion and sink to the cluster centre through gas drag. In doing so, they bind to each other, forming a non-hierarchical multiple. Typically, a central binary comprising most of the mass forms. The other objects are ejected from the cloud or to large distances, where they cannot accrete much. Thus, if the cloud mass is low initially, the ejectae are likely to be substellar (this is one of the proposed formation mechanisms for brown dwarfs [8, 40]). Due to the dynamical decay, most of the binaries are close. The most important feature of the simulation is the *runaway formation of a massive binary*, which then dominates the cluster dynamics. As a result, other binary pairs are very unlikely to form and the other cluster members have comparatively low mass. *Binary pairing is therefore not random for the closest systems.* We will see that this feature is also common in simulations with more realistic initial conditions.

3 Episode II: Attack of the Turbulence

Molecular clouds are seen to display random motions that are typically described as 'turbulent'. Thus, it is a natural choice to impose a turbulent field as initial condition for the gas velocities. Turbulence also provides the seed for the generation of cloud sub-structure, which is subsequently amplified by gravity, leading to the 'dynamic' formation of stellar objects. The chaotic nature of turbulence guarantees that the protostars have an initial spatial distribution that cannot be predicted a priory. This property is welcome, as it decreases the ability of the modeller to pre-determine the outcome. In this section we present the setup and results from a series of 'turbulent' SPH simulations, which constitute the next step in refinement from the 'small-N cluster' simulations discussed before.

3.1 Numerical Scheme and Initial Conditions

We performed 10 calculations of small fragmenting gas clouds, using the SPH technique. Sink particles replace bound blobs after a critical densityis reached [5]. We apply standard viscosity with $\alpha = 1$ and $\beta = 2$, and a binary tree to find nearest neighbours and calculate self-gravity. The opacity limit for fragmentation is modelled using an equation of state $p \propto \rho^{\gamma}$, where the gas is isothermal at low densities ($\leq 10^{-13}$ g cm^{-3}) and polytropic with $\gamma = 5/3$ at higher densities.

Each cloud is initially spherical, has radius of $\approx 10^4$ AU, 5 $M_{\odot}$ and density and temperature of $\approx 10^{-18}$ g cm^{-3} and 10 K respectively. The initial Jeans mass is ≈ 0.5 $\mathrm{M}_{\odot}$. We use 100 SPH particles to resolve the minimum mass of few $\mathrm{M_J}$ that can occur in the calculation [7]), thus resulting in a total of 3.5×10^5 SPH particles.

We impose an initial random 'turbulent' velocity field, defined by a power-law spectrum. The values for the power-law exponent bracket the observed uncertainty in Larson's 'velocity-size' relation. The velocity field is normalised so that there is equipartition of kinetic and gravitational energy initially. We are imposing a parameterised initial velocity field which approximately reproduces observed bulk motions in molecular clouds (often described as 'turbulent' motions) but this term ('turbulence') should not be taken to imply that we are modeling what a fluid dynamicist would recognise as fully developed turbulence.

The hydro-dynamical calculations are run until ≈ 0.5 Myr. Thereafter the remaining gas is removed and the stellar system is evolved as a pure N-body system, using NBODY2 [1]. After 10 Myr we find that 95% of the multiples have decayed into stable configurations (using the criterion by Eggleton & Kiseleva [23]), and we stop the integration. The calculations produce 145 stars and brown dwarfs; 40% of the objects are substellar. The calculations have been performed using the United Kingdom Astrophysical Fluids Facility (UKAFF). Animations are available on request to the first author.

3.2 Triples and Higher-order Multiples

Our simulations produce a wealth of multiple systems. The multiplicity fraction at 0.5 Myr after the initiation of star formation is close to 100%. It is apparent that multiple star formation is a major channel for star formation in turbulent flows. The systems can adopt a variety of configurations, like binaries orbiting binaries or triples. Such exotic systems have been observed, and currently, the occurrence of high-order multiples is being revised upwards (15-25% of all systems, [44] and this volume) as large surveys and high-resolution techniques begin to expose the closer and wider companions.

3.3 Multiplicity as a Function of Age

The companion frequency decreases during the first few Myr of N-body evolution, as many of the multiples are unstable. The total companion frequency decays from ≈ 1 to ≈ 0.3. This internal decay affects mostly low-mass outliers, which are released in vast amounts to the field. We expect that in a real cluster the multiplicity would drop even further as star forming cores do not form in isolation but close to one another. Some of our binaries orbiting binaries might not have survived in a more realistic environment. The predicted decrease in the multiplicity frequency has been quantitatively observed by Duchêne et al. [20]. In less dense star forming environments, such as associations or moving groups, we expect that dynamical interactions among different cores should not be that important and that many ejected low-mass objects should have been able to leave the group early on. Therefore the observed companion frequency should, on average, be larger than in dense clusters (notice e.g. the high companion frequencies found among members of the TW Hydrae and MBM 12 associations [14]).

3.4 Multiplicity as a Function of Primary Mass

We find a positive dependence of the multiplicity fraction on primary mass (see Fig. 3 in [17]), in qualitative agreement with observations. This dependence can also be illustrated by a direct comparison with the infrared colour-magnitude diagram of the 600 Myr old Praesepe cluster (Fig. 1). The cluster was observed by Hodgkin et al. [30]; the masses of simulated stars were converted to magnitudes using the tracks by Baraffe et al. [3]. Binaries with less than 200 AU separation are considered as unresolved.

Two features from Fig. 1 are worth noting: first, the simulated cluster shows a binary sequence whose width is comparable to that of the Praesepe, except for systems redder than $I - K = 2.5$. This seems to suggest that the formation of a significant number of triples, quadruples, etc. may indeed be common in real clusters. Second, although our binary fraction for G stars is in agreement with observations, our models fail to produce as many low-mass binaries as observed. For example, a binary fraction of at least 15% is seen among brown dwarfs, e.g. [13, 35], although values as high as $30 - 40\%$ have been predicted [38] (but see [31]).

3.5 Bound Brown Dwarfs

During the first few $\times 10^5$ yr most brown dwarfs are locked in multiple systems, often orbiting a binary or triple in eccentric orbits at large separations. Most of these systems are unstable and decay in a few Myr, releasing individual brown dwarfs to the field. Only a few substellar objects survive as bound to stars. Of these, the majority orbit a binary or triple at distances

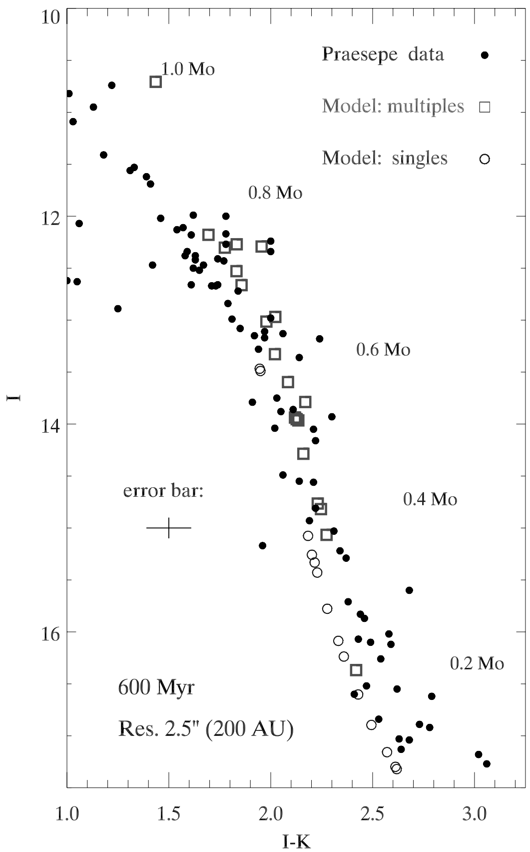

Fig. 1. Colour-magnitude diagram (I vs $I - K$) for the Praesepe cluster, with our results superimposed. Binaries closer than 200 AU are considered as unresolved

greater than 100 AU. One case out of 4 consists of a brown dwarf orbiting an M star at 10 AU. Our results are in agreement with the observed brown dwarf desert at very small separations. However, more than a dozen substellar companions to stars at wide separations are known [26]. According to our results, we would expect that a large fraction of the primaries in these wide systems should turn out, in closer examination, to be $N \geq 2$ multiples.

3.6 Velocity Dispersion

Single and binary stars attain comparable velocities in the range $1{-}10\ \mathrm{km\ s^{-1}}$. Higher-order multiples display lower velocity dispersions (Fig. 2). This kine-

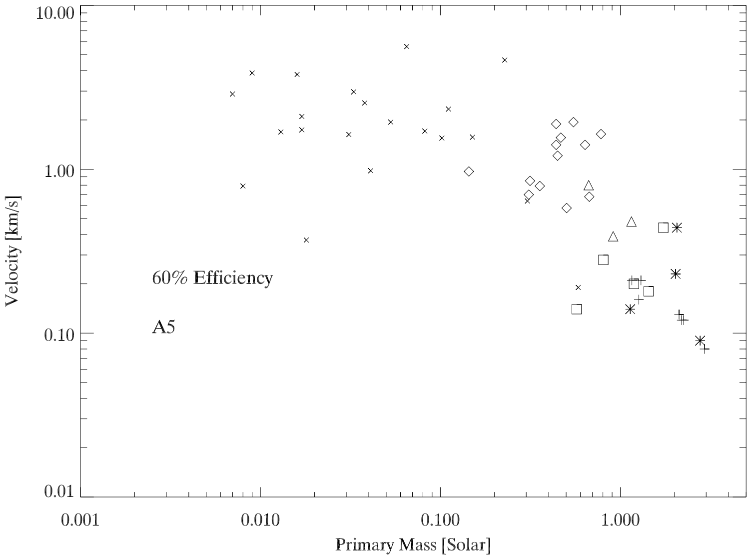

Fig. 2. Velocity (in km s^{-1}) versus primary mass (in $M_{\odot}$), after the end of the hydro calculations (60% efficiency). Small crosses represent singles and the other symbols refer to $N > 1$ multiples. A5 is a simulation label

matic segregation as a function of N is the expected outcome of the break-up of unstable multiples, whereby the ejected objects (typically singles, or less often binaries) acquire large velocities whereas the remaining more massive multiple recoils with a lower speed. Therefore, we would expect low-mass star-forming regions like Taurus, where a local kinematic segregation may survive against the influence of large scale dynamics, to display an overabundance of multiple systems in the densest regions, from where the low mass singles can escape more easily. This prediction was made by Delgado-Donate et al. [17, 18], and has been recently supported by the simulations [4]. On the observational side, it must be noted that the most recent survey of Taurus [29], covering several times the area of previous surveys, has found that the fraction of brown dwarfs increases as one moves away from the densest cores, known before to be over-abundant in binaries. This seems to be an indication for an average larger speed of the lower-mass single objects, as predicted.

4 Episode III: Revenge of the Binaries

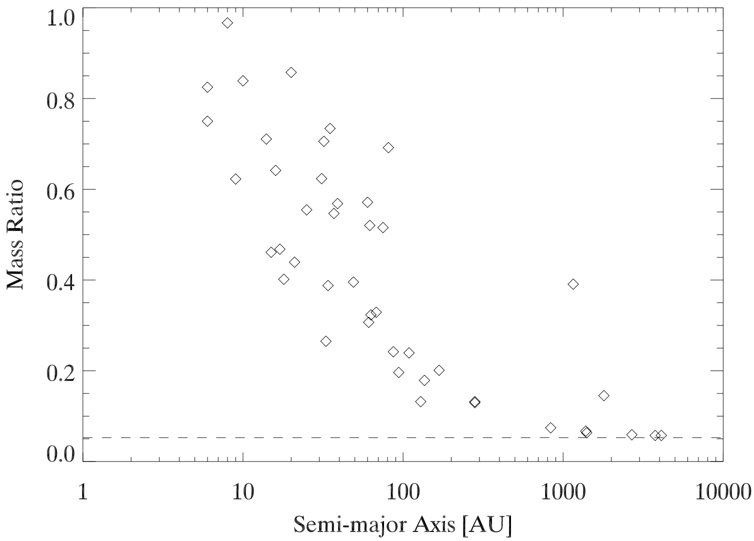

Fig. 3. Mass ratio q versus semi-major axis a [in AU] for different values of the initial specific angular momentum of the two-body system in the 'toy models'. The dashed horizontal line marks the minimum value the mass ratio can have, given the initial setup of the models

We have shown that 'turbulent' calculations are able to form a large fraction of multiples systems. For a significant range of primary masses, we reproduce the observed multiplicity fractions and the basic features of the IMF, and provide a viable formation mechanism for brown dwarfs. This is a substantial achivement. However, we must look more closely at the distribution of binary parameters, which is the most exacting area in which star formation theories can be compared with observations, and check critically against solid empirical results. Presently we have focused on low mass ratio binaries, i.e. those whose component masses differ by at least a factor of 2–3 – these are known to comprise roughly half of the population of binaries. We will argue that the high occurrence of this type of binary cannot be explained within current and past star formation models.

4.1 Where are the Low Mass Ratio Binaries?

Binaries with a relatively low binding energy (wide, low mass ratio q or low-mass binaries) are seen to be under-produced by all star formation calculations to date. N-body models, e.g. [22, 43], and hydrodynamic simulations, e.g. [12, 17, 18], run into difficulties to produce systems of this type, as dynamical interactions – which play a vital role in the formation of multiples and the ejection of low-mass objects – also act to disrupt systems with a low binding energy, low-q binaries among them. Even 'turbulent' calculations with subsonic Mach numbers [27, 28] also fail to produce enough low binding energy binaries despite the lower mean number of objects formed per cloud.

We have studied this problem by reviewing the existing literature and performing simple 'toy models' of $N = 2$ embedded stars [15]. We find that most models to date fail to produce low-q binaries due to the production and mutual interaction of several binary pairs (which promotes the exchange of higher-mass components as binary companions) and due to the fact that the first binary, which goes on to accrete rapidly and thus dominate the dynamics of the system, forms with a rather high mass ratio initially. These problems are hard to avoid as the components form in collapsing filaments and are thus pre-destined to interact shortly after formation, decreasing the chances of attaining different masses before a bound pair is formed. In addition, for a bound system, the accretion of high angular momentum material is seen to increase q, as matter is preferentially accreted onto the secondary. This result has tentatively been called into question by Ochi et al. [39].

4.2 Possible Solutions to the Riddle

In order to investigate possible solutions to the puzzle of low-q binary formation, we have performed simple 'toy models' of the evolution of an embedded protobinary, where the relative specific angular momentum of the binary is chosen as a free parameter. The models are very similar to those described in Section 2, except that now $N = 2$. These simulations show that, provided that the specific angular momentum of the protobinary is weakly coupled to the specific angular momentum of the gas it accretes, a binary with initially nearly equal mass components can end up with a very low mass ratio. From these models it is possible to obtain a relation between semi-major axis and mass ratio (Fig. 3) which is in close agreement to that observed among wide binaries. Thus, it seems that the condition of weak angular momentum coupling may be of relevance to the formation of wide low-q pairs. It remains unclear, however, how such binaries can form under more realistic initial conditions.

From our study, we tentatively conclude that low-q systems can either form in cores where the proto-binary has lower specific angular momentum than its gas reservoir or else where a low-mass companion forms through *delayed* disk fragmentation. In both situations, the system has to form in relative isolation, to survive disrupting encounters with other binaries. It is unclear, however, how any of these conditions can be met in practice. We thus flag the creation of extreme mass ratio and brown dwarf binaries as an unsolved problem and challenge to theorists.

5 Conclusions

Gas is a very important actor in the theatre of star formation. Even after the fragmentation and collapse phase, gas plays a vital role through the dissipation of energy during encounters, accretion, disk fragmentation and drag in the more diffuse background. We have presented simple models of small clouds with a few accreting point masses, that represent a first step towards the investigation of the role of gas in star formation. From them, we can see that the formation of a dominant binary, with lower mass objects orbiting at large separations or ejected from the cloud, is a typical outcome of the break-up of an accreting multiple.

On a more realistic ground, we have undertaken the first hydrodynamical + N-body simulations of multiple star formation to produce a statistically significant number of stable hierarchical multiple systems, with components separations in the range $1 - 1000$ AU. We have shown that a high multiplicity fraction is typical of the very early stages, a few $\times 10^5$ yr after star formation begins, with many different possible multiple configurations. At later stages (a few Myr), many systems have decayed, ejecting brown dwarfs to the field and decreasing the companion frequency. Both the high initial multiplicity and its dependence on age seem to be in accord with recent observations.

We find a positive dependence of multiplicity on primary mass, with few low-mass stars being primaries. The paucity of brown dwarf binaries in our simulations indicate that the models need finer tuning. Brown dwarfs are found, however, orbiting binaries or triples at large distances, and thus we suggest that a good test of our models is to look into the primaries of wide brown dwarf companions in search of multiplicity. The velocity dispersion among multiples is seen to be, on average, somewhat lower than for the singles, and thus we would expect this weak kinematic segregation to show up in regions where the large scale dynamics are not very relevant (low-mass star forming regions, associations).

We have also shown that hydrodynamic simulations of binary formation fail to produce extreme mass ratio binaries with anything like the frequency with which they are observed. Too efficient fragmentation, intersecting flows, the formation of a dominant binary and the accretion of high angular momentum material from a circumbinary disk are key factors that reduce the formation and survival probability of low-q binaries. Possible solutions to this riddle have been identified – weak coupling of the specific angular momentum of a protobinary with its surrounding material, initial conditions less prone to fragmentation – but it remains unclear how they may occur naturally under realistic initial conditions.

References

1. S. Aarseth: PASP **111**, 1333 (1999)
2. P. Artymowicz, S. H. Lubow: ApJ **467**, L77 (1996)
3. I. Baraffe, G. Chabrier, F. Allard, P. H. Hauschildt: A&A **337**, 403 (1998)
4. M. R. Bate: MNRAS (2005) accepted
5. M. R. Bate, I. A. Bonnell, N. M. Price: MNRAS **277**, 362 (1995)
6. M. R. Bate, I. A. Bonnell: MNRAS **285**, 33 (1997)
7. M. R. Bate, A. Burkert: MNRAS **288**, 1060 (1997)
8. M. R. Bate, I. A. Bonnell, V. Bromm: MNRAS **332**, L65 (2002)
9. M. R. Bate, I. A. Bonnell, V. Bromm: MNRAS **339**, 577 (2003)
10. I. A. Bonnell, M. R. Bate, C. J. Clarke, J. E. Pringle: MNRAS **285**, 201 (1997)
11. I. A. Bonnell, M. R. Bate, C. J. Clarke, J. E. Pringle: MNRAS **323**, 785 (2001)
12. I. A. Bonnell, M. R. Bate, S. G. Vine: MNRAS **343**, 413 (2003)
13. H. Bouy, W. Brandner, E. Martín et al.: AJ **126**, 1526 (2003)
14. A. Brandeker, R. Jayawardhana, J. Najita: AJ **126**, 2009 (2003)
15. C. J. Clarke, E. J. Delgado-Donate: MNRAS (2005) submitted
16. E. J. Delgado-Donate, C. J. Clarke, M. R. Bate: MNRAS **342**, 926 (2003)
17. E. J. Delgado-Donate, C. J. Clarke, M. R. Bate: MNRAS **347**, 759 (2004a)
18. E. J. Delgado-Donate, C. J. Clarke, M. R. Bate: MNRAS **351**, 617 (2004b)
19. G. Duchêne: A&A **341**, 547 (1999)
20. G. Duchêne, J. Bouvier, S. Bontemps et al.: A&A **427**, 651 (2004)
21. A. Duquennoy, M. Mayor: A&A **248**, 485 (1991)
22. R. H. Durisen, M. F. Sterzik, B. K. Pickett: A&A **371**, 952 (2001)
23. P. Eggleton, L. Kiseleva: ApJ **455**, 640 (1995)
24. D. A. Fischer, G. W. Marcy: ApJ **396**, 178 (1992)
25. C. F. Gammie: ApJ **553**, 174 (2001)
26. J. E. Gizis, J. D. Kirkpatrick, A. Burgasser et al.: ApJ **551**, 163 (2001)
27. S. P. Goodwin, A. P. Whitworth, D. Ward-Thompson: A&A **414**, 633 (2004a)
28. S. P. Goodwin, A. P. Whitworth, D. Ward-Thompson: A&A **423**, 169 (2004b)
29. S. Guieu, C. Dougados, J.-L. Monin, E. Magnier, E. L. Martín: New brown dwarfs in the Taurus SFR. In: *Memorie della Societa Astronomica Italiana*, vol 76, no 2, ed by L. Testi & A. Natta (Roma 2005) pp 253–258
30. S. T. Hodgkin, D. J. Pinfield, R. F. Jameson et al.: MNRAS **310**, 87 (1999)
31. V. Joergens: in *Protostars and Planets V*, Oct. 24-28, 2005, Waikoloa, Hawaii. LPI Contr. No. 1286., p.8034 (2005)
32. P. Kroupa: New Astronomy **4**, 615 (2000)
33. P. Kroupa, J. Bouvier, G. Duchêne, E. Moraux: MNRAS **346**, 354 (2003)
34. G. Lodato, W. K. M. Rice: MNRAS **358**, 1489 (2005)
35. E. L. Martín, D. Barrado y Navascués, I. Baraffe, H. Bouy, S. Dahm: ApJ **594**, 525 (2003)
36. R. D. Matthieu, H. Zinnecker: *The Formation of Binary Stars: IAU Symposium 200*, (PASP, Volume 112, Issue 777, 2000) pp 1512–

37. J. M. McDonald, C. J. Clarke: MNRAS **275**, 671 (1995)
38. P. F. L. Maxted, R. D. Jeffries: MNRAS (2005), accepted, astro-ph/0507177
39. Y. Ochi, K. Sugimoto, T. Hanawa: ApJ **623**, 922 (2005)
40. B. Reipurth, C. J. Clarke: AJ **122**, 432 (2001)
41. L. di G. Sigalotti, J. Klapp: International Journal of Modern Physics D, vol. 10 **2**, 115 (2001)
42. M. F. Sterzik, R. H. Durisen: A&A **304**, L9 (1995)
43. M. F. Sterzik, R. H. Durisen: A&A **339**, 95 (1998)
44. A. Tokovinin: RMxAC **21**, 7 (2004)

Roger Griffin

Population of Dynamically Formed Triples in Dense Stellar Systems

Natalia Ivanova

Physics and Astronomy, Northwestern University, 2145 Sheridan Rd, Evanston, IL 60208 USA nata@northwestern.edu

Summary. In dense stellar systems, frequent dynamical interactions between binaries lead to the formation of multiple systems. In this contribution we discuss the dynamical formation of hierarchically stable triples: the formation rate, main characteristics of dynamically formed population of triples and the impact of the triples formation on the population of close binaries. In particular, we estimate how much the population of blue stragglers and compact binaries could be affected.

1 Introduction

In globular clusters, the most plausible way for the dynamical formation of hierarchical triples is via binary-binary encounters. As numerical scattering calculations show, the probability of triple formation is quite substantial and for equal masses, a hierarchical triple is formed in roughly 50% of all encounters [3]. The probability is reduced by only a factor of a few when original semi-major axes of binaries are about equal [9]. The consideration of stars as non-point masses can decrease this probability further, as the physical collisions enhance strongly the destruction of close binaries during binary-binary encounters [2]. The formation of triple stars have often been noticed in numerical simulations of dense stellar systems using $N-$body codes (e.g. [4,10]), however so far there has been no attempt to study in detail the population of triple systems as well as their effect on the close binaries and blue stragglers. In this contribution we report the preliminary results of our study of triples population.

2 Method and Assumptions

We use a *Monte Carlo* method described in detail in [6]. This method assumes a static cluster background, all relevant dynamical parameters being kept constant throughout dynamical simulation. In particular, the cluster model we consider here has central density $n_{\rm c} = 10^5$ [$\rm pc^{-3}$], velocity dispersion $\sigma = 10$ [km/s], escape velocity $v_{\rm esc}$ [km/s] and half-mass relaxation time $t_{\rm rh} = 10^9$ [yr]. The code takes into account such important dynamical processes as mass segregation and evaporation, recoil, physical collisions, tidal captures, and binary–single and binary–binary encounters. For dynamical encounters that involve binaries we use `Fewbody`, a numerical toolkit for direct N-body integrations of small-N gravitational dynamics [2]. This toolkit is particularly suited to automatically recognize a hierarchical triple (formed via an encounter) using the stability criterion from Mardling & Aarseth [8]. In order to get large statistics on triples formation rate, we start with 1.25×10^6 stars, 100% are in primordial binaries; the modeled cluster has mass $\sim 250\,000 M_\odot$ at 10 Gyr and the core mass is 10-20% of the total cluster mass. This cluster model represents well a "typical" globular cluster.

There is no developed population synthesis methods for triples evolution. As a result, we can not keep the triples once they were dynamically formed and have to break a triple into a binary and a single star. This approach is suitable as it is likely that a dynamically formed hierarchical triple will be destroyed during next dynamical encounter. In our standard runs, we break a triple while conserving the energy: the energy required to eject the outer companion is acquired from shrinking of the inner binary orbit. The outer companion is released unless the required shrinkage is such that the inner binary merges. In the latter case the inner system is allowed to merge and the outer companion is kept at its new, wider orbit to form the final binary system. On the other hand, it is possible that in a triple system the inner eccentricity will be later increased via the Kozai mechanism [7]. This mechanism causes large variations in the eccentricity and inclination of the star orbits and could drive the inner binary of the triple system to merge before next interaction with other stars. To check how strongly this affects the binary population, we compare two cluster models with identical initial populations of 5×10^5 stars. In one model, we use our standard treatment for triples breaking. In the second model, we compare the Kozai time-scale $\tau_{\rm Koz}$ (taken as in [5]) with the collision time-scale $\tau_{\rm coll}$. Inner binaries in the formed triples are merged if $\tau_{\rm Koz} < \tau_{\rm coll}$ (we define these triples as Kozai triples). We expect that some of the triples can also have a secular eccentricity evolution even in the case of inclinations smaller than the Kozai angle (see e.g. [1]), but we neglect this possibility.

3 Numerical Results on Dynamically Formed Triples

3.1 Formation Rates

From our standard model, we find that a "typical" cluster has about 5000 hierarchically stable triples formed in its core throughout its evolution. As our triples are formed via binary-binary encounters, the resulting formation rate intrinsically depends on the binary fraction, the binary cross-section and the total number of binaries. Hence the obtained formation rate can be written as:

$$\Delta N_{\rm tr}/N_{\rm bin} = 0.05 f_{\rm bin} \langle m_{\rm b} \rangle \langle a \rangle \text{ per Gyr.} \tag{1}$$

Here $f_{\rm bin}$ is the binary fraction, $\langle m_{\rm b} \rangle$ is the average binary mass and $\langle a \rangle$ is the average binary separation. In particular, at 10 Gyr $\langle m_{\rm b} \rangle \approx 1 M_\odot$, $\langle a \rangle \approx 10 R_\odot$ and $f_{\rm bin} \approx 10\%$. The formation rate at 10 Gyr is therefore such that as many as 5% of all core binaries have sucesfully participated in the formation of hierachically stable triples during 1 Gyr. We stress that the expression above is fitted to numerical simulations; it does not include directly the expected dependence on the core number density and velocity dispersion because only one set of these parameters was used in simulations.

The formation rate of triples can also be written as a function of the cluster age (for ages > 1 Gyr):

$$\Delta N_{\rm tr} = 600\ T_9^{-1/3} \text{ per Gyr,} \tag{2}$$

where T_9 is the cluster age in Gyr.

3.2 Masses, Orbital Periods and Eccentricities

In Fig. 1 we show the distributions of companions masses in triple systems (the mass of the inner binary and of the outer companion), of inner and outer orbital periods, and of outer eccentricities, for all dynamically formed triples throughout the entire cluster evolution. The inner eccentricities did not show strong correlation with any other parameters and are distributed rather flatly. A "typical" triple has the mass ratio $M_3/(M_1 + M_2) \approx 0.5 \pm 0.1$, the total mass of the inner binary is $M_1 + M_2 \approx 1.3 \pm 0.3 M_\odot$ (such a binary, if merges, will likely produce a blue straggler), $P_{\rm in} \approx 1$ day. The typical period ratio is high, $P_{\rm out}/P_{\rm in} \approx 1000$, the ratio of the orbital separations $a_{\rm out}/a_{\rm in} \approx 100$ and the outer eccentricity is very large, $e_{\rm out} \approx 0.95 \pm 0.05$.

3.3 Hardness and the Kozai Mechanism

Only those triples that have the binding energy of the inner binary with the outer companion greater than a kinetic energy of an average object in the field are stable against subsequent dynamical encounters. The ratio of these energies is the triple's hardness, η. We find that 45% of all triples have $\eta > 1$ and only 7% of all triples have $\eta > 10$. In our numerical simulation we find that for binaries, to likely survive subsequent dynamical encounters, a hardness should be about few times larger than 1. Therefore we can assume that most of the formed triples can be easily destroyed in their subsequent evolution in the dense core. However, we find also that about a third of all triples are the Kozai triples. The probability that a triple is affected by Kozai mechanism does not correlate with the triple's hardness, the orbital periods or the eccentricities. In the result, a significant fraction of all triples can evolve not as our triples-breaking treatment predicts.

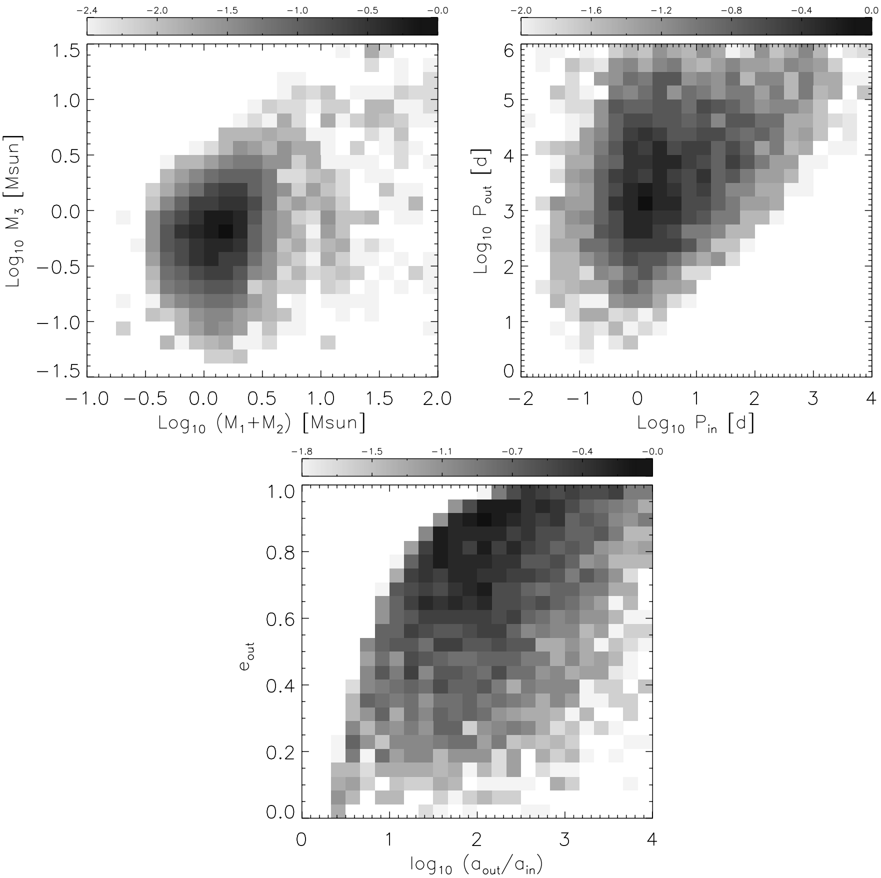

Fig. 1. The distributions of masses of inner binaries and outer companions (left panel), of inner and outer orbital periods (right panel) and the plot of outer companion's eccentricities versus the orbital separation ratio (bottom panel) in the dynamically formed hierarchically stable triples. The colors correspond to the logarithm of the probability density

3.4 Population of Kozai Triples

About 60% of all triples have inner binaries with both components on the Main Sequence (MS-MS binaries), and 30% of them are Kozai triples. A typical total mass of such binary is $1.3 \pm 0.2\ M_\odot$ (see also Fig. 2). If Kozai mechanism leads to a merger, we find that these triples can provide 10% of all blue stragglers ever created.

About 40% of all triples have inner binaries with a compact object (WD for white dwarf and NS for neutron star) and 35% (40% for WD-WD inner binaries) of them are Kozai triples. A typical WD-MS binary affected by the Kozai evolution consists of a $0.8\ M_\odot$ WD and $0.8\ M_\odot$ MS star. It is not clear

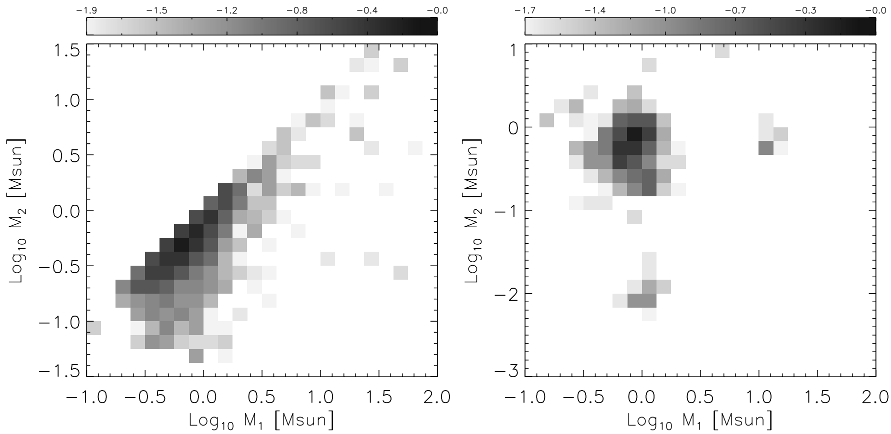

Fig. 2. The population of inner binaries in Kozai triples: MS-MS sequence binaries (left panel) and inner binaries with a compact object (right panel). The colors correspond to the logarithm of the probability density, M_1 is the mass of the more massive companion in the case of MS-MS binary or the mass of a compact companion

Table 1. The stellar population of close binaries and triples in the cluster core at the age of 10 Gyr. MS stands for a Main Sequence star, RG for a red giant, WD for a white dwarf and NS for a neutron star.

	Binaries		Triples, inner	binaries	Triples, outer companions
	MS	WD	MS	WD	
MS	79%	13%	60%	20%	79%
RG	0.7%	0.3%	2%	1%	0.7%
WD		7%		15%	20%
NS	0.3%	0.3%	0.6%	0.7%	0.3%

if the Kozai mechanism will lead to the merger or to the start of the mass transfer and will create therefore a cataclysmic variable. In the latter case, the formation rate of cataclysmic variables via Kozai mechanism is rather large. For example, in a typical globular cluster at the age of 10 Gyr, it can provide in 1 Gyr as many new cataclysmic variables as 25-50% of all cataclysmic variables that were created by all other channels and are present in the cluster at this age.

3.5 Comparison of the Close Binaries Population and the Triples Population

In Table 1 we provide the complete statistics for the stellar population of close binaries and triples in the cluster core at the age of 10 Gyr. We find that the inner binary of a triple is more likely to contain a compact object than a core binary at 10 Gyr. The statistics for outer stars follows that of the binariy populations.

3.6 Comparison of Models with and without Kozai Triples Mergers

We find that different treatments of Kozai triples (our standard breaking of triples based on the energy balance or the enforced merge of the inner binary in a Kozai triple) do not lead to significantly different results for the binary fractions (the difference is less than 1%). Some difference is noticed for the distribution of binary periods of core binaries with a WD companion: in the model where Kozai triples, once formed, had their inner binaries merged, the relative number of binaries with the periods less than 0.3 day is smaller than in the model where Kozai triples were treated as usual, and for binaries with periods between 0.3 and 3 days the situation is reversed.

Acknowledgments

The author thanks John Fregeau for the useful discussion on triples stability and acknowledges the support by a *Chandra* Theory Award.

References

1. E. B. Ford, B. Kozinsky, F.A. Rasio: ApJ **535**, 385 (2000)
2. J. M. Fregeau, P. Cheung, S. F. Portegies Zwart et al.: MNRAS **352**, 1 (2004)
3. D. Heggie, P. Hut: *The Gravitational Million-Body Problem: A Multidisciplinary Approach to Star Cluster Dynamics* (Cambridge University Press 2003)
4. J. R. Hurley, O. R. Pols, S. J. Aarseth, S. J. at al: ArXiv Astrophysics e-prints, arXiv:astro-ph/0507239 (2005)
5. K. A. Innanen, J. Q. Zheng, S. Mikkola et al: AJ **113**, 1915 (1997)
6. N. Ivanova, K. Belczynski, J. M. Fregeau et al: MNRAS **358**, 572 (2005)
7. Y. Kozai: AJ **67**, 591 (1962)
8. R. A Mardling, S. J. Aarseth: MNRAS 2001 **321**, 398 (2001)
9. S. Mikkola: MNRAS **207**, 115 (1984)
10. S. McMillan, P. Hut, J. Makino: ApJ **372**, 111 (1991)

Interferometric Studies of Multiple Stars

Christian A. Hummel

European Southern Observatory, Casilla 19001, Santiago 19, Chile
chummel@eso.org

Summary. Long baseline optical and infrared interferometry (LBI) has been immensely successful in resolving spectroscopic binaries in order to enable the determination of stellar masses and luminosities. However, the technique has been applied to only a very few cases of higher multiplicity, namely triple stars. I will discuss in the following a specific case, η Virginis, while I provide other references on the technique instead of repeating them here.

1 If you have been Thinking of Using LBI...

Long baseline interferometry (LBI) is a special technique to achieve the highest spatial resolution at the expense of being able to image complex structure with high dynamic range. Therefore, single and multiple stars have been the main target over the past couple of decades, with astrophysically important results [5].

The observations of simple targets such as single and multiple stars are no exception to the rule that in general, interferometry has to be combined with other techniques since it probes only limited spatial frequencies. If one considers LBI for a target, one should therefore consult a checklist [4] in order assess the feasibility of the observations. Most importantly, the expected target size needs to be known, and matched to the available baselines. In addition, the homepage of the European Southern Observatory (ESO) provides tools such as VisCalc and CalVin (http://www.eso.org/observing/etc/index.html) supporting observations with the Very Large Telescope Interferometer (VLTI).

As the number of stations in the interferometric arrays has increased, albeit modestly and slowly, interferometers may now be considered as telescopes and no longer as a sort of ruler. In the following I will point out the important but perhaps less obvious consequences of this classification.

1.1 Imaging, Dynamic Range, and Fidelity

Naturally, imaging is what a telescope should be able to perform, and interferometers are no exception [2]. However, those arrays which have a sufficient number of elements are capable to produce images of only simple structures having to do with the limited sampling of the aperture plane. Just as in the radio where interferometric imaging techniques have been pioneered, the dynamic range, i.e. the ratio of the peak map intensity to the lowest believable contour, is a function of the quality of the data, including calibration. However, fidelity to complex structures is only a function of aperture coverage, and can be limited even if the dynamic range is high.

As of 2005, images from LBI are usually made for public relations, as structural parameters are always obtained by fitting the appropriate models directly to the visibility (and other complementary) data.

1.2 Photometric Field of View

In terms of the photometric field of view (FOV), three classes can be identified, a wide field belonging to Fizeau-type combiners, intermediate belonging to the Michelson type, and narrow belonging to the Michelson type but using single-mode fibers for improved data quality. The Large Binocular Telescope's LINC-NIRVANA beam combiner belongs to the first class, while VLTI's MIDI and AMBER beam combiners belong to the second and third class, respectively. MIDI's FOV is about 2 arcseconds using the UTs, while AMBER's FOV is only about 60 mas using the UTs.

1.3 Interferometric Field of View

As the observable of an interferometer is the visibility, the amplitude of which is related to the contrast of the fringes in the interference pattern, or fringe packet, and as the latter is a superposition of the fringe packets across the (photometric) field of view, the interferometer is insensitive to directions falling outside the central fringe packet located at the phase center of the pointing direction. The area over which photons contribute to the central fringe packet is called the interferometric field of view. It is roughly equal to $R\lambda/B$, where R is the spectral resolution, and λ/B is the fringe spacing (B being the length of the projected baseline).

The width of the fringe packet is inversely proportional to the bandwidth of the received radiation. In Fig.1 one can see the two well separated fringe packets produced by the two components of the binary star 12 Persei. The same star was observed by the Mark III interferometer in a narrow channel centered at 800 nm, and one can see from the typical variation of the visibility amplitude during the night that in this case the fringe packets overlapped (see Fig. 2).

If a component from a multiple star systems falls *outside* the interferometric but *inside* the photometric field of view, the visibility amplitude will be decreased by a factor $f = 1 + 10^{-\Delta m/2.5}$, where Δm is the magnitude difference between that component and the combination of all others.

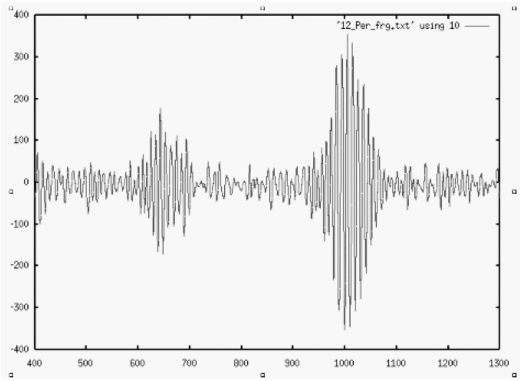

Fig. 1. The two fringe packets produced by the 40 mas-separated components of 12 Persei, as observed on Oct 9, 2001, with the 330 m baseline of the CHARA Array in the K'-band

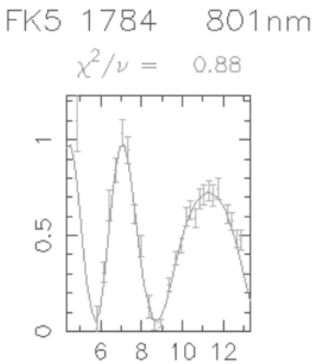

Fig. 2. Visibility amplitude of 12 Persei observed October 8, 1992, at 50 mas separation on a 12 m baseline of the Mark III interferometer at 800 nm, bandwidth of 22 nm

1.4 Broadband Aperture Synthesis

Various interferometers are also acting as spectrometers, which is to say that the visibility is measured in several, and in some cases many hundreds of wavelength channels. If these cover significant fractions of the spectrum, so will the aperture coverage be increased due to the spatial frequency being the ratio of baseline length over wavelength. However, the increase in aperture coverage is offset in a way due to the fact that the target structure most likely will vary with wavelength, thus prohibiting the simple combination of all visibility data to obtain an image of the target. Also, the interpretation of the visibility spectrum is complicated by the changing spatial resolution along the wavelength axis.

2 Modeling of Interferometric Observations of η Virginis

The triple star η Virginis was the first triple system to be fully resolved by LBI, and these observations at the same time constituted the first successful operation of a six-station array [3].

2.1 Visibility Function and Data

The first epoch (of 27) observations are shown in Fig.3, more specifically the location in the aperture plane (also called *uv*-plane) of the measurements taken by the 11 baselines of the NPOI [1] during the night. The longest NPOI baselines resolved the close pair in this triple system, while the shorter baselines were sensitive to the wide separation.

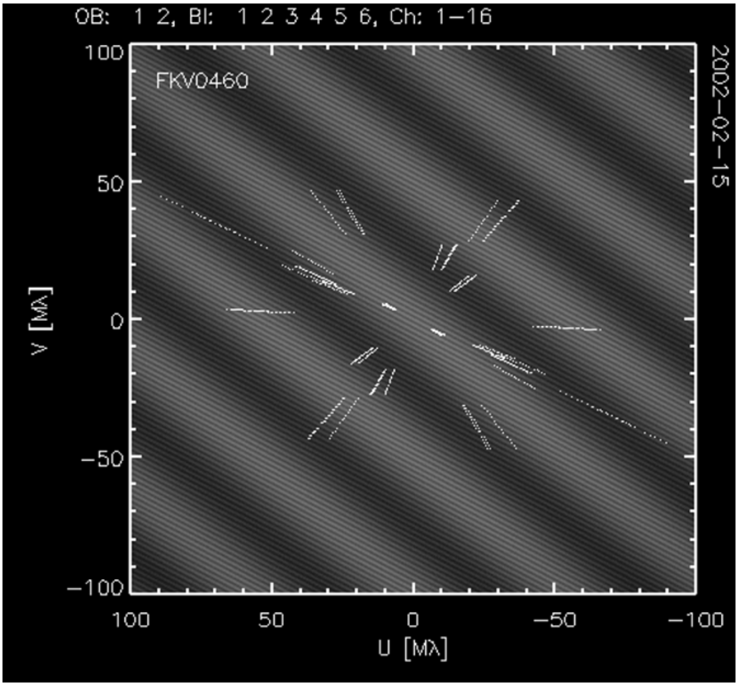

Fig. 3. Aperture coverage provided by the NPOI six-station array for the observations of η Virginis on February 15, 2002. The grey-scale image corresponds to the amplitude of the squared visibility function predicted by a model of the triple system and fitted to the data. One can discern two systems of stripes corresponding to the two binary components in this hierarchical system, with the narrow stripes due to the larger spacing

2.2 Hierarchical Model Format

As we are for the time being only interested in hierarchical systems, which cover most of the cases of higher multiplicity anyway, we developed the format shown below to specify component and orbital parameters. For each component in a multiple system, e.g. A, B, C for the components in a triple system, we specify the stellar parameters which can be fitted to the data, including radial velocities if available. In a triple system, the binary components to be specified can then be A-B and AB-C, or B-C, A-BC.

```
name(0)          ='A'              component(0)     ='A-B'
wmc(0)           ='Aa'             method(0)        =1
mode(0)          =1                semimajoraxis(0)=7.36
mass(0)          =2.68             inclination(0)   =45.5
diameter(0)      =0.46             ascendingnode(0)=129.5
magnitudes(*,0) =[4.2,4.2]         eccentricity(0) =0.244
;                                  periastron(0)    =196.9
name(1)          ='B'              epoch(0)         =2452321.4
wmc(1)           ='Ab'             period(0)        =71.7916
mode(1)          =1
mass(1)          =2.04             component(1)     ='AB-C'
diameter(1)      =0.21             method(1)        =1
magnitudes(*,1) =[6.0,6.0]         semimajoraxis(1)=133.7
;                                  inclination(1)   =50.6
name(2)          ='C'              ascendingnode(1)=170.8
wmc(2)           ='B'              eccentricity(1) =0.087
mode(2)          =1                periastron(1)    =2.3
mass(2)          =1.66             epoch(1)         =2447896.2
diameter(2)      =0.15             period(1)        =4774.0
magnitudes(*,2) =[6.5,6.3]
```

Diameters and magnitude differences can be constrained by the interferometry; individual magnitudes are then constrained by the combined magnitudes known for the system. Magnitudes and semi-major axes can be used to predict the motion of the photocenter if the close pair should not be resolved by the interferometer. The masses are constrained if radial velocity data are added to the interferometric data (discussed below).

2.3 Astrometric Mass Ratio

Both pairs in the triple system η Virginis have been resolved and the orbital motion measured by NPOI [3]. Since the tertiary component is only slowly moving and its motion can be modeled using the extensive speckle interferometric data, it provides a reference position for the component motions in the close pair. This enabled the measurement of the component mass ratio in the close pair, providing an estimate independent of the one derived by the semi-amplitudes of the radial velocity curves.

2.4 Combined Modeling

Stellar masses are model parameters since we fit the model to a combination of spectroscopic and interferometric data, allowing to make the fit more robust and obtain astrophysically relevant parameters more directly. In the case of η Virginis, the close pair is a double-lined spectroscopic binary, allowing to measure masses of and distance to this pair. Therefore, even without the radial velocity curve of the tertiary, its mass can be determined also.

We implemented combined modeling with the safeguards provided by the Singular-Value-Decomposition method [6] against inadvertently selecting unconstrained parameters for a fit, and use the Levenberg-Marquardt implementation of non-linear least-squares fitting [6]. Relative weights of the data sets are set to normalize the reduced χ^2 for them individually before combination.

3 ...Now is a Good Time to do it

The VLTI operated by ESO is the first to offer LBI in service mode, which enables astronomers to have observations executed in absentia and raw data delivered to them meeting certain quality contol criteria. Software for the data reduction is available, e.g. through JMMC (http://mariotti.ujf-grenoble.fr/) and NOVA (http://www.strw.leidenuniv.nl/ nevec/index.html).

References

1. Armstrong, J. T., et al. 1998, ApJ, 496, 550
2. Baldwin, J. E., & Haniff, C. A. 2001, Phil. Trans. A, 360, 969
3. Hummel, C.A., Benson, J.A., Hutter, D.J., Johnston, K.J., Mozurkewich, D., Armstrong, J.T., Hindsley, R.B., Gilbreath, G.C., Rickard, L.J, & White, N.M. 2003, AJ, 125, 2630
4. Hummel, C. A. 2004, in Spectroscopically and Spatially Resolving the Components of Close Binary Stars, ed. by R.W. Hilditch, H. Hensberge, and K. Pavlovski (San Francisco: ASP), p. 13
5. Hummel, C. A. 2005, in The Power of Optical/IR Interferometry: Recent Scientific Results and 2nd Generation VLTI Instrumentation, ed. by F. Paresce and A. Richichi (Garching: ESO Astrophysics Symposia), in press
6. Press, W. H., Flannery, B. P., Teukolsky, S. A., & Vetterling, W. T. 1992, Numerical Recipes (Cambridge University Press, Cambridge)

Interferometric Orbits of New Hipparcos Binaries

I.I. Balega[1], Y.Y. Balega[2], K.-H. Hofmann[3], E.V. Malogolovets[4], D. Schertl[5], Z.U. Shkhagosheva[6] and G. Weigelt[7]

[1] Special Astrophysical Observatory, Russian Academy of Sciences ildiko@sao.ru
[2] Special Astrophysical Observatory, Russian Academy of Sciences balega@sao.ru
[3] Max-Planck-Institut für Radioastronomie khh@mpifr-bonn.mpg.de
[4] Special Astrophysical Observatory, Russian Academy of Sciences evmag@sao.ru
[5] Max-Planck-Institut für Radioastronomie ds@mpifr-bonn.mpg.de
[6] Special Astrophysical Observatory, Russian Academy of Sciences zalikha@sao.ru
[7] Max-Planck-Institut für Radioastronomie weigelt@mpifr-bonn.mpg.de

Summary. First orbits are derived for 12 new Hipparcos binary systems based on the precise speckle interferometric measurements of the relative positions of the components. The orbital periods of the pairs are between 5.9 and 29.0 yrs. Magnitude differences obtained from differential speckle photometry allow us to estimate the absolute magnitudes and spectral types of individual stars and to compare their position on the mass-magnitude diagram with the theoretical curves. The spectral types of the new orbiting pairs range from late F to early M. Their mass-sums are determined with a relative accuracy of 10-30%. The mass errors are completely defined by the errors of Hipparcos parallaxes.

1 Introduction

Stellar masses can be derived only from the detailed studies of the orbital motion in binary systems. To test the models of stellar structure and evolution, stellar masses must be determined with $\approx 2\%$ accuracy. Until very recently, accurate masses were available only for double-lined, detached eclipsing binaries [1]. The empirical mass-luminosity relation is therefore well-constrained for late-B to late-F stars of the main sequence. At the end of the 1990s, new accurate masses were determined at the bottom of the main sequence using the combination of very precise radial velocities with adaptive optics [5], [11]. With an accuracy of 2-10%, masses for very low-mass stars were also provided by precise astrometric measurements using the Fine Guidance Sensors on board of HST [3], [12]. However, for the mass range between $0.6\,\mathcal{M}_{\odot}$ and $0.9\,\mathcal{M}_{\odot}$, the lack of empirical data for stellar masses remains noticeable. This gap can be bridged using the speckle imaging of nearby short-period (P<20 yr) G, K, and M pairs, in combination with the long-term monitoring of their radial velocities.

Since 1998, precise relative positions and magnitude differences for more than 200 new Hipparcos binaries [4] have been measured using the speckle interferometric technique. Many of them show fast relative motion of the components, denoting a possibility of an orbit definition within one decade. The majority of speckle observations was collected by our team at the 6 m BTA telescope in Zelenchuk and by Horch et al. at the WIYN 3.5 m telescope in the USA [7], [8]. Presently, the orbital parameters for approximately 20 new Hipparcos pairs can be obtained. Here we present the orbits for 12 systems from the list. Five pairs belong to the K and M dwarfs, while seven others are late F to G-type stars.

2 Orbits and Masses

Due to the high accuracy of speckle measurements (typically 1 to 3 mas), most of the orbits can be considered definitive, despite the small number of observations. The orbital periods and the major semiaxes are defined with a typical accuracy of 1%. However, the relative error of the parallaxes for the stars from our sample is changing in the range between 5 and 10%. This means that the total masses of the systems can be estimated with an accuracy of only 10% or worse. To improve the mass accuracies, we need additional data about the radial velocities of the components or more precise parallaxes.

The main parameters of the orbits for twelve new pairs, together with their physical properties, are given in Table 1. To derive the orbits, in a few cases we made use of the published speckle measurements from other telescopes. For convenience, the Hipparcos parallaxes of the pairs are included in the table. The absolute magnitudes and spectral types of the components were estimated from speckle interferometric magnitude differences in the visible and infrared bands with regard for their Hipparcos parallaxes. Note that two pairs in the list, HIP 4809 and HIP 5531, have evolved components. The last column in Table 1 gives the relative errors of the masses.

The orbital ellipses for our 12 pairs are shown in Fig. 1 and Fig. 2. For convenience, the binaries are grouped according to the spectral types of the components: 6 pairs belong to the F-G spectral types, and the 6 others are K- to M-type dwarfs.

The positions of the components on the $\mathcal{M}/M$ diagram are presented in Fig. 3. The mass ratios of the systems were derived from speckle photometric data and the empirical $\mathcal{M}/M_V$ relation [9]. For two systems, HIP 5531 and HIP 19206, we used mass ratios from the spectroscopic survey [10]. For comparision, two theoretical isochrones for 5 Gyr and solar metallicity taken from [2] and [6] are plotted on the diagram. The components of the systems with magnitude differences less than 1 magnitude are given as circles, while for designation of the components with larger magnitude differences we use asterisks. This helps to single out those systems which can be observed as SB2. The components of evolved pairs are shown by the larger circles.

Table 1. Main parameters of the orbits, properties of the components, and total masses for 12 new Hipparcos binaries

HIP	π_{hp} mas	σ_π mas	M_{VA}	M_{VB}	Sp_A	Sp_B	P yrs	a AU	$\mathcal{M}$ $\mathcal{M}_\odot$	$\sigma_\mathcal{M}$ $\mathcal{M}_\odot$	$\sigma_\mathcal{M}/\mathcal{M}$ %
4809	13.94	0.90	3.1	3.3	G6-G9IV	G6-G9IV	16.41	9.18	2.90	0.57	20
4849	46.61	1.61	6.7	8.4	K3	K8	28.99	9.77	1.17	0.14	12
5531	17.41	0.67	3.2	4.0	G0IV	G0IV	7.30	5.00	2.33	0.30	13
11352	23.19	1.21	5.5	5.7	G8	G9	6.85	4.31	1.71	0.27	16
14075	15.17	1.44	5.5	5.5	G8	G8	13.89	7.07	2.03	0.58	29
14230	29.62	1.09	4.7	6.4	G2	K2	5.91	3.71	1.47	0.26	18
14669	64.83	4.26	9.5	11.2	M2	M4	28.31	8.78	0.84	0.17	20
19206	24.00	0.92	4.1	5.5	G0	G8	21.33	9.29	1.75	0.25	14
105947	17.11	1.13	3.9	5.4	F8	G8	18.79	9.82	2.68	0.58	22
106972	39.78	3.70	9.9	11.1	M2	M4	18.57	6.74	0.89	0.25	28
111685	52.94	1.94	8.2	10.2	K7	M3	16.77	6.23	0.86	0.10	12
114922	31.50	3.85	9.4	9.6	M1	M2	19.72	6.95	0.87	0.32	37

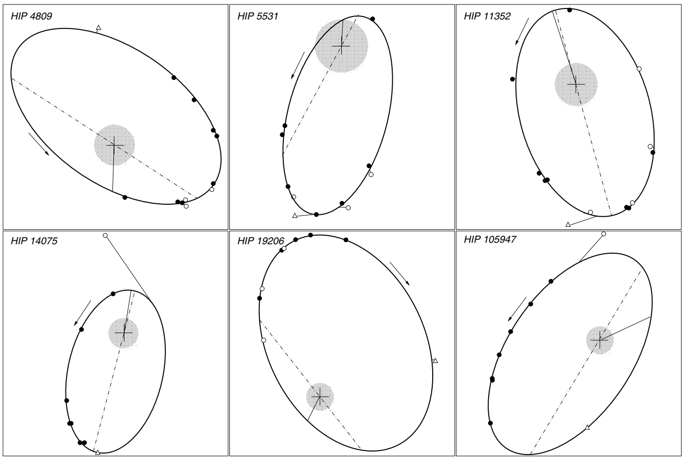

Fig. 1. Apparent ellipses for six F-G type new Hipparcos binaries. BTA speckle data are indicated by filled circles, other interferometric data by open circles, and Hipparcos first measurements by triangles. Residual vectors for all measurements are plotted, but in most cases they are smaller than the points themselves. The orbital motion directions are indicated by arrows. Solid lines show the periastron positions, while the dot-dashed lines represent the lines of nodes. North is up and east is to the left. The shaded circle at the position of the brighter component has a radius of 0.02", corresponding to the diffraction limit of a 6 m aperture

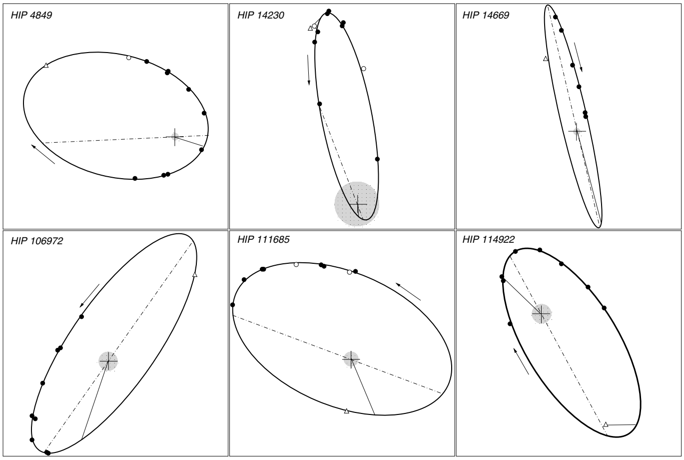

Fig. 2. Apparent ellipses for six K-M type new pairs

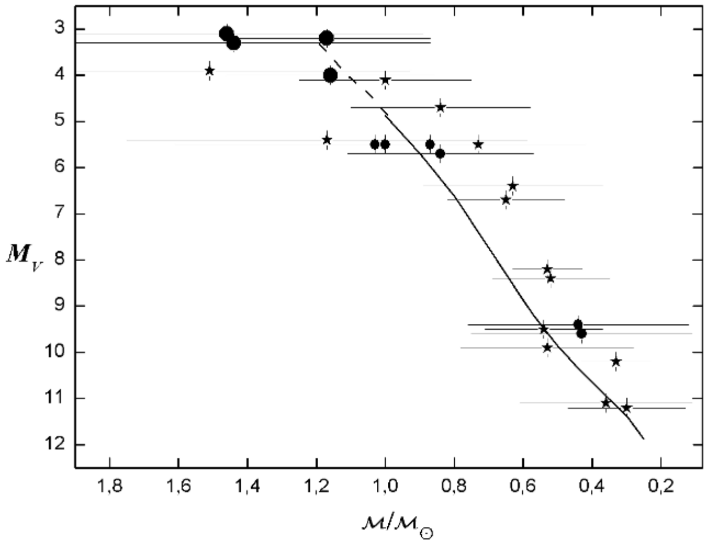

Fig. 3. Positions of the components of 12 new Hipparcos binaries on the mass-magnitude diagram. Binaries with $\Delta m < 1$ are plotted as filled circles, while those with $\Delta m > 1$ are shown as stars. The larger circles indicate two systems with evolved components, HIP 4809 and HIP 5531. Error bars are the same as for the mass-sums. The two curves are 5 Gyr theoretical isochrones from [2] (solid line) and [6] (dashed line) for solar metallicities

3 Conclusions

Speckle monitoring of new nearby (distance less than 77 pc) Hipparcos binaries and Hipparcos "problem" stars allows us to determine new orbits in a comparatively short time interval. Differential speckle interferometry helps to estimate the individual luminosities and spectral types of the components. In view of the results given above for 12 pairs, we can make the following concluding remarks. First, the semimajor axes of the systems lie in the rather narrow range between 4 and 10 AU. This fact reflects the optimal range of orbital periods and angular separations for the nearby binaries (median distance 50 pc), which can be studied by means of speckle interferometry. About 40 new orbits for the nearby Hipparcos binaries could be obtained before 2010 if the speckle monitoring of fast pairs continues. Second, we note the higher luminosity for the components of most of the systems in comparison with the theory for the mass range 0.5-1.0 $\mathcal{M}_{\odot}$. This can be a sign of the evolved status of the stars or the result of their lower metallicity. Third, the calculated mass-sums of the pairs have comparatively low relative accuracy, between 10 and 30%, which is explained by the dominating input of the Hipparcos parallax errors. The further improvement of speckle orbits will not lead to significantly more precise masses. To reduce the mass-sum errors to 5% or below, it is necessary to collect systematic data of their radial velocities with a precision of $\sim 0.5\ \mathrm{km\,s^{-1}}$ or to measure the parallaxes with a typical accuracy of 0.1 mas.

References

1. J. Andersen: Astron. Astrophys. Rev. **3**, 91 (1991)
2. I. Baraffe, G. Chabrier, F. Allard et al: Astron. Astrophys. **337**, 403 (1998)
3. G.F. Benedict, B.E. McArthur, O.G. Franz et al: Astron. Journal **120**, 1106 (2000)
4. ESA: The Hipparcos and Tycho Catalogues ESA SP-1200 (1997)
5. T. Forveille, J-L. Beuzit, X. Delfosse et al: Astron. Astrophys. **351**, 619 (1999)
6. L. Girardi, A. Bressan, G. Bertelli et al: Astron. Astrophys. Suppl. Ser. **141**, 371 (2000)
7. E.P. Horch, Z. Ninkov, W.F. van Altena et al: Astron. Journal **117**, 548 (1999)
8. E.P. Horch, S.E. Robinson, R.D. Meyer et al: Astron. Journal **123**, 3442 (2002)
9. K.R. Lang: Astrophysical Data: Planets and Stars (Springer-Verlag, N.Y.) (1992)
10. B. Nordström, M. Mayor, J. Andersen et al: Astron. Astrophys. **418**, 989 (2004)
11. D. Segransan, X. Delfosse, T. Forveille et al: Astron. Astrophys. **364**, 665 (2000)
12. G. Torres, T.J. Henry et al: Astron. Journal **117**, 562 (1999)

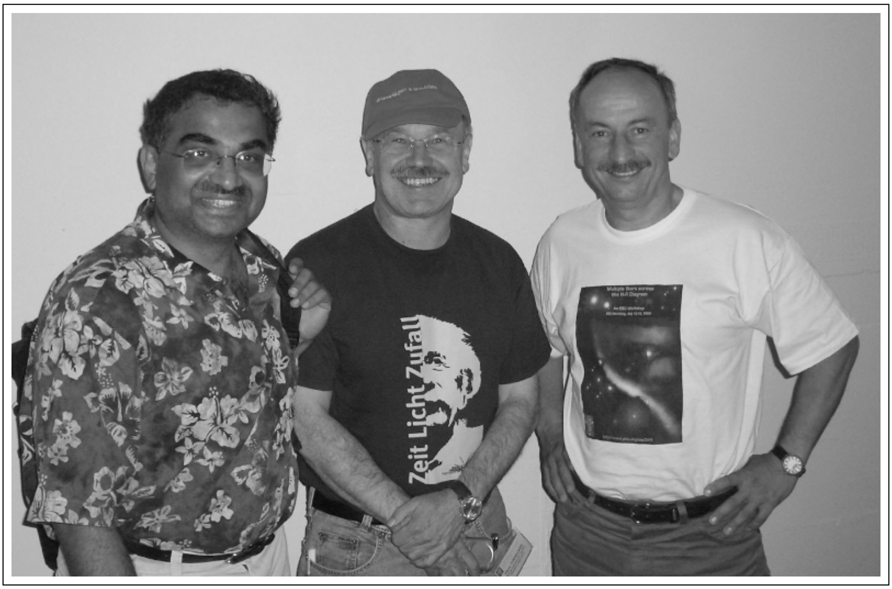

Shri Kulkarni, Hans Zinnecker, Yuri Balega (from left to right)

New Facts about δ Velorum: Fewer but Larger Components

A. Kellerer[1], M.G. Petr-Gotzens[1], P. Kervella[2] and V. Coudé du Foresto[2]

[1] European Southern Observatory, Karl-Schwarzschild-Str. 2, D-85748 Garching, Germany akellere@eso.org, mpetr@eso.org

[2] LESIA, Observatoire de Paris-Meudon, 5 place Jules Janssen, 92195 Meudon Cedex, France pierre.kervella@obspm.fr, vincent.foresto@obspm.fr

Summary. Interferometric observations of the nearby eclipsing binary δ Vel A were obtained with VLTI/VINCI and AMBER. The measurements, which for the first time resolve the two components, are analysed with non-linear least-square fitting methods and provide estimates of the orbital parameters and the stellar properties. We derive a system mass of $M_{Aa+Ab} = (4.05 \pm 0.30) M_\odot$ and an eccentric binary orbit ($e \approx 0.26$). The observations further indicate that the components' diameters are much larger than expected for main-sequence stars, implying that Aa and Ab are in evolved post main-sequence evolutionary phases.

1 A Nearby (~24pc) Eclipsing Binary System

An observer gazing at the southern sky constellation Vela will easily make out the bright star δ Velorum, since it is one of the 50 visually brightest stars on the sky. In the Cape Photographic Durchmusterung (1895-1900) δ Vel is listed with a photographic magnitude of 3.5 mag [1], while more modern measurements yield consistent values of V=1.9–2.0 mag (the *Hipparcos* magnitude is $H_p = 1.95$ mag). Already in 1847, Herschel [2] published the detection of two faint visual companions, δ Vel C and D, at $\sim 80''$ distance from δ Vel A. Even another companion, δ Vel B, had been discovered by Innes in 1895 [3]. The Washington Visual Double Star Catalogue [4] describes δ Vel as a quadruple stellar system: it reports that δ Vel consists of two pairs, AB (sep$\sim 2.6''$) and CD (sep$\sim 6''$), separated approximately by $70''$. Only recently, the most luminous component, component A, was discovered to be itself an eclipsing binary with a period of 45.15 days [5].

2 VLTI Observations of the Eclipsing Binary

The eclipsing binary δ Vel A (components designated as Aa and Ab) was observed in April and May 2003 at four orbital phases using two siderostats and the K-band beam recombination instrument VINCI on the ESO Very Large Telescope Interferometer (VLTI). In February 2005, during the AMBER science demonstration phase, medium resolution ($\lambda/\Delta\lambda = 1500$) K-band data of

Aa+Ab were obtained, using three Unit Telescopes of the VLTI. The observations were combined with observations of HD63744, for calibration purposes. We used the data reduction routines described by [6] and [7] for VINCI and AMBER data reduction, and obtained as a result 26 squared visibilities (V^2) at 5 different orbital phases.

3 Results and Discussion

3.1 Physical Parameters of the Close Eclipsing Binary (Aa+Ab)

The visibility measurements were fitted onto the model of a binary system made out of two uniformly bright circular disks, observed at K-band with filters of finite bandwidths. Five parameters of the binary model (stellar diameters D_1, D_2, position angle of the ascending node Ω, semi-major axis a, eccentricity e) were adjusted with non-linear least-squares fitting to best match the measured visibilities. Table 1 lists orbital and physical parameters corresponding to the best fit of the interferometric data, along with parameters estimated from other techniques.

Most interestingly, our results indicate stellar diameters for Aa and Ab of $6.1 \pm 0.4\ D_\odot$ and $3.5 \pm 0.6\ D_\odot$ respectively. Given the fact that many authors classify δ Vel A as A1V (e.g. [8]) much smaller diameters ($\sim 2D_\odot$) were expected. We further deduce a system's total mass of $M_{Aa+Ab} = (4.05 \pm 0.30)M_\odot$ based on the orbital period of 45.15 d and the size of the semi-major axis as constrained by our interferometric measurements.

The results need to be compared to predictions made by stellar evolutionary models. In Fig. 1 we plot the measured radii and absolute V magnitudes of δ Vel Aa and Ab against isochrones of evolutionary models published by Yi et al. [9]. The comparison suggests that the age of δ Vel is about $(0.9 \pm 0.1)10^9$yr. Separate masses of δ Vel Aa and Ab are then derived by tracing the relevant isochrones in the radius versus mass diagram, which yields $M_{Aa} = 2.23 \pm 0.10\ M_\odot, M_{Ab} = 2.15 \pm 0.10\ M_\odot$, and hence $M_{Aa+Ab} = 4.38 \pm 0.14\ M_\odot$, in agreement with the value above. Finally, the resulting locations of δ Vel Aa, Ab in the HR-diagram, assuming an age of $(0.9 \pm 0.1)10^9$yr, suggest that δ Vel Aa and δ Vel Ab are in evolved evolutionary states, i.e. have left the main-sequence.

3.2 On the Physical Association of δVel C and D

Since the observations of Herschel [2], δVel has been quoted as a visual multiple star, with δVel C and D representing the "outer" components. With apparent V magnitudes of 11.0 and 13.5 for C and D respectively [11], they should be of late spectral type, certainly no earlier than M, *if* they are at similar distance as δVel (Aa+Ab+B). To our knowledge, the only existing spectra of C and D were recorded during a survey of nearby M dwarfs [12].

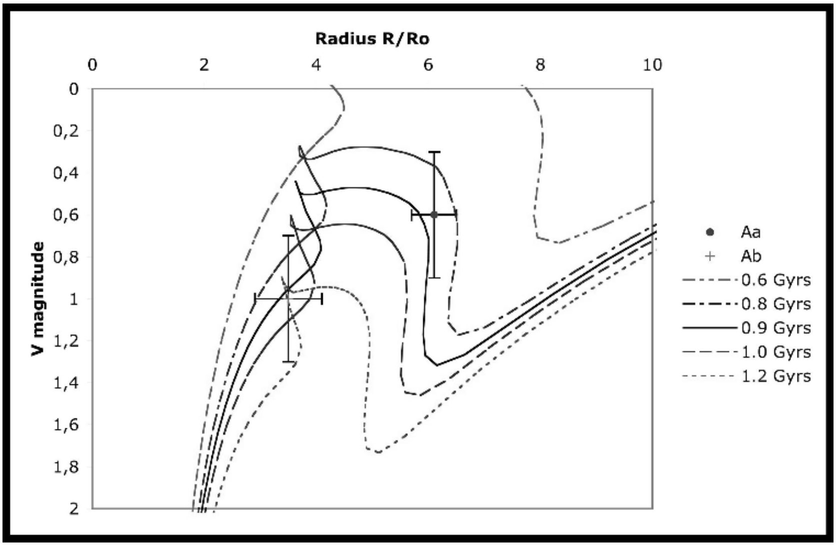

Fig. 1. Observations of δ Vel A compared to evolutionary models by [9], for solar chemical composition. The age of δ Vel A appears to be $(0.9 \pm 0.1)10^9$yr

While the limited range and resolution of the spectra precluded ready determination of the spectral types of C and D, they were nevertheless estimated as ~G8V and ~K0V. Therefore, given their apparent magnitudes, C and D must be at much further distances than δVel (Aa+Ab+B). We conclude, that δVel C and D are not physically associated and hence, δVel should be designated as a triple stellar system only.

4 Conclusions

New interferometric data of the eclipsing binary δVel A have been combined with existing photometric and spectroscopic observations in order to analyse the physical properties of this multiple system. One of our main results is that the eclipsing binary components show large radii that are incompatible with the general classification of δVel Aa, Ab as early A-type main-sequence stars. While fitting the interferometric data we also varied the stellar diameter values of δVel Aa, Ab within ranges more appropriate for main-sequence A-type stars, but it was impossible to achieve any acceptable solution this way. Our analysis therefore suggests that δVel Aa, Ab are in a post main-sequence phase of their evolution. The result is puzzling and certainly deserves further investigation. Our understanding would benefit from precise photometry during the eclipses in order to provide separate intensities of Aa and Ab and a confirmation of the ratio of their stellar diameters. Moreover, high resolution

Table 1. Parameters of δ Vel (Aa+Ab) involved in the analysis of the interferometric data. Second column: values estimated without the present interferometric measurements (References: [5, 10]). Last two columns: estimates derived from our measurements.

Parameter	estimate based on		
	light curves + astrometry	interferometry	evolutionary models
d: distance to δ Vel (Aa+Ab) [pc]	24.450±0.001		
T: orbital period [days]	45.150±0.001		
τ: fraction of orbital period from primary to secondary eclipse	0.435±0.005		
t_1: duration of primary eclipse [days]	0.51±0.05		
t_2: duration of secondary eclipse [days]	0.91±0.01		
e: eccentricity of orbit	0.300 ± 0.045	0.2581 ± 0.0004	
ω: angle of periastron [rad]	0.33±0.07	0.395 ± 0.001	
Ω: position angle of the ascending node [rad]		0.47±0.01	
a: semi-major axis [m]	$(6.0 \pm 0.4)10^{10}$	$(5.92 \pm 0.15)10^{10}$	
M_{Aa+Ab}: total mass of δ Vel (Aa+Ab) [$M_\odot$]	4.2 ± 0.7	4.05 ± 0.30	4.38 ± 0.14
M_{Aa}: mass of δ Vel Aa [$M_\odot$]			2.23 ± 0.10
M_{Aa}: mass of δ Vel Aa [$M_\odot$]			2.15 ± 0.10
$\phi = \frac{\phi_2}{\phi_1}$: surface intensity ratio	2.0±0.7		
D_1: diamater of Aa [$D_\odot$]		6.1 ± 0.4	
D_2: diameter of Ab [$D_\odot$]		3.5 ± 0.6	
Age of δ Vel [yr]			$(0.9 \pm 0.1)10^9$

spectra of (Aa+Ab) during and out of the eclipses should enable a better determination the stars' effective temperatures and luminosity classes.

References

1. Gill D., Kapteyn J. C: Ann. Cape Obs. **5**, part III (1900)
2. Herschel, J.F.W.: QB **3**, H52, Smith, Elder and co. (publisher), London (1847)
3. Innes, R.T.A.: MNRAS **55**, 312 (1895)
4. Worley C.E., Douglass G.G.: A&AS **125**, 523 (1997)
5. Otero, S.A., Fieseler, P.D., Lloyd, C.: IBVS **4999**, 1 (2000)
6. Kervella, P., Thévenin, F., Ségransan, D. et al.: A&A **404**, 1087 (2003)
7. Millour, F., Tatulli, E., Chelli, A.E. et al.: SPIE **5491**, 1222 (2004)
8. Royer, F., Gerbaldi, M., Faraggiana, R., Gómez, A.E.: A&A **381**, 105 (2002)

9. Yi, S., Demarque, P., Kim, Y-C., Lee, Y-W. et al.: ApJS **136**, 417 (2001)
10. Argyle, R.W., Alzner, A., Horch, E.P.: A&A **384**, 171 (2002)
11. Jeffers, H.M. et al.: Publications of the Lick Observatory, icvd.book (1963)
12. Hawley, S.L., Gizis, J.E., Reid, I.N. Hawley: AJ **112**, 2799 (1996)

Speckle Interferometry of Two Low-mass Triple Systems in the Solar Neighbourhood

E.V. Malogolovets[1], Y.Y. Balega[2], K.-H. Hofmann[3], D.A. Rastegaev[4] and G. Weigelt[5]

[1] Special Astrophysical Observatory Russian Academy of Sciences evmag@sao.ru
[2] Special Astrophysical Observatory Russian Academy of Sciences balega@sao.ru
[3] Max-Planck-Institut fuer Radioastronomie khh@mpifr-bonn.mpg.de
[4] Special Astrophysical Observatory Russian Academy of Sciences leda@sao.ru
[5] Max-Planck-Institut für Radioastronomie weigelt@mpifr-bonn.mpg.de

1 Introduction

Multiple systems with low levels of hierarchy are important targets for the study of formation, evolution, and dynamical stability of multiple stars. Two such triple stars with low mass components, GJ 900 and KUI 99, have been observed during the last six years at the 6 m BTA telescope (Zelenchuk). The first object is a young system with projected distances between the components in the range of 200-700 mas. The second one is a group of middle-aged K dwarfs.

In the V and I bands, the observations were performed using the speckle camera described in [7]. In the K-band the data were obtained with the speckle camera of the Max-Planck-Institut fuer Radioastronomie in Bonn. The mean square error of the speckle measurements is 2-4 mas, depending on seeing conditions. The speckle images were reconstructed using the triple correlation method [6]. Below, we present the results of the relative motion study in the systems and give conclusions about their hierarchy.

2 GJ 900

GJ 900 is a young nearby (π_{hip}=51.8 mas) K7 star. It was first resolved as a triple system with speckle interferometry at the 6 m BTA telescope in November 2000. The bispectrum reconstruction of the K-band image is shown in Fig. 1. Later, the system was observed in the H and K bands with the 8 m Subaru telescope using adaptive optics [8]. From the apparent configuration of the components, it was supposed that it could be a low-mass Trapezium-type system. If this is the case, GJ 900 is the first known Trapezium-type star at the bottom of the main sequence.

Presently, 4 speckle interferometric observations and 2 adaptive optics measurements allow us to follow the relative motion of the components. Speckle photometry gives the following magnitude differences between the stars: $\triangle I_{AB}$=2.42±0.08, $\triangle I_{AC}$=3.67±0.22, $\triangle K_{AB}$=1.92±0.18,

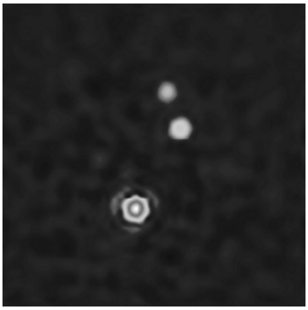

Fig. 1. The bispectrum reconstruction of the GJ 900 image in the K-band

$\triangle K_{AC}$=2.55±0.30. These differences are approximately 0.2 mag larger than those given by adaptive optics. With magnitude differences in the I-band and Hipparcos parallaxes in hand, we obtain the following absolute magnitudes for the components: M_{IA}=10.5, M_{IB}=12.9, M_{IC}=14.2. The corresponding spectral types of the individual stars are: K7, M5 and M7.

The relative positions of the AB pair changed linearly during the period 2000-2004, showing a mean motion of 48 mas/yr (Fig. 2). The angular separation in the AC pair remains constant within the errors of measurements. These observations are represented in Fig. 3. We expect that the period of the AB pair lies between 50 and 100 yrs, while for the AC subsystem it can be over 1000 yrs. It looks as if the GJ 900 apparent configuration is caused by a chance projection.

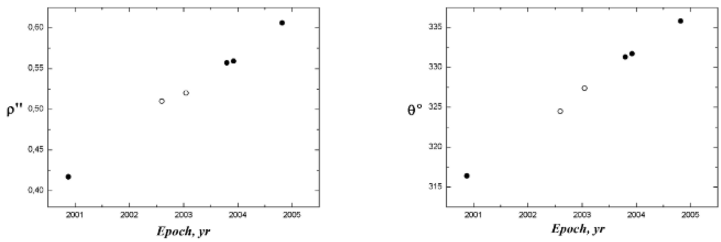

Fig. 2. Relative positions for GJ 900 AB between 2000.8754 and 2004.8208. Filled circles are from the 6 m BTA speckle measurements; open circles are the adaptive optics data from Martin [8]

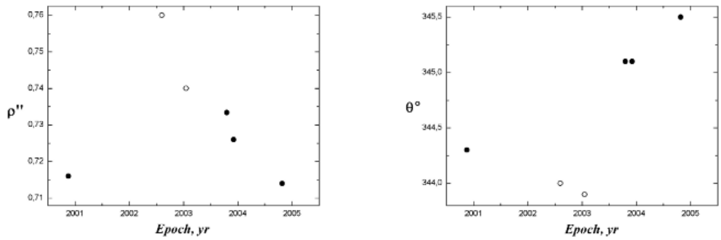

Fig. 3. Relative positions for GJ 900 AC between 2000.8754 and 2004.8208

3 KUI 99=GJ 795

KUI 99 is a late-type K star from the solar neighbourhood (π_{hip}=53.82 mas). In 1943, Kuiper [5] first resolved KUI 99 as a visual binary star. Duquennoy [3] found that the brighter component of KUI 99 is itself a spectroscopic binary. Orbital solutions for the outer pair were proposed by Baize [1], Heintz [4] and Soderhjelm [10]. In 1998, KUI 99 was directly resolved as a triple star for the first time using the speckle interferometer at the 6 m BTA telescope [2]. The differential magnitude speckle measurements showed that the components B and C have similar brightness: $\triangle m_{AB}$=0.94±0.03, $\triangle m_{AC}$=1.14±0.03. Differential speckle photometry and Hipparcos parallax give the following absolute magnitudes and spectral types for the stars: M_{VA}=7.2, M_{VB}=8.1, M_{VC}=8.3 and K4, K7 and K8.

Interferometric orbits for the AB and AC pair can be derived from the 1998-2004 data. The apparent ellipses of the KUI 99 AC and KUI 99 AB pair are shown in Fig. 4

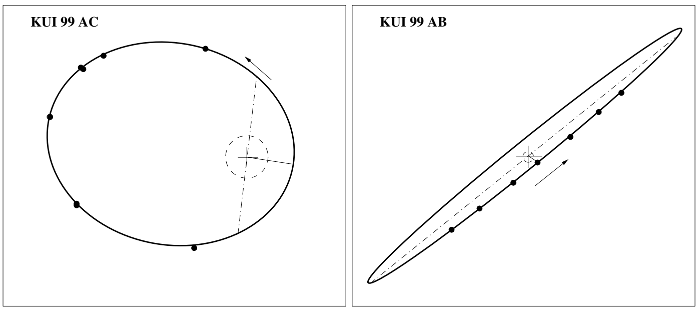

Fig. 4. Speckle interferometric orbits for the inner (KUI 99 AC) and the outer (KUI 99 AB) pair. The line of nodes is shown by the dash-dotted line. The arrow shows the direction of motion. North is up, east is to the left. The dashed circle has a radius of 20 mas

For the inner AC pair the speckle orbit parameters are in good agreement with the spectroscopic orbit of Duquennoy [3]. The orbital elements for the inner and outer subsystems are given in Table 1.

Table 1. Orbital elements for the inner (KUI 99 AC) and outer (KUI 99 AB) pair

Comp.	P(yr)	T	e	a(″)	i°	Ω°	ω°
AC	2.51 ± 0.01	2000.55 ± 0.01	0.620 ± 0.006	0.120 ± 0.002	18.2 ± 2.5	173.6 ± 10.9	87.1 ± 10.3
AB	39.55 ± 0.37	2001.83 ± 0.07	0.161 ± 0.075	0.690 ± 0.074	85.9 ± 0.8	128.6 ± 0.4	92.0 ± 0.8

We can state from the orbital solutions that KUI 99 is a low-hierarchical system with an angle between the two orbital planes of about 70°. It is necessary to continue the monitoring of the relative motion in the systems in order to detect possible oscillations of the orbital parameters, which can be caused by the Kozai mechanizm [9].

References

1. P. Baize: A&AS **44**, 199 (1981)
2. I.I. Balega, Y.Y. Balega, K.-H. Hofmann et al: A&A **385**, 87 (2002)
3. A. Duquennoy: A&A **178**, 114 (1987)
4. W.D. Heintz: A&AS **56**, 5 (1984)
5. G.P. Kuiper: PASP **46**, 285 (1934)
6. A.W. Lohmann, G. Weigelt, B. Wirnitzer: Appl. Opt. **22**, 4028 (1983)
7. A.F. Maksimov, Y.Y. Balega, U. Beckmann et al: Bull. Special Astrophys. Obs. **56**, 25 (2003)
8. E. Martin: AJ **126**, 918 (2003)
9. S. Soderhjelm: A&A **107**, 54 (1982)
10. S. Soderhjelm: A&A **341**, 121 (1999)

Tertiary Companions to Close Spectroscopic Binaries

A. Tokovinin[1], S. Thomas[1], M. Sterzik[2] and S. Udry[3]

[1] Cerro Tololo Inter-American Observatory, Casilla 603, La Serena, Chile
atokovinin, sthomas@ctio.noao.edu
[2] European Southern Observatory, Casilla 19001, Santiago 19, Chile
msterzik@eso.org
[3] Observatoire de Genève, CH-1290 Sauverny, Switzerland
Stephane.Udry@obs.unige.ch

Summary. Preliminary results of a survey of nearby solar-type spectroscopic binaries (SB) with orbital periods $1 < P_1 < 30$ days for tertiary companions are presented. Observations with adaptive optics and data from the 2MASS sky survey permitted to discover new tertiary components and to sharpen statistical limits on their frequency. We find that 0.86 ± 0.07 SBs with $P_1 < 5$ d have tertiaries, but this fraction drops to 0.49 ± 0.06 for $P_1 > 5$ d. The periods of tertiary companions are distributed in a wide range, from 2 to 10^5 yr, with most frequent periods of few thousand years.

1 The Goals and the Sample

All binaries were likely formed by fragmentation of molecular clouds with subsequent dynamical evolution. The formation of close binaries remains an unsolved problem, however [1]. It is believed that some mechanisms of angular momentum transport lead to shrinkage of their orbits. But were is that angular momentum deposited? Larson [4] argues that the momentum goes to a more distant tertiary component (or components). Current data indicate that almost half of spectroscopic binaries (SB) with periods below 10 d indeed have such companions [6], and it is possible that *all* close SBs are triple. Here we put this hypothesis to a stringent observational test.

We define a sample of SBs where the chance of discovering tertiary companion is maximized: nearby (within 100 pc) solar-type dwarfs with periods between 1 d and 30 d, selected from the catalogue of spectroscopic orbits, recent literature, and ongoing CORALIE survey. The sample contains 166 SBs belonging to 161 stellar systems. Some primaries turn out to be moderately evolved, despite their short orbital periods. The masses of spectroscopic components were estimated from spectral types and orbital parameters. Data on known wide components come from [5].

Using a combination of complementary observing techniques, it is possible to put strong constraints on potential tertiaries. Each method has its own detection range, depending on the tertiary period P_3 and the mass ratio q_3 (q_3

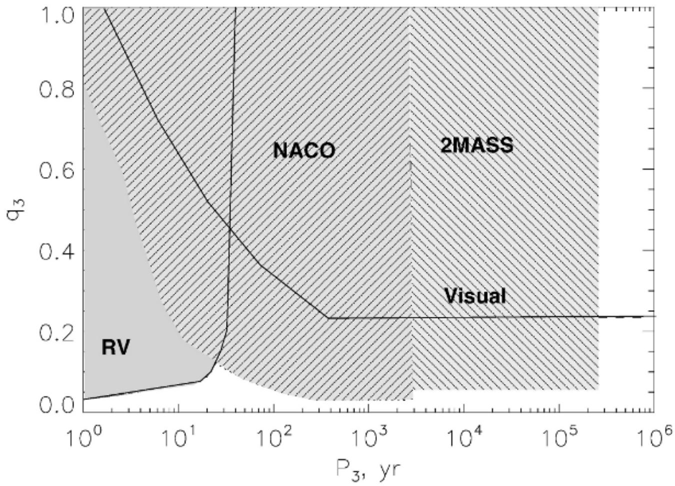

Fig. 1. Limits for detecting a tertiary component by different techniques as a function of tertiary period P_3 and its mass ratio q_3, for one target HIP 2790. Radial velocities (RV) cover short periods, adaptive-optics observations (NACO) probe companions with periods less than ~3000 yr, still wider components can be detected with 2MASS, if not known already from historical visual and proper motion surveys

is defined here with respect to the spectroscopic primary, rather than total mass of the SB). Figure 1 illustrates these limits for one specific system.

2 Adaptive Optics Observations

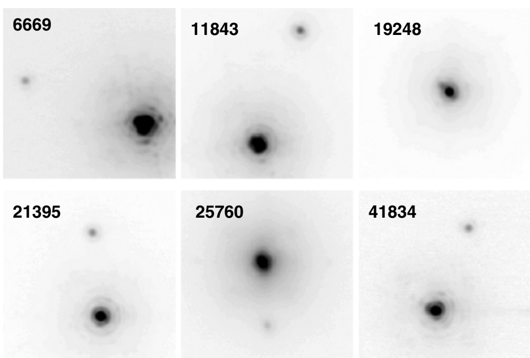

Fig. 2. Examples of new components detected with adaptive optics. The HIPPARCOS numbers of each target are given. The field size is $2'' \times 2''$

High spatial resolution images of target stars have been obtained using the NAOS-Conica adaptive optics system[4] mounted at the VLT on November 8-9, 2004. We observed 52 targets and two astrometric calibrators in a narrow-band filter centered at the wavelength 2.12 μm, to avoid detector saturation. Only targets without known tertiary components (or with very distant tertiaries) were on this program. We detected 11 certain and 3 suspected tertiaries among 52 targets (Fig. 2). The observations were pursued in July 2005, but these data are not included in the present analysis.

3 Search of Companions in 2MASS

The SBs were examined for the presence of wide visual companions using Two Micron All-Sky Survey (2MASS) and Digital Sky Survey (DSS). The JHK_s photometry provided by 2MASS enabled us to construct $J_{\rm abs}, (J-K)$ color-magnitude diagrams for all stars within 2 arcmin. radius from each target. The standard main sequence (MS) was traced as well because the distance to each SB is known. All stars within 0.2^m from the MS were considered as photometric candidates, i.e. potential physical companions. We checked that this criterion selects known physical companions, but it cannot be made "sharper" without risk of losing companions.

Among 6079 point sources around our targets, 202 photometric candidates were selected. Most of these stars, of course, are optical, as can be inferred from their statistics (mostly faint and distant from targets). A chance of detecting a *real* physical component depends on the total number of point sources in each field, N_*. We abandoned 1/3 fields with $N_* > 40$ (near the Galactic plane) where confusion makes the companion search hopeless. For the remaining targets, we found 35 new candidates, in addition to those previously known. New candidates with separations above $20''$ were then checked for common proper motion by comparing their positions in 2MASS and DSS, on a time base ranging from 10 to 50 yr. We finally retrieved from 2MASS 22 known and 13 new companions (8 certain and 5 tentative, i.e. still unconfirmed).

4 Parameters of Tertiary Companions

Known and new tertiary companions are plotted in the (P_3, q_3) plane in Fig. 3. Their masses are estimated from magnitude difference with the help of standard MS relations, their orbital periods are evaluated statistically by the third Kelper's law from the separations, unless known from exact orbital solutions. Indicative detection limits for the whole sample are also shown.

[4] `http://www.eso.org/instruments/naco`

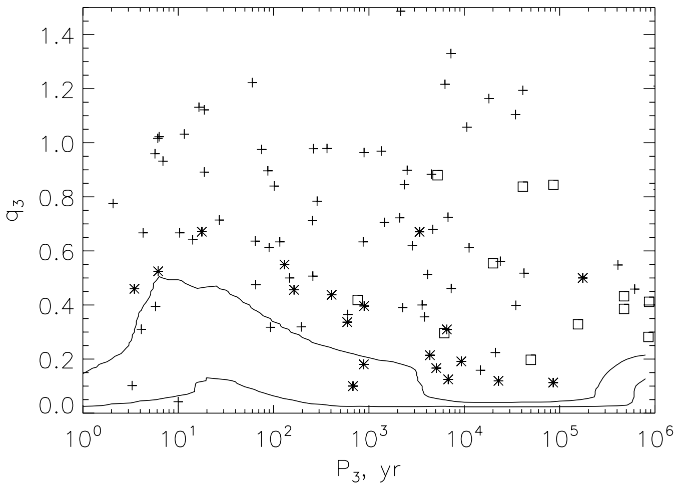

Fig. 3. Mass ratios and periods of tertiary companions. Known components are plotted as pluses, new components as asterisks. The squares denote components at the next hierarchical level, not considered in the main statistics. The lines trace detection probabilities of 10% and 50%

For comparison, Fig. 3 shows even more distant, higher-level companions (squares) that dominate at the longest periods. Hence, the paucity of tertiaries with $P_3 > 10^5$ yr is real, not a selection effect. Similarly, we see only few tertiaries with $P_3 < 3$ yr (the shortest period is 2.1 yr), despite a good coverage of this region by spectroscopy. Discovering spectroscopic tertiaries with periods of few years is relatively straightforward, so that many more would have been known now if they were really abundant.

New components have, mostly, low mass ratios q_3. On the other hand, some previously known tertiaries are more massive than their respective spectroscopic primaries. The fraction of tertiaries with $q_3 > 1$ is 0.18 ± 0.04 – still smaller than 1/3 expected for a random choice of component masses. Thus, there is a tendency for the most massive companions of each system to belong to the SB.

We looked for correlations between orbital parameters of SBs and those of tertiaries and found that SBs with tertiaries have, on average, shorter orbital periods P_1 (Fig. 4). The difference of period distributions between SBs within triple (or higher-order) multiples and "simple" SBs is highly significant. Considering that there are still undiscovered triple stars in the sample, this difference is in fact even larger. If all SBs were triple, no such difference of their period distributions would be expected. We consider Fig. 4 as a strong (although indirect) proof that *SBs without tertiary companions do exist.* On the other hand, the distributions of the mass ratio of SBs with and without

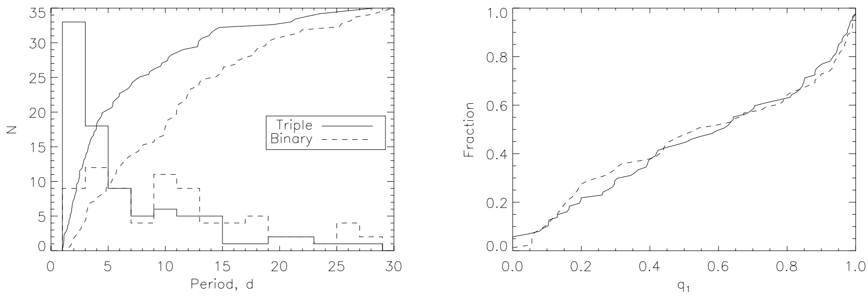

Fig. 4. Distributions of periods (left) and mass ratios (right) of spectroscopic binaries with (full lines) and without (dashed lines) tertiary components

tertiaries are indistinguishable. No correlation between the periods of SBs and tertiaries is apparent in Fig. 5. Unlike visual triples, all systems in our sample are quite far from the dynamical stability limit $P_3/P_1 \sim 5$.

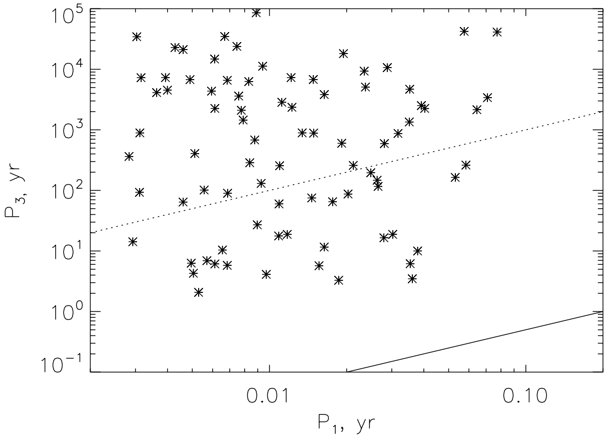

Fig. 5. Comparison of tertiary periods P_3 with the SB periods P_1. The full line denotes the stability limit $P_1 = 5P_3$, the dotted line corresponds to the period ratio of 10 000

The true frequency of tertiary components in our sample has been determined by taking into account known selection effects. We used the maximum likelihood technique for estimating unbiased distribution of tertiaries in (P_3, q_3) coordinates, and for deriving the errors of such estimates. The analysis of the whole sample has been complemented by the analysis of subsamples, split accordingly to SB periods. It could be anticipated from Fig. 4

Table 1. Frequency of Tertiary Components

Sample	N	f
$P_1 < 5$d	72	0.86 ± 0.07
$P_1 > 5$d	94	0.49 ± 0.06
All	166	0.66 ± 0.05

that short-period SBs have a higher fraction of tertiary components, and the actual numbers in Table 1 confirm this.

The frequency of tertiaries can be compared to the frequency of wide binary companions to field dwarfs with periods above 1 yr, which is about 50% [2]. It is indistinguishable from the observed proportion of tertiaries among long-period SBs. On the other hand, almost all short-period SBs are triple. However, even in this group the existence of pure binaries cannot be excluded: we estimate their fraction as 14% ± 7%.

5 Discussion

We establish that the frequency of tertiary companions to close ($P_1 < 5$ d) SBs is higher than for wider SBs. In other terms, the period distributions of SBs with and without tertiaries are different. This points to the mechanism of Kozai cycles with tidal friction (KCTF) [3] as a way of creating SBs with periods of few days. The KCTF process works even for very wide and low-mass tertiaries, although it may take a long time to act.

Some SBs could have had wide companions that were later stripped away by dynamical interactions with members of their primordial clusters, preventing or restricting KCTF evolution. These SBs have, on average, longer orbital periods than SBs within multiple systems. These periods are still too short to be explained by fragmentation, however. We speculate that the period distribution of "pure" binaries (Fig. 4, dashed line) may be close to the initial period distribution, unmodified by the KCTF. The origin of these short periods can be tentatively related to processes like disk braking and accretion.

References

1. M.R. Bate, I.A. Bonnell, V. Brown: MNRAS **336**, 705 (2002)
2. A. Duquennoy, M. Mayor: A&A **248**, 485 (1991)
3. P. Eggleton, L. Kiseleva-Eggleton: ApJ **562**, 101 (2001)
4. R.B. Larson: MNRAS **332**, 155 (2002)

5. A. Tokovinin: A&AS **124**, 75 (1997)
6. A. Tokovinin: Statistics of multiple stars: Some clues to formation mechanisms. In: *The formation of binary stars*, ASP Conf. Ser., vol. 84, ed. by H. Zinnecker, R.D. Mathieu (ASP, San Francisco 2001) pp 84–92

Spectroscopic Subcomponents in Visual Double Stars: The Most Probable Values of their Physical and Orbital Parameters. Application to the System WDS 14404+2159

José A. Docobo and Manuel Andrade

Astronomical Observatory R.M. Aller
Universidade de Santiago de Compostela
P.O. Box 197
Santiago de Compostela, Spain
oadoco@usc.es, oandrade@usc.es

Summary. Double stars with spectroscopic subcomponents are very interesting objects from many points of view. In this way, determination of their orbits and masses has become a key step in its study. We show a method that allows to calculate, both from orbits and Hipparcos parallax, the most probable values of all stellar masses, spectroscopic binary inclination, angular separation between their components and even a spectral types' estimate. We apply this method to triple system WDS 14404+2159 (a double star with a single-lined spectroscopic subcomponent) and compare our results with other estimations.

1 Methodology

1.1 Notation

We will use 1, 2 and 3 subscripts to refer to Aa, Ab and B components, respectively. M_j will be the absolute magnitude of the component j; m_j, the apparent visual magnitude and $\mathcal{M}_j$, its mass. The subscript 12 is used to refer to the spectroscopic subsystem. Moreover, ΔM will be the difference between absolute magnitudes of the components of the spectroscopic subsystem.

Once we have calculated the masses, the semi-major axis and the inclination of the spectroscopic orbit can be computed. New apparent visual magnitudes are also given, as well as spectral types of all components.

The semi-major axis and inclination can be added to the known spectroscopic orbital elements. Therefore, the angle of node will be the only orbital element that remains unknown.

1.2 Jaschek's Criterion

If the subsystem is a single-lined spectroscopic binary, we can suppose from [1] that $\Delta M = M_2 - M_1 \geq 1$.

1.3 Basic Steps

Compatible Parallax Values

We compute the parallax by means of:

$$\log \pi = \frac{M_1 - m_{12} - 5}{5} - \frac{1}{2}\log(1 + 10^{-0.4\Delta M}). \tag{1}$$

Eq. 1 provides the parallax values depending on M_1 and ΔM, which are compatible with the margin of error given by Hipparcos.

For each value of M_1 and π, we calculate the corresponding value of M_2 (obtained from ΔM) and M_3 (inferred from m_3 and π).

From now on, we will work with mean values of the three absolute magnitudes and the mean parallax.

Estimation of Spectral Types and Masses

The spectral types will be estimated from the calibration given in [2], and the individual masses will be calculated from a statistical fit given in [3] and reproduced here in Table 1. These equations, valid only for a certain range of spectral types, Table 1, give functional relations between the mass and the spectral type for components of a binary system, where the coefficients a and b take several values depending on the luminosity class. On the other hand, s is a continuous variable defined in [4] that represents the spectral class.

Table 1. Estimation of masses $\mathcal{M}$ from the spectral type s

$\mathcal{M}$	a	b	Spectral range
$(a + b\,e^{-s})^2$	1.34 ± 0.17	20.8 ± 2.5	$B4 - K4$
$a\,s^b$	19.29 ± 0.86	-1.660 ± 0.065	$B0.5 - K3.5$
$a + \frac{b}{s^2}$	-0.117 ± 0.090	27.47 ± 0.61	$B0.5 - M6$

Note: Here e is the number e.

Moreover, the mass function for the spectroscopic binary is:

$$\frac{(\mathcal{M}_2 \sin i)^3}{(\mathcal{M}_1 + \mathcal{M}_2)^2} = 3.985 \cdot 10^{-20} k_1^3 P (1 - e^2)^{\frac{3}{2}}, \tag{2}$$

with $\mathcal{M}_1$ and $\mathcal{M}_2$ the masses of components 1 and 2, respectively; i, the inclination; k_1, the radial velocity amplitude; P, the period; and e, the eccentricity. In this way, we can estimate the minimum mass and the latest spectral type of the secondary spectroscopic component.

2 Application to WDS 14404+2159

2.1 Data

HD 129132 is known as a triple system, see [5]. Its Hipparcos parallax is $\pi_{\rm Hip} = 9.47 \pm 0.71$ mas.

The combined apparent magnitude of the spectroscopic subsystem is $m_{12} = 6.05$, while the magnitude of the visual component B is $m_3 = 7.1$.

The visual binary orbit was calculated by Barlow and Scarfe [6], who obtained a period of $9.^y268 \pm 0.^y019$ and a semi-major axis of $0.''074 \pm 0.''001$. From the same reference we take the following orbital elements of the close pair: $P = 101.^d606 \pm 0.^d008$, $e = 0.117 \pm 0.007$, $\omega_1 = 140.^\circ7 \pm 2.^\circ9$ and $K_1 = 19.0 \pm 0.1$ km s^{-1}.

2.2 Results

Table 2. The final results for WDS 14404+2159

$\mathcal{M}_1$ ($\mathcal{M}_\odot$)	2.66 ± 0.24	Sp_1	A3IV
$\mathcal{M}_2$ ($\mathcal{M}_\odot$)	1.44 ± 0.10	Sp_2	F2V
$\mathcal{M}_3$ ($\mathcal{M}_\odot$)	2.13 ± 0.10	Sp_3	A5V
$\mathcal{M}$ ($\mathcal{M}_\odot$)	6.23 ± 0.28		
π (mas)	9.48 ± 0.30	M_1	1.14 ± 0.05
a (AU)	7.81 ± 0.27	M_2	2.98 ± 0.07
a_{12} (AU)	0.656 ± 0.023	M_3	1.99 ± 0.17
a_{12} (mas)	6.22 ± 0.29	m_1	6.26 ± 0.05
a_1 (AU)	0.231 ± 0.019	m_2	8.09 ± 0.07
i (°)	$49.8(130.2) \pm 5.5$	m_3	7.11 ± 0.17

The results are shown in Table 2 and the orbit is drawn in Fig. 1. We have also calculated the maximum separation of the spectroscopic subsystem $\rho_{\rm max} = 6.78$ mas.

A plausible model for this system is given in [6], with $\mathcal{M}_1 = 1.97\ \mathcal{M}_\odot$, $\mathcal{M}_2 = 1.29\ \mathcal{M}_\odot$ and $\mathcal{M}_3 = 1.82\ \mathcal{M}_\odot$. Later, different values were calculated by [7] with the total mass ($6.633 \pm 1.694\ \mathcal{M}_\odot$) about 30% larger than the previous estimate by [6] ($5.08\ \mathcal{M}_\odot$) and about 6.6% larger than the mass obtained by us ($6.22 \pm 0.28\ \mathcal{M}_\odot$). The estimation given in [6] for the inclination ($i = 45°$) is in good agreement with our result, $i = 49.^\circ8 \pm 5.^\circ5$.

3 Remarks

Although in this work we are dealing with single-lined spectroscopic binaries, we know that this method can also be applied to double-lined spectroscopic binaries. Usually, in this case, we can expect even more accurate results.

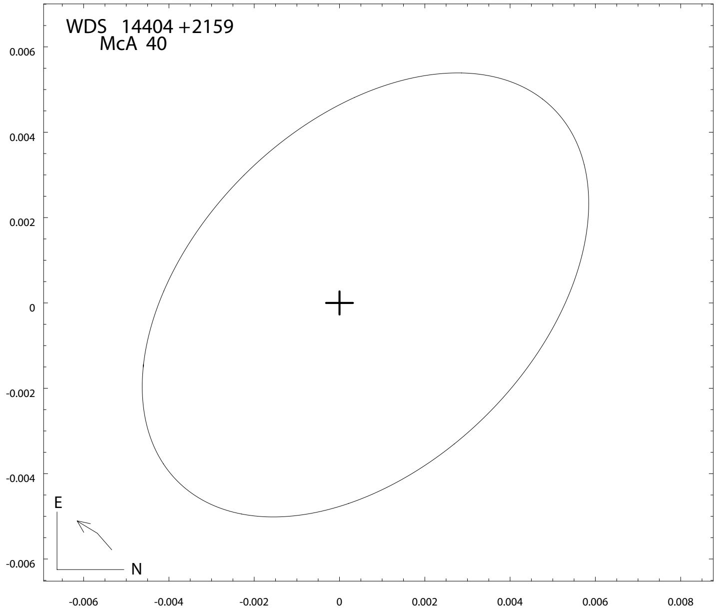

Fig. 1. Apparent orbit of the spectroscopic sub-component in WDS 14404+2159. Axis scale in arcseconds

With regard to the possibility of optically resolving these systems, it can be noted that angular separations will never be larger than a few miliarcseconds.

Theoretically, it would be possible to determine the direction of the motion in the spectroscopic orbit by studying the perturbations due to the visual component B. A secular increase of the argument of periastron will suggest retrograde motion ($i > 90°$), while its decrease will correspond to a direct motion ($i < 90°$).

References

1. C. Jaschek, M. Jaschek: *The Classification of Stars*, 1nd edn (Cambridge Univ. Press 1987)
2. D.F. Gray: *The Observation and Analysis of Stellar Photospheres*, 2nd edn (Cambridge Univ. Press 1992) pp 430–434
3. N.A. Belikov: BICDS **47**, 9 (1995)
4. C. de Jager, H. Nieuwenhuijzen: A&A **177**, 217 (1987)
5. W.E. Harper, G.H. Blanchet: Publ. DAO **7**, 99 (1937)
6. D.J. Barlow, C.D. Scarfe: AJ **102**, 2098 (1991)
7. C. Martin, F. Mignard, W.I. Hartkopf, H.A. McAlister: AASS **133**, 149 (1998)

Multiple Stars in the Field

Brian D. Mason[1,2] and William I. Hartkopf[1,3]

[1] U.S. Naval Observatory 3450 Massachusetts Avenue NW, Washington, DC 20392-5420 USA
[2] bdm@usno.navy.mil
[3] wih@usno.navy.mil

Summary. When examining the statistics of multiple stars in the field, especially coming from visual binary star point of view, several problems present themselves. First, and most importantly, is distinguishing between physical multiples and optical pairs. Establishing physicality is not a simple "binary" response as there are degrees of certainty. We discuss some of the reasons for caring about non-physical pairs, as well as the tools for establishing or more correctly identifying apparent kinematic properties which hopefully result in dynamic solutions. The Washington Double Star Catalog, the Visual Orbit Catalog, and the US Naval Observatory speckle program are used as examples in many of these cases. The magnum opus for a global characterization of these systems is the Washington Multiplicity Catalog (WMC). Selected as a catalog and a method to "develop a simple, unambiguous, flexible, and computer friendly designation scheme for stellar companions (including planets)" at a multi-commission meeting in Manchester (GA24). This was re-affirmed at Special Session 3 in Sydney (GA25) by Commissions 5, 8, 26, 42, 45 and the Working Group on Interferometry when a sample (1/2 hour band) WMC was produced. An all-sky WMC is in progress the binary sources utilized in its construction and the implications resulting from it with regards to multiple stars in the field are discussed.

1 It's the WDS, not the WBS!

Double Stars are not necessarily Binary Stars![1]

1.1 Who Cares about Doubles?

Since binaries are physical pairs and optical doubles are geometrical constructs, one may well ask: are doubles of any value, and if so, what? Distinguishing between these two has primarily been more a problem for imaging techniques than for other methods. For the WDS we keep track of doubles as well as binaries for several reasons:

[1]While this talk will periodically focus on binaries rather than physical multiples, the same principles apply.

– We don't know which doubles are binary. Characterizing a pair as a binary requires some sort of Keplerian arc to be distinguished or some other parameter such as the system binding energy to be known. Until physicality is established many doubles are simply unknown possible pairs.

– We don't want to keep "discovering" new pairs. Once a pair is established as optical, retaining it in the databases but flagged it as optical can save resources spent chasing down possible binaries.

– The psf of imaging as well as spectroscopy and photometry are affected by unresolved pairs and the scattered light of wider pairs. For example, many doubles detected by Tycho were anomalous grid-step ghost doubles caused by scattered light from nearby bright stars.

– Differential proper motions from the WDS are often more accurate than those derived through more classical proper motion techniques [11]. This is due to the often much longer observational baseline, although the $\sqrt{N}$ improvement due to frequent observations is also a factor.

– Well characterized linear motion systems may be better scale calibrators than even definitive orbits.

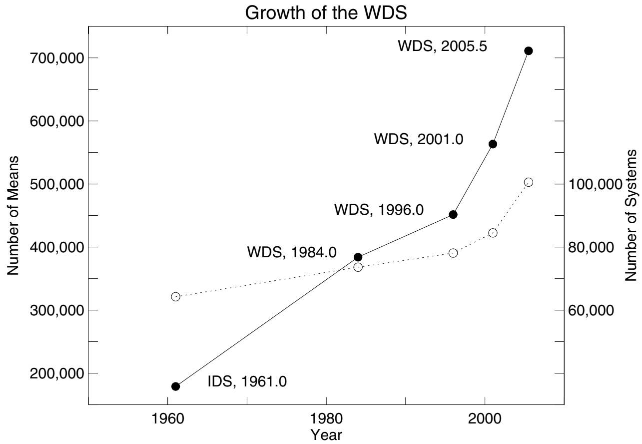

Fig. 1. Over the past twenty years the WDS has grown substantially: a 37% increase in numbers of systems (open circles) and an 85% increase in numbers of measures (filled circles). The first edition (1984) included 5.22 mean positions per pair. This number has improved with each subsequent edition (1996: 5.78 means/pair, 2001: 6.67 means/pair) to the current value of 7.11 mean positions per pair.

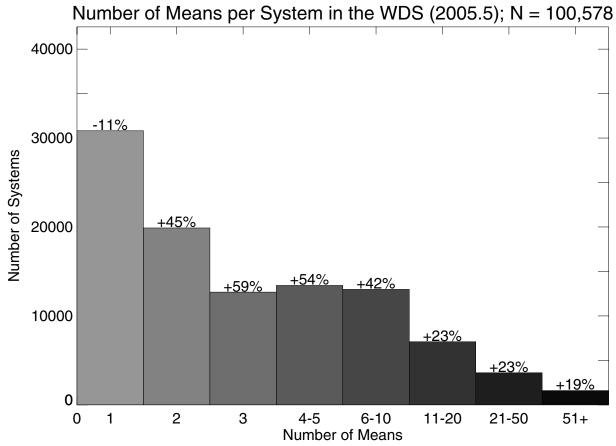

Fig. 2. The number of means per system, compared with the 1996 edition of the WDS. Despite the large number of new systems added to the catalog from Hipparcos, Tycho, etc. over the past 9 years, all bins except for the first have increased, as more systems have received follow-up observations.

1.2 Growth of the WDS

1.3 How do we Find Physical Binaries and Multiples?

There are a variety of methods for distinguishing between optical doubles/multiples and physical binaries/multiples. "Separating the wheat from the chaff" requires some sort of parameter that characterizes a pair of stars as either gravitationally bound or chance alignment. These include:

– orbits (or some portion of a Keplerian arc),
– common proper motion (although pairs may be physically related, this relationship could be tenuous),
– common parallax (i.e., at the same approximate distance), and
– proximity (in other words, just close to each other in an angular sense).

2 Orbits

Absolutely, positively, without a doubt binaries (most of the time).

In addition to establishing physicality there are many compelling reasons for observing binaries to measure orbital motion — mass being the most obvious.

2.1 Combined Solution Orbits

The "best case" orbits are those which have gone through numerous revolutions. Sometimes, however, a small magnitude difference may result in two possible solutions (with periods $\sim P$ and $2P$). Other parameters can often help determine which solution is correct.

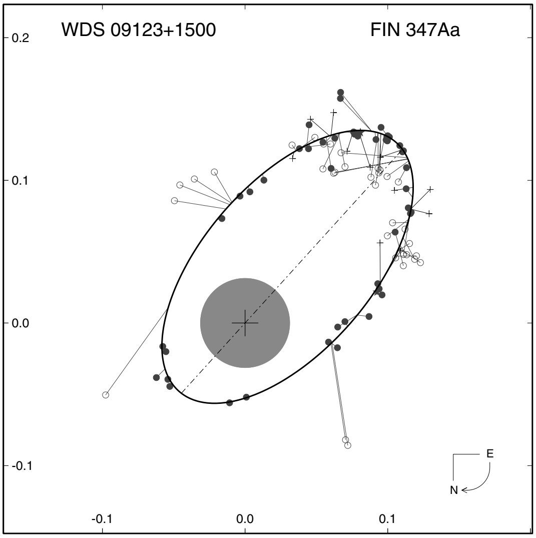

Fig. 3. Astrometric orbit plot of FIN 347 (= 81 Cancri), data 1959-2001, P = 2.7yrs., 14 rev. Scales are in arcseconds, and the large shaded region represents the resolution limit of a 4-m telescope. Filled and open circles indicate measures by speckle and eyepiece interferometry, respectively. See [13] for relative astrometry which uses the spectroscopic orbit from [5].

2.2 Preliminary Orbits

There are a variety of reasons, some scientific and others more sociological, why visual binary orbits are often calculated when orbital coverage is still marginal. The long orbital period relative to the scientist's career is a factor, but usually there is a compelling reason why the orbit should be calculated. Even with scant coverage, the astrophysically important derived parameter

$$3log(a) - 2log(P)$$

is often not grossly erroneous. Also, physicality is often ascertained from some other parameter, such as common parallax or proper motion, which would seem to indicate that any apparent motion may be more than "two ships passing in the night."

Regardless, many binaries have solutions which can be generously called "preliminary" and might more accurately be called "indeterminate" (or "nearly worthless"). The criteria for characterizing visual binary orbits are clearly spelled out in the *Sixth Catalog of Orbits of Visual Binary Stars* [7]. Figure 4 gives an example of a less well determined orbit.

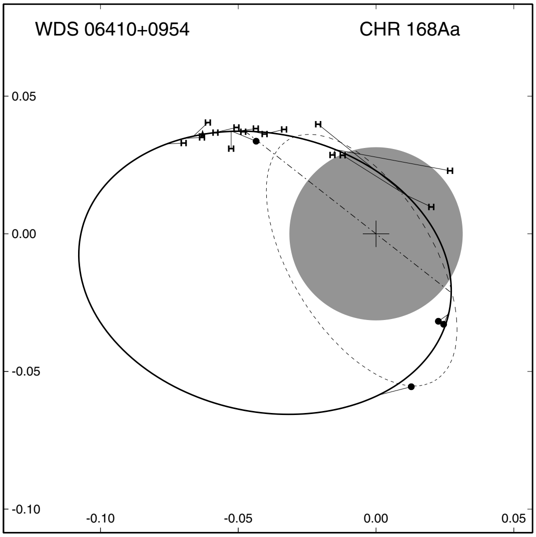

Fig. 4. Preliminary orbit of 15 Mon, from data taken with the CHARA and USNO speckle cameras, the Navy Prototype Optical Interferometer, and HST. The NPOI measure is a filled circle. Speckle measures are open circles (CHARA) or stars (USNO). HST-FGS measures are indicated by the letter **H**. The dot-dash line is the line of nodes, and the dotted ellipse is the orbit of [4]. The large shaded region represents the resolution limit of a 4-m telescope. HST measures were of noticeably lower quality in 1996-97 when FGS3 was in use. All later HST data were taken with FGS1r.

3 Common Proper Motion

Are they binaries or are they simply members of the same moving group?

3.1 Proper Motion Doubles

The first known major survey for common proper motion (CPM) pairs was that of S.W. Burnham. He found 360 BUP pairs, which at present have an average of 4.14 measures/system. Since his work in the early part of the 20^{th} Century, 15 of them (4%) have been determined to have linear solutions and thus are likely non-physical doubles.

Around the middle of the last century H. Giclas and collaborators at the Lowell Observatory began an examination for additional CPM pairs. They found 197 GIC pairs (currently with 2.48 measures/system), all of which are apparently physical.

The greatest contribution, by far, was that of W.J. Luyten. Over the course of nearly 50 years he found 6,170 LDS pairs whose proper motion indicated they were related. Only two presently have linear solutions, which could be due either to better proper motions available to Luyten or (more likely) to the small number of observations to date (only 1.67 measures/system). This low observation rate is due to the faintness of targets and the difficulty in finding them. Due to the tireless work of Richard Jaworski [9], about $\frac{2}{3}$ of the LDS pairs now have modern $0''\!.1$ positions and the number of measures per system will increase once these coordinates have been matched against other deep astrometric catalogs.

Recent work has been done by John Greaves using UCAC2 to look for CPM pairs. He has found 1143 GRV pairs thus far, but there is as yet only 1 meas/sys, limited to a portion of the Northern hemisphere. Before additional searches of this type are carried out it may be more appropriate to wait for the all-sky UCAC3, which will come out in 2006. Totalling about 60 million stars, UCAC3 will include final block adjustments and solutions for tens of thousands of doubles too close for earlier reduction. The expected precision of the proper motions will be primarily a function of magnitude: 2 mas/yr to 13^{th} mag and 4-6 mas/yr for those fainter.

Future proper motion work may include re-analysis of AGK2 data, now in process at USNO, which will supersede the AC data and give 1 mas/yr proper motion to 13^{th} mag for stars north of $2^\circ\!.5$.

4 Common Parallax

True Nearest Neighbors

Components of pairs with different parallaxes in the Hipparcos Catalogue were examined to see if they were actually close to each other. These included separate parallax values for Component (C) solution doubles in Vol. 10 of the Hipparcos Catalogue as well as the double entry systems. This work, done by USNO Summer Student Will Levine, defined pairs as physical if

$$|\pi_A - \pi_B| < \frac{3}{4}(\sigma\pi_A + \sigma\pi_B)$$

and optical if

$$|\pi_A - \pi_B| > \sigma\pi_A + \sigma\pi_B.$$

Following these criteria, 11,564 pairs were determined to be physical, with 234 optical and 6,998 indeterminate. Referring back to §2, four pairs with orbits of the lowest grade (5) have statistically different parallaxes and are probably optical.

5 Proximity

Binaries or physical multiples identified by compelling closeness.

The closer one "looks" for companions the less likely is the chance of random alignment. High-resolution techniques typically observe pairs with separations under an arcsecond, with some techniques reaching the sub-milliarcsecond level. The fact that these techniques, especially dilute aperture interferometry, are limited to the brightest (and preferentially closest) stars, decreases the odds of chance alignment even further. An example is HIP 40001, which was observed with the USNO speckle camera on the KPNO 4m telescope in January 2001, at a separation of 270 mas. At this separation and relatively small magnitude difference the chance of random optical co-alignment is small, but non-zero. While it can be argued statistically, the true physicality of the system can only be established through follow-up observations.

This sort of statistical culling of the BDS [2] was done by Aitken [1] during construction of the ADS catalog in the early 1930's. To avoid some of the problems described in §1.1 above, most of Aitken's rejected pairs were added back in by the time the IDS [10] was released. Retaining all pairs, but indicating physical or optical nature when possible, is the current modus operandi of the WDS [14].

5.1 Determining Physicality: Iota Ori

Arguments related to the physicality of close doubles are often made based on star counts and proximity. Since the true number of doubles is not known, these numbers, often based on observations by techniques with limited angular resolution, can undercount the true number of stars of a given magnitude. An example is ι Ori (= CHR 250Aa; see Figure 6). N-body simulations of the ι Ori / μ Col / AE Aur dynamical interaction [6] suggest that the speckle pair is extremely unlikely to be physical, despite the close angular separation.

6 The Washington Multiplicity Catalog (WMC)

an IAU sanctioned method for finding binaries and physical multiples from the vast number of catalogs that contain doubles

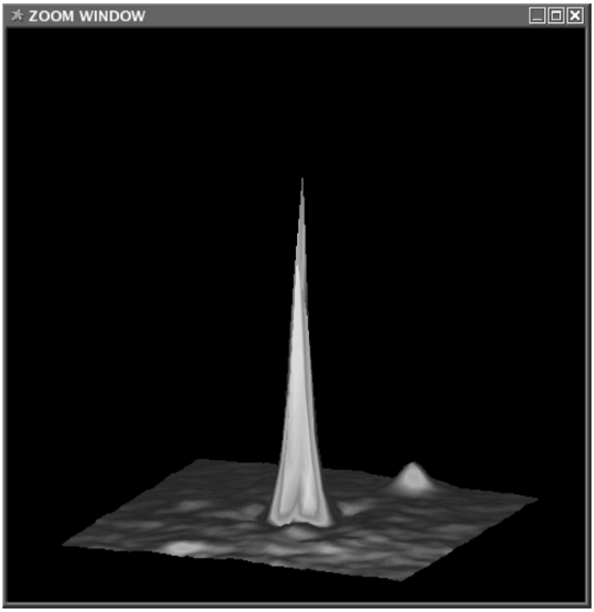

Fig. 5. HIP 40001 and its companion star.

6.1 Roots of the WMC

Historically, double stars have been categorized by the method of detection: photometric, spectroscopic, or visual. This also generally corresponded to their periods, from shortest to longest, respectively. While this categorization did not always apply, the regions where these methods could overlap corresponded to a relatively few systems. However, because of the synergy of the techniques, these systems were often the most astrophysically important.

Each of the many techniques for investigating components to stars independently developed its own nomenclature scheme. While the separation/period regimes accessible to these different techniques remained mostly separate, the inconsistencies in these nomenclature schemes were of little consequence. However, with modern cross-correlation techniques detecting smaller ΔV_r systems with longer period and optical interferometry (first filled and later delute aperture) resolving shorter period systems, the historically disparate techniques are now seeing increasing overlap, with a commensurate increase in possibilities for component confusion.

The idea behind the Washington Multiplicity Catalog (WMC) was discussed in 1997 at the Manchester IAU-GA, as a means of addressing this nomenclature confusion. As many of these are multiple systems, there was also a desire for a flexible system which could retain hierarchical information.

Starting with the WDS nomenclature scheme, the WMC component designation was expanded through a series of lower case letters and numbers to

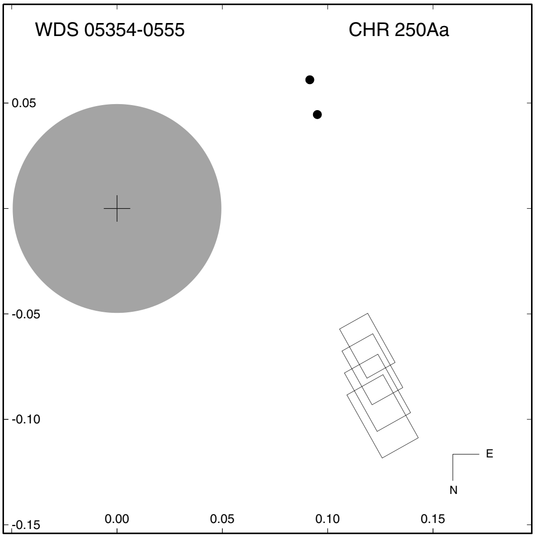

Fig. 6. At left is the double star CHR 250, with small filled circles indicating the 1994 and 1996 speckle measures reported in [12]. Scales are in arcseconds, and the large shaded circle represents the $0\overset{''}{.}054$ resolution limit of the 100-inch telescope. The four small error boxes indicate the predicted location of the secondary in 2006.0, 2007.0, 2008.0, and 2009.0, assuming the motion is linear and both speckle measures are characterized by errors of $\Delta\theta = 0\overset{\circ}{.}5$, $\frac{\Delta\rho}{\rho} = 0.5\%$. Finding the companion within a box appropriate to the observation date would be a strong indication that the relative motion of the pair is linear (i.e., non-Keplerian) as has been suggested [6].

take into account multiple hierarchies. At the Sydney GA in 2000 a sample WMC ($\frac{1}{2}$ hour of the sky) was presented which gave examples of the methods for addressing various nomenclature problems.

6.2 Applying WDS rules to the WMC

The WDS is a complete listing of all resolved systems (i.e., visual and interferometric doubles). There are an abundance of components to stars which are detected but not resolved (and are thus not in the WDS), however. These include:

1. spectroscopic doubles (single- or double-lined),
2. photometric or eclipsing binaries,
3. astrometric doubles (While not included in the WDS, several astrometric systems in the Orbit Catalog are given component designations as if they are resolved subcomponents, thus "reserving" these designations for their eventual resolution),

4. lunar occultation doubles,
5. contact systems and other doubles, and
6. planets.

6.3 Rules of Component Designation

The WDS at present extends nomenclature to second level hierarchies. The WMC will extend this nomenclature to cover more complex systems, however. Capital letter are used to indicate top level hierarchies (e.g., `012345.6+112233 AB`). Second- and third-level hierarchies are denoted by lower case letters (e.g., `Aa,Ab`) and numbers (e.g., `Ba1,Ba2`), respectively. Alternating lower case letters and numbers will be used to indicate progressively higher levels.. The coordinates used for the WMC are J2000, truncated to $0^{\mathrm{s}}\!.1$ and $1''$ precision in RA and DEC, respectively.

6.4 Sources of Multiplicity

Since the majority of known doubles are visual pairs, the catalogs maintained at the USNO make an excellent starting point for the WMC. The following sources have been consulted:

- USNO Double Star Catalogs: WDS [14], ORB6 [7], INT4 [8], DM2 [17]
- *A Catalog and Atlas of Cataclysmic Variables: On-line Version*,[2] [3]
- *Ninth Catalogue of Spectroscopic Binary Orbits*,[3] [15]
- *Catalog of Orbital elements, Masses and Luminosities of close double stars*, [16]
- California & Carnegie Planet Search website[4] and their links

6.5 Coordinate Matching

System matches are based on the stars arcsecond precise coordinates. The most time-consuming aspect of the WMC construction (by far!) has been the improvement of the WDS arcminute coordinates, which has been completed for more than 95% of these systems. Improvement of the remaining systems is on-going, although it will not be possible for some subset of these systems[5].

[2] `http://icarus.stsci.edu/~downes/cvcat/`

[3] `http://sb9.astro.ulb.ac.be/`

[4] `http://exoplanets.org/`

[5] **You** try to find a 15^{th} (± 2) magnitude pair with arcminute-precision coordinates and unknown proper motion seen only once in the mid-19^{th} century! Other pairs are lost due to errors at the telescope or typographical errors in the original publications, while still others are misdentifications of photographic plate flaws, etc.

6.6 Multiplicity Statistics

Combining the WDS and other catalogs, then making a first pass at merging duplicate information (e.g., SB and EB pairs with two entries) yields 115,904 pairs. "Physicality" codes are assigned, as follows:

Code	Characterization	Source
P	"definitely" physical	systems with orbits, (incl. Hipparcos O systems), exoplanets, cataclysmic pairs
p	"probably" physical	astrometric/interferometric/ occultation pairs, Hipparcos G systems, proximity (see text)
O	"definitely" optical	linear solution pairs
o	"probably" optical	proximity (see text)
C	"definitely" cpm	LDS, BUP, GIC, LPM, GRV pairs
c	"probably" cpm	similar proper motions, published comments, etc.
?	binarity uncertain	Hipparcos suspected non-singular, (X,S,V)
X	probably not real	plate flaws, misidentifications, etc

Other codes are assigned based on notes in the WDS and other catalogs. The remaining systems were assigned p or o code based on proximity:

$$log(\rho) = 2.8 - 0.2 \times V$$

with a minimum value of $2''$.

6.7 Grouping Pairs

Cluster members are flagged based on designations or proximity to known cluster members. The following pairs were removed:

- X and ? pairs: N=7,251
- Optical pairs: N=38,116
- Cluster members: N=543 (to get statistics for field stars)
- CPM pairs: N=7,811

The remaining pairs were checked for other entries within 3 arcmin in δ and $\alpha\cos(\delta)$ to differentiate simple binaries from multiples, then component designations are assigned for members of multiples.

6.8 Results

Simple binaries: N=57,562
Multiple systems: N=1,901 (N=4,293 pairs)

Number of Components	Hierarchy Level 1	Hierarchy Level 2	Hierarchy Level 3
3	471	1101	0
4	44	134	56
5	9	29	19
>5	6	18	14

6.9 Results (Including CPM Pairs)

Simple binaries: N=62,005
Multiple systems: N=2,257 (N=5,069 pairs)

Number of Components	Hierarchy Level 1	Hierarchy Level 2	Hierarchy Level 3
3	650	1230	0
4	60	146	63
5	13	35	20
>5	7	19	14

References

1. R.G. Aitken: *New General Catalogue of Double Stars within 121 degrees of the North Pole*, (Carnegie Institution of Washington 1932)
2. S.W. Burnham: *General Catalogue of Double Stars within 121 degrees of the North Pole*, (Carnegie Institution of Washington 1906)
3. R.A. Downes, R.F. Webbink, M.M. Shara, H. Ritter, U. Kolb, & H.W. Duerbeck: PASP **113**, 764 (2001)
4. D.R. Gies, B.D. Mason, W.G. Bagnuolo, Jr., M.E. Hahula, W.I. Hartkopf, H.A. McAlister, M.L. Thaller, W.P. McKibben, & L.R. Penny: ApJL **475**, 49 (1997)
5. R. Griffin & R. Griffin: Observatory **102**, 217 (1982)
6. A. Gualandris, S. Portegies Zwart, & P.P. Eggleton: MNRAS **350**, 615 (2004)
7. W.I. Hartkopf, B.D. Mason, & C.E. Worley: AJ **122**, 3472 (2001); see also `http://ad.usno.navy.mil/wds/orb6.html`
8. W.I. Hartkopf, H.A. McAlister, & B.D. Mason: AJ **122**, 3480 (2001); see also `http://ad.usno.navy.mil/wds/int4.html`
9. R. Jaworski: Webb Soc., Double Star Circ. **13**, 74 (2005)
10. H.M. Jeffers & W.H. van den Bos: *Index Catalogue of Visual Double Stars, 1961.0*, (Pub. of the Lick Observatory, vol. 21, 1963)
11. G.H. Kaplan & S.C. Snell: BAAS **33**, 1493 (2001)

12. B.D. Mason, D.R. Gies, W.I. Hartkopf, W.G.Bagnuolo, Jr., T.A. ten Brummelaar, & H.A. McAlister: AJ **115**, 821 (1998)
13. B.D. Mason, H.A. McAlister, & W.I. Hartkopf: AJ **112**, 276 (1996)
14. B.D. Mason, G.L. Wycoff, W.I. Hartkopf, G.G. Douglass, & C.E. Worley: AJ **122**, 3466 (2001); see also `http://ad.usno.navy.mil/wds/wds.html`
15. D. Pourbaix, A.A. Tokovinin, A.H. Batten, F.C. Fekel, W.I. Hartkopf, H. Levato, N.I. Morrell, G. Torres, & S. Udry: A&A **424**, 727 (2004)
16. M.A. Svechnikov, & L.A. Bessonova: Bull. d'Inf. Cent. Donnees Stellaires, #26, 99 (1984)
17. C.E. Worley, B.D. Mason, & G.L. Wycoff: AJ **122**, 3482 (2001); see also `http://ad.usno.navy.mil/wds/dm2.html`

Multiplicity of Chemically Peculiar Stars

Swetlana Hubrig[1], Nancy Ageorges[1] and Markus Schöller[1]

European Southern Observatory (ESO), Casilla 19001, Santiago, Chile

Summary. Recently, with the goal to study multiplicity of chemically peculiar stars, we carried out a survey of 40 stars using diffraction limited near infrared (IR) imaging with NAOS-CONICA (NACO) at the VLT. Here, we announce the detection of 27 near IR companion candidates around 25 late B-type chemically peculiar stars exhibiting strong overabundances of the chemical elements Hg and Mn in their atmospheres. A key point for the understanding of the abundance patterns in these stars may be connected with binarity and multiplicity. It is intriguing that more than half of the sample of HgMn stars studied previously by speckle interferometry and recently using the adaptive optics system NACO belong to multiple systems.

1 Introduction

Chemically peculiar (CP) stars are main sequence A and B type stars in the spectra of which lines of some elements are abnormally strong or weak. The class of CP stars is represented by roughly three subclasses including magnetic Ap and Bp stars, metallic-line Am stars and HgMn stars which are late B-type stars showing extreme overabundances of Hg (up to 6 dex) and/or Mn (up to 3 dex). Among the magnetic Ap stars the rate of binaries is 43% [1]. The main result of this most recent study of multiplicity of magnetic stars is that, statistically, the orbital parameters of Ap stars do not differ from those of normal stars, except for an almost complete lack of orbital periods shorter than 3 days. The studies of the evolutionary state of magnetic Ap stars in binaries indicate that all of them are rather old main sequence stars and are well evolved from the zero-age main sequence (e.g. Wade et al. (1996) [2]), fully in agreement with results of the study of single magnetic Ap stars by Hubrig et al. (2000) [3].

The number of double-lined spectroscopic binary (SB2) systems among magnetic Ap stars is abnormally low (only 3 SB2 systems are known to date) and no eclipsing binary comprising a magnetic Ap star has ever been identified. The rate of binaries is much smaller among magnetic Bp stars, ∼20%, and only two double-lined eclipsing binaries have recently been discovered: HD 123335 was discussed by Hensbergen et al. (2004) [4] and AO Vel by González et al. (2005) [5]. A total of six magnetic Bp/Ap stars are known to be multiple and are listed in the Multiple Star Catalogue of Tokovinin (1997) [6].

The metallic-line Am stars show an overabundance of heavy elements and an underabundance of Ca and Sc. A very high fraction of these stars, at least 90%, are SB systems with orbital periods between 2.5 and 100 days.

HgMn stars are rather young objects and many of them are found in young associations like Sco-Cen, Orion OB1 or Auriga OB1. HgMn stars do not have strong large-scale organized magnetic fields and exhibit marked abundance anomalies of numerous elements. In contrast to Bp and Ap stars with large-scale organized magnetic fields, they generally do not show overabundances of rare earths, but exhibit strong overabundances of heavy elements like W, R, Os, Ir, Pt, Au, Hg, Tl, Pb, Bi. Another important distinctive feature of these stars is their slow rotation ($\langle v \sin i \rangle \approx 29\,\mathrm{km\,s^{-1}}$, Abt et al. (1972) [7]). The number of HgMn stars decreases sharply with increasing rotational velocity [8]. Evidence that stellar rotation does affect abundance anomalies in HgMn stars is provided by the rather sharp cutoff in such anomalies at a projected rotational velocity of 70–80 $\mathrm{km\,s^{-1}}$ [9].

The mechanisms responsible for the development of the chemical anomalies of HgMn stars are not fully understood yet. A key point for the understanding of the abundance patterns may be connected with binarity and multiplicity. More than 2/3 of the HgMn stars are known to belong to spectroscopic binaries [10]. Quite a number of HgMn stars belong to triple or even quadruple systems [11, 12]. Out of 30 SB HgMn stars observed in speckle interferometry, 15 appear to have more than two components. Indirect evidence for the presence of a third component was found in four other HgMn SBs (HD 11905, HD 34364, HD 78316 and HD 141556) on the basis of spectroscopic and photometric arguments. Further evidence that other HgMn stars frequently are members of multiple systems is inferred from the results of the ROSAT all-sky survey. X-ray emission was detected through this survey in 12 HgMn stars (7 SB1s, 3 SB2s and 2 for which no radial velocity data are available). Previous X-ray observations with the Einstein Observatory and theoretical estimates had suggested that stars in the spectral range B2–A7 are devoid of any significant X-ray emission. In most cases when emission had been detected in such stars, it was found to originate from a cool companion. This suggests that the X-ray emission found in HgMn SBs does not originate from the HgMn primary. From observations investigating late-B X-ray sources using the ESO 3.6-m with ADONIS [13] we found faint companions for 4 HgMn stars that were part of the X-ray selected late-B stars observed, strengthening this interpretation.

In the catalogue of multiple stars by Tokovinin (1997) [6], which compiles data on 612 stellar systems of different spectral types, we found four additional multiple systems containing HgMn stars. It is especially intriguing that if the relative frequency of HgMn stars in multiple systems is studied, every third system with a primary in the spectral range between B6 and

B9 involves an HgMn star. These observational results clearly show that the study of multiple systems with an HgMn component is of prime interest for star formation. In the following we report our results of the recent study of multiplicity of this amazing class of objects using NACO K-band imaging.

2 Observations

Observations of 40 HgMn stars have been carried out with NACO in service mode from October 2004 to March 2005. We used the S13 camera, to be able to discover practically all components down to K=14 with a signal-to-noise ratio of the order of 12.

Here, we announce the detection of 27 near IR companion candidates in eight binaries, 16 triple and one quadruple system. The detected companion candidates have K magnitudes between $5\overset{\rm m}{.}5$ and $13\overset{\rm m}{.}5$ and angular separations ranging from $0\overset{\prime\prime}{.}1$ to $7\overset{\prime\prime}{.}3$ (7-1500 AU).

In Figs. 1–3 we show adaptive optics K-band images obtained with NACO. The field of view displayed was selected according to the angular distances of the companions. The intensity scale was adjusted to visualize the respective companions.

One of our NACO targets, the HgMn star HD 75333, has already been observed in May 2001 with the adaptive optics system at Keck II. The Keck images of this system have been presented in Hubrig et al. (2005) [14]. These observations revealed that this star has two low-mass companions in a binary system at a separation of $1\overset{\prime\prime}{.}34$. This system is not displayed in Figs. 1–3, since the separation between the two low-mass companions in the binary system is only $0\overset{\prime\prime}{.}06$. The diffraction limit for NACO installed at the 8 m telescope is lower than that for Keck II, hence these companions do not appear resolved in our NACO images. In Fig. 4 we show the distribution of the projected separations for the studied multiple systems with HgMn primaries. For most of the systems the separations are smaller than 100 AU.

If all detected IR objects around the HgMn stars are true companions, the resulting multiplicity rate is 68%. In Table 1 we present the list of the observed HgMn stars. Their visual magnitudes and spectral types were retrieved from the SIMBAD data base. In the last column we give some remarks about their multiplicity.

3 Discussion

The results of our study clearly confirm that HgMn stars are frequently found in multiple systems. It is especially intriguing that out of the 40 HgMn stars in the sample studied only two stars, HD 65950 and HD 70235, are not known to belong to a binary or multiple system. However, companionship can not be

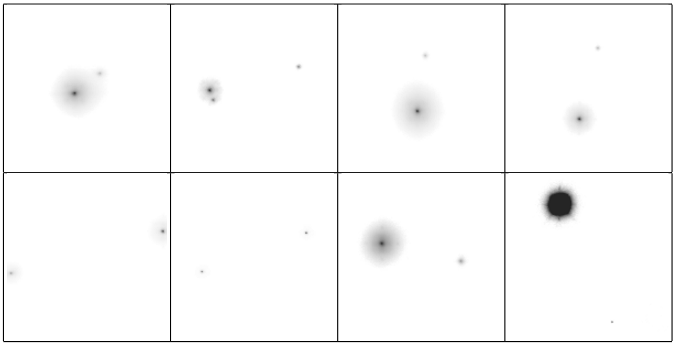

Fig. 1. NACO images of the wide systems in our sample. Upper row from left to right: HD 32964, HD 34880, HD 36881 and HD 53929. Lower row from left to right: HD 120709, HD 129174, HD 165493 and HD 178065. The field of view in each frame is $7.95'' \times 7.95''$

established based on K photometry alone, and confirming the nature with a near infrared spectrograph is essential for establishing their true companionship. Our program to carry out NACO K-band spectroscopy of the discovered IR-candidate companions has been scheduled at the VLT in service mode for the period October 2005 to March 2006. Using these observations we will be able to determine the mass of the IR companions much more accurately, and explore the physics in their atmospheres by comparison of observed and synthetic spectra. Since the HgMn type primaries have all Hipparcos parallaxes ($\sigma(\pi)/\pi < 0.2$), their age is known, and assuming coevality we will have an unprecedented set of data for the confirmed very young or even PMS companions.

We would like to note that our observations contribute not only to the understanding of the formation mechanism of HgMn stars but also to the general understanding of B-type star formation. An interesting result about the combination of long- and short-period systems has been presented by Tokovinin a few years ago [15]. He suggested that the fraction of SBs belonging to multiple systems probably depends on the SB periods. It is much higher for close binaries with 1 to 10 day periods than for systems with 10 to 100 day periods. The statistics of multiple systems is still very poor and much work remains to be done. The proposed survey of binarity and multiplicity of HgMn stars will help to understand the connection between close binaries and multiplicity, and especially the formation of close binary systems. To find out which role membership of HgMn stars in multiple systems plays for the development of their chemical peculiarities, it would be important to compare the ranges of periods, luminosity ratios, and orbital eccentricities, as well as hierarchy of multiples with the same characteristics of normal late B systems.

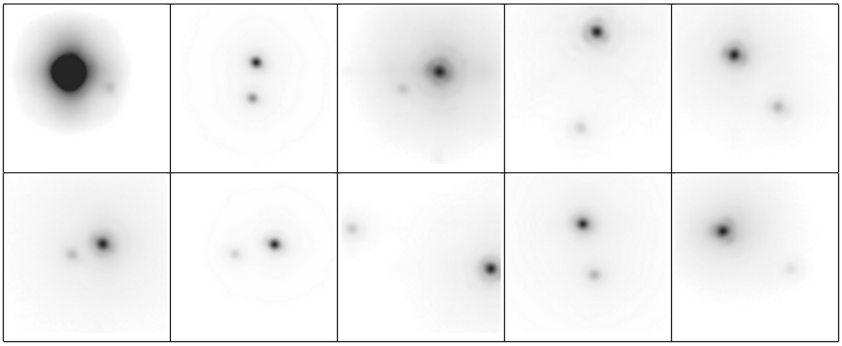

Fig. 2. NACO images of the intermediate systems in our sample. Upper row from left to right: HD 33904, HD 35548, HD 53244, HD 59067 and HD 73340. Lower row from left to right: HD 78316, HD 101189, HD 110073, HD 158704 and HD 221507. The field of view in each frame is $1.33'' \times 1.33''$

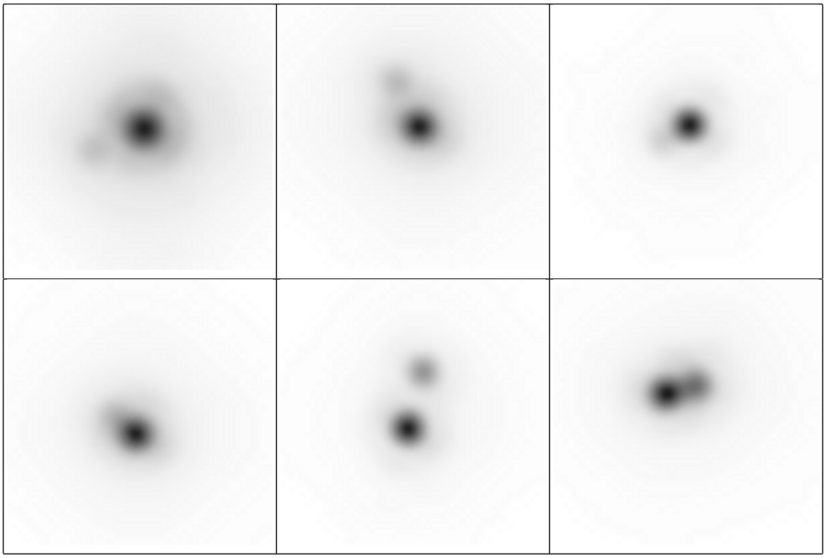

Fig. 3. NACO images of the close systems in our sample. Upper row from left to right: HD 21933, HD 28217 and HD 29589. Lower row from left to right: HD 31373, HD 33647 and HD 216494. The field of view in each frame is $0.66'' \times 0.66''$

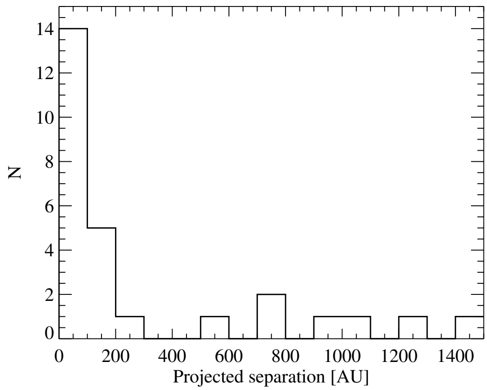

Fig. 4. Distribution of the projected separations for the studied systems with HgMn primaries

Table 1. List of HgMn stars observed with NACO.

HD	V	Sp. Type	Remarks	HD	V	Sp. Type	Remarks
1909	6.6	B9IV	SB2	70235	6.4	B8Ib/II	
7374	6.0	B8III	SB1	71066	5.6	A0IV	vis. binary
19400	5.5	B8III	vis. binary	71833	6.7	B8II	vis. binary
21933	5.8	B9IV	IR comp.	72208	6.8	B9	SB2
27295	5.5	B9IV	SB1	73340	5.8	B8	IR comp.
28217	5.9	B8IV	vis. binary + IR comp.	75333	5.3	B9	two IR comp.
29589	5.4	B8IV	SB1 + IR comp.	78316	5.2	B8III	SB2 + IR comp.
31373	5.8	B9V	IR comp.	101189	5.1	B9IV	IR comp.
32964	5.1	B9V	SB2 + IR comp.	110073	4.6	B8II/III	SB1 + IR comp.
33904	3.3	B9IV	IR comp.	120709	4.6	B5III	IR comp.
33647	6.7	B9V	SB2 + IR comp.	124740	7.9	A	SB2
34880	6.4	B8III	SB1 + two IR comp.	129174	4.9	B9	SB1 + IR comp.
35548	6.6	B9	SB2 + IR comp.	141556	4.0	B9IV	SB2
36881	5.6	B9III	SB1 + IR comp.	144661	6.3	B8IV/V	SB1
49606	5.9	B7III	SB1	144844	5.9	B9V	SB2
53244	4.1	B8II	SB1 + IR comp.	158704	6.1	B9II/III	SB2 + IR comp.
53929	6.1	B9.5III	SB1 + IR comp.	165493	6.2	B7.5II	SB1 + IR comp.
59067	5.9	B8	IR comp.	178065	6.6	B9III	SB1 + IR comp.
63975	5.1	B8II	SB1	216494	5.8	B8IV/V	SB2 + IR comp.
65950	6.9	B8III		221507	4.4	B9.5IV	IR comp.

A further remarkable feature of HgMn spectroscopic binaries is that many of them have orbital periods shorter than 20 days. However, binary periods of less than three days are absent, while they are quite common among normal late B systems. Interestingly, from a survey of the Batten et al. catalogue [16] limited to systems brighter that V = 7, it appears that only six normal B8 and B9 stars are known to be members of SBs with orbital periods between 3 and 20 days. Four of them are very fast rotating with $v \sin i$ values of the order of $100\,\mathrm{km\,s^{-1}}$ and more, i.e. much faster than typical HgMn stars. For the remaining two systems no information on the rotational velocity could be found in the literature.

In some binary systems with an HgMn primary, the components definitely rotate subsynchronously [17]. It is striking that the majority of these systems have more than two components. Probably the most intriguing and most fundamental question is whether all late-B close binaries with subsynchronously rotating companions belong to more complex systems.

References

1. Carrier F., North P., Udry S., Babel J., 2002: A&A 394, 151
2. Wade G.A., North P., Mathys G., Hubrig S., 1996: A&A 314, 491
3. Hubrig S., North P., Mathys G., 2000: ApJ 539, 352
4. Hensberge H., Nitschelm C., Freyhammer L. M., et al., 2004: ASP Conference Series, Vol. 318, 309
5. González J.F., Hubrig S., Nesvacil N., North P., 2005: A&A submitted
6. Tokovinin A., 1997: A&AS 124, 75
7. Abt H.A., Chaffee F.H., Suffolk G., 1972: ApJ 175, 779
8. Wolff S.C., Wolff R.J., 1974: ApJ 194, 65
9. Hubrig S., Mathys G., 1996: Carrier F., North P., Udry S., Babel J., 2002: A&A 120, 457
10. Hubrig S., Mathys G., 1995: Comm. on Astroph. 18, 167
11. Cole W.A., Fekel F.C., Hartkopf W.I., et al., 1992: AJ 103, 1357
12. Isobe S., 1991: Proceedings ASA 9, 270
13. Hubrig S., Le Mignant D., North P., Krautter J., 2001: A&A 372, 152
14. Hubrig S., Schöller M., Le Mignant D., et al., 2005: Proceedings of the ESO Workshop “High resolution infrared spectroscopy in astronomy”, p. 499
15. Tokovinin A., 2001: IAU Symposium 200, p. 84
16. Batten A.H., Fletcher J.M., MacCarthy D.G., 1989: Eighth Catalogue of the Orbital Elements of Spectroscopic Binary Systems, Publ. Dominion Astrophys. Obs. 17
17. Guthrie B.N.G., 1986: MNRAS 220, 559

Multiplicity of Contact Binary Stars

T. Pribulla[1] and S.M. Rucinski[2]

[1] Astronomical Institute of the Slovak Academy of Sciences, 059 60 Tatranská Lomnica, Slovak Republic, pribulla@ta3.sk
[2] David Dunlap Observatory, University of Toronto P.O. Box 360, Richmond Hill, Ontario, Canada L4C 4Y6, rucinski@astro.utoronto.ca

Summary. We present results of a preliminary investigation of triple star incidence for contact binary stars. The goal is to shed light on the possible role of distant companions which may have acquired and/or absorbed AM during evolution of multiple systems facilitating or enabling formation of contact binaries. We used several techniques but mostly disregarded their detection biases in an attempt to establish a low limit to the frequency of triple systems. The result for the much better observed Northern-sky subsample is 56% $\pm$8%, whereas subsamples of systems best observed using individual techniques indicate apparent frequencies as high as 60% to 67%; this is consistent with the hypothesis that all contact binary stars exist in multiple systems.

1 Introduction

Formation of binary stars is a fascinating subject [21]. Especially, formation of short-period binaries ($P <$ 3-5 days) is still not understood, because during the T Tauri stage the components would have to overlap. Formation in triple (or multiple) systems may alleviate the problem through the so called Kozai cycles [6, 7]. Confirmation of the triple body formation of very close binaries can only come through observations and careful statistical investigations. We limit our scope to contact binaries [15] with orbital periods shorter than 1 day, the most extreme objects in the sense of the lowest angular momentum content among all Main Sequence binary stars.

There are several known multiple systems containing contact binary stars, e.g., visual binary consisting of two contact binaries, BV Dra and BW Dra. Several new triple systems were detected during the David Dunlop Observatory (DDO) radial velocity program (see [19]). In the present study, we consider only systems brighter than $V = 10$ at light maximum. The contact binaries were selected from the updated version of the Catalogue of Contact Binary Stars (hereafter CCBS, [12]) currently containing 391 systems. We use new direct imaging and DDO spectroscopy and published astrometric, photometric and X-ray observations. In this preliminary contribution, we give just a short description of the data, techniques and results. A detailed study containing a final table of the detected triples has been submitted for publication [13].

2 Detection techniques

2.1 Direct imaging and astrometry

The most important data sources here are the Hipparcos Catalogue [4] and The Washington Double Star (WDS) Catalog [11]. 40 contact binaries from our sample are already listed in WDS as members of visual binaries.

The Hipparcos catalogue contains large number of apparently single stars which show astrometric perturbations due to unseen, but gravitationally bound companion(s). Six systems show enhanced scatter of positions indicating a third body orbiting a contact binary on a short-period orbit ($P_3 < 1$ year), two systems (ER Ori and V2388 Oph) required an acceleration term in their astrometric solution. 26 systems with a possible non-single astrometric solution are also listed. A good indicator of possible third-body astrometric or photometric perturbations is the Hipparcos parallax error. Contact binaries in most visual binaries have large parallax errors. Three systems not suspected before, but having parallax errors larger than 3σ relative to the error median, have been found: UX Eri, V1363 Eri and DY Cet. Another astrometric indicator is a large proper-motion error in the TYCHO-2 catalogue [5], which can indicate the presence of a third body on a relatively longer orbit (see Fig. 1).

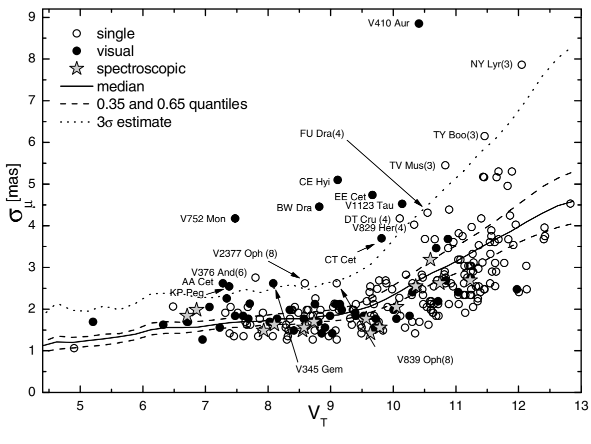

Fig. 1. Dependence of the combined proper motion error, σ_μ, on the median V_T magnitude for all contact binaries in the TYCHO-2 catalog. Numbers written in parentheses are given for systems currently not identified as multiple systems, they give the number of positions used for the proper-motion determination.

A program of direct detection of infrared companions using the adaptive optics system on the Canada France Hawaii Telescope was undertaken by one of the authors (SMR) in 1998. The observations were obtained with the PUEO instrument and KIR camera combination in the H and K infrared bands. The measured FWHM of corrected images was 0.143 arcsec in the K band. We used the PSF subtraction only for obvious companions at separations below 1 arcsec. In spite of this cursory treatment, we detected seven previously not identified companions at separations smaller than 5 arcsec to GZ And, AH Aur, CK Boo (separation only 0.12 arscec), SW Lac, V508 Oph, U Peg and RZ Tau. In all those cases, judging by the values of magnitude differences ΔK and ΔH, we suspect the companions to be M-type dwarfs.

2.2 Spectroscopy

Spectroscopy offers one of the most direct methods of discovery of companions to contact binaries. When a companion is present, extraction techniques utilizing deconvolution of spectra, such as the broadening functions (BF, see [17]), often show one sharp peak superimposed on a background of a broad and rapidly changing projection of the contact binary brightness onto the radial-velocity axis. The radial velocity program at the David Dunlap Observatory (see [19]) has led to the discovery of several new triple or multiple systems containing contact binaries: V899 Her and VZ Lib [9], V401 Cyg [18], as well as VW LMi, TV UMi and AG Vir (to be published).

The detection limit for third components, given by the ratio of the third component light to the total light of the eclipsing pair $\beta = L_3/(L_1 + L_2)$, is about 0.03 – 0.04. Averaging of individual spectra may show much fainter companions to the level of $\beta \simeq 0.01$ or even below (see [2]). We use all detections of [2] for our statistics.

Another spectroscopic technique are systemic-velocity changes. Because radial velocities usually come from different sources with different systematic errors and because contact binaries show large broadening of spectral lines, this is a relatively poor indicator of multiplicity. Available radial-velocity studies of contact binaries suggest only two suspect cases, W UMa and AW UMa.

2.3 The light-time effect "LITE"

Sinusoidal modulation of times of eclipses in binaries may result from the binary revolution on a wide orbit around a center of mass with a companion, the LITE or the LIght-Time Effect [1]. Because intrinsic period changes in close binaries are quite common due to their strong physical interaction, the presence of the LITE is usually not conclusive, but can prompt other observations. 129 systems having more than 15 CCD or *pe* minima in the Cracow database (the May 2004 version, [8]) were selected and analyzed. Only 18 out of 129 systems provided stable LITE solutions. The LITE interpretation was found for the first time for TY Boo, TZ Boo, CK Boo, GW Cep, UX Eri, V566 Oph and BB Peg. Predicted mean separations for several systems (e.g., AB And, CK Boo, V566 Oph) are accessible to speckle or direct detection. In fact, CK Boo was independently detected as visual double during CFHT observations (see Section 2). For the 20 best observed systems (with largest number of available minima), the multiplicity rate is 60% ± 5%.

2.4 The period–color relation

The period – color relation for contact binary stars was discovered observationally by [3]. The relation is a consequence of contact binaries being Main Sequence objects, with all implied correlations between the mass, effective temperature and radius, hence the size and thus the period. As pointed out before [16] the period – color relation must have a short-period, blue envelope (SPBE). Its locus corresponds to the Zero Age Main Sequence of least evolved stars. Evolution and expansion of components can lead to lengthening of the period and to reddening of the color index; reddening may be also caused by the interstellar matter. Thus, one does not expect contact binaries to appear blue-ward of the SPBE. Some blue outliers which do exist may be multiple systems with the color index peculiarity caused by a blue companion. The most deviating systems from our sample are V523 Cas, V1191 Cyg, XY Boo, V445 Cep and V758 Cen.

2.5 X-ray emission

Contact binary stars consist of solar-type stars spun into very rapid rotation by the tidal forces. As a consequence, they are very active and show elevated chromospheric and coronal activity [20]. X-ray coronal emission correlates with the effective temperature, T_{eff}, and the orbital period, P. A convenient distance independent quantity is the ratio of the apparent X-ray and bolometric fluxes, f_X/f_{bol}. X-ray fluxes were estimated from RASS counts by the procedure described in [20]. The scatter in f_X/f_{bol} reaches factors of 10 or 100 times from the average. We argue that companions to contact binaries may be the cause of these large deviations and that the deviations may go both ways: (i) When an early-type contact binary has an M-dwarf companion or even a binary M-dwarf companion then f_X/f_{bol} can be strongly elevated, but (ii) when the contact binary is of solar or later spectral type, its inactive early-type companion may reduce the value of f_X/f_{bol}. In fact we detected several early-type, long-period contact systems, showing enhanced X-ray flux (V335 Peg, DO Cha or RS Col) which may indicate that they host a late-type, active companion.

2.6 Other possible methods

There are other feasible methods and indicators of multiplicity which were not applied in the present investigation: (i) lunar occultations [14]: from among

391 contact binary stars in the electronic version of CCBS, 26 lie within the path of the Moon; (ii) the third light in light curve solutions: usually not reliable due to correlations with other photometric elements; (iii) precession of the orbital plane: a close and massive third body orbiting a binary system can cause precession of the orbital plane resulting in the changes of its orbital inclination and thus changes of the photometric amplitude of the eclipses [10].

3 Statistics and results

We have carefully inspected our list of contact binaries brighter than $V = 10$ with periods shorter than one day to establish all cases which appear to indicate multiplicity. We see 58 triple systems among 138 objects of our sample, giving the nominal lower limit to the frequency of triple systems of $42\% \pm 5\%$. While on the Northern sky ($\delta > 0$), using all available techniques, we see 47 triple systems among 84 objects, giving the frequency of $56\% \pm 8\%$, the Southern sky yields only 11 systems out of 54, corresponding to $20\% \pm 6\%$. Our estimate for the Northern hemisphere may be taken as a confirmation of the multiplicity hypothesis in production of close binary stars.

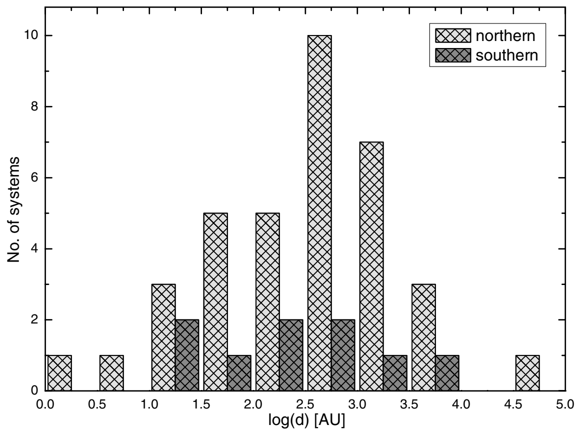

Fig. 2. The projected separations (in AU) shown for all systems with astrometric data, separately for both hemispheres (relative to the celestial equator). EM Cep (the only system in the bin with $4.5 < \log d < 5$), previously considered to be in a visual binary with a very large separation, is probably not a physically bound system.

The visual technique, combined with the parallax data permits to evaluate projected physical separations between the companions. The projected separations are moderate and distributed in the range between 3 and 5,700

AU, or 1.4×10^{-5} pc and 0.027 pc. Fig. 2 shows a histogram of the projected separations. The distribution may in fact reflect observational biases, but it does show that the separations are much smaller than typical distances between stars in the solar neighborhood of about one parsec. Thus, even the widest pairs with angular separations of several tens of arcsec can be regarded as gravitationally bound. But – physically – can these stars be evolutionary connected to the contact binaries? Can the Kozai cycle work at such large distances or do we see now only the results of it acting well in the past? Answers to these exciting questions are beyond the scope of this paper.

Acknowledgement. The conference participation of TP was supported by the Slovak Science and Technology Assistance Agency under the contract No. APVT-20-014402. The research made use of the SIMBAD database and the Washington Double Star (WDS) Catalog.

References

1. Borkovits, T., Hegedus, T., 1996, Astron. Astrophys. Suppl. Series, **120**, 63
2. D'Angelo, C., van Kerkwijk, M. & Rucinski, S.M., 2005, in preparation
3. Eggen, O.J., 1967, Mem. Roy. Astr. Soc., **70**, 111
4. European Space Agency, 1997, *The Hipparcos and Tycho Catalogues* (ESA SP-1200)(Noordwijk: ESA) (HIP)
5. Høg, E., Fabricius, C., Makarov, V.V. et al., 2000, Astron. Astrophys., **355**, 27
6. Kiseleva, L.G., Eggleton, P.P., Mikkola, S., 1998, Mon. Not. Roy. Astron. Soc., **300**, 292
7. Kozai, Y., 1962, Astron. J., **67**, 591
8. Kreiner, J.M., Kim, C.H., Nha, I.S., 2001, *An atlas of (O-C) diagrams of eclipsing binary stars*, Wydawnictvo Naukowe Akademii Pedagogicznej, Krakow
9. Lu, W., Rucinski, S.M., Ogloza, W., 2001, Astron. J., **122**, 402
10. Mayer, P., Pribulla, T., Chochol, D., 2004, Inf. Bull. Var. Stars, No. 5563
11. Mason, B.D., Wycoff, G.L., Hartkopf, W.I. et al., 2001, Astron. J., **122**, 3466 (WDS)
12. Pribulla, T., Kreiner, J.M., Tremko, J., 2003, Contrib. Astron. Obs. Skalnaté Pleso, **30**, 117
13. Pribulla, T., Rucinski, S.M., 2006, Astron. J., submitted
14. Richichi, A., Calamai, G., Stecklum, B., 2002, Astron. Astrophys., **382**, 178
15. Rucinski, S.M., 1993, in *The Realm of Interacting Binary Stars*, J. Sahade et al. (eds.), p.111
16. Rucinski, S.M., 1998, Astron. J., **116**, 2998
17. Rucinski, S.M., 2002a, Astron. J., **124**, 1746
18. Rucinski, S.M., Lu, W., Capobianco, C.C. et al., 2002, Astron. J., **124**, 1738
19. Rucinski, S.M., Pych, W., Ogloza, W. et al., 2005, Astron. J., **130**, 767
20. Stepien, K., Schmitt, J.H.M.M. & Voges, W., 2001, Astron. Astrophys., **370**, 157
21. Zinnecker, H. Mathieu, R.D. (eds), 2001, *The Formation of Binary Stars*, IAU Symp. 200 (ASP Publ.)

Extrasolar Planets in Double and Multiple Stellar Systems

A. Eggenberger[1], S. Udry[1], M. Mayor[1], G. Chauvin[2], B. Markus[3], J.-L. Beuzit[4], A.-M. Lagrange[4], T. Mazeh[3], S. Zucker[5] and D. Ségransan[1]

[1] Observatoire de Genève, 51 ch. des Maillettes, CH-1290 Sauverny, Switzerland
anne.eggenberger@obs.unige.ch
[2] European Southern Observatory, Alonso de Cordova 3107, Casilla 19001, Santiago 19, Chile
[3] School of Physics and Astronomy, Raymond and Beverly Sackler Faculty of Exact Sciences, Tel Aviv University, Tel Aviv, Israel
[4] Laboratoire d'Astrophysique, Observatoire de Grenoble, 414 rue de la piscine, 38041 Saint-Martin d'Hères, France
[5] The Weizmann Institute of Science, PO Box 26, Rehovot 76100, Israel

Summary. About 60% of G and K dwarfs belong to double or multiple stellar systems, making these a common environment in which planets may form. Despite this, close binaries have often been rejected from radial-velocity searches for extrasolar planets because they present observational difficulties. Planet formation and survival in binaries is thus a poorly known issue, though interesting in several respects. In particular, stellar duplicity could be used to test planet formation models and possibly identify the main formation mechanism for giant planets. For a few years we have been conducting two observational programmes dedicated to the study of extrasolar planets in binaries. The first one is a radial-velocity search for short-period giant planets in spectroscopic binaries, while the second one is a systematic adaptive optics search for stellar companions to nearby stars with and without planetary companions. In this contribution we first review some observational and theoretical aspects related to extrasolar planets in binaries. We then present some preliminary results from our two observational programmes.

1 Introduction

The study of extrasolar planets in double and multiple stellar systems is a rather new and fast developing facet of the extrasolar planet research field. In this section we present a brief review of some observational and theoretical results related to planets in binaries[1]. The emphasis is not on completeness, but on sketching out the general framework in which current research is taking place.

[1]For conciseness, planets in double and multiple stellar systems will often be referred to as planets in binaries, it being understood that for multiple stellar systems the binary denotes the planet-host star and its nearest stellar companion, or its nearest close pair considered as a unique object for highly hierarchical systems.

1.1 The Observational Perspective

A real interest for planets in binaries emerged only a few years ago. On the one hand, a dozen of planets were then known to orbit the component of a double or triple system, proving that planets can form and survive in certain types of stellar systems. On the other hand, [24] suggested that planets found in binaries may have different properties than planets orbiting single stars. This claim was based on an analysis of the mass-period diagram, emphasizing a paucity of short-period massive planets and the fact that the most massive short-period planets belong to binaries. Hence a possible different mass–period correlation for the two populations (planets in binaries vs planets around single stars), which was found to be highly significant despite the small number of planets in binaries.

The first observational programmes dedicated to the study of extrasolar planets in binaries started around 2001. Radial-velocity searches for planets in spectroscopic binaries (see Sect. 2) and in wide binaries (see Desidera et al., this volume) were thus launched. Some other programmes followed a different approach, namely searching for stellar companions to planet-host stars (see Sect. 3 or [11,13,15]). Such an approach is also worth pursuing since a precise knowledge of the multiplicity status of each planet-host star is a prerequisite for any study aiming at comparing the properties of planets found in binaries and around single stars. Many of these observational programmes are still ongoing and only preliminary results are available yet.

Finally, we also studied the eccentricity–period diagram and pointed out that short-period planets found in binaries tend to have a low eccentricity when their period is shorter than about 40 days [6]. That is, the minimum period for a significant eccentricity may be longer for planets in binaries than for planets orbiting single stars. But again, this trend is based on a small sample of planets in binaries, and a larger sample will be needed to settle once and for all whether or not planets found in binaries possess different properties than planets orbiting single stars.

1.2 The Theoretical Perspective

Two major scenarios have been proposed to explain giant planet formation: core accretion and disc instability (see e.g. [2, 18]). Several aspects of planet formation are still poorly known, and it is clear that adding a stellar companion does not simplify the problem. Nevertheless, a few aspects of planet formation in binaries have been studied, on the assumption that the binary was already formed when planet formation began. In such a case, each star may affect a potential circumstellar protoplanetary disc formed around the other component. In close systems, angular momentum transfer between the binary and a (circumstellar) protoplanetary disc will lead to a truncation of the disc's outer radius [1]. Assuming that the protoplanetary disc is still large and massive enough to sustain planet formation, will a planet persist in the long term? Stability zones have been shown to exist in such systems [8], and, generally speaking, if a planet can form in a truncated disc, it is likely to survive in the long term.

The efficiency of forming giant planets in binaries is a less studied and more debated issue. [3] claimed that the presence of a stellar companion located at about 40 AU could favour planet formation via disc instability. On the other hand, [14] showed that planet formation, either via disc instability or via core accretion, is unlikely in binaries with a separation of about 50 AU. More recently, [12] revisited the question and made a more extensive study. Their main conclusions can be summarized as follows: (i) planet formation in massive discs is not possible, whatever the mechanism (core accretion or disc instability), (ii) in intermediate-mass discs, both mechanisms may work, provided cooling is very efficient, (iii) core accretion remains the only viable mechanism in light discs, and (iv) for binaries wider than 120 AU planet formation proceeds very similarly to the isolated case. A very important conclusion can be drawn from these results: fewer planets should be found in binaries with a separation below 100 AU if disc instability is the main formation mechanism [12]. Studying planet formation in binaries may thus be a means of identifying the main formation mechanism for giant planets.

Once a planet has formed, the stellar companion may still affect its evolution. [9] studied the evolution of a Jupiter-mass protoplanet still embedded in a protoplanetary disc and showed that for systems with a separation in the range 50–100 AU both the mass accretion rate onto the planet and the migration rate of the planet are enhanced due to the presence of the stellar companion. These results constitute a first argument in favour of different properties for planets in binaries.

To sum up, even if several aspects of planet formation and survival in binaries are still debated and unclear, models have come up with a few very interesting predictions that could be confronted with observations. For some time, we have been working on gathering observational material to be used to test some of these predictions. Preliminary results from this work are presented in the following sections.

2 Searching for Short-Period Planets in Spectroscopic Binaries

In 2001 we initiated a systematic radial-velocity search for short-period circumprimary giant planets in single-lined spectroscopic binaries (SB1). This programme is aiming at obtaining a first quantification of the frequency of giant planets in close binaries. Our sample of binaries has been selected on the basis of former CORAVEL surveys for G and K dwarfs of the solar neighbourhood [4, 7]. All single-lined spectroscopic binary candidates with a period longer than approximately 1.5 years were retained, providing us with a sample of about 140 binaries covering both hemispheres. For each binary, 10 to 15 high-precision radial-velocity measurements were taken, either with the CORALIE spectrograph (ESO La Silla Observatory, Chile) or with the ELODIE spectrograph (Haute-Provence Observatory, France). The data acquisition phase is now completed and data analysis is under way.

2.1 Data Reduction

Stellar spectra obtained with ELODIE or CORALIE are reduced online. Radial velocities are computed by cross-correlating the measured stellar spectra with a numerical binary mask whose nonzero zones correspond to the theoretical positions and widths of stellar absorption lines at zero velocity. The resulting cross-correlation function (CCF) therefore represents a flux-weighted mean profile of all the stellar lines selected by the mask. For stars with a low projected rotational velocity the CCF has a Gaussian shape, and the radial velocity is determined by fitting the CCF with a Gaussian function. What we are interested in for the planet search are not the radial velocities themselves but the residual (radial) velocities around the binary orbit. Residual velocities are obtained by subtracting the binary orbit (if known on the basis of CORAVEL data) or a drift (for systems with periods much longer than the duration of the CORAVEL surveys) to the high-precision radial velocities obtained with ELODIE or CORALIE. Note that CORAVEL velocities are used to ensure that the system is a binary and to determine (if possible) its orbit, but they are not directly used to obtain residual velocities. The planet search is based solely on ELODIE or CORALIE high-precision measurements and is carried out by searching for short-period radial-velocity variations in the residual velocities.

2.2 Preliminary Results

The sample used for the final analysis is made of about 100 SB1s. The reduction in the sample size is mainly due to the rejection of CORAVEL SB1s candidates that turned out to be double-lined spectroscopic binaries (SB2) at the higher precision of the ELODIE and CORALIE spectrographs (see Sect. 2.3 for a justification regarding SB2s rejection). Figure 1 shows the residual-velocity variation for all our targets, as quantified by the normalized root-mean-square (rms). Most targets (74%) have a normalized rms close to 1, indicating that no source of radial-velocity variation other than the orbital motion is present. In contrast, some systems are clearly variable (12.5% of the targets exhibit a normalized rms larger than 3), while some others

(13.5%) are marginally variable with a normalized rms between 2 and 3. Mean measurement uncertainties indicate that the precision achieved on the radial-velocity measurement for the nonvariable systems is as good as the one commonly achieved by radial-velocity planet searches targeting single stars. The varying systems are, of course, the most interesting ones since the observed variability may be due to a planet orbiting the primary star. Variable and marginally variable systems are currently being analysed in detail as described in Sect. 2.4, but no convincing planetary candidate has been found yet.

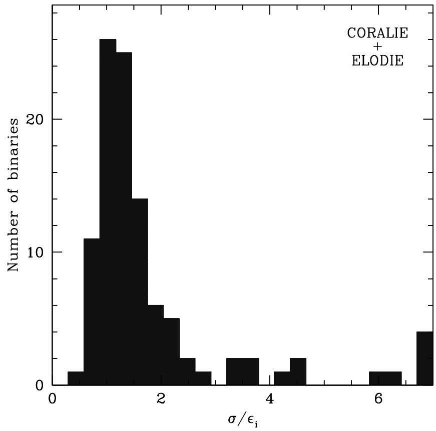

Fig. 1. Normalized residual velocity root-mean-square for all our targets. σ is the rms around a Keplerian orbit or around a drift, and ϵ is the mean measurement uncertainty. Systems with a rms larger than 7 are all gathered together in the last bin

2.3 Origin of Observed Radial-Velocity Variations

Does Fig. 1 imply that the frequency of short-period planets in our sample of spectroscopic binaries is quite high? Unfortunately not, for there exist several alternative effects that can produce residual-velocity variations such as the ones observed. The possibilities include: (i) the system is an unrecognized double-lined spectroscopic binary (i.e. a SB2 that happens to be observed when the two correlation peaks are superimposed, thus mimicking a SB1 system), (ii) the primary star is intrinsically variable, (iii) the pair is also a visual binary and there is light contamination from the secondary visual component, and (iv) the system is in fact triple, the secondary itself being a binary.

For visual systems, when the binary separation is close to the diameter of the spectrograph's fiber (2 arcsec for ELODIE and CORALIE) the fraction of light, coming from the secondary, that enters the fiber is variable and depends on the seeing and on the telescope guiding. As discussed in [16], different light contributions produce radial-velocity variations of the cross-correlation function. The amplitude of the variation strongly depends on the binary magnitude difference, the lower the magnitude difference the stronger the perturbations. This is the reason why we selected single-lined spectroscopic binaries. By considering SB1s we make sure that the magnitude difference is not too small, therefore minimizing the perturbations which are then usually smaller than the photon-noise error.

When the binary is a triple system whose secondary is itself a binary, the secondary spectrum will be varying periodically in time. If the secondary is bright enough, then a shallow and moving secondary CCF will be present, inducing asymmetry variations in the primary CCF, part of which are going to be interpreted as radial-velocity variations (see [20] for further details). Note that such a varying secondary CCF can usually not be detected directly by inspecting the cross-correlation profile since it is very shallow (flux ratio of a few percents), usually very broad (large projected rotational velocity), and is blended with the primary CCF most, if not all of the time (small velocity difference). Such triple systems can be dangerously misleading since they can perfectly mimic the presence of a planet orbiting the primary star, which is precisely what we are looking for.

To differentiate between these effects, tests including analysis of the CCF bisector span, analysis of the CCF parameters and their correlations, cross-correlation with different sets of lines, activity indicators, and photometric data can be used. All these tests are of great help, especially for identifying the cause of the residual-velocity variation observed for the most varying systems, but, in general, the lack of individual radial velocities for the two components is a major drawback.

2.4 Turning SB1s into SB2s Using Multi-Order TODCOR

As just mentioned, identifying the cause of the observed residual-velocity variation is usually not easy. In particular, differentiating between a light body (a planet) orbiting the primary star and a heavier body (a low-mass star or a brown dwarf) orbiting the secondary component may be very tricky using one-dimensional cross-correlation techniques. One way to solve the problem is to use two-dimensional cross-correlation techniques. TODCOR (TwO-Dimensional CORrelation) is such an algorithm developed by Zucker & Mazeh to deal with the difficulties encountered in double-lined spectra when the lines of the two components could not be easily resolved [23]. Assuming the observed spectrum to be the sum of two known templates with unknown Doppler shifts and a given flux ratio, TODCOR calculates the two-dimensional cross-correlation function, whose maximum gives simultaneously the radial velocities of both components. One advantage of TODCOR is its ability to use different templates for the primary and the secondary component, enabling to derive radial velocities for faint secondaries. TODCOR was originally designed to handle single-order spectra, but it is now also working with multi-order spectra [22, 25].

All variable and marginally variable systems from our programme are currently being analysed with TODCOR, trying to obtain the radial velocities of the two components individually. This analysis is still in its early stages, but a few SB1s have already been turned successfully into SB2s or into triple systems. One example is presented in the next subsection.

2.5 HD 223084

According to the Hipparcos catalogue, HD 223084 is a bright ($V = 7.23$) G0 star at a distance of 39 pc from the sun. CORAVEL measurements revealed the star as a long-period SB1 candidate and we consequently included HD 223084 in our planet search sample. A first series of CORALIE measurements exhibited a periodic residual-velocity variation compatible with the presence of a planetary companion orbiting the primary star. Pursuing the observations, tests such as those discussed in Sect. 2.3 began to indicate that the planetary hypothesis was not the best one, and that HD 223084 was probably rather a triple system, the secondary being the variable star (see [5] for a discussion of the one-dimensional radial-velocity analysis). HD 223084 was therefore one of the first candidates for a TODCOR analysis.

Our multi-order TODCOR analyses rely on a template library built from CORALIE and ELODIE spectra. When analysing a binary, we do not select the templates a priori, but rather try different configurations and select the one giving the best results (i.e. lowest rms) for the radial velocities of both components. The flux ratio is a function of the wavelength, and is calculated for the spectral types of the two chosen templates using the spectral energy distribution library by [17].

Applying multi-order TODCOR to our CORALIE spectra of HD 223084 we were able to separate the two components, thus obtaining the individual radial velocities for both components. As we suspected, the B component was found to be a SB1, but looking at the secondary cross-correlation function we occasionally saw a third correlation peak. On some spectra it was thus possible to separate Ba from Bb, turning the B component itself into a SB2. HD 223084 is therefore a triple system made of a G0 star (A) and two M stars (M0–M1 for Ba and M1–M2 for Bb according to the best-fit templates). The outer orbit (AB) is not well constrained since CORALIE data only cover a small fraction of the orbital period, but the inner orbit (Ba-Bb) is well defined. The parameters for this orbit are $P = 202.02 \pm 0.09$ days, $e = 0.272 \pm 0.006$, $K_1 = 16.14 \pm 0.09\,\mathrm{km\,s^{-1}}$, $K_2 = 18.0 \pm 0.4\,\mathrm{km\,s^{-1}}$. The residuals are $\sigma_A =$

$25\,\mathrm{m\,s^{-1}}$, $\sigma_{Ba} = 494\,\mathrm{m\,s^{-1}}$ and $\sigma_{Bb} = 663\,\mathrm{m\,s^{-1}}$, showing that for this system the precision on the radial velocity of the primary star is degraded, implying a lessened sensitivity for the planet search. But this is not a general truth. For instance, [26] obtained a $10\,\mathrm{m\,s^{-1}}$ precision on the radial velocity of the primary component for the HD 41004 system, which allowed them to find a planet in this close (23 AU) triple system.

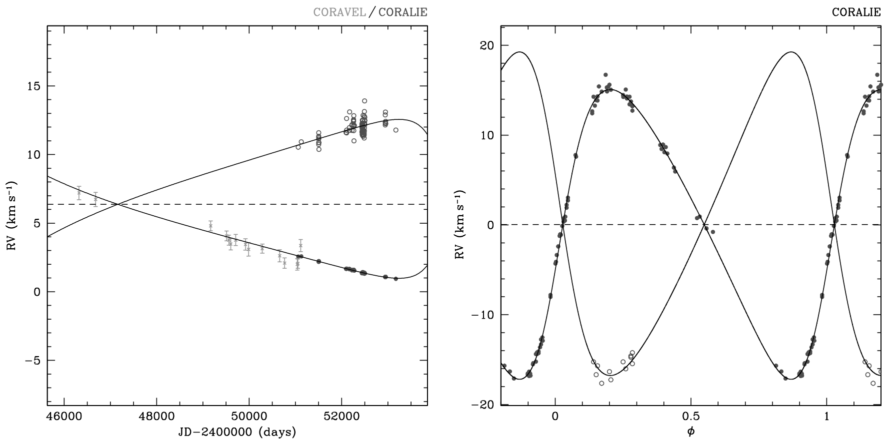

Fig. 2. Left: Radial velocities and tentative orbital solution for HD 223084 AB. CORAVEL data (stars) essentially represent the A component. Radial velocities obtained with TODCOR on the basis of CORALIE observations are shown as dots for the A component and as circles for the B component. **Right:** SB2 orbit for HD 223084 B (see text for orbital parameters). Dots represent Ba and circles Bb

3 Probing the Multiplicity Status of Nearby Stars with VLT/NACO

Since 2002 we have been carrying out a systematic adaptive optics (AO) search for stellar companions to nearby southern stars with and without planetary companions using the NAOS–CONICA facility [10,19] at the ESO Very Large Telescope (VLT, Chile). This programme is mainly aiming at characterizing and quantifying the influence of stellar duplicity on planet formation and evolution. But, as a by-product, this survey will also provide us with a precise knowledge of the multiplicity status of many planet-host stars, allowing us to confirm or infirm some of the trends emphasized in Sect. 1.1.

3.1 Programme Description

The programme relies on a sample of 110 dwarf stars of the solar neighbourhood divided into two subsamples. The planet-host star subsample comprises about 50 stars known to harbour at least one planetary companion. The comparison star subsample consists of about 60 stars belonging to our CORALIE planet search sample [21], not showing "large" radial-velocity variations and not known as Hipparcos close visual binaries. Comparison stars have been chosen very carefully, so that we can use them both as statistical references for the scientific analysis, and as point spread function reference stars in the data reduction process. This means that each comparison star has its coordinates, visual magnitude, color and parallax as close as possible to the actual values of one of the planet-host star. Conceptually, comparison stars must not be planet-bearing stars, but in practice this can never be completely known. Selecting comparison stars within the CORALIE planet search sample is one of the best way to approximate the ideal definition. The main reason for choosing a larger comparison star sample is that a few planet-host stars appearing in other published AO surveys will be added to the planet-host star subsample for the final analysis.

The programme strategy consists of searching for stellar companions around each of our 110 targets in order to see whether the binary fraction is the same for the two subsamples. Different binary fractions would indicate that the presence of a stellar companion either favours or inhibits planet formation and/or survival, depending on which subsample has the highest binary fraction.

3.2 Observations

Each star of a pair planet-host star – comparison star is observed in succession, taking unsaturated images through narrow-band filters within the H ($\lambda_c = 1.644\,\mu$m, field of view = $14'' \times 14''$, scale = 13.25 mas/pixel) or K ($\lambda_c = 2.166\,\mu$m, field of view = $28'' \times 28''$, scale = 27.03 mas/pixel) band. Whenever a companion is detected, an additional image is taken in narrow-band filter within the J band for color information. The total integration time is 10–15 min to allow for the detection of almost all stellar companions. Given the large proper motion of most of our targets, second-epoch observations taken after one year usually provide a good test regarding the optical or physical status of the pair. This is of importance since only physical binaries must be considered for the analysis.

3.3 Detection and Detection Limits

The survey itself (i.e. one observation per target) is almost completed, but second-epoch observations are still ongoing. So far we have found 7 companions to planet-host stars and 12 companions to comparison stars. Our detections and detection limits are shown in Fig. 3. In addition, several much fainter companions have been detected, but those have a very high probability of being background stars. The physical or optical status of some of the brightest companions can be assessed by combining our measurements with data from the 2MASS catalogue, but for many pairs this is not feasible since the secondary component is either too close and/or too faint to be listed in the 2MASS catalogue.

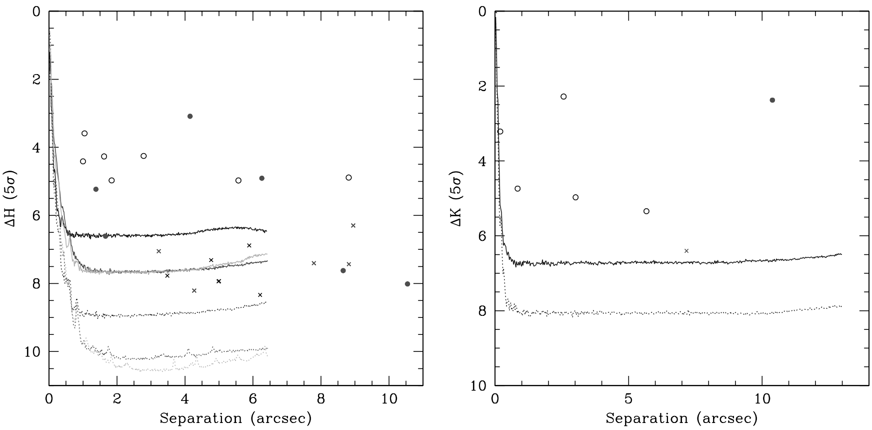

Fig. 3. Detection limits for our 4 observing runs. For each run, the best (dotted line) and worst (solid line) detection curve is given. The survey is preferentially made within the H band, but in case of degraded AO correction the K band is used. The detector of CONICA was changed in the middle of the programme, resulting in better detection curves for the last runs. Dots are companions to planet-host stars, circles are companions to comparison stars. Crosses are much fainter companions with a very high probability of being optical. A few companions were observed in H and in K and are therefore present on both diagrams

3.4 Effect of Stellar Duplicity on Planet Formation and Survival

Using the available data, a preliminary statistical analysis can be made in order to get a first quantification of the global effect of stellar duplicity on planet formation and survival. The subsamples considered for the statistics comprise 45 planet-host stars and 60 comparison stars from our survey, to which we add 10 planet-host stars from the AO survey by [15]. Only the companions with a projected separation in the range 0.8–6.5″ and located within the most restrictive detection limit for each band (K or H) are considered for this preliminary analysis. Companions with only one measurement but with a high probability of being optical were discarded. Using these subsamples, the binary fraction for planet-host stars is $5.5 \pm 3.0\%$. For comparison stars the binary fraction is in the range 8.3 ± 3.5–$16.7 \pm 4.8\%$, the uncertainty stemming from the fact that the physical or optical status of several of the bright companions to comparison stars is unknown. But once second-epoch observations will be completed, this binary fraction will be known exactly. For comparison, the binary fraction for field stars can be computed. Using the distributions for nearby stars [4], and the restrictions used for our analysis, the binary fraction for field stars is 11%, in good agreement with our results for comparison stars. Therefore, on the basis of the present results there may be a small difference between the two subsamples, but the two binary fractions may also be compatible within the error bars. In this context, results from second-epoch observations are crucial as they will remove the ambiguity. Furthermore, with the aim of improving the statistics, we are conducting a northern counterpart to our NACO programme using the PUEO–KIR facility at the 3.6-m Canada-France-Hawaii Telescope.

4 Conclusion

The sample of planets found in binaries has almost doubled since 2002, and as of July 2005, 25 of the known planet-host stars were also part of a double or multiple stellar system with a separation in the range 20–6500 AU. Note that this amounts to 31 planets since multiple planetary systems also exist in wide binaries.

Preliminary results from our radial-velocity search for short-period giant planets in spectroscopic binaries indicate that for a large fraction of our targets a precision as good as the one obtained for single stars can be achieved. No convincing planetary candidate has been found yet, but the detailed analysis is in progress.

Globally, stellar duplicity does not favour planet formation for binaries with a separation between 35 and 230 AU. In fact, for this separation range, stellar duplicity could have a negative effect on planet formation and survival. Final results from our adaptive optics programme should soon settle this question.

Regarding the properties of extrasolar planets found in binaries, the new data are, globally, in agreement with the proposed trends. But whether or not planets found in binaries possess different properties than planets orbiting single stars is still an open question.

References

1. P. Artymowicz and S. H. Lubow. *ApJ*, 421:651–667, 1994.
2. A. P. Boss. *Science*, 276:1836–1839, 1997.
3. A. P. Boss. *Bulletin of the American Astronomical Society*, 30:1057, 1998.
4. A. Duquennoy and M. Mayor. *A&A*, 248:485–524, August 1991.
5. A. Eggenberger, S. Udry, and M. Mayor. Planets in Binaries. In *ASP Conf. Ser. 294: Scientific Frontiers in Research on Extrasolar Planets*, pages 43–46, 2003.
6. A. Eggenberger, S. Udry, and M. Mayor. *A&A*, 417:353–360, 2004.
7. J. L. Halbwachs, M. Mayor, S. Udry, and F. Arenou. *A&A*, 397:159–175, 2003.
8. M. J. Holman and P. A. Wiegert. *AJ*, 117:621–628, 1999.
9. W. Kley. Evolution of an embedded Planet in a Binary System. In *IAU Symposium*, page 211, 2000.
10. R. Lenzen, R. Hofmann, P. Bizenberger, and A. Tusche. CONICA: the high-resolution near-infrared camera for the ESO VLT. In *Proc. SPIE Vol. 3354, Infrared Astronomical Instrumentation, Albert M. Fowler; Ed.*, pages 606–614, 1998.
11. K. L. Luhman and R. Jayawardhana. *ApJ*, 566:1132–1146, 2002.
12. L. Mayer, J. Wadsley, T. Quinn, and J. Stadel. *astro/ph-0405502*, 2004.
13. M. Mugrauer, R. Neuhäuser, T. Mazeh, M. Fernandez, E. Guenther, and C. Broeg. A Direct Imaging Search for Wide (Sub)Stellar Companions around Rad-vel Planet Host Stars. In *ASP Conf. Ser. 321: Extrasolar Planets: Today and Tomorrow*, page 127, 2004.
14. A. F. Nelson. *ApJ*, 537:L65–L68, 2000.
15. J. Patience, R. J. White, A. M. Ghez, C. McCabe, I. S. McLean, J. E. Larkin, L. Prato, S. S. Kim, J. P. Lloyd, M. C. Liu, J. R. Graham, B. A. Macintosh, D. T. Gavel, C. E. Max, B. J. Bauman, S. S. Olivier, P. Wizinowich, and D. S. Acton. *ApJ*, 581:654–665, 2002.
16. F. Pepe, M. Mayor, D. Queloz, and S. Udry. Towards 1 $\mathrm{m\,s^{-1}}$ RV Accuracy. In *IAU Symp. 202, Planetary Systems in the Universe: Observation, Formation and Evolution*, 2000. In press but available at http://www.unige.ch/sciences/astro/fr/Recherches/.
17. A. J. Pickles. *PASP*, 110, 1998.
18. J. B. Pollack, O. Hubickyj, P. Bodenheimer, J. J. Lissauer, M. Podolak, and Y. Greenzweig. *Icarus*, 124:62–85, 1996.
19. G. Rousset, F. Lacombe, P. Puget, N. N. Hubin, E. Gendron, T. Fusco, R. Arsenault, J. Charton, P. Feautrier, P. Gigan, P. Y. Kern, A.-M. Lagrange, P.-Y. Madec, D. Mouillet, D. Rabaud, P. Rabou, E. Stadler, and G. Zins. NAOS, the first AO system of the VLT: on-sky performance. In *Adaptive Optical System Technologies II. Edited by Wizinowich, Peter L.; Bonaccini, Domenico. Proceedings of the SPIE, Volume 4839*, pages 140–149, 2003.
20. N. C. Santos, M. Mayor, D. Naef, F. Pepe, D. Queloz, S. Udry, M. Burnet, J. V. Clausen, B. E. Helt, E. H. Olsen, and J. D. Pritchard. *A&A*, 392:215–229, 2002.
21. S. Udry, M. Mayor, D. Naef, F. Pepe, D. Queloz, N. C. Santos, M. Burnet, B. Confino, and C. Melo. *A&A*, 356:590–598, 2000.
22. S. Zucker. *MNRAS*, 342:1291–1298, 2003.
23. S. Zucker and T. Mazeh. *ApJ*, 420:806–810, 1994.
24. S. Zucker and T. Mazeh. *ApJ*, 568:L113–L116, 2002.

25. S. Zucker, T. Mazeh, N. C. Santos, S. Udry, and M. Mayor. *A&A*, 404:775–781, 2003.
26. S. Zucker, T. Mazeh, N. C. Santos, S. Udry, and M. Mayor. *A&A*, 426:695–698, 2004.

Monika Petr-Gotzens

Homogeneous Comparison of Directly Detected Planet Candidates: GQ Lup, 2M1207, AB Pic

Ralph Neuhäuser

Astrophysikalisches Institut, Schillergässchen 2-3, D-07745 Jena, Germany,
rne@astro.uni-jena.de

Summary. We compile the observational evidence for the three recently presented planet candidates imaged directly and derive in a homogeneous way their temperatures and masses. For both AB Pic b and 2M1207 b, we derive a larger temperature range than in Chauvin et al. (2004, 2005b) [7] [9]. AB Pic b appears to be quite similar as GQ Lup b, but older. According to the Tucson and Lyon models, all three companions could either be planets or brown dwarfs. According to the Wuchterl formation model, the masses seem to be below the D burning limit. We discuss whether the three companions can be classified as planets, and whether the three systems are gravitationally bound and long-term stable.

1 Introduction: Direct Imaging of exo-planets

Direct imaging of planets around other stars is difficult because of the large dynamic range between faint planets very close to much brighter primary stars. Few Myr young planets and young sub-stellar companions in general including both brown dwarfs are much brighter than Gyr old sub-stellar objects because of on-going contraction and possibly accretion (e.g. Burrows et al. 1997 [4]; Wuchterl & Tscharnuter 2003 [30]).

Below, we will compile the observational evidence published for the three currently discussed exo-planets detected directly, namely around GQ Lup (Neuhäuser et al. 2005a [24]; henceforth N05a), 2M1207 (Chauvin et al. 2005a [8]; henceforth Ch05a), and AB Pic (Chauvin et al. 2005b [9]; henceforth Ch05b). From the published observables, we derive in a homogeneous way the parameters needed for placement in the H-R diagram, i.e. luminosity and temperature. Then, we compare the loci of these three planet candidates with different model tracks to determine the masses.

2 Observational Evidence: Three Candidates

N05a presented astrometric and spectroscopic evidence for a sub-stellar companion around the well-known classical T Tauri star GQ Lup, for which also radius and gravity could be determined. Chauvin et al. (2004) [7] presented a companion candidate near 2MASSWJ 1207334-393254 (or 2M1207 for short), JHK imaging and a low-resolution, low S/N spectrum (both with AO at the VLT), which still needed astrometric confirmation. Schneider et al. (2004) [26] also detected the companion candidate using the HST/Nicmos a few weeks later, too early for astrometric confirmation (2 σ only). Then, Ch05a published the astrometric confirmation for the two objects (companion candidate and primary object) to have the same proper motion. Also very recently, Ch05b presented evidence for another possibly planetary-mass companion around yet another young nearby star, namely AB Pic.

The directly observed parameters are presented in Table 1, keeping the preliminary designations (A for the primary object, b for the companion, always regarded as a planet candidate). We also would like to note that both GQ Lup A and AB Pic A are normal stars, while 2M1207 A is a brown dwarf.

Table 1. Observables published

Object	Spec type	J [mag]	H [mag]	K [mag]	L or L' [mag]	distance [pc]
GQ Lup A	K7	8.605 (21)	7.702 (33)	7.096 (20)	6.05 (13)	140 ± 50
GQ Lup b	M9-L4			13.10 (15)	11.7 (3)	
2M1207 A	M8	12.995 (26)	12.388 (27)	11.945 (26)	11.38 (10)	70 ± 20 (*)
2M1207 b	L5-9	≥ 18.5	18.09 (21)	16.93 (11)	15.28 (14)	
AB Pic A	K2	7.576 (24)	7.088 (21)	6.981 (24)		47.3 ± 1.8
AB Pic b	L0-3	16.18 (10)	14.69 (10)	14.14 (8)		

Note: Numbers in brackets are error margins on last digits. (*) Mamajek 2005 [20] give 53 ± 6 pc for 2M1207 A, within the Ch05a error.
Ref.: N05a, Ch05a, Ch05b, 2MASS, Jayawardhana et al. 2003 [15], Chauvin et al. 2004 [7].

3 Derived Parameters

Based on the directly observable parameters listed in Table 1, we can now homogeneously derive some other parameters, which are not observable directly. Those other parameters are in particular luminosity and temperature, which are neccessary for placement into the H-R diagramm.

The derivation of temperature from the spectral type also needs the gravity as input (see e.g. Gorlova et al. 2003 [14]). For none of the six objects involved, the gravity is measured directly by high-resolution spectra; only for GQ Lup b, there is a measurement (from a low-resolution spectrum, R$\simeq$ 700). Only one of the six objects is already on the zero-age main-sequence, namely AB Pic A, so that we can assume dwarf gravity. GQ Lup A is a pre-MS star, 2M1207 A a brown dwarf, and the other companions are sub-stellar and, hence, above the main sequence, probably intermediate between dwarfs and giants. Hence, it is best to derive the full possible range in temperature, given several different spectral type to temperature scales. We list the temperature ranges for all available scales in Table 2 - together with the bolometric corrections used to estimate the luminosities, which are also given, as well as absolute K-band magnitudes.

Table 2. Derived parameters for sub-stellar objects involved

Temp. scale below	GQ Lup b	2M1207A	2M1207 b	AB Pic b
Spectral type:	M9-L4	M8	L5-9	L0-3
Luhmann 1999 (a)	≤ 2550	≤ 2720	n/a	< 2550
Reid et al. 1999	2100-1800	~ 2200	2000-1850	2000-1850
Kirkpatrick et al. 2000	2050-1650	n/a	2000-1750	2000-1750
Basri et al. 2000	2500-1850	~ 2500	1750-1600	2250-1950
Stephens et al. 2001	2320-1820	~ 2400	1720-1320	2220-1920
Leggett et al. 2002 (b)	2500-1700	~ 2200	1650-1150	2350-1650
Burgasser et al. 2002	2300-1740	~ 2400	1625-1170	2190-1850
Dahn et al. 2002	2500-1900	~ 2550	1900-1300	2400-1950
Nakajima et al. 2004	2520-1830	~ 2650	1690-1140	2380-1970
Golimowski et al. 2004	2400-1600	~ 2500	1950-1100	2400-1600
mean	2060 ± 180	2425 ± 160	1590 ± 280	2040 ± 160
range	2520-1600	2650-2200	2000-1100	2400-1600
M_K [mag]	7.37 ± 0.96	7.72 ± 0.66	12.70 ± 0.75	10.77 ± 0.14
B.C.$_K$ (*)	3.3 ± 0.1	3.1 ± 0.1	3.25 ± 0.1	3.3 ± 0.1
$\log L_{bol}/L_{\odot}$	-2.37 ± 0.41	-2.43 ± 0.20	-4.49 ± 0.34	-3.730 ± 0.039

Remarks: (a) Luhman 1999 [19] intermediate scale; (b) compilation in Leggett et al. (2002) [17]; n/a for not applicable; all temperatures are given in [K], (*) bolometric correction B.C.$_K$ in [mag] for the K-band according to Golimowski et al. (2004) [13].

The temperature mean and range for GQ Lup b is almost identical to the one given in N05a (mean ~ 2050 K, range 1600 to 2500 K), where a few scales listed in Table 2 here were not included.

Chauvin et al. (2004) [7] derive the age of 2M1207 A by assuming it to be co-eval with the mean TWA age and then assume that 2M1207 b has the same distance and age. For 2M1207 b, Chauvin et al. (2004) [7] give a temperature of only 1250 ± 200 K, obtained from the absolute magnitudes in H, K, and L' with Chabrier et al. (2000) [5] and Baraffe et al. (2002) [1]; apparently, this temperature range is obtained from *http://perso.ens-lyon.fr/isabelle.baraffe/DUSTY00* models for 10 Myrs, roughly the age of the TW Hya association. They also obtain 1000 to 1600 K from Burrows et al. (1997) [4] for 70 pc and 5-10 Myrs age. Hence, they have obtained the temperature from uncertain models tracks and an assumed distance and age, and not from converting the observed (distance-independant) spectral type to a temperature. Our temperature range is larger and its upper limit is shifted to higher values compared to Chauvin et al. (2004) [7]. The situation is similar for AB Pic b, for which we obtain a temperature of 2040 ± 160 K from its spectral type and considering all scales (table 2). Ch05b, however, only use the models by Burrows et al. (1997) [4] yielding 1513 to 1856 K and Chabrier et al. (2000) [5] and Baraffe et al. (2002) [1] giving 1594 to 1764 K. Hence, one could conclude that the models underestimate the temperature.

On the other hand, if one gives a correct absolute magnitude (or luminosity) as input (assuming a correct distance), and also taking into account that the Lyon models used in Ch05b were previously found to *under*estimate the radii (Mohanty et al. 2004 [21]), one would expect that the resulting temperature is an *over*estimate. This shows that the determination of the temperature should be done with great care under full consideration of the young age and, hence, low gravity of the involved objects.

4 Mass Determination by Model Tracks

Once temperatures, absolute magnitudes, and luminosities are determined homogeneously, we can derive the masses of the objects, see Table 3.

Table 3 shows that for all three planet candidates, there is a large mass range when employing the full possible range of luminosities, temperatures, and age, at least when using the Lyon or Tucson models. For 2M1207 b, those models tend to give masses below $\sim 20\ M_{\rm jup}$ from luminosities, temperatures, and age, but higher masses are not excluded.

For young objects as the ones considered here, one has to take into account the formation, i.e. initial conditions matter, so that models starting with an assumed internal structure are highly uncertain. Stevenson (1982) [28] wrote about such collapse calculations: *Although all these calculations may reliably represent the degenerate cooling phase, they cannot be expected to provide accurate information on the first* 10^5 *to* 10^8 *years of evolution because of the artificiality of an initially adiabatic, homolously contracting state.*
Baraffe et al. (2002) [1] also wrote that *assinging an age* (or mass) *to objects younger than a few Myrs is totally meaningless when the age is based on models using oversimplified initial conditions.*
Chabrier et al. (2005) [6] assertain that *both models and observations are hampered by nummerous uncertainties and great caution must be taken when considering young age* (≤ 10 *Myr) objects.*

Chauvin et al. (2004) [7] state in their section 3.5 ... *although the models are reliable for objects with age* ≥ 100 *Myr, they are more uncertain at early phases of evolution* (≤ 100 *Myr). As described by Baraffe et al. (2002), the choice of the initial conditions for the model adds an important source of uncertainty which is probably larger than the uncertainties associated with the age and distance of 2M1207. ... We then consider the new generation of models developed by Chabrier et al. (2000) and Baraffe et al. (2002) ...* (to determine the mass of 2M1207 b).

Ch05b write in their section 5 ... *as described in Baraffe et al. (2002), model predictions must be considered carefully as they are still uncertain at early phases of evolution* (≤ 100 *Myrs; see also Mohanty et al. 2004 and*

Table 3. Masses of sub-stellar objects involved (masses in [M_{jup}])

Model Reference	Figure used	Input parameters	Object GQ Lup b	2M1207 A	2M1207 b	AB Pic b
		(age used:)	1-2 Myr	5-12 Myr	5-12 Myr	30-40 Myr
masses derived from temperatures and ages:						
Burrows et al. 1997	Fig. 9/10	T & age	4-15	14-25	4-14	13-25
Chabrier et al. 2000	Fig. 2	T & age (a)	≤ 20	15-25	≤ 15	15-30
Baraffe et al. 2002	Fig. 2	T & age (b)	3-16	15-25	2-12	12-50
Baraffe et al. 2002	Fig. 3	T & age	5-30	20-45	≤ 20	15-30
Wuchterl model	(f)	T & age	1-3	1-5	n/a (c)	n/a (c)
masses derived from luminosities and ages:						
Burrows et al. 1997	Fig. 7	L & age	12-32	20-30	2-10	14-15
Baraffe et al. 2002	Fig. 2	L & age	12-42	12-30	2-5	~ 20
Baraffe et al. 2002	Fig. 3	L & age	10-30	10-50	n/a (c)	n/a (c)
Baraffe et al. 2002	(b)	L & age	18-50	25-60	3-6	11-18
Wuchterl model	(f)	L & age	1-3	1-5	n/a (c)	n/a (c)
masses derived from luminosities and temperatures (H-R diagram):						
Burrows et al. 1997	Fig. 11	L & T	≤ 15	≤ 25	2-70 (d)	2-70 (d)
Baraffe et al. 2002	Fig. 1	L & T	≤ 20	≤ 20	n/a (d)	n/a (d)
Baraffe et al. 2002	Fig. 6	L & T	≤ 30	10-35	n/a (c)	n/a (e)
Wuchterl model	(f)	L & T	1-3	1-5	n/a (c)	n/a (c)

Remarks: n/a for not applicable, (a) Similar for Dusty, Cond, and NextGen, (b) see also http://perso.ens-lyon.fr/isabelle.baraffe/DUSTY00 models, (c) outside of range plotted or calculated, (d) full mass range possible; for additional contraint of assumed age, i.e. to be located on the correct isochrone, the mass would be ≤ 20 M_{jup}, (e) ≤ 60 M_{jup} from L & T in Fig. 8, (f) Fig. 4 in N05a.

Table 4. Summary of parameters for the three planet candidates

Parameter	Objects		
	GQ Lup b	2M1207 b	AB Pic b
distance [pc]	140 ± 50	70 ± 20:	47.3 ± 1.8
membership	Lupus I	TWA (?)	TucHorA
age [Myr]	≤ 2	5-12:	30-40
epoch difference [yr]	5	1	1.5
separation	0.7", 100 AU	0.8", 54 AU	0.5", 258 AU
sign. for CPM (1) [σ]	$6+4+7$	$2+2+4+4$	$3+5$
remaining motion A/b [mas/yr]	1.4 ± 2.2	4.1 ± 8.2	6.9 ± 13.2
orbital motion exp. [mas/yr]	3.7 ± 1.5	1.9 ± 0.6	6.9 ± 0.4
escape velocity exp. [mas/yr]	5.2 ± 2.1	2.7 ± 0.9	9.8 ± 0.6
long-term stable ? (2)	yes	no	yes
SpecType	M9-L4	L5-L9.5	L0-3
spectrum resolution	700	< 700	700
spectrum S/N ratio	45	low	high
T_{eff} [K]	2520-1600	2000-1100	2400-1600
gravity $\log g$ [cgs]	2.0-3.3 (3)	unknown	unknown
radius [R_{jup}]	1.2 ± 0.6 (4)	unknown	unknown
M_K [mag]	7.37 ± 0.96	12.70 ± 0.75	10.77 ± 0.14
$\log L_{bol}/L_\odot$	-2.37 ± 0.41	-4.49 ± 0.34	-3.730 ± 0.039
mass [M_{jup}] Lyon/Tucson	1-42	2-70	11-70
mass [M_{jup}] Wuchterl	1-3	n/a (5)	n/a (5)

Remarks: (1) significance for common proper motion in Gaussian σ; (2) according to criteria in Weinberg (1987) [29] and Close et al. (2003) [10] (3) from fit to theoretical GAIA-dusty template spectrum; (4) from fit to spectrum with flux and temperature known; (5) not applicable, because outside of plotted or calculated range.
Ref.: this paper, N05a, Mugrauer & Neuhäuser 2005 [22], Ch05a, Ch05b, Hipparcos.

Close et al. 2005). We then considered the most commonly used models of Burrows et al. (1997), Chabrier et al. (2000), and Baraffe et al. (2002) ... (to determine the mass of AB Pic b).

It is surprising that Chauvin et al. (2004) [7] and Ch05b first ascertain that the Lyon (Chabrier et al. 2000 [5] and Baraffe et al. 2002 [1]) and Tucson (Burrows et al. 1997 [4]) models, which both do not take into account the collapse and formation, are not applicable for 2M1207 and AB Pic, and then use them. Given the fact that these models are not applicable, as correctly stated by Chauvin et al. (2004) [7] and Ch05b, one has to conclude that the temperatures and, hence, masses of 2M1207 b and AB Pic b were essentially undetermined.

The model by Wuchterl & Tscharnuter (2003) [30] for stars and brown dwarfs does take into account their formation, so that it can be valid for very young objects. The tracks for planets shown in Fig. 4 in N05a are calculated based on the nucleated instability hypothesis (Wuchterl et al. 2000 [31]).

Finally, we would like to point out, that neither distance nor age are directly derived parameters in the cases of the companions, and that only the distance towards AB Pic A is determined directly as parallaxe by Hipparcos. In all three cases, the age and distance of the companion is assumed to be the same as for the primary because of common proper motion. However, there are counter-examples.

5 Summary and Discussion on Planethood

We compile all information relevant for our discussion in Table 4.

Gravitationally bound ? While the remaining possible motion between GQ Lup A and b (change in separation and position angle) is smaller than both the expected orbital motion and the expected escape velocity, this system may well be gravitationally bound. This may be different for 2M1207 A+b: The remaining motion between the two objects may be larger than the expected escape velocity (Table 4), so that it is not yet shown to be bound. The GQ Lup system has a total mass and bounding energy sufficient for being long-term stable according to the criteria by Weinberg et al. (1987) [29] and Close et al. (2003) [10], while the 2M1207 system is not – too low in mass(es) for the given separation. See Mugrauer & Neuhäuser (2005) [22] for a discussion. 2M1207 A+b, if formed together and if still young, may be an interesting case as a low-mass binary just desintegrating. The remaining motion between the AB Pic A and b is not yet shown to be smaller than the expected escape velocity (Table 4), so that is not yet shown to be bound, but it could be stable.

Masses: Chauvin et al. (2004) [7] and Ch05b may have underestimated the range in possible temperatures of both 2M1207 b and AB Pic b by using models rather than spectral type to temperature conversions.

According to the Lyon and Tucson models, GQ Lup b and 2M1207 b may either be planet or brown dwarf, while AB Pic b would be a low-mass brown dwarf. According to both the Wuchterl model and our K-band spectrum compared with the Hauschildt GAIA-dusty model, GQ Lup b is a planet; the mass, age, and planethood of AB Pic b and 2M1207 b cannot yet be discussed using the Wuchterl model, because it is not yet available in the neccessary parameter range regarding temperatures, luminosities, and ages (outside the range in fig. 4 in N05a). An extrapolation would indicate that AB Pic b has a mass around one Jupiter mass, but it is probably much harder to form a one Jupiter mass object at 258 AU separation (AB Pic b) than at 100 AU separation (GQ Lup b). 2M1207 A, according to the Wuchterl model, appears to be below the D burning mass limit at roughly a few Jupiter masses. It would need to be more nearby and/or older to be above 13 M_{jup}.

Lodato et al. (2005) [18] argue that 2M1207 system may rather be seen as a binary pair of two very low-mass objects than a planet around a primary, due to the similar masses of both objects at the given relatively large separation. A several Jupiter mass object at 55 AU separation could not have formed by planet-like core accretion from a (low-mass) disk around a brown dwarf such as 2M1207 A. GQ Lup b may have been able to form as a planet at 100 AU separation around an almost solar-mass star (Lodato et al. 2005 [18]), while AB Pic b with 258 AU separation is again to far off.

The GQ Lup b K-band spectrum resembles well the spectra of isolated, free-floating young objects previously classified as brown dwarfs. However, the mass range of brown dwarfs and planets may well overlap: The Saturnian moon Titan has both a solid core and an atmosphere. It is regarded as a moon, because it orbits Saturn, a planet. If Titan would orbit the Sun directly (without other objects of similar mass in a similar orbit), it would be regarded a planet. The mass range of moons and planets overlaps. Analogously, if an object below 13 Jupiter masses with a solid or fluid core formed in a disk and orbits a star, then its a planet, otherwise a low-mass brown dwarf.

Those young objects with similar spectra as GQ Lup b were classified as 13 to 78 Jupiter mass brown dwarfs based on Tucson or Lyon models, which may not be valid until at least 10 Myrs, as recently specified in Chabrier et al. (2005) [6]. Hence, they may be lower in mass, maybe around a few to 10 Jupiter masses. If GQ Lup b has the same spectrum and mass as those young free-floating objects, the free-floating objects may be low-mass brown dwarfs (or planemos), because they are free-floating, while GQ Lup b with the same mass can be a planet, namely if formed with a core in a disk.

References

1. Baraffe I., Chabrier G., Allard F., Hauschildt P., 2002, A&A 382, 563
2. Basri G., Mohanty S., Allard F., et al., 2000, ApJ 538, 363
3. Burgasser A.J., Kirkpatrick J.D., Brown M.E. et al. 2002, ApJ 564, 421
4. Burrows A., Marley M., Hubbard W. et al. 1997, ApJ 491, 856
5. Chabrier G., Baraffe I., Allard F., Hauschildt P., 2000, ApJ 542, 464
6. Chabrier G., Baraffe I., Allard F., Hauschildt P., 2005, *Review on low-mass stars and brown dwarfs*, in: Valls-Gabaud D. & Chavez M. (Eds.) Resolved Stellar Populations, ASP Conf. Series, in press
7. Chauvin G., Lagrange A.M., Dumas C., Zuckerman B., Mouillet D., Song I., Beuzit J.L., Lowrance P., 2004, A&A 425, L29
8. Chauvin G., Lagrange A.M., Dumas C., Zuckerman B., Mouillet D., Song I., Beuzit J.L., Lowrance P., 2005a, A&A 438, L25 (Ch05a)
9. Chauvin G., Lagrange A.M., Zuckerman B., et al., 2005b, A&A 438, L29 (Ch05b)
10. Close L.M., Siegler N., Freed M., Biller B., 2003, ApJ, 587, 407
11. Close L.M., Lenzen R., Guirado J.C., 2005, Nature 433, 286
12. Dahn C.C., Harris H.C., Vrba F.J., et al., 2002, AJ 124, 1170
13. Golimowski D., Leggett S., Marley M. et al. 2004, AJ 127, 3516
14. Gorlova N.I., Meyer M.R., Rieke G.H., Liebert J., 2003, ApJ 593, 1074
15. Jayawardhana R., Ardila D.R., Stelzer B., Haisch K.E., 2003, AJ 126, 1515
16. Kirkpatrick J.D., Reid I.N., Liebert J., et al., 2000, AJ 120, 447

17. Leggett S.K., Golimowski D.A., Fan X., et al., 2002, ApJ 564, 452
18. Lodato G., Delgado-Donate E., Clarke C.J., 2005, MNRAS 364, L91
19. Luhmann K.L., 1999, ApJ 525, L466
20. Mamajek E., 2005, ApJ 634, 1385
21. Mohanty S., Jayawardhana R., Basri G., 2004, ApJ 609, 885
22. Mugrauer M. & Neuhäuser R., 2005, AN 326, 701, astro-ph/0509162
23. Nakajima T., Tsuji T., Yanagisawa K. 2004, ApJ 607, 499
24. Neuhäuser R., Guenther E.W., Wuchterl G., Mugrauer M., Bedalov A., Hauschildt P., 2005a, A&A 435, L13 (N05a)
25. Reid I.N., Kirkpatrick J., Liebert J. et al. 1999, ApJ 521, 613
26. Schneider G., Song I., Zuckerman B., et al., 2004, BAAS 36, No. 5, 11.14
27. Stephens D.C., Marley M.S., Noll K.S., Chanover N. 2001, ApJ 556, L97
28. Stevenson D.J., 1982, Planet. Space Sci. 30, 755
29. Weinberg M.D., Shapiro S.L., Wasserman I., 1987, ApJ, 312, 367
30. Wuchterl G. & Tscharnuter W.M., 2003, A&A 398, 1081
31. Wuchterl G., Guillot T., Lissauer J. 2000, Protostars and Planets IV, (Eds. Mannings V. et al.), 1081

Searching for Planets Around Stars in Wide Binaries

Silvano Desidera[1], Raffaele Gratton[1], Riccardo Claudi[1], Mauro Barbieri[1], Giovanni Bonannno[2], Mariangela Bonavita[3], Rosario Cosentino[2,4], Michael Endl[5], Sara Lucatello[1], Aldo F. Martinez Fiorenzano[1,3], Francesco Marzari[6] and Salvo Scuderi[2]

[1] INAF - Osservatorio Astronomico di Padova desidera@pd.astro.it
[2] INAF - Osservatorio Astrofisico di Catania
[3] Dipartimento di Astronomia, Università di Padova
[4] INAF - Centro Galileo Galilei
[5] McDonald Observatory, University of Texas at Austin
[6] Dipartimento di Fisica, Università di Padova

Summary. We present the status of the radial velocity planet search ongoing at TNG. We are observing about 50 wide binaries with similar components, searching for planets and abundance anomalies caused by the ingestion of metal-rich planetary material. A by-product of our project is the detection of several new spectroscopic binaries. No clear planet detection emerged up to now. Evaluation of the statistical significance in terms of frequency of planets in binaries is in progress. The abundance analysis of half of the sample revealed no pair with large difference.

1 Scientific Motivations

The search for planets in multiple systems allows to improve our knowledge on planet formation and evolution. On one hand, the frequency of planets in binary systems has a strong effect on the global frequency of planets, more than half of solar type stars being in binary or multiple systems [4]. On the other hand, the properties of planets in binaries, and any difference with those of the planets orbiting single stars would shed light on the effects caused by the presence of the companions. The occurrence of some difference on the period-mass relation was indeed suggested [12]. It is also possible that the binary companion of a planet host forces the planet to reach high eccentricities through the Kozai mechanism [11].

Moreover, binarity can be used also to study the origin of the planet-metallicity connection [6]: if the ingestion of planetary material occurs, increasing the metallicity of the outer layer of the star, a chemical abundance difference between the components should be detectable. This is much easier to indentify than a chemical anomaly in a normal field star, for which no proper reference is available.

With these two science goals, we started a radial velocity (RV) survey of the components of wide binaries. We are using SARG, the high resolution spectrograph of the TNG ([7]), equipped with an iodine cell to derive high precision RVs.

2 The Sample

The sample was selected from the Hipparcos Multiple Star Catalog, considering binaries in the magnitude range $7.0 < V < 10.0$, with magnitude difference between the components of $\Delta V < 1.0$, projected separation larger than 2 arcsec (to avoid contamination of the spectra), parallax larger than 10 mas and error smaller than 5 mas, with $B - V > 0.45$ and spectral type earlier than F7. About 50 pairs (100 stars) were selected. The sample is then formed by wide binaries with mass ratio close to 1. Considering systems with similar components is crucial for the accuracy of the differential chemical abundance analysis. Fig. 1 shows the distribution of the projected separation in AU. For most of the pairs, it results between 50 and 600 AU.

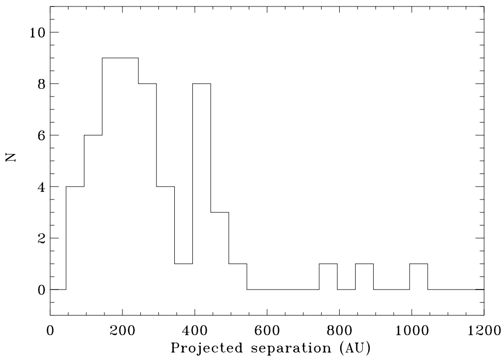

Fig. 1. Distribution of the projected separation in AU of the binaries in the sample

3 Abundance Analysis

Differential abundance analysis was performed as described in [2], reaching errors of about 0.02 dex in the iron content difference. We fully exploit the physical link between the components (same distance from the Sun), deriving effective temperatures difference from ionization equilibrium and gravity difference from the magnitude difference.

The analysis of 23 pairs, about half of the sample, shows that most of the pairs have abundance differences smaller than 0.02 dex and there are no pairs with differences larger than 0.07 dex. The four cases of differences larger than

0.02 dex may be spurious because of the larger error bars affecting pairs with large temperature difference ($\Delta T_{eff} \geq 400$ K), cold stars ($T_{eff} \leq 5500$ K) and stars with rotational velocity larger than 5 km/s.

Figure. 2 shows the amount of iron accreted by the nominally metal richer component to explain the observed abundance difference. For most of the slow-rotating stars warmer than 5500 K, characterized by a thinner convective envelope and for which our analyis appears to be of higher accuracy, this is similar to the estimates of rocky material accreted by the Sun during its main sequence lifetime (about 0.4 Earth masses of iron, [10]).

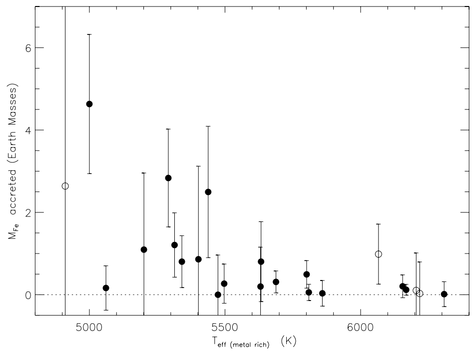

Fig. 2. Estimate of iron accreted by the metal-rich component of each pair as a function of its effective temperature, taking into account the mass of the mixing zone as in [10]. Empty circles: Stars with significant rotation broadening, for which our analysis is less accurate. Filled circles: Other stars. The less severe limits at lower effective temperatures are mostly due to the more massive convective zone of cool stars. The mass of meteoritic material is about 5.5 times the mass of iron

4 Radial Velocities

RVs were determined using the AUSTRAL code [8] as described in [1]. Typical errors are 2-3 m/s for bright stars observed as standards to monitor instrument performances and 5-10 m/s for the $V \sim 8-9$ program stars.

4.1 New Triple Systems

A by–product of our project is the detection of new spectroscopic binaries among the components of the wide binaries. These systems are then composed by at least three components.

Double-lined spectroscopic binaries were excluded from the sample when their nature emerged. An example, HD 17785, is shown in Fig. 3.

Figure. 4 shows the radial velocity curve of HD 8071 A, with overplotted the preliminary best-fit orbital solution (P=567 days, e=0.39, K=8.8 km/s). Considering a primary mass of 1.25 $M_\odot$ [2], the minimum mass of the companion is then 0.44 $M_\odot$.

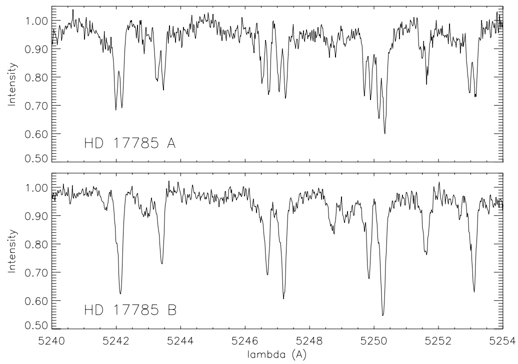

Fig. 3. A small portion of spectra of the components of HD 17785. The primary clearly is a double-lined spectroscopic binary

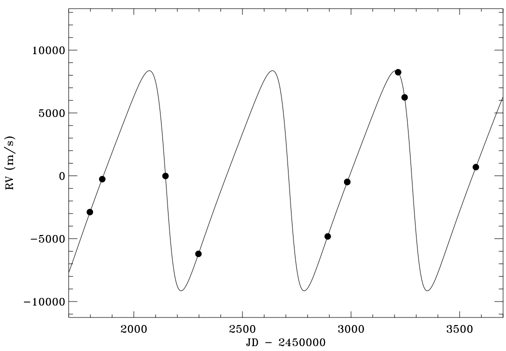

Fig. 4. Radial velocities of HD 8071 A. The preliminary orbital solution is overplotted as a solid line

4.2 Stars with Long Term Trends

About 10% of the stars in the sample show long term linear or nearly linear trends. In one case the trend is due to the known companion, as trends with opposite sign and nearly the same magnitude are observed for the two components. In the other cases the trends are due to low mass, possibly substellar companions. Direct imaging to search for such systems is planned. The direct identification of substellar objects as companions of stars for which age and chemical composition can be derived would play a relevant role in the calibration of models of substellar objects.

4.3 Low Amplitude Variables and Planet Candidates

Some further stars show RV variability above internal errors. One case we investigated in detail is that of HD 219542 B. The 2000-2002 data indicated a possible periodicity of 111 days with a significance of about 97% [1]. However, the continuation of the observations revealed that the RV variations are likely due to stellar activity [3]. Other candidates, mostly of fairly low amplitude, are emerging from our sample. Further observations are in progress.

4.4 Line Bisectors: a Tool to Study Stellar Activity and Contamination

The relevance of activity jitter for the interpretation of the RV data promped us to develop a tool to measure the profile of the spectral lines. The existence of a correlation between the variations of the RV and those of the line profile might indicate a non-Keplerian origin for the observed RV variations. Our approach allows to use the same spectra acquired for the derivation of RVs, removing the iodine lines by means of a suitable spectrum of a fast rotating early type star with iodine cell in the optical path. The procedure is described in detail in [9].

The study of line shape is relevant for our program also as a diagnostic for the contamination of the spectra by the wide companion. In the case of HD 8071 B, we indeed observe a correlation likely due to the contamination of HD 8071 A. We are confident that this is the worst case, as this pair is one of the closest in our sample (separation 2.1 arcsec) and the large amplitude RV variations of HD 8071 A (Fig. 4) should increase the effect of a variable contamination of the observed RVs of HD 8071 B.

4.5 Upper Limits on Planetary Companions

While no confirmed planet detection emerged up to now from our survey, a detailed analysis of the negative results would allow to constrain the frequency of planets in binary systems. Since we are focusing on a specific type of binaries, wide binaries with similar components, such a study is complementary to other studies of planets in binaries [5].

To this aim, we are deriving upper limits on the planetary companions still compatible with the observations. We consider eccentric orbits in our estimation, as described in [1]. The effect of the inclusion of eccentric orbits can be clearly seen in Fig. 6. A full statistical evaluation of the upper limits is in progress.

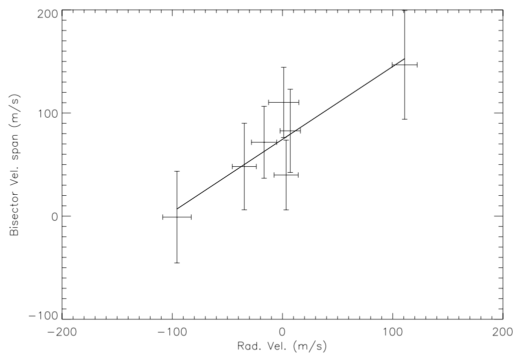

Fig. 5. Radial velocity - line bisector correlation for HD 8071 B. This is likely due to the comtamination by the companion HD 8071 A

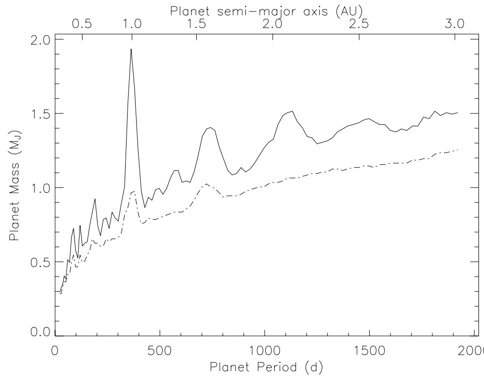

Fig. 6. Upper limits on planetary companion on circular (dashed line) and eccentric (solid line) orbits for a star in our sample

References

1. S. Desidera, R. Gratton, M. Endl et al: A&A **405**, 207 (2003)
2. S. Desidera, R. Gratton, S. Scuderi et al: A&A **420**, 683 (2004)
3. S. Desidera, R. Gratton, M. Endl et al: A&A **420**, L27 (2004)
4. A. Duquennoy & M. Mayor: A&A **248**, 485 (1991)
5. A. Eggenberger et al: this volume (2005)
6. D. Fischer & J. Valenti: ApJ **622**, 1102 (2005)
7. R. Gratton, G. Bonanno, P. Bruno et al: Exp. Astr. **12**, 107 (2001)
8. M. Endl, M. Kürster, S. Els: A&A **362**, 585 (2000)
9. A.F. Martinez Fiorenzano, R. Gratton, S. Desidera, et al: A&A, in press (2005)
10. N. Murray, B. Chaboyer, P. Arras et al. : ApJ **555**, 810 (2001)
11. Y. Wu & N. Murray: ApJ **589**, 605 (2003)
12. S. Zucker & T. Mazeh: ApJ **568**, L113 (2002)

Multiplicity at the Very Low Mass End of the H-R Diagram

H. Bouy[1], E.L. Martín[1], W. Brandner[2] and J. Bouvier[3]

[1] Instituto de Astrofísica de Canarias, C/ Vía Láctea, s/n, E-38200 - La Laguna, Tenerife, Spain
bouy@iac.es, ege@iac.es

[2] Max-Planck Institut für Astronomie, Königstuhl 17, D-69117 Heidelberg, Germany
brandner@mpia.de

[3] Laboratoire d'Astrophysique de l'Observatoire de Grenoble, 414 rue de la piscine, F-38400 Saint Martin d'Hère, France
Jerome.Bouvier@obs.ujf-grenoble.fr

Summary. We review the properties of multiplicity of very low mass stars and brown dwarfs in different environments and at different ages. We will compare the main results of surveys performed in the field, where the objects are relatively old (1–5 Gyrs) and isolated, in the Pleiades young (∼120 Myr) open cluster, and in the young (∼5 Myr) Upper Scorpius OB association (USco). While the field and Pleiades populations seem to have very similar properties, the preliminary results obtained in Usco seem to show significant differences. If confirmed, it would mean that the phenomenons responsible for the "final" properties of multiplicity of ultracool dwarfs (spectral type later than M6) are still at work at the age of Usco, but are already over at the age of the Pleiades. We will also discuss the observed properties in the context of the predictions of the most recent models of formation and evolution.

1 Introduction

Multiple systems are important testimonies of the formation and evolution of a population of astrophysical objects. The properties of the out-coming population, and in particular the properties of multiplicity, depend directly on both the mechanisms involved and on the initial conditions. Little is known about the formation processes responsible for the formation of very low mass stars and brown dwarfs. In order to address these questions, a large number of authors have performed detailed studies of the properties of multiplicity of very low mass stars and brown dwarfs over the last 5 years (see e.g [1, 3, 4, 6, 8–10, 15, 17, 19, 23, 25, 27, 34]). The major observed properties, such as the apparent lack of wide multiple systems at evolved ages and the possible preference for equal-mass systems, provide important constraints for the models of formation and evolution. The relatively low multiplicity fraction observed in the field and in the Pleiades for visual binaries still needs to be complemented by spectroscopic studies before a meaningful comparison can be made with the predictions of the models. In section 2, we will review in details the results obtained in the field, then in sections 3 and 4, we will compare it to the properties observed in the younger Pleiades cluster and Usco OB association. Finally in section 5 we will give a brief overview of other types of multiple systems including ultracool dwarfs, and in section 6, we will discuss the comparison between these different environments/ages, and the predictions of the most recent models of formation and evolution.

2 Multiplicity of Ultracool Dwarfs in the Field

The study of multiplicity of ultracool dwarfs in the field has been an intense field of research over the last few years. Several teams have been doing a lot of work in this field. Table 1 gives a very brief overview of the different studies reported in the literature on that topic over the last two years. The different results are consistent, as one could expect since they use overlapping samples coming from the 2MASS, SDSS and DENIS surveys.

Table 1. Study of multiplicity among field ultracool dwarfs

Authors	Spectral range	Binary Fraction
[9]	M8–L0.5	15±7%
[15]	M8–L5	15±5%
[6]	T5–T8	9^{+15}_{-4}%
[4]	M7–L8	15±5%
[34]	M6–M7.5	9^{+4}_{-3}%

Figure 1 shows the multiplicity fraction (defined as the number of multiple systems divided by the total number of objects) as a function of the spectral type. Although it is strictly incorrect to quantitatively compare these results, because they were obtained under very different conditions, covering very different ranges of mass ratios and separations, we observe a clear trend for a decreasing multiplicity fraction toward lower effective temperatures.

Figure 2 shows the distribution of mass ratio of ultracool field dwarfs, compared to that of more massive early-M dwarfs from [11, 21] and to that of F–G dwarfs from [12]. There is an apparent preference for equal mass systems among ultracool binaries. This result is only preliminary and must be considered with great caution, because the sample of ultracool dwarfs was unfortunately limited in magnitude rather than in volume (see e.g [4, 15]), implying a strong bias toward equal-mass systems. Assuming it is real, it would mean a great difference with the early-M dwarfs, which distribution is rather flat, only slightly increasing toward mass ratios of unity, and with more massive F–G dwarfs, which show a peak at about q =0.4.

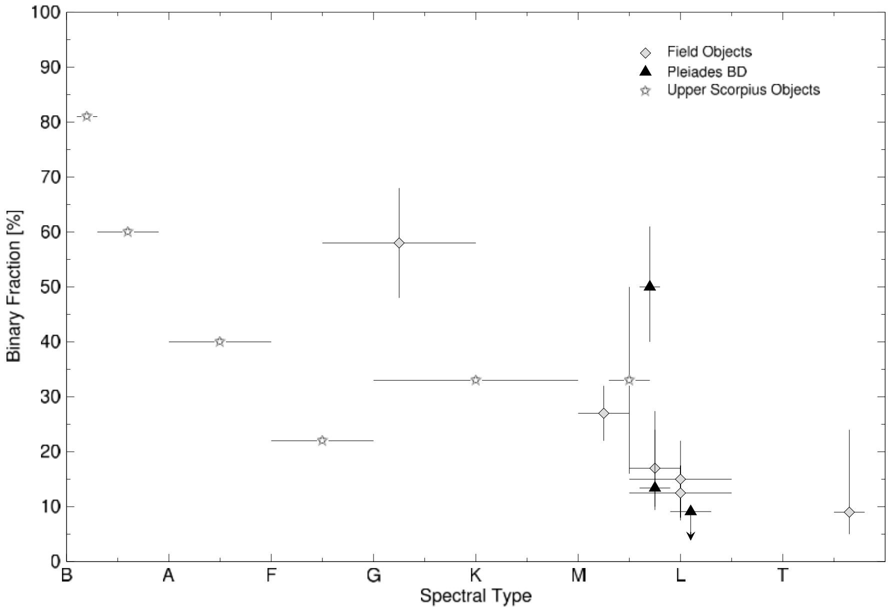

Fig. 1. Binary fraction vs Spectral type. Although these results have been obtained under very different conditions, and should therefore not be compared, there seems to be a trend for decreasing binary fraction toward cooler effective temperatures

The distribution of separation of ultracool dwarfs gives the most peculiar and constraining parameter. Figure 3 compares the distribution of separations of ultracool dwarfs to that of F–G dwarfs reported by [12]. The shape is similar (gaussian like), with a peak at 8 AU. While the different surveys were more sensitive to multiple systems with large separations, they did not discover any companion at separation greater than ∼20 AU, indicating a strong cut-off in the distribution of separation and a lack of wide multiple systems. This remarkable difference with more massive objects gives major constraints on the models of formation and evolution. To date, only few wide multiple systems have been observed. [26] first reported a binary with a separation of 30 AU, just above the cut-off. [14] and [16] simultaneously reported another interesting binary at a separation of ∼30 AU [31] recently reported another of these objects with a separation of 30 AU. The most interesting wide-binary was recently reported by [2], with a separation over 200 AU. Another candidate was reported by [20], with a separation of 240 AU. These two objects really contrast with any other companion ever observed, at a separation ∼8 times larger than the largest multiple systems reported to date.

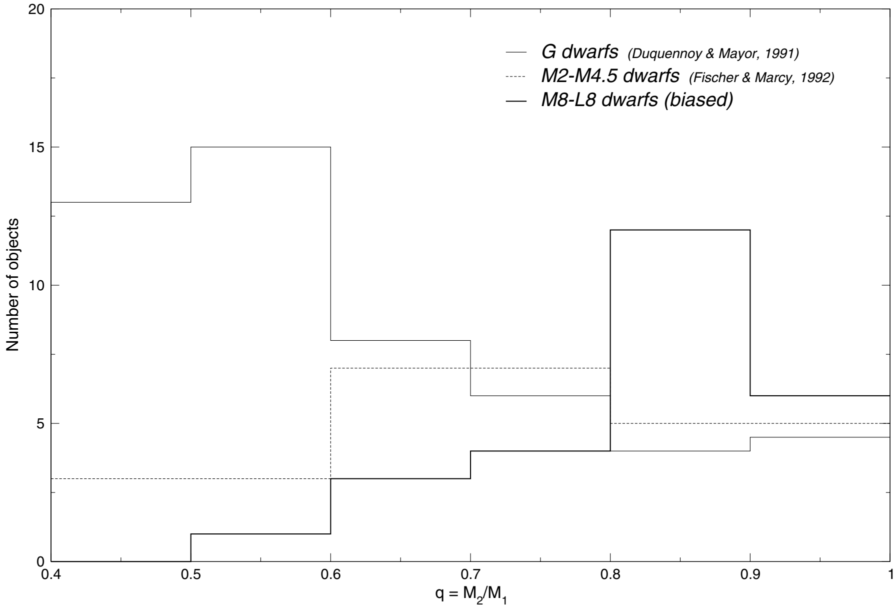

Fig. 2. Distribution of mass ratio of field ultracool binaries, compared to that of G and early-M dwarfs. There seems to be a preference for equal mass ultracool binaries, but this result should be considered with caution since the corresponding sample was biased toward equal mass systems

3 Multiplicity of Ultracool Dwarfs in the Pleiades Open Cluster

The study of multiplicity of ultracool dwarfs in the Pleiades open cluster has also been an intense field of research. One of the first brown dwarfs discovered in the Pleiades was a spectroscopic binary (PPL15, [1]). Table 2 gives a brief overview of the different results obtained over the last few years.

3.1 Binary Fraction

The **visual** binary fractions reported successively by [23, 26] and [5] are consistent one with each other. The first upper limit found by [26] at less than 3% only is not so surprising. Considering the cut-off at about 20 AU in the distribution of separation observed for field objects, and assuming that the properties in the field and in the Pleiades are similar, one indeed expects to find only very few multiple systems at separations greater than the limit of sensitivity of their HST/NICMOS survey (27 AU). The next results obtained at higher angular resolutions with WFPC2 [23] and ACS [5] are consistent one with the other, but disagree completely with the **photometric** binary frequency reported by [32]. Using colour-magnitude diagrams, they report a

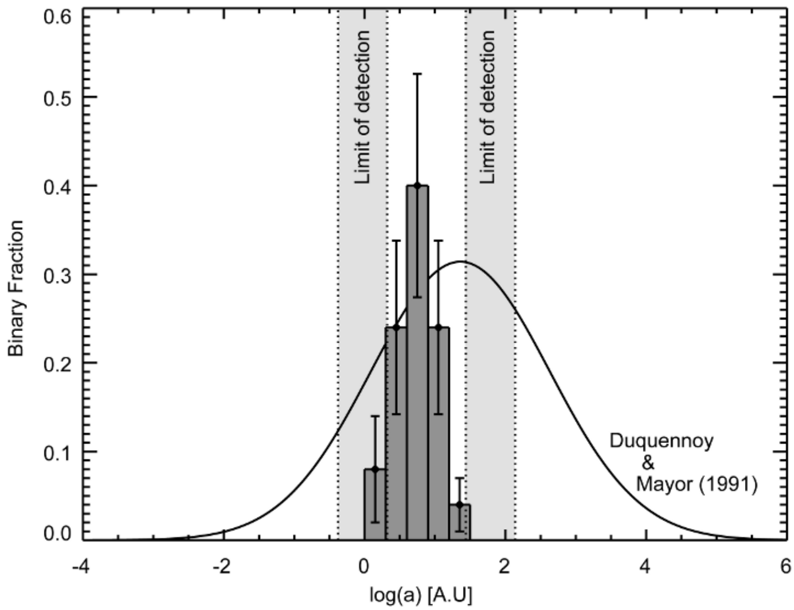

Fig. 3. Distribution of separation of field ultracool binaries, compared to that of G dwarfs from [12]

binary fraction as high as 50%. The 3 surveys covered similar ranges of mass ratios. The discepancy could therefore only be due to the limit of separation of the HST surveys. If confirmed, this difference would mean that most of the brown dwarf binaries in the Pleiades are spectroscopic binaries. The values obtained with the HST surveys are only lower limit on the overall binary fraction. The spectroscopic binary fraction has not been measured neither in the field nor in the Pleiades, but statistical studies have shown that it could be as high as ∼35% ([28]), leading to an overall binary fraction consistent with that reported by [32]. We nevertheless suspect the photometric survey to suffer, among other things, from a significant contamination by foreground objects, leading to an overestimated binary fraction. Similar photometric surveys using 3 colours have been shown to give a contamination as high a 20% ([29]). Surveys looking for spectroscopic binaries will be the main challenge of the coming years in order to precisely and accurately determine the properties of ultracool binaries over the whole separation range.

Figure 1 shows the multiplicity fraction reported in the Pleiades by [5] and [32]. The [5] values are very similar to that observed in the field for objects with similar masses ([6]).

Finally, there seems to be a difference in the multiplicity fraction within the brown dwarf regime itself. Table 2 shows that the binary fraction for M6–M9 dwarfs might be slightly higher than that for cooler objects between

Table 2. Study of multiplicity among Pleiades ultracool dwarfs

Reference	Spectral range	Binary Fraction
[26]	M5–L0	<3% for sep.>27 AU
[23]	M6–M9.5	15±5% for sep.>7 AU
[32]	M6–M8	50±10% photom.
[5]	M6–M9	13^{+14}_{-4}% for sep.>7 AU
[5]	M9–L3	<9.1% for sep.>7 AU

M9-L3, although the small number statistics and the large error bars do not allow to draw any firm conclusion.

Since only few multiple systems have been discovered in the Pleiades, it is not possible to perform any statistically meaningful analysis of the distribution of mass ratio and separations. One must nevertheless note that all the multiple systems resolved have separations less than 12 AU, and all have mass ratio close to unity. If confirmed, it would mean that the properties of multiplicity of ultracool dwarfs in the Pleiades are very similar to that of older isolated field objects. Any mechanism responsible for these properties should therefore have occurred before the age of the Pleiades.

4 Multiplicity of Ultracool Dwarfs in the Upper Scorpius OB Association

Two studies have been recently performed in the Upper Scorpius OB association, one with ACS on-board HST looking for companions among a sample of 12 M5.5–M7.5 dwarfs ([19]), and one with adaptive optics on the VLT among a sample of 58 M0-M7.5 dwarfs. In both cases the targets are confirmed members of the association. As shown in Figure 4, the two studies have similar sensitivities, although NACO proves to give a better resolution at closer separation. The HST study used 3 optical colours which were used to perform a preliminary selection of non-physical pairs, while in its current state the NACO study used only K-band images, therefore with no mean to distinguish real companions from foreground/background sources. The HST optical colours (V, i' and z') providing only poor constraints, second epoch measurements proving common proper motion and spectroscopy are required in both studies to confirm the multiplicity of the candidates.

[19] have performed a search for multiple systems among a sample of 12 bona-fide brown dwarfs using HST/ACS. They resolve 3 candidates, leading to a raw observed **visual** binary fraction of 25±14%, and deduce a binary fraction corrected for biases of 42%. This value is clearly higher than that obtained in the field and in the Pleiades, and if confirmed, would indicate that the dynamical evolution is still on-going at the age of Usco (∼5 Myr).

In June 2005 we resolved 9 binary candidates among the 58 targets of our NACO sample, leading to an observed binary fraction of ∼15%, consistent

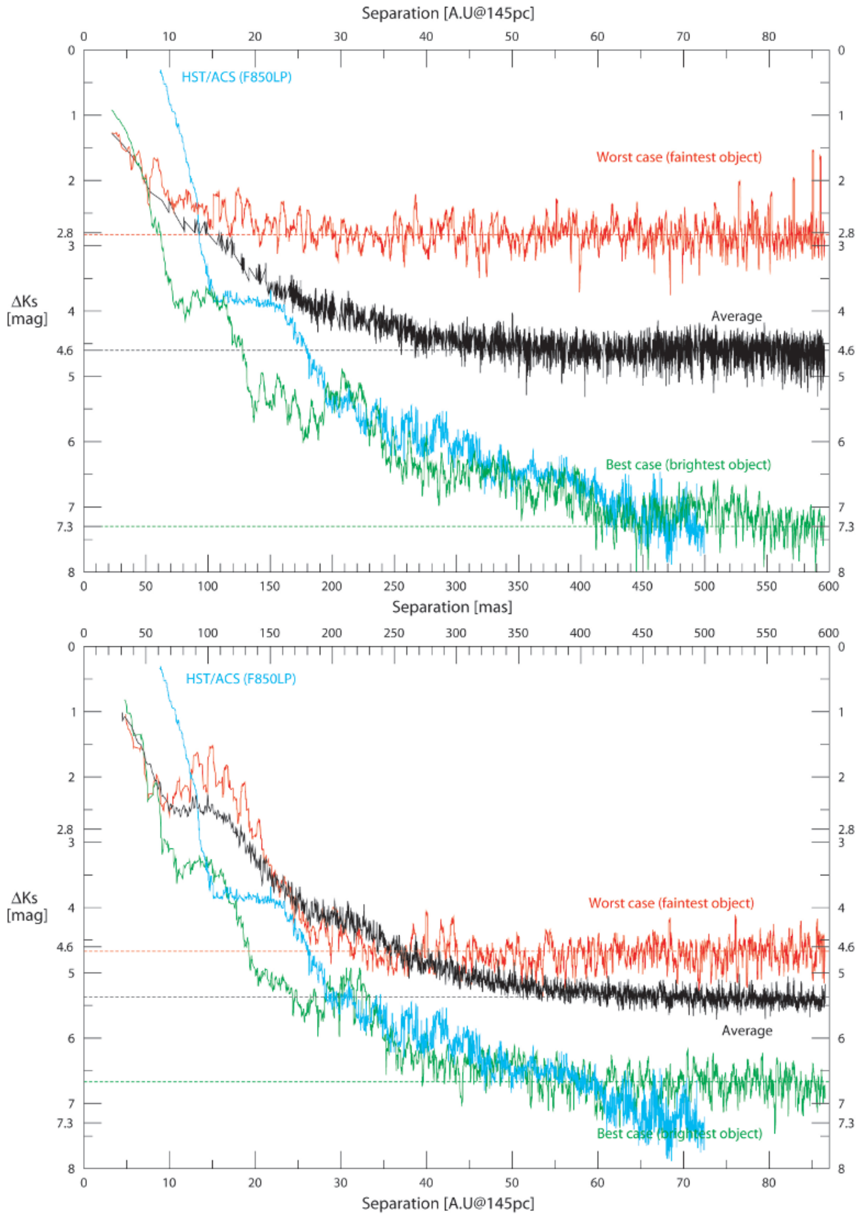

Fig. 4. Sensitivity of the NACO and HST ([19]) studies of Upper Scorpius VLMS and BD. At shorter separation, diffraction limit on an 8 m telescope wins. Moreover, the Ks band images of NACO are much more sensitive to low mass companions than the optical ACS images

within the large error bars with the one reported by [19], eventhough it covers a larger spectral class range. Considering only the 28 objects of our sample within the same spectral class range as [19], we resolve 5 binary candidates among a total sample of 28 objects, leading to a slightly higher observed binary frequency of ∼18%. These values must be corrected for biases, which has not been done at the time this proceeding is written, since most of the candidates still need confirmation by second epoch imaging and spectroscopy.

Two wide binary candidates (separation of 0.9″, corresponding to ∼120 AU at the distance of USco) have been observed with LIRIS at the WHT in La Palma. In both cases the companions have near-infrared J, H and K colours consistent with a spectral type similar to that of the primary. We acquired a spatially resolved spectrum for one the two, which confirm that the companion has the same spectral type as the primary within 1 subclass. The probability to find two objects with similar spectral class within 1” being extremely low, we consider that these objects are physical pairs. The first one still requires spectroscopic measurements to confirm its multiplicity, but the probability to find an object with consistent near-infrared colours within 1” is also very low. With separations of ∼120 AU, these two objects indicate that the frequency of wide multiple systems among ultracool dwarfs might be higher than that observed in the field or in the Pleiades.

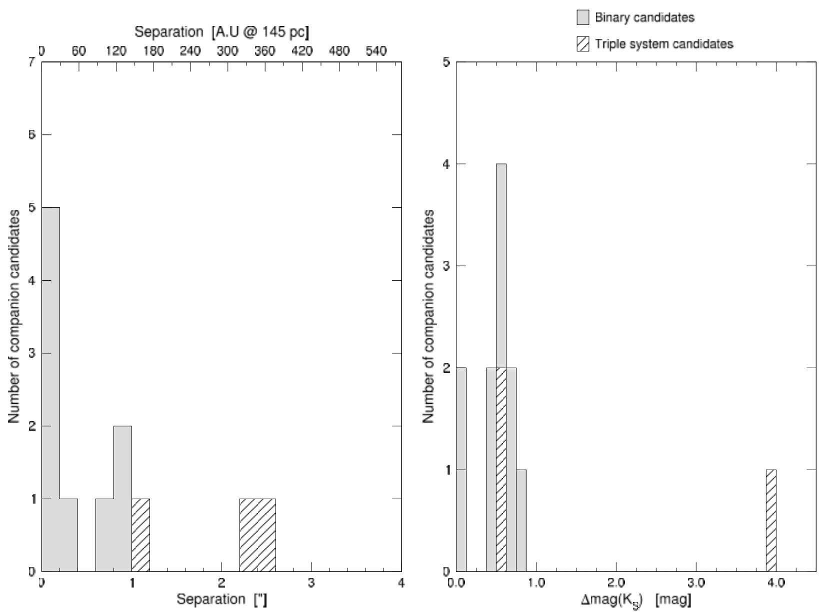

Fig. 5. Distribution of separations and of difference of magnitude (Ks) of the sample of multiple systems discovered with NACO in USco

All three candidates resolved by [19] have mass ratios close to unity. Figure 5 shows the distribution of difference of magnitude of the binary candidates we resolve with NACO. It shows that all objects have small differences of magnitude (less than 1.5 mag). This effect must be real, since we were sensitive to difference as large as 7.3 mag, and it indicates that most of the candidates have mass ratios close to unity, as observed in the field and in the Pleiades. Second epoch images confirming the multiplicity of the candidates are required to confirm this result.

5 Ultracool Dwarfs in other Types of Multiple Systems

Ultracool dwarfs have been found in many other types of multiple systems. [13] have observed a white dwarf-ultracool dwarf pair. Oppenheimer et al. (private comm.) have recently reported a new case of a brown dwarf orbiting an A star. Surveys around G-dwarfs have found few ultracool dwarf companions and the enigmatic "brown dwarf desert". Several multiple systems of higher orders including very low mass stars and brown dwarfs companions have been reported to dates, such as GJ 569B ([18]), GJ 900 ([22]) and HD 130948 ([33]). The properties of all these multiple systems give very important constraints on the formation and evolution of these objects, and possibly indicate that ultracool dwarfs form in several competing or complementary ways.

6 Discussion

The properties of visual multiple systems among the Pleiades and field ultracool dwarfs appear to be very similar, while there seems to be major differences between these two and the population of young Upper Scorpius very low mass stars and brown dwarfs. If, as it is thought, most objects are born in OB associations like Upper Scorpius, this would mean that dynamical evolution is still actively on-going at the age of Upper Scorpius ($\sim$5 Myr). In particular, the larger fraction of wide multiple systems observed in Upper Scorpius must be disrupted within the age of the Pleiades ($\sim$120 Myr), since only few of them are reported either in the Pleiades or in the field.

The two most accepted scenarios of formation of very low mass stars and brown dwarfs are the so-called "star-like" model, which assumes that very low mass stars and brown dwarfs form like stars from the contraction of a molecular cloud, and the "ejection" models, which assume that ultracool dwarfs are ejected embryos from protostellar clusters (see e.g contribution by Delgado-Donate in this volume, and references therein). Although these two models are sometimes presented as distinct and independent mechanisms occurring in separate places, recent hydrodynamical simulations show that the contraction of a molecular cloud leads to the formation of ultracool objects via both processes. The real question of the origin of ultracool dwarfs is therefore not so much which of these two processes is at work, but what are their respective efficiencies, and under which conditions. The properties of multiplicity can address this question, and tentatively give hints of the answers. Together with the growing number of wide multiple systems reported recently by various authors in the field ([2,14,16,24,31]) and in young associations ([7,20,30]), the wide multiple systems we report in USco challenge the models of formation involving gravitational interactions and ejection. That scenario cannot produce such a significant number of wide multiple systems, since they would be destroyed very early in the process of ejection. Although certainly at work, this mechanism can probably not explain the formation of the majority of the very low mass objects. On the other hand, the star-like model fails to explain the cut-off in the distribution if separations at evolved ages, as well as the preference for equal mass systems. While important and fast progresses have been made both on the theoretical and observational sides over the last five years, it seems still too early to draw any firm conclusions regarding the validity of the different models of formation and evolution. These models have not reach yet a level of sophistication allowing direct comparisons with the observations, while the observations must provide improved statistical studies, spanning a larger range of separations and of mass ratios, on larger samples, and should be extended to more environments (young, evolved, dense and loose associations, as well as isolated objects).

References

1. Basri, G. & Martín, E. L. 1999, AJ, 118, 2460
2. Billeres, M., Delfosse, X., Beuzit, J. ., et al. 2005, ArXiv Astrophysics e-prints
3. Bouy, H., Brandner, W., Martín, E. L., et al. 2004, A&A, 424, 213
4. Bouy, H., Brandner, W., Martín, E. L., et al. 2003, AJ, 126, 1526
5. Bouy, H., Moraux, E., & Bouvier, J. et al., 2005, submited to A&A
6. Burgasser, A. J., Kirkpatrick, J. D., Reid, I. N., et al. 2003, ApJ, 586, 512
7. Chauvin, G., Lagrange, A.-M., Dumas, C., et al. 2005, A&A, 438, L25
8. Close, L. M., Lenzen, R., Guirado, J. C., et al. 2005, Nature, 433, 286
9. Close, L. M., Siegler, N., Freed, M., & Biller, B. 2003, ApJ, 587, 407
10. Close, L. M., Siegler, N., Potter, D., Brandner, W., & Liebert, J. 2002, ApJl, 567, L53
11. Delfosse, X., Beuzit, J.-L., Marchal, L., et al. 2004, in ASP Conf. Ser. 318: Spectroscopically and Spatially Resolving the Components of the Close Binary Stars, 166–174
12. Duquennoy, A. & Mayor, M. 1991, A&A, 248, 485
13. Farihi, J., Zuckerman, B., & Becklin, E. E. 2005, ArXiv Astrophysics e-prints
14. Forveille, T., Ségransan, D., Delorme, P., et al. 2004, A&A, 427, L1
15. Gizis, J. E., Reid, I. N., Knapp, G. R., et al. 2003, AJ, 125, 3302
16. Golimowski, D. A., Henry, T. J., Krist, J. E., et al. 2004, AJ, 128, 1733
17. Joergens, V., Neuhäuser, R., Guenther, E. W., Fernández, M., & Comerón, F. 2003, in IAU Symposium, 233–+

18. Kenworthy, M., Hofmann, K., Close, L., et al. 2001, ApJl, 554, L67
19. Kraus, A. L., White, R. J., & Hillenbrand, L. A. 2005, ArXiv Astrophysics e-prints
20. Luhman, K. L. 2004, ApJ, 614, 398
21. Marchal, L., Delfosse, X., Forveille, T., et al. 2003, in SF2A-2003: Semaine de l'Astrophysique Francaise
22. Martín, E. L. 2003, AJ, 126, 918
23. Martín, E. L., Barrado y Navascués, D., Baraffe, I., Bouy, H., & Dahm, S. 2003, ApJ, 594, 525
24. Martín, E. L., Basri, G., Brandner, W., et al. 1998, ApJl, 509, L113
25. Martín, E. L., Brandner, W., & Basri, G. 1999, Science, 283, 1718
26. Martín, E. L., Brandner, W., Bouvier, J., et al. 2000, ApJ, 543, 299
27. Martín, E. L., Koresko, C. D., Kulkarni, S. R., Lane, B. F., & Wizinowich, P. L. 2000, ApJl, 529, L37
28. Maxted, P. F. L. & Jeffries, R. D. 2005, Arxiv Preprint, astro-ph/0507177
29. Moraux, E., Bouvier, J., Stauffer, J. R., & Cuillandre, J.-C. 2003, A&A, 400, 891
30. Neuhäuser, R., Guenther, E. W., Wuchterl, G., et al. 2005, A&A, 435, L13
31. Phan-Bao, N., Martín, E. L., Reylé, C., Forveille, T., & Lim, J. 2005, A&A, 439, L19
32. Pinfield, D. J., Dobbie, P. D., Jameson, R. F., et al. 2003, MNRAS, 342, 1241
33. Potter, D., Martín, E. L., Cushing, M. C., et al. 2002, ApJl, 567, L133
34. Siegler, N., Close, L. M., Cruz, K. L., Martín, E. L., & Reid, I. N. 2005, ApJ, 621, 1023

Spectroscopic Companions of Very Young Brown Dwarfs

Viki Joergens

Leiden Observatory, P.O.Box 9513, 2300 RA Leiden, Netherlands,
viki@strw.leidenuniv.nl

Summary. I review here the results of the first RV survey for spectroscopic companions to very young brown dwarfs (BDs) and (very) low-mass stars in the ChaI star-forming cloud with UVES at the VLT. This survey studies the binary fraction in an as yet unexplored domain not only in terms of primary masses (substellar regime) and ages (a few Myr) but also in terms of companion masses (sensitive down to planetary masses) and separations (< 1 AU). The UVES spectra obtained so far hint at spectroscopic companions of a few Jupiter masses around one BD and around one low-mass star (M4.5) with orbital periods of at least several months. Furthermore, the data indicate a multiplicity fraction consistent with field BDs and stellar binaries for periods $<$100 days.

1 Introduction

The multiplicity properties of brown dwarfs (BDs) are key parameters for their formation. For example, embryo-ejection scenarios predict few binaries in only close orbits (see Delgado-Donate, this proceeding [4]), while isolated fragmentation scenarios allow for an abundance of binaries over a wide range of separations.

In recent years, numerous low-mass and BD binaries were detected by direct imaging in the field and in young clusters and associations (see Bouy, this proceeding [2]). Based on these observations, it was found that very low-mass stars (VLMSs) and BDs pair less frequently in binary systems than solar-like stars. However, these surveys cannot resolve the inner $\sim$3 to 10 AU (depending on distance) around the objects. Companions orbiting at such close separations may have originated based on a substantially different companion formation mechanism than the one found so far by direct imaging. They can be detected indirectly by spectroscopic Doppler surveys. Precise monitoring of the radial velocities (RVs) of BDs became possible in the last years with the generation of 8–10 m class telescopes. Shortly after the high-resolution echelle spectrograph UVES at the VLT saw its first light in October 1999, two programs were started with this instrument in spring 2000 and 2001 in order to systematically search for close companions to BDs and VLMSs in the very young Cha I star-forming region (Joergens & Guenther 2001 [9]; Joergens 2005 [10]) and in the field (Guenther & Wuchterl 2003 [7]). In this article, we present and discuss the current results of the survey in Cha I.

2 Results of RV Survey in Cha I

In order to probe BD multiplicity at very young ages an RV survey of BDs/VLMSs in the Cha I star-forming region (~2 Myr) was started by Joergens & Guenther (2001 [9]). Among a subsample of ten BDs/VLMSs ($M \leq 0.12\,M_{\odot}$, M5–M8), nine do not show signs of companions down to masses of giant planets. The sampled orbital periods for them are < 40 day corresponding to separations <0.1 AU (Joergens 2005 [10]). Monte-Carlo simulations show that the data set provides a fair chance (> 10%) to detect companions even out to 0.4 AU (Maxted & Jeffries 2005 [12]). For the BD candidate Cha Hα 8 (M6.5), RV data were recorded with a time base of a few years and they indicate the existence of a spectroscopic companion of planetary or BD mass with an orbital period of at least several months or even years (Fig. 1). Thus, among ten BDs/VLMSs, none shows signs of BD companions with periods less than 40 days and one with a period > 100 days. Furthermore, the low-mass star CHXR74 (M4.5) also exhibits long-term RV variations (Fig. 4) that are attributed to an orbiting companion with at least 19 Jupiter masses.

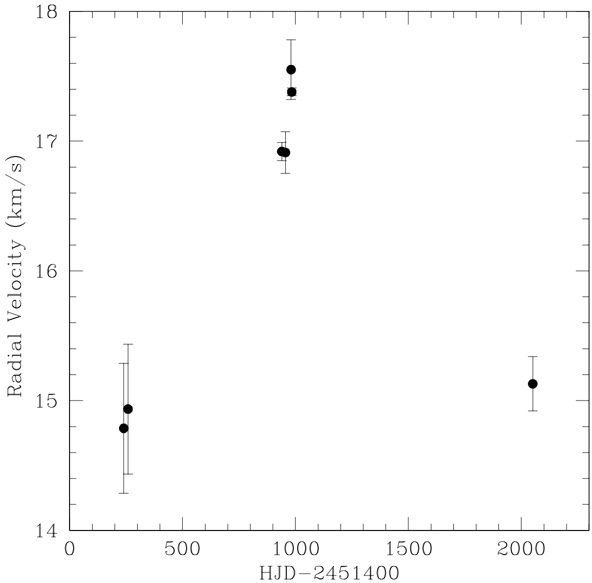

Fig. 1. Radial velocity data for the young BD candidate Cha Hα 8 (M6.5) recorded with UVES/VLT: significant variability occurring on time scales of months to years hints at a companion at $a > 0.2$ AU and a mass $M \sin i$ of at least 6 $M_{\rm Jup}$ (Joergens 2005 [10])

3 Detection of RV Planets around BDs in Cha I Feasible

The RV survey in Cha I revealed that very young BDs/VLMSs exhibit no RV noise due to surface activity down to the precision required to detect Jupiter mass planets (Joergens 2005 [10]). They are, therefore, suitable targets when using the RV technique to search for planets. In the upper panel of Fig. 2, the distribution of RV differences recorded for very young BDs and VLMSs ($M \leq 0.12\,M_\odot$, M5–M8) is compared to the RV signal caused by a planet of 1-10 M_{Jup}. It shows that the RV signal of a giant planet is detectable well above the RV noise level for a BD primary. The lower panel of Fig. 2 displays as comparison RV data for T Tauri stars recorded by Guenther et al. (2001 [6]). The RV amplitude of a planet is completely swallowed by the large systematic RV errors of up to 7 km/s for them making planet detections by the RV technique around very young stars quasi impossible.

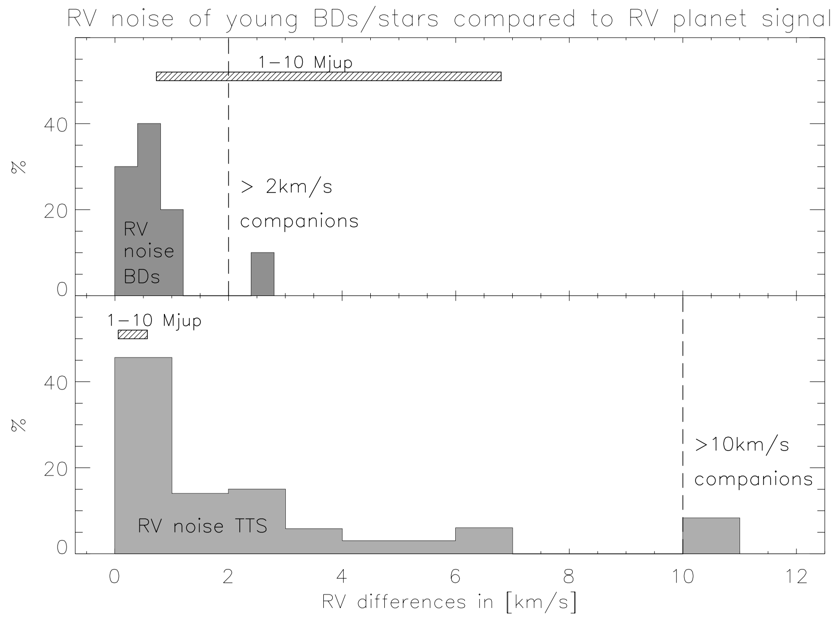

Fig. 2. Distribution of RV differences for very young BDs/VLMSs (upper panel, Joergens 2005 [10]) and for T Tauri stars (lower panel, Guenther et al. 2001 [6]). The plot shows that systematic errors caused by activity at very young ages are sufficiently small in the substellar mass regime to allow for detections of giant planets by the RV technique, which is not the case for T Tauri stars. RV differences/amplitudes in the plot are peak-to-peak values. Inserted ranges of RV planet signals were calculated based on circular orbits, a semi major axis of 0.1 AU and a primary mass of $0.06\,M_\odot$ for BDs, and 1 AU and $1\,M_\odot$ for T Tauri stars, respectively

4 Is the BD Desert a Scalable Phenomenon?

If BDs form in the same way as stars, we should observe an equivalent companion mass distribution for both. Then, the BD desert observed for solar-like stars could exist as a scaled-down equivalent also around BD primaries, this would be a *giant planet desert*, as illustrated in Fig. 3 (Joergens 2005 [10]). The here presented RV survey started to test its existence for BDs in Cha I. For higher than solar-mass primaries, there are indeed hints that the BD desert might be a scalable phenomenon: while RV surveys of K giants detected a much higher rate of close BD companions compared to solar-like stars (e.g. Hatzes et al. 2005 [8], Mitchell et al. 2005 [13]), with only one exception they all do not lie in the BD desert when scaled up for the higher primary masses.

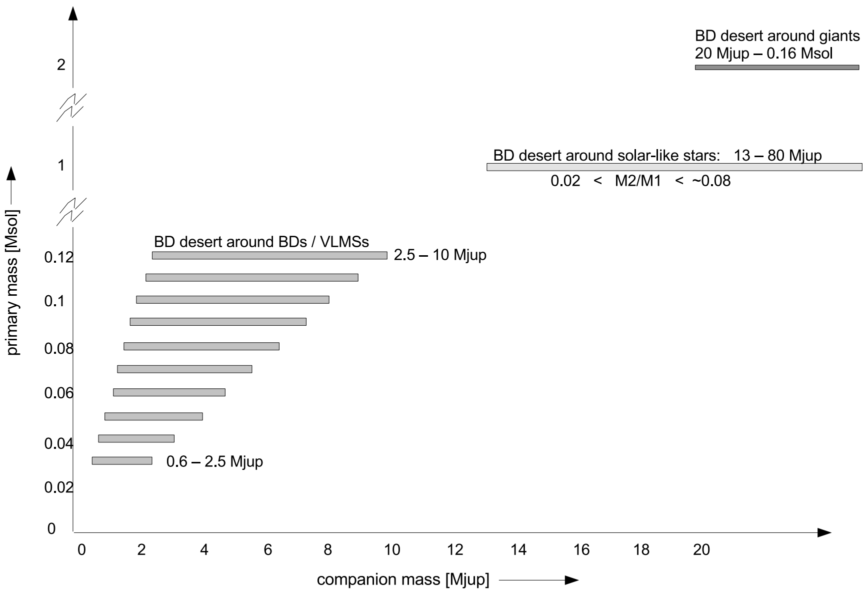

Fig. 3. Schematic illustration of the BD desert as observed for solar-like stars, and of a scaled version of it for lower primary masses (BDs/VLMSs), and for higher primary masses (giants)

5 Conclusions

The study of the multiplicity properties of BDs for separations of less than ∼3–10 AU has been recognized as one of the main observational efforts that are necessary in order to constrain the formation of BDs. This can be done by means of high-resolution spectroscopic surveys. We have presented here the current results of the first RV survey of very young BDs (Joergens 2005 [10]). It exploits the high resolving power and stability of the UVES spectrograph and the large photon collecting area of the VLT. A remarkable feature of this survey is that it is sensitive to planetary mass companions. This is due to a precise RV determination and to the fact that systematic RV errors caused by activity are sufficiently small for the targets to allow for the detection of Jupiter mass planets around them, as shown for the first time by this survey. Thus, very young BDs, at least in Cha I, are suitable targets for the search for close extrasolar planets in contrast to very young stars.

None of the BDs and VLMSs monitored shows signs of BD or planetary companions for separations smaller than 0.1 AU. This hints at a small binary fraction and a low frequency of giant planets in this separation range (zero

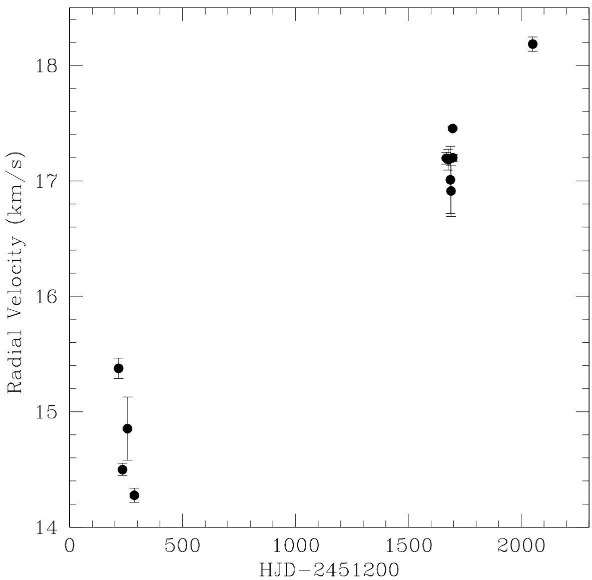

Fig. 4. Radial velocity data for the low-mass star CHXR 74 (M4.5) recorded with UVES/VLT: significant variability occurring on time scales of months to years hints at a companion at $a > 0.4$ AU and a mass $M\sin i$ of at least 19 M_{Jup} (Joergens 2005 [10])

of ten). Within the limited statistics, this result is consistent with the binary frequency found for field BDs/VLMSs (12±7%, Guenther & Wuchterl 2003 [7]) and with the frequency of stellar G dwarf binaries (7%, [5]) in the same separation range. For some of the Cha I targets also larger separations were probed leading to the detection of two candidates for spectroscopic systems: Both the BD candidate Cha Hα 8 (M6.5) and the low-mass star CHXR74 (M4.5) exhibit long-term RV variations that were attributed to orbiting companions with several Jupiter masses at minimum. Orbit solutions have to await follow-up observations. However, the data suggest orbital periods of at least several months, i.e. separations of > 0.2 AU and 0.4 AU, resp.

Direct imaging surveys found a significantly lower frequency of BD binaries with separations a >3–10 AU compared to solar-like stars [2]. This might be (partly) caused by a shift to smaller separations for lower mass primaries. The first surveys that probe the inner few AU around BDs by spectroscopic means are the one presented here (Joergens & Guenther 2001 [9], Joergens 2005 [10], fair detection efficiency for a <0.4 AU [12], sensitive to M_{jup} planets), and the following ones by other groups: Basri & Martín (1999 [1], detection of first spectroscopic BD binary), Reid et al. (2002 [14], single epoch spectra, sensitive to double-lined spectroscopic binaries), Guenther & Wuchterl (2003 [7], fair detection efficiency for a <0.7 AU [12], sensitive to planetary masses) and Kenyon et al. (2005 [11], fair detection efficiency for a <0.02 AU [12], sensitive to BD companions). These surveys do not hint at a higher BD binary fraction at a <1 AU compared to stellar binaries indicating that also the overall binary frequency is lower in the substellar than in the stellar regime. While corrections have to be applied to the observed values because of selection biases (e.g. Burgasser et al. 2003 [3]) and sparse sampling of the velocity data (e.g. Maxted & Jeffries 2005 [12]), a primary gaol is to enlarge and improve the available data set for BD spectroscpic binary studies in terms of sample sizes, phase coverage, and precision of RV data.

References

1. G. Basri, E. L. Martín: ApJ, **118**, 2460 (1999)
2. H. Bouy: Multiplicity at the very low-mass end of the HRD. this proceeding
3. A.J. Burgasser, J.D. Kirkpatrick, I.N. Reid et al. ApJ **586**, 512 (2003)
4. E. Delgado-Donate: the formation of multiple stars. this proceeding
5. A. Duquennoy, & M. Mayor: A&A, **248**, 485 (1991)
6. E. W. Guenther, V. Joergens, R. Neuhäuser et al: A spectroscopic and photometric survey for pre-main sequence binaries. In: *IAU Symposium No. 200*, ed by H. Zinnecker, R.D. Mathieu (ASP, San Francisco) p.165 (2001)
7. E. W. Guenther, G. Wuchterl: A&A, **401**, 677 (2003)
8. A. P. Hatzes, E. W. Guenther, M. Endl et al: A&A, **437**, 743 (2005)
9. V. Joergens, E. Guenther: A&A, **379**, L9 (2001)

10. V. Joergens: A&A, in press, astro-ph/0509134 (2005)
11. M. J. Kenyon, R. D. Jeffries, T. Naylor et al: MNRAS **356**, 89 (2005)
12. P. F. L. Maxted, R. D. Jeffries: MNRAS **362**, L45 (2005)
13. D. S. Mitchell, S. Frink, A. Quirrenbach et al: subm. (2005)
14. I. N. Reid, J. D. Kirkpatrick, J. Liebert et al: AJ **124**, 519 (2002)

The Observed Multiplicity of Low-mass Stars: From Embedded Protostars to Open Clusters

Gaspard Duchêne and Jérôme Bouvier

Laboratoire d'Astrophysique de Grenoble - Université Joseph Fourier - BP 53 - 38041 Grenoble cedex 9 - France
gaspard.duchene@obs.ujf-grenoble.fr, jerome.bouvier@obs.ujf-grenoble.fr

Summary. The multiplicity of stars is a direct tracer of the conditions under which they form and, in particular, it provides constraints on the modes of fragmentation for pre-stellar cores. For several years, we and other groups have conducted systematic surveys for the multiplicity of solar-like and lower-mass stars in nearby young open clusters (a few to a few hundred Myr) to investigate the impact of environmental conditions and/or dynamical processes. These surveys have led to the conclusion that the multiplicity of low mass stars is established by an age of a few million years at most. They have left open, however, the possibility that significant changes occur in the earlier, more embedded phases of protostellar evolution. We have recently started a statistical survey for multiplicity among embedded protostars in order to probe such a possibility. In this contribution, we summarize both types of surveys, i.e., the multiplicity of low-mass stars in young open clusters and that of embedded protostars. Using direct and high-angular resolution imaging, tens of companions have been discovered, leading to statistically significant multiplicity rates that can be compared with the predictions of (multiple) star formation models.

1 Introduction

Multiple systems result from the fragmentation of low-mass molecular cores, a process that occurs for virtually all cores. Studying the statistical properties of multiple systems can therefore provide important clues regarding the physics of this process. For many years now, numerical simulations have attempted to describe the entire sequence of collapse and fragmentation of a molecular core. Unfortunately, this numerical approach is a daunting task in large parts, because of the huge dynamic ranges in density, temperature and relevant timescales required to follow the entire process. For a long time, simplified simulations had to be performed: use of 2-dimensional calculations; impossibility to deal simultaneously with rotation, magnetic field, turbulence and viscosity; calculations halted at the opacity limit without following through until the formation of dense star-like objects, etc. These first simulations were nonetheless highly informative, proving among other things that many physical effects could lead to cloud fragmentation, hinting towards the possibility of a high frequency of multiple systems, and suggesting that the final properties of multiple systems (frequency, distribution of orbital elements) could strongly depend on the physical conditions reigning in the pre-collapse core. In the last few years, new efforts have led to the first simulations of the collapse of entire cores all the way to the formation of disk-surrounded pre-main sequence stars (Bate et al. 2003; Delgado-Donate et al. 2004; Goodwin et al. 2004). With "realistic" initial conditions, these simulations have led to the conclusion that, somewhat independently of the initial conditions, each core would fragment into many objects, typically as many as there are Jeans masses in the core. Most of these objects are then scattered away and ejected as single stars due to the strong dynamical interactions occurring in the center of the cores. The predicted average multiplicity rates are relatively low, though with a strong dependence on stellar mass. These are excellent predictions to confront with observations. The existence of young, unstable several-bodies systems is another prediction that could be tested by imaging young stellar objects with high-angular resolution devices, for instance.

It is now a well-established fact that binaries and higher-order multiple systems are prevalent among field stars of all masses. Duquennoy & Mayor (1991) conducted the most complete multiplicity survey for field stars to date, focusing on solar-type stars and determining an average companion star fraction (number of companions per number of primaries) of $61 \pm 3\,\%$ and a $\sim$10:1 binary:triple ratio. Tokovinin (2004), focusing on previously known binaries, identified additional, usually faint and distant visual, companions leading to a substantially revised 4:1 binary:triple ratio and a slightly higher total companion star fraction. The occurrence of stellar companions in lower mass Main Sequence stars is somewhat lower, especially at separations beyond $\sim$ 10 AU (Delfosse et al., in prep.). More surprising was the discovery in the early 1990s that pre-main sequence solar-type may stars host even more companions. Systematic surveys of Myr-old T Tauri stars in several well-known star forming regions, such as the Taurus-Auriga molecular cloud, discovered almost twice as many visual companions as were expected from the field star population, opening a long standing debate regarding the origin of the discrepancy (see discussion in Duchêne 1999). The fact that the Orion Trapezium low-mass star population showed a "normal" fraction, i.e., field-like, of multiple systems further complicated the situation. Should the Taurus-Auriga or Orion populations be considered exceptions to an almost universal behavior or is it a clear evidence that the fragmentation of pre-stellar cores really depend on environment conditions?

Clearly, the observed properties of $\sim$ 1 Myr-old young multiple stars vary from cloud to cloud, but ten years ago, it was not possible to single out only one scenario that could account for all observations. For instance, Durisen & Sterzik (1994) argued that the range of multiplicity rates observed in different star-forming regions could be accounted for by a difference in initial gas temperature between giant molecular clouds, such as Orion, and smaller clouds, such as Taurus-Auriga. On the other hand, Kroupa (1995) explored the possibility that fragmentation produces a universal population of so-called primordial[1] multiple systems that then could evolve differently based on the environment in which they are. For instance, Kroupa et al. (1999) showed that a single model, in which all stars form as binaries could account simultaneously for the observed multiplicity rate for the low-mass star population in the Taurus-Auriga and Orion clouds as well as in the 100 Myr-old Pleiades open cluster. In this model, the frequent direct system-system interactions during the early stages of the cluster evolution resulted in the disruption of many low binding energy wide systems, naturally explaining the difference between clusters and loose associations.

Among all types of multiple systems, binaries are by far the most frequent. In field solar-type stars, triple and higher-order multiple are 4 to 10 times less frequent than binaries; a somewhat lower ratio seems to apply to T Tauri stars although binaries may still represent the dominant multiplicity mode (Koresko 2002; contribution by Correia et al. in this volume). Being able to explain the (high) frequency of binary systems among low-mass stars in various environments is therefore a key test of star formation theories. However, high-order multiple systems may prove even more useful as both, their formation and survival, is more sensitive to a number of processes, such as direct encounters and complex gas-stars interactions. Systems in which three stars have commensurable separations are prone to N-body dynamical instability and will likely decay into an ejected low-mass single object and a lower-order multiple. This decay, which has been suggested as a possibility for forming brown dwarfs if it happens before the end of the main gas accretion phase (Reipurth & Clarke 2001), appears to occur frequently in numerical simulations, suggesting that it may be hard for multiple systems to survive for millions or billions of years. For all these reasons, determining the properties (frequency, separations, mass ratios) of high order multiples could prove highly valuable in constraining the star formation processes. And we now start to consider the single:binary:triple:quadruple ratios as more valuable than the total number of companions to a sample of targets.

With these goals in mind, we have conducted systematic surveys to determine the frequency and properties of visual companions among low-mass young stars in a variety of environments. In particular, we first studied several open clusters of various ages to constrain the time evolution of multiplicity in clusters on timescales of 1–100 Myr and test whether the Orion population is an exception or a rather normal case. More recently, we have started probing the multiplicity of embedded protostars, which are in a much earlier phase than the previously-studied T Tauri stars, thereby probing the evolution of multiplicity on timescales of 0.1–1 Myr. In the following, we first present our survey of open clusters (Sect. 2) and of embedded protostars (Sect. 3). We then compare the observational results with other multiplicity surveys and with predictions of numerical models to place constraints on the star formation process (Sect. 4).

[1] The term "initial" would actually be more appropriate.

2 Multiplicity in Young Open Clusters

The multiplicity of low-mass members of young open clusters was extensively studied by us (Bouvier et al. 1997, 2001; Duchêne et al. 1999) and by another group (Patience et al. 1998, 2002). The clusters that were surveyed are the following: IC 348 ($\sim$2 Myr), α Perseus ($\sim$90 Myr), the Pleiades ($\sim$125 Myr), M 34 ($\sim$220 Myr), the Hyades ($\sim$600 Myr) and Praesepe ($\sim$700 Myr). Note that in the case of IC 348, a significant age spread has been demonstrated in the low-mass population and only the average age is used here. All clusters are located within 320 pc of the Sun, favoring the detection of close companions, around the 30 AU peak of the separation distribution in Main Sequence binary systems. Depending on observing constraints, the samples that were surveyed encompassed slightly different mass ranges. Only solar-like members were studied in α Perseus, the Pleiades and Praesepe clusters, whereas a $\sim$0.5–2 $M_{\odot}$ mass range was probed in the Hyades, for instance. In IC 348, which is young enough that most targets were in their pre-main sequence phase, masses are less accurately known; all 0.1–2 $M_{\odot}$ members that were bright enough to be observed were targeted.

Altogether, a total of about 730 objects were targeted with near-infrared high angular resolution devices (adaptive optics and speckle interferometry), leading to well over a hundred new companions being discovered and to robust estimates of the statistical properties of multiple stars. Typically, speckle interferometry allows detection of tighter companions, even below the diffraction limit of a telescope, whereas adaptive optics provides a larger dynamic range and therefore a good sensitivity for very faint companions; they are therefore complementary techniques. Because of the limited field-of-view of the instruments used in these surveys, an upper limit of a few to 10 arcseconds on the multiple system projected separations was considered and unrelated background companions were excluded through their near-infrared colors and, in the case of IC 348, of their extreme faintness. Even though future analyses may reveal a few background stars that were not excluded in these surveys, these are unlikely to affect significantly our statistical results.

All clusters yielded remarkably similar results in terms of multiplicity. The raw detection rate for companions is $\sim$20 % for all clusters over almost two decades in projected separations, typically 30–1500 AU. Once completeness corrections are applied to account for tight faint companions that are difficult to detect, this implies a typical companion star fraction, i.e. number of companion per target, of 25–30 %. Within a few percent, this is equal to the fraction expected for Main Sequence solar-type stars as determined by Duquennoy & Mayor (1991) in the same separation range and, consequently, a factor of two lower than what is observed for T Tauri stars in Taurus-Auriga, for instance. The lowest fraction observed, in IC 348, is on order $\sim$20 %, only a few percent lower than solar-type field stars but this is consistent with the fact that a significant fraction of that sample consists of low-mass stars

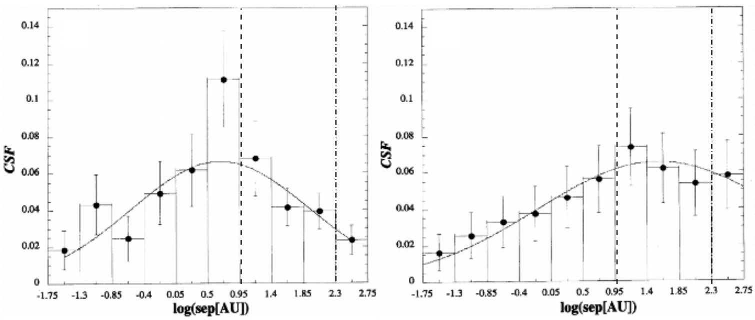

Fig. 1. The projected separation distribution of companions to low-mass stars for a combination of several open clusters (*left*) and for field stars (*right*); adapted from Patience et al. (2002). A Gaussian fit to both distribution is also plotted. Note the relative deficit of companions in clusters beyond ~ 200 AU (dot-dashed lines) whereas the cluster surveys are typically complete down to ~ 10 AU (dashed lines)

($< 0.5\,M_\odot$) for which the companion star fraction is somewhat lower in the field, especially for wide companions.

The separations of the multiple systems detected in the course of these surveys sample the entire range that was probed, from a few AUs to up to 3000 AU in some clusters. In logarithmic bins, the distribution increase towards small separations, in a trend that agrees nicely with that observed for solar-type field binaries (see Fig. 1). There is marginal evidence for a slightly lower proportion of the widest binaries probed in these surveys, i.e., for projected separation beyond ~ 200 AU. This apparent deficit is not significant in any single cluster but appears in all clusters, making it a possibly significant clue for the formation and early evolution of low-mass multiple systems.

For all clusters but IC 348, the mass of the companions can be inferred from their brightness since they are already on the zero-age Main Sequence. In IC 348, the near-infrared brightness ratio of binary systems was converted into a mass ratio assuming an average mass-luminosity relationship appropriate for the age of the cluster. While near-infrared excesses induced by dusty circumstellar disks may lead to misestimates in some systems, this should not affect the entire sample, leading to robust statistical results. The distribution of mass ratios inferred for all clusters is slowly rising towards low values ($q < 0.5$), as observed for wide companions in Main Sequence solar-type binaries (Duquennoy & Mayor 1991). It must be noted that in IC 348, companions much less massive than the brown dwarf limit could have been easily detected; yet, none was found (Duchêne et al. 1999). This is reminiscent of the observed paucity of brown dwarfs in wide orbits around stellar objects, a possible consequence of the low binding energy that such systems would have.

The detection rate of triple and higher-order multiple systems is small, on order 1 % or so. However, there is a clear detection bias against triple systems in these surveys. Broadly speaking, binary systems span rather evenly the entire separation range from contact binaries to 10^6 yr orbital periods, and roughly half of them are located in the separation range probed by the imaging surveys presented here. In triple and higher order systems, however, three-body interactions play an important role and, in order to remain stable for millions of years, the systems must be hierarchical. Typically, a factor of at least 10 between the inner and outer orbital periods is required. Therefore, triple systems that have a companion at a separation of, say, 100 AU must have their third component either too close or too wide to be detected in these surveys. At this point, it is almost impossible to interpret the observed frequency of multiple systems other than to say that their frequency in open clusters is not in excess of what is found among field stars.

An interesting point to note is the fact that the multiple systems in IC 348, the youngest cluster in our sample, are as frequent as among field stars, and not higher. The age of IC 348 is comparable to that of the pre-main sequence populations that were studied in the early 90s and its low-mass members are T Tauri stars. This clearly shows that the Trapezium cluster cannot be considered an exception among all other star-forming regions. Rather, it suggests that all few million years-old clusters have a substantially lower companion star fraction than other loose star-forming regions such as Taurus-Auriga. This leaves both scenarios presented in Sect. 1 (sensitivity to initial conditions on one hand and universal primordial population combined with dynamical interactions/disruptions in dense clusters) open, with the only new constraint that, if dynamical interactions in clusters are at play, they must occur on a timescale shorter than $\sim$1 Myr.

3 Multiplicity among Embedded Protostars

Since the observations of stellar populations that are a few Myr-old could not discriminate between the two main scenarii put forward several years ago, it became clear that the solution may come from the observations of even younger populations. Therefore, the study of low-mass star multiplicity shifted in recent years towards the first Myr of stellar evolution, before the T Tauri phase itself. The youngest such systems, Class 0 protostars that are only $\sim 10^4$ yrs-old, have most of their mass in the envelope and emit principally in the far-infrared and radio domains. Class I sources are in an intermediate evolutionary stage and are increasingly bright at longer infrared wavelengths. High-angular resolution observations of these objects, which are necessary to probe their multiplicity, were not feasible until a few years ago, but recent surveys have taken advantage of the newest generation of instruments. In this section, we present results from various surveys for embedded multiple systems, conducted in the radio and near-infrared regimes.

A first systematic survey was conducted by Looney et al. (2000) with interferometric observations in the millimeter regime, where they were sensitive to the thermal emission from the cold dust surrounding embedded young stellar objects. Concentrating on the 6 Class 0 and 2 Class I sources in their sample (which also included some T Tauri stars), they found that every single protostar had at least one additional companion within their field of view. However, because of the broad ranges of angular separations probed and of distances to the targets, many of these systems had projected separations of several to ten thousand AUs. This implies that some of these systems are likely to be unbound and, in any case, that this survey cannot easily be compared to previous multiplicity surveys which focused on tighter systems. Using a 2000 AU upper limit for projected separation, their surveys was composed of 16 independent systems, including 3 binaries and no higher order multiples. The absence of triple systems can be understood given the small range of separations probed by these observations and, within that range, a $\sim$ 20% companion star fraction should be considered quite substantial. Despite the small number statistics associated to this study that precludes any meaningful comparison to other surveys, this work confirmed that binary (and possibly multiple systems) are prevalent among embedded protostars.

Focusing on a sample of 14 embedded young stellar objects that drive giant molecular outflows (mostly embedded protostars) and gathering near-infrared and radio high-angular resolution data, Reipurth (2000) found an observed binary frequency of order 80%, the highest ever measured in a population of young stars. The projected separations ranged from less than 10 to several thousand AUs and, due to the variety of distance and instrumental technique involved, it is difficult to extract a multiplicity rate that could be compared to other surveys. Yet, the observed multiplicity was so high that it led Reipurth to argue that the presence of giant outflows is directly related to multiplicity, possibly through the dynamical decay of unstable high-order multiples. If true, this would imply, however, that the high multiplicity rate he estimated is actually an overestimate of the intrinsic rate for all embedded sources. Following on this idea, Reipurth et al. (2002; 2004) obtained centimeter-wave high-angular resolution maps of a sample of 21 young stellar objects, mostly Class I sources, and observed a well-defined 33% multiplicity rate over the 0.5–12" angular separation range (distances ranged from 140 to 800 pc). Among these sources, 4 out of 7 objects that drive giant outflows were found to be multiples, a marginally higher rate. Overall, the multiplicity rate of embedded sources is in good agreement with that of T Tauri stars in star-forming regions such as Taurus-Auriga and Ophiuchus.

In a complementary approach, Haisch et al. (2002; 2004) and Duchêne et al. (2004) conducted direct near-infrared imaging surveys of Class I sources in nearby star-forming regions. A total of 119 protostars in the Perseus, Chamaeleon, Serpens, Ophiuchus and Taurus-Auriga have been targeted; in the latter two clouds, the surveys are essentially complete. The importance of these new surveys resides in their larger and better-defined samples, allowing robust statistical analyses. The observed multiplicity rate is again in the 20–30% range, in agreement with the radio surveys described above over

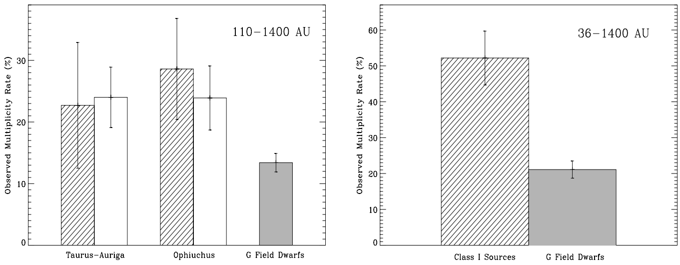

Fig. 2. *Left:* The observed frequency of visual companions for Class I protostars from direct imaging surveys (hatched histograms) and T Tauri stars (empty histograms) in the Taurus and Ophiuchus star-forming regions, from Duchêne et al. (2004). *Right:* Similar histogram after the higher angular resolution surveys, merging all star-forming regions together

similar separation ranges. The observed companion frequency of embedded protostars is also in agreement with surveys of optically-detected T Tauri stars in the Taurus and Ophiuchus clouds (see Fig. 2). In addition to these surveys, we have recently obtained adaptive optics images of a subsample of 44 Class I sources in order to probe a broader range of projected separations for these objects (Duchêne et al., in prep.). With such observations, we can both increase significantly the number of known companions and detect hierarchical multiple systems that were not present in the direct imaging surveys. In the 36–1400 AU separation range, and limiting ourselves to flux ratios not larger than $\Delta K = 4$ magnitudes, we find a 52.2±7.5% companion star fraction for Class I sources. This is about two and a half times higher than the multiplicity rate of solar-type field stars (see Fig. 2) and it is at least as high as the highest rate observed in a population of T Tauri stars.

Of particular interest is the finding that the clustered Perseus and Orion (L1641) populations of embedded protostars show the same multiplicity rates as the Taurus-Auriga and Ophiuchus populations. This is a different behavior than what is observed for T Tauri stars, suggesting that there is indeed a substantial decrease of the multiplicity rate in dense clusters between the embedded protostar and revealed T Tauri phases. Indeed, Duchêne et al. (2004) found evidence that protostars in Taurus-Auriga and Ophiuchus that still possess a substantial envelope revealed by millimeter mapping had a somewhat higher companion star fraction than those who do not. This may be the first direct evidence that the frequency of multiple systems actually evolves during the first million year, possibly as a result of direct system-system interactions in clusters, as suggested by Kroupa (1995).

The observed distribution of projected separations is consistent with that observed for somewhat older T Tauri stars, although small number statistics prevent definitive conclusions in this respect. Mass ratios cannot be inferred from a single near-infrared flux ratio given the complex nature of protostars: ongoing accretion and the details of their opaque environment can result in a wide range of near-infrared fluxes almost independently of the system's total mass. However, a few interesting systems were found with extremely large flux ratios (up to $\Delta K = 6$ magnitudes). Given the rather low luminosities of the primaries, these companions could be very low-mass companions, potentially proto-brown dwarfs. Only spectroscopic follow-up, which is already under way for some systems, will help determining the exact nature of these objects but they represent a potentially crucial population for our understanding of the formation and early evolution of brown dwarfs.

The observed frequency of triple systems (there are no higher order systems), about 14% in the 36–1400 AU range, is relatively high, yielding an observed binary:triple ratio on order 4:1 even though we have sampled a somewhat limited range of projected separations. Extrapolating this ratio to account for much tighter and wider systems, one could expect a $\sim$30% frequency of high order multiple systems, much higher than observed among field stars, for which the binary:triple ratio is merely equal to our *observed* ratio. The proportion of triple and higher-order systems among T Tauri stars is also very high, however, and this may simply reveal the existence of unstable systems yet to be disrupted over longer timescales. Most of the triple systems we have found (5 out of 6) are hierarchical with a ratio of projected separations of at least a factor of 4.7 and therefore a ratio of orbital periods larger than $\sim$10; they are therefore likely to be long-term stable.

4 Implications for the Star Formation Process

Overall, the multiplicity surveys summarized here reveal a relatively clear picture of the early evolution of multiple systems. First of all, it is now clear that low-mass stars in all open clusters have indistinguishable multiplicity properties from field stars, with the possible exception of the frequency of the systems with separations of several hundred AUs. The fact that young cluster and field populations of multiple systems are so similar should not be considered a surprise, since it is believed that most stars form in such clusters (but see Adams & Myers 2001). Still, this independent confirmation is reassuring in that multiple systems can indeed be considered as good tracers of the evolution of stellar population. In addition, it confirms that most multiple systems are already settled by the age of these clusters and little, if any, evolution occurs beyond a few million years. From a dynamical standpoint, this was to be expected, as clusters are usually already relaxed on the large scale by that age and individual unstable multiple systems decay on a much shorter timescale. We note, however, that some of the least dense cluster-like populations of Myr-old stars, like the optically-detected young stars in ρ Ophiuchus, possess a high multiplicity rate, similar to Taurus. This can be interpreted as evidence that the cluster is not dynamically evolved yet, i.e., its crossing time is still longer than its current age, so that most stars have not yet interacted with other members of the cloud. One therefore predicts a significant decrease of the multiplicity rate in this cloud over the next few million years, although we will not be able to test this hypothesis.

Moving in towards younger sources, observations suggest that only few unstable systems decay over the $\sim 10^5$–10^6 yrs timescale probed between Class I protostars and T Tauri stars in loose associations. It is possible that many systems have decayed much earlier on ($<< 10^5$ yrs), but it must be noted that the limited number of isolated single stars is so limited that it is hard to imagine that each pre-stellar core led to the formation of $>$ 4–5 stars. This reasoning has led Goodwin & Kroupa (2005) to conclude that most cores fragment in only 2 or 3 stars. This seems to contradict the results of numerical simulations of turbulent core fragmentation, which tend to form many stars per core. We note, however, that if the strength of the turbulent velocity field is significantly reduced, fragmentation becomes much less efficient, leading to a smaller number of stars formed from a single core.

Another observational-established fact is the moderate mass dependence of the multiplicity rates between $\sim 0.1 M_\odot$ and $\sim 1 M_\odot$, for both main sequence and T Tauri populations. Numerical simulations of turbulent fragmentation predict much stronger mass-dependencies as a consequence of the violent system-system interactions within a single core. The formation and survival of a significant population of low-binding energy systems probably indicates that fragmentation occurs in a much quieter way. It is still too early to use the observed properties of young multiple systems to derive physical parameters of the pre-collapse cores, such as their total mass or turbulent strength (contribution by Delgado-Donate et al. in this volume). A more stringent constraint on the model may eventually come from multiplicity surveys among young brown dwarfs that are already underway.

Possibly the most important results from the multiplicity surveys of embedded protostars is the absence of significant differences between star-forming regions, even though moderate and dense clusters as well as loose associations have been studied. This seems to indicate that the core fragmentation process proceeds to a rather universal set of properties for wide multiple systems despite the wide range of physical properties probed. Most likely, this indicates that the large scale properties of the cloud (such as its total mass or initial gas temperature, before the collapse of the entire cloud) play almost no role on the fragmentation itself, which could be influenced by local properties (e.g., gas temperature just before fragmentation of individual cores). In turn, these properties could be more uniform than expected, even though pre-stellar cores are known to be denser and more compact in cluster-like environments than in loose associations (Motte & André 2001). In any

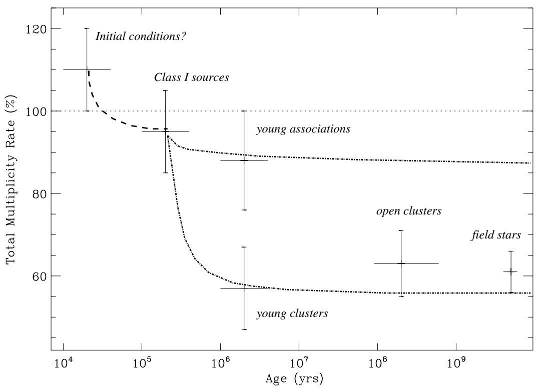

Fig. 3. Time evolution of the *total* multiplicity frequency (extrapolated from the number of visual companions) as a function of time. Horizontal errorbars represent the range of objects observed in each type of populations. The rate for the youngest sources in this plot has *not* been observed so far; we simply estimate it to be somewhat higher than that of Class I sources based on the limited number of ejected single stars. The dashed curve represents the decay of initially unstable multiple systems and the dot-dashed curve the decay due to system-system encounters in stellar populations; these are much stronger in clusters (lower curve) than in loose associations (upper curve), accounting for the dual multiplicity mode around 1 Myr

case, this finding is well in line with the assumption of Kroupa's models, i.e., a universal initial population of multiple systems.

Taking all observations into account, we propose the following scenario for the formation and early evolution of low-mass stars; this scenario is illustrated in Fig. 3. First of all, most low-mass (a few $M_\odot$ at most) pre-stellar cores fragment into 2–4 objects, resulting in a high frequency of both binaries and higher order multiple systems with an overall proportion of 1 or slightly more companion per primary. Over a timescale of $\sim 10^4$ yrs, the multiple systems that are internally unstable decay, thus freeing a few single stars and thereby reducing somewhat the total multiplicity rate (through both the loss of a companion and the addition of a new single primary). Then, each core may interact with its neighbors, at least in dense enough star-forming regions, resulting in a new decrease of the multiplicity frequency on a time scale of a few 10^5 yrs. In loose star-forming regions, this effect is barely noticeable, but it can remove up to 50% of all companions in clusters. After about 1 Myr, the evolution is almost over, as dense clusters have already been dynamically stirred up whereas associations are already almost dissipated in the field. Only intermediate clusters, such as Ophiuchus, may decay on a timescale of several Myr. Finally, field stars are the sum of all stars, i.e., some weighted average of the various star formation channels. While this scenario is entirely consistent with current observations, it still needs confirmation, especially at the youngest ages and, as far as understanding the initial conditions, the universality of the properties of multiple systems still needs to be explained.

As a final thought, we note that the frequency of high-order multiple systems (triples, quadruples, ...) among low-mass embedded protostars has not yet been established with a sufficient statistical significance to be conclusive. However, it seems plausible that they are more frequent than among field stars which could be due to the existence of unstable systems early on. If this is correct, then the disruption of unstable systems should be a rather common phenomenon that could occur on a timescale on order a few 10^4 yrs, so that it is not so unlikely that such events could be witnessed among the youngest systems. While recent claims of dynamical ejection in the T Tau triple system need further monitoring (and may well be wrong), it is important to keep track of proper motion and radial velocities within known multiple systems and for single stars in the vicinity of known multiple systems. In any case, we reiterate the importance of understanding not only the total number of companions in a given sample, but the relative frequency of single, binary, triple, quadruples, ..., systems, as these carry crucial information regarding the processes that occur during the first ~ 1 Myr of their evolution.

References

1. F.C. Adams, P.C. Myers: ApJ, **553**, 744 (2001)
2. M.R. Bate, I.A. Bonnel, V. Bromm: MNRAS, **339**, 577 (2003)
3. J. Bouvier, F. Rigaut, D. Nadeau: A&A, **323**, 139 (1997)
4. J. Bouvier, G. Duchêne, et al.: A&A, **375**, 989 (2001)
5. E.J. Delgado-Donate, C.J. Clarke, et al.: MNRAS, **351**, 617 (2004)
6. G. Duchêne: A&A, **341**, 547 (1999)
7. G. Duchêne, J. Bouvier, T. Simon: A&A, **343**, 831 (1999)
8. G. Duchêne, J. Bouvier, et al.: A&A, **427**, 651 (2004)
9. A. Duquennoy, M. Mayor: A&A, **248**, 485 (1991)
10. R.H. Durisen, M.F. Sterzik: A&A, **286**, 84 (1994)
11. S.P. Goodwin, A.P. Whitworth, D. Ward-Thompson: A&A, **414**, 633 (2004)
12. S.P. Goodwin, P. Kroupa: A&A, **439**, 565 (2005)
13. K.E. Haisch, M. Barsony, et al.: AJ, **124**, 2841 (2002)
14. K.E. Haisch, T.P. Greene, et al.: AJ, **127**, 1747 (2004)
15. C.D. Koresko: AJ, **124**, 1082 (2002)
16. P. Kroupa: MNRAS, **277**, 1491 (1995)
17. P. Kroupa, M.G. Petr, M.J. McCaughrean: New A., **4**, 495 (1999)
18. L.W. Looney, L.G. Mundy, W.J. Welch: ApJ, **529**, 477 (2000)
19. F. Motte, P. André: A&A, **365**, 440 (2001)
20. J. Patience, A.M. Ghez, et al.: AJ, **115**, 1972 (1998)
21. J. Patience, A.M. Ghez, et al.: AJ, **123**, 1570 (2002)
22. B. Reipurth: AJ, **120**, 3177 (2000)

23. B. Reipurth, C.J. Clarke: AJ, **122**, 432 (2001)
24. B. Reipurth, L.F. Rodríguez, et al.: AJ, **124**, 1045 (2002)
25. B. Reipurth, L.F. Rodríguez, et al.: AJ, **127**, 1736 (2004)
26. A.A. Tokovinin: RMxAA, **21**, 7 (2004)

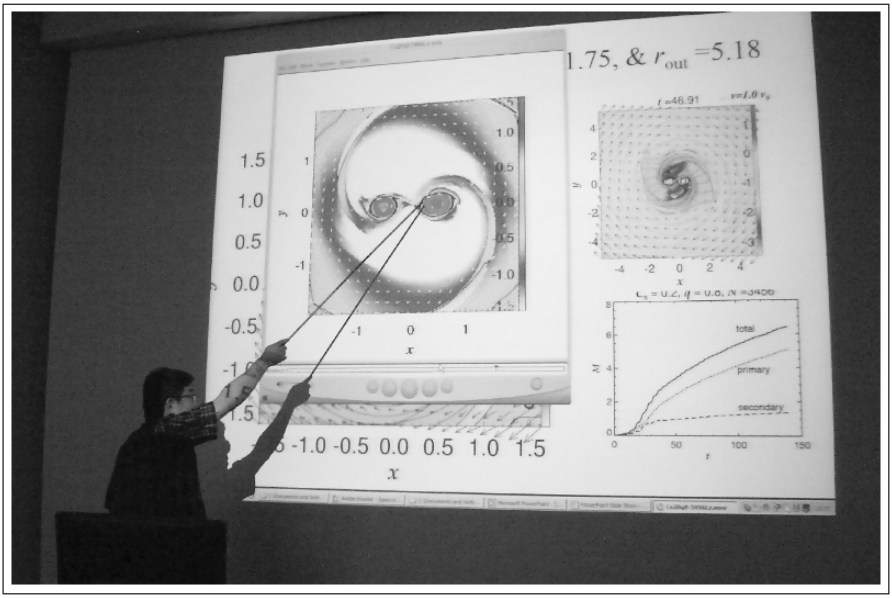

Tomoyuki Hanawa

High-order Multiplicity of PMS Stars: Results from a VLT/NACO Survey

S. Correia[1], H. Zinnecker[1], Th. Ratzka[2] and M.F. Sterzik[3]

[1] Astrophysikalisches Institut Potsdam, An der Sternwarte 16, D-14482 Potsdam, Germany scorreia@aip.de hzinnecker@aip.de
[2] Max-Planck-Institut für Astronomie, Königstuhl 17, D-69117 Heidelberg, Germany ratzka@mpia.de
[3] European Southern Observatory, Casilla 19001, Santiago 19, Chile msterzik@eso.org

Summary. We report on our survey for high-order multiplicity among wide visual Pre-Main Sequence (PMS) binaries conducted with NACO at the VLT. The sample comprises 55 T Tauri systems from various star-forming regions. Of these systems, 8 are found to be triple and 7 quadruple. The corresponding degree of multiplicity among binaries (number of triples and quadruples divided by the number of systems) is 27.3 ±7.0% in the projected separation range $0\farcs07$-$12''$, with the largest contribution from the Taurus cloud. The observed frequency agrees with results from previous multiplicity surveys within the uncertainties, but seems lower than current predictions from numerical simulations of multiple star formation. CTTS-WTTS type statistics among the components of multiple systems is such that half of the systems have mixed-types (i.e. at least one component with a different type), and close pairs are predominantly WTTS pairs. The degree of multiplicity may be higher if we could include spectroscopic components.

1 Observation and Data Reduction

Observations were carried out during two periods. A first set of 37 objects was observed from October 22^{th} 2002 to March 26^{th} 2003 while observations of another 21 systems were conducted from April 4^{th} 2004 to June 17^{th} 2004 (Table 1). A report about the first data set has already been published in [1]. Each object of the first set was observed through the three narrow-band filters Brγ (2.166 μm, 0.023 μm width), H_2 (2.122 μm, 0.022 μm width), and [FeII] (1.644 μm, 0.018 μm width). Objects of the second set were observed only through the [FeII] filter. The combination of natural guide star magnitude and seeing lead to AO-corrections with typical Strehl ratios of $\sim$30% in Brγ, which provides mainly diffraction-limited cores. Data reduction was performed in the usual way: sky subtraction, flat-fielding, bad-pixels and cosmics corrections.

2 Results

All candidate triples/quadruples of our survey are shown in Fig. 1.

Table 1. Observed sample of wide PMS binaries.

Name	R.A. [J2000.0]	Decl. [J2000.0]	Cloud	Dist. [pc]	V [mag]	K [mag]	Obs. date [UT]
LkHα 262/263 ..	02 56 08.4	+ 20 03 40	MBM 12	275	14.6	9.5	2002 Nov 14
J 4872	04 25 17.6	+ 26 17 51	Taurus	142	13.0	8.6	2002 Nov 13
FV Tau	04 26 53.6	+ 26 06 55	Taurus	142	15.4	7.4	2002 Nov 13
UX Tau	04 30 04.0	+ 18 13 49	Taurus	142	10.7	7.6	2002 Oct 22
DK Tau	04 30 44.3	+ 26 01 25	Taurus	142	12.6	7.1	2002 Nov 13
HK Tau	04 31 50.6	+ 24 24 18	Taurus	142	15.0	8.6	2003 Feb 17
LkHα 266	04 31 57.8	+ 18 21 37	Taurus	142	14.6	8.5	2002 Oct 22
GG Tau	04 32 30.3	+ 17 31 41	Taurus	142	12.3	7.4	2002 Oct 22
UZ Tau	04 32 43.0	+ 25 52 32	Taurus	142	12.9	7.4	2002 Nov 14
HN Tau	04 33 39.3	+ 17 51 53	Taurus	142	13.7	8.4	2003 Feb 18
IT Tau	04 34 13.9	+ 26 11 42	Taurus	142	14.9	13.7	2003 Feb 19
L1642-1	04 35 02.3	− 14 13 41	L1642	100	13.7	7.7	2003 Feb 20
RW Aur	05 07 49.6	+ 30 24 05	Auriga	142	10.3	7.0	2002 Nov 17
CO Ori	05 27 38.3	+ 11 25 39	Orion	460	10.6	6.5	2002 Nov 13
AR Ori	05 35 54.1	− 05 04 14	Orion	460	13.9	9.8	2003 Feb 19
LkHα 336	05 54 20.1	+ 01 42 56	L1622	460	14.4	9.2	2003 Feb 19
CGHα 5/6	07 31 37.4	− 47 00 22	Gum Neb.	450	14.2	9.1	2002 Dec 23
PHα 14	08 08 33.8	− 36 08 10	Gum Neb.	450	15.8	10.3	2002 Dec 23
PHα 30	08 12 05.6	− 35 31 45	Gum Neb.	450	15.1	12.2	2003 Jan 17
vBH 16	08 27 39.0	− 51 09 50	Gum Neb.	450	15.6	9.3	2003 Jan 27
PHα 51	08 15 55.3	− 35 57 58	Gum Neb.	450	15.9	11.1	2003 Jan 23
HD 76534	08 55 08.7	− 43 28 00	DC164.3+1.5	830	8.0	7.8	2003 Jan 20
SX Cha	10 55 59.9	− 77 24 41	Cha I	160	14.7	8.7	2003 Jan 22
Sz 15	11 05 41.5	− 77 54 44	Cha I	160	...	10.6	2003 Jan 22
ESO Hα 281	11 07 04.0	− 76 31 45	Cha I	160	...	9.7	2003 Jan 22
Sz 19	11 07 20.7	− 77 38 07	Cha I	160	10.9	6.2	2003 Jan 20
VV Cha	11 07 28.4	− 76 52 12	Cha I	160	14.8	9.5	2003 Feb 19
VW Cha	11 08 01.8	− 77 42 29	Cha I	160	12.6	7.0	2003 Feb 20
Glass I	11 08 15.4	− 77 33 54	Cha I	160	13.3	6.9	2003 Feb 20
CoD −29 8887 ...	11 09 14.0	− 30 01 39	TW Hya	50	11.1	6.7	2003 Jan 20
Sz 30	11 09 12.3	− 77 29 12	Cha I	160	13.2	9.0	2003 Jan 20
Hen 3-600	11 10 28.9	− 37 32 05	TW Hya	50	12.1	6.8	2003 Feb 20
Sz 41	11 12 24.5	− 76 37 06	Cha I	160	11.6	8.0	2003 Jan 22
CV Cha	11 12 27.8	− 76 44 22	Cha I	160	11.0	6.9	2003 Jan 20
Sz 48	13 00 53.2	− 77 09 10	Cha II	178	...	9.5	2004 Apr 06
BK Cha	13 07 09.3	− 77 30 24	Cha II	178	15.2-16.5	8.4	2004 Apr 03
Sz 60	13 07 23.4	− 77 37 23	Cha II	178	...	9.5	2004 Apr 05
Sz 62	13 09 50.7	− 77 57 24	Cha II	178	15.6	9.1	2003 Jan 22
Herschel 4636	13 57 44.1	− 39 58 45	NGC 5367	630	9.7	7.2	2003 Jan 20
ESO Hα 283	15 00 29.6	− 63 09 46	Circinus	700	...	10.3	2003 Mar 26
Sz 65	15 39 27.7	− 34 46 17	Lupus I	190	12.7	8.0	2004 Apr 06
Sz 68	15 45 12.9	− 34 17 31	Lupus I	190	10.4	6.5	2004 Apr 06
HO Lup	16 07 00.6	− 39 02 19	Lupus III	190	13.0	8.6	2004 Apr 06
Sz 101	16 08 28.4	− 39 05 32	Lupus III	190	15.5	9.4	2004 Apr 10
Sz 108	16 08 42.7	− 39 06 18	Lupus III	190	13.1	8.8	2004 Apr 10
Sz 120	16 10 10.6	− 40 07 44	Lupus III	190	7.1	6.2	2004 Apr 10
WSB 3	16 18 49.5	− 26 32 53	Ophiuchus	160	...	9.3	2004 May 01
WSB 11	16 21 57.3	− 22 38 16	Ophiuchus	160	18.5	10.1	2004 Jun 18
WSB 20	16 25 10.5	− 23 19 14	Ophiuchus	160	13.4	7.5	2004 May 01
WSB 28	16 26 20.7	− 24 08 48	Ophiuchus	160	...	9.5	2004 May 01
SR 24	16 26 58.8	− 24 45 37	Ophiuchus	160	...	7.1	2004 May 01
Elias 2-30	16 27 10.2	− 24 19 16	Ophiuchus	160	14.1	6.7	2004 May 01
WSB 46	16 27 15.1	− 24 51 39	Ophiuchus	160	...	9.4	2004 May 01
Haro 1-14c	16 31 04.4	− 24 04 32	Ophiuchus	160	12.7	7.8	2004 May 01
ROX 43	16 31 20.1	− 24 30 05	Ophiuchus	160	10.6	6.7	2004 May 04
Elias 2-49	16 40 17.9	− 23 53 45	Ophiuchus	160	8.9	5.5	2004 May 01
HBC 652	16 48 18.0	− 14 11 15	L162	160	13.5	7.5	2004 May 01
B59-1	17 11 03.9	− 27 22 57	B59	160	...	8.1	2004 May 01

2.1 Chance Projections

In order to discriminate systems whose components are gravitationally bound from those that are only the result of chance projection, we used two approaches. The first one is a statistical approach which consists of estimating the probability that the companions we found are physically bound to their primary based on the local surface density of background/foreground sources in each field. The details of the method are reported in Correia et al. [2]. We found that all but three of the companions detected in our survey have probabilities for chance projection well below the 1% level. This means that most are very likely bound to their systems, although considering probabilities to individual sources is known to be prone to errors (see e.g. [3] for a discussion). The candidate companions (ESO Hα 283 C, ESO Hα 283 D, and PHα 30 C) show a non-negligible probability of being chance projections, with probabilities of 2.9%, 37%, and 8.8%, respectively. The second approach is an attempt to determine the nature of the new or so far unconfirmed candidate companions through the use of a color-color J-H/H-K diagram and has already been shown [1]. Although spectroscopy and common proper-motion

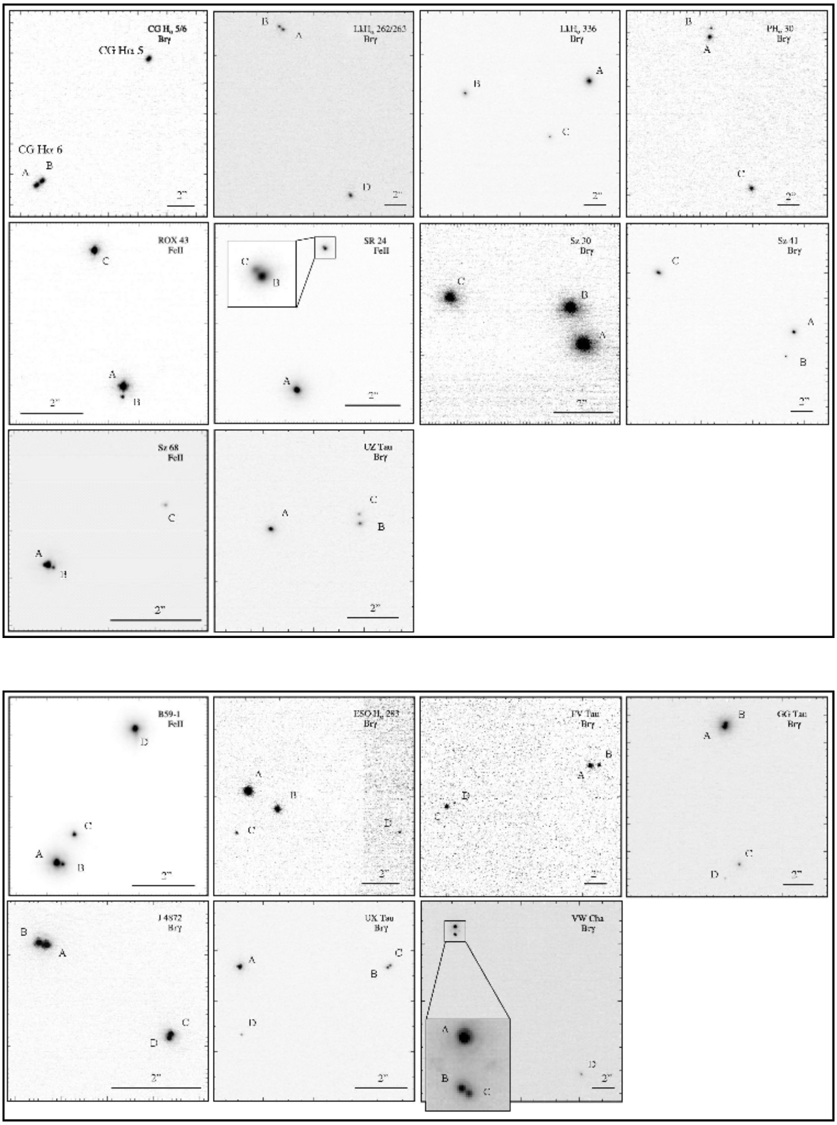

Fig. 1. Apparent triple (upper panel) and apparent quadruple (lower panel) systems detected in our VLT/NACO survey, showing the adopted nomenclature. North is up, east is left

evidence are necessary in order to unambiguously identify any chance projection, we conclude from the above analysis that PHα 30 C, ESO Hα 283 C and ESO Hα 283 D are consistent with being projected background stars. We will not consider further these companion candidates in our analysis.

2.2 Multiplicity Statistics

Among the 58 wide binaries surveyed, two are Herbig Ae/Be binary stars (HD 76534 and Herschel 4636) and one is likely to be a foreground (older) object (Sz 15). We excluded these systems from the statistics and take into account an additional faint companion known from other studies but undetected here for sensitivity reasons (LkHα 262/263C that was found recently as an edge-on disk [4]). We have thus 40 binaries, 8 triples and 7 quadruples. We did not attempt to correct for incompleteness. Therefore, the number of triple/quadruple systems identified should be considered as lower limits, given our sensitivity limits (discussion in [2]).

In order to characterize the multiplicity, we here define a quantity that we call *degree of multiplicity per wide binary* (or a multiplicity frequency per wide binary, MF/wB) :

$$MF/wB = \frac{T + Q + ...}{wB + T + Q + ...}, \tag{1}$$

where wB represents the number of wide binaries (with projected component separations typically $\gtrsim 1''$), T the number of triples and Q the number of quadruples. This quantity here equals 27.3 $\pm$7.0%.

The question that arises naturally is the one about the multiplicity frequency in different clouds, although the latter is of lower statistical significance than that of the total sample. The cloud with the highest value is Taur-Aur (5 triples-quadruples/10 wide binaries, MF/wB=50 $\pm$22%), followed by Cha I (3/10, MF/wB=30 $\pm$17%) and Ophiuchus (2/10, MF/wB=20 $\pm$14%).

We considered a distance-limited sample in order to ensure a similar range of linear projected separations probed. Limiting ourselves to only the wide binaries of the sample at distance 140-190pc (i.e. for which multiples have companions in the separation range 10/14 AU - 1700/2300 AU corresponding to a projected separation between $0.''07$ and $12''$), one obtains MF/wB=28.6 $\pm$8.3% (30 binaries, 6 triples, 6 quadruples).

Comparison with Previous Multiplicity Surveys

We compared our result with the proportion of triples/quadruples found in previous multiplicity surveys with similar separation range and sensitivity. These are the studies by Leinert et al. [5] and Köhler & Leinert [6] in Tau-Aur, Ghez et al. [7] in Chamaeleon, Lupus and CrA, and Köhler et al. [8] in the Scorpius-Centaurus OB association. We based this comparison on the multiplicity frequency per wide binary, as defined above (Eq.1), including in these surveys only binaries with separations larger than about $1''$ (i.e. ∼140 AU). On our side, we had to restrict the separation range to the resolution achieved by those surveys (i.e. typically $\sim 0\farcs1$-$12''$ at 140 pc that is ∼14-1700 AU). This means that, when considering the systems from the distance-limited sample as defined above, we had to discard two companions (VW Cha C and SR 24 C, with projected separations $0\farcs11$ and $0\farcs08$, respectively), ending up with MF/wB=26.2 ±7.9% (31 binaries, 6 triples, 5 quadruples). The result, as summarized in Table 2, is that our newly derived multiplicity agrees with the previous surveys, within the uncertainties.

Comparison with Theory

There is a probable overabundance of high-order multiples produced by the current simulations of star formation with respect to current observations. Direct comparison is not possible since theoretical multiplicity frequencies include both, all the binaries with separations < 140 AU, down to $\sim$ 3-5 AU, and wider high-order companions (with separations $\gtrsim 2000$ AU), unlike the observations. However, we assumed here that the corrections to be applied in order to obtain MF/wB in the same separation range are minor [2]. In the following, we summarize the theoretical studies used for the comparison.

Sterzik & Durisen [9] performed few-body cluster decay simulations. Although that study neglected the effect of remnant molecular gas and disk accretion and treated only the process of dynamical evolution of young small N-body clusters, it yields highly significant and robust statistics since a large number of realizations (10 000) has been computed. A degree of multiplicity of 34% was found. Delgado-Donate et al. [10] modeled the dynamical decay of a large number (a hundred) of small-N (N=5) star-forming clusters including the effects of competitive accretion and dynamical evolution through 3D hydrodynamical simulations with a ∼1AU spatial resolution, and found a rather high multiplicity frequency close to 50%. A similar high frequency of multiple systems was the outcome of two other recent and more sophisticated hydrodynamical simulations. Delgado-Donate et al. [11] simulated the fragmentation of 10 small-scale turbulent molecular clouds and their subsequent dynamical evolution, including this time the effect of accretion disks into the evolution of multiples. Goodwin et al. [12] followed the collapse and fragmentation of 20 dense star-forming cores with a low-level of turbulence. In both cases a high frequency of high-order multiples was obtained (Table 2).

3 CTTS vs WTTS Companion Statistics

We performed a compilation of T Tauri types for both individual components and pairs of the triple/quadruple systems from the available literature [2]. It turns out that, among the systems with CTTS/WTTS information for each component (8 systems), one half are systems of mixed type (i.e. at least

Table 2. Comparison of the multiplicity frequency per wide binary (MF/wB) of our work with those derived from previous multiplicity surveys among T Tauri stars in the same separation range ∼14-1700 AU, and with recent numerical simulations (bottom part).

Reference	cloud	MF/wB
This work	several	$26.2 \pm 7.9\%$
Leinert et al. (1993)	Tau-Aur	$18.5 \pm 8.3\%$
Koehler et al. (1998)	Tau-Aur	$41.2 \pm 15.6\%$
Ghez et al. (1997)	Cha/Lup/CrA	$13.6 \pm 7.9\%$
Koehler et al. (2000)	Sco-Cen OB assoc.	$26.1 \pm 10.6\%$
Sterzik & Durisen (2003)		34%
Delgado-Donate et al. (2003)		49.8%
Delgado-Donate et al. (2004)		$38.9 \pm 14.7\%$
Goodwin et al. (2004)		$56.3 \pm 18.8\%$

one component with a different type). This is quite in contrast with what is known for binaries (e.g. [13, 14]). Another interesting point is that close pairs are usually non-accreting in these systems. In fact, here almost all pairs with separations $\lesssim 0.''3$ (∼50 AU) are WTTS-WTTS pairs. There are two important exceptions : GG Tau AB and UZ Tau BC. However, GG Tau AB is known to be surrounded by a massive circumbinary disk for resplenishment.

References

1. Correia, S., Ratzka, Th., Sterzik, M.F., Zinnecker, H. : A VLT/NACO Survey for Triple Systems among Visual Pre-Main Sequence Binaries. In: *Science with Adaptive Optics*, eds. W. Brandner & M. Kasper (Springer-Verlag 2004).
2. Correia, S., Zinnecker, H., Ratzka, Th., Sterzik, M.F. : 2006, to be published in A&A.
3. Brandner, W., Zinnecker, H., Alcalá, J.M. et al. 2000, AJ, 120, 950.
4. Jayawardhana, R., Luhman, K.L., D'Alessio, P. et al. 2002, ApJ, 571, L51.
5. Leinert, Ch., Zinnecker, H., Weitzel, N. et al. 1993, A&A 278, 129.
6. Köhler, R. & Leinert, Ch. 1998, A&A 331, 977.
7. Ghez, A.M., McCarthy, D.W., Patience, J.L. et al. 1997, ApJ, 481, 378.
8. Köhler, R., Kunkel, M., Leinert, Ch. et al. 2000, A&A 356, 541.
9. Sterzik, M.F. & Durisen, R.H. 2003, A&A, 400, 1031.
10. Delgado-Donate, E.J., Clarke, C.J., Bate, M.R. 2003, MNRAS, 342, 926.
11. Delgado-Donate, E.J., Clarke, C.J., Bate, M.R. et al. 2004, MNRAS, 351, 617.
12. Goodwin, S.P., Whitworth, A.P., Ward-Thompson, D. 2004, A&A, 414, 633.
13. Prato, L. & Simon, M. 1997, ApJ, 474, 455.
14. Hartigan, P. & Kenyon, S.J. 2003, ApJ, 583, 334.

Accretion onto Binary YSOs Through Gap from Their Circum-binary Disk

Tomoyuki Hanawa[1,2], Yasuhiro Ochi[2] and Koichi Ando[2]

[1] Center for Frontier Science, Chiba University, Yayoi-cho 1-33, Chiba 263-8522, Japan hanawa@cfs.chiba-u.ac.jp

[2] Graduate School of Science and Technology, Chiba University, Yayoi-cho 1-33, Chiba 263-8522, Japan

Summary. We have reexamined gas accretion onto YSO binary from the circum-binary disk on the basis of 2D numerical simulations with very high spatial resolution. The binary was assumed to have either a circular or an elliptic orbit. At the initial stage, the circum-binary disk has an inner edge at $r_{\rm in} \geq 1.75a$, where a denotes the mean separation of the binary. The disk is assumed to rotate with the Keplerian velocity. We have confirmed that gas accretes from the circum-binary disk through the L_2 point into the Roche lobe. The gas accretes mainly onto the primary after circulating half around the secondary. This means that the accretion decreases the mass ratio. The accretion through gap is due to some pairs of two-armed spiral shock waves. While a pair of them corotates with the binary, the other pairs rotate more slowly, e.g., at $\Omega = \Omega_*/4$ in most models, where Ω_* denotes the mean angular velocity. Whenever the slowly rotating shock waves get accross the L_2 point, the gas flow increases. Thus the accretion rate of the binary changes with the frequency, $\nu = (3/2)\,(\Omega_*/2\pi)$, in the case of a circular orbit. When the orbit is eccentric, the accretion rate changes mainly with the binary orbit but not purely periodically.

1 Introduction

Stars acquire their zero age masses mainly thorough accretion in the protostellar phase. Since majority of protostars have their companions, we should take account of the effects of their companions on the gas accretion. First, the gas accretion is shared between the primaries and secondaries in binaries. Second, the gravitational torque may induce gas accretion from the circum-binary disk in binaries. The former tends to lower the gas accretion, while the latter tends to enhance it. We have performed numerical simulations with extremely high spatial resolution to evaluate the two effects. From the numerical simulations we have found two new features. First, the accretion rate is highly oscillatory even when the binary orbit is circular. Second, the accretion rate on the primary is much larger than on the secondary. We show the results of our numerical simulations and discuss the implications.

2 Model and Method of Computation

We consider a binary system accreting gas from the circum-binary disk. We ignore the self-gravity of the accreting gas for simplicity. The binary is assumed to have either a circular or an eccentric orbit. We assume further that the binary and circum-binary disk are coplanar and hence the gas flow is two-dimensional for simplicity. The accreting gas is assumed to be isothermal. Then we solve the two-dimensional hydrodynamical equations,

$$\frac{\partial \Sigma}{\partial t} + \boldsymbol{\nabla} \cdot (\Sigma \boldsymbol{v}) = 0 \,, \tag{1}$$

and

$$\frac{\partial \boldsymbol{v}}{\partial t} + (\boldsymbol{v} \cdot \boldsymbol{\nabla})\, \boldsymbol{v} + {c_{\mathrm{s}}}^2 \,\boldsymbol{\nabla} \ln \Sigma + \boldsymbol{\nabla} \Phi \,, \tag{2}$$

where Σ, $\boldsymbol{v}$, c_{s}, and Φ denote the surface density of the gas, the gas velocity, the sound speed, and the gravitational potential, respectively. The gravitational potential is evaluated to be

$$\Phi(\boldsymbol{r},\, t) = \Phi_1 + \Phi_2 \,, \tag{3}$$

$$\Phi_i = \begin{cases} -\dfrac{GM_i}{|\boldsymbol{r} - \boldsymbol{r}_i|} & \text{for } |\boldsymbol{r} - \boldsymbol{r}_i| \geq R_i \\ -\dfrac{GM_i}{2R_i^3}\,(3R_i^2 - |\boldsymbol{r} - \boldsymbol{r}_i|^2) & \text{otherwise,} \end{cases} \tag{4}$$

where $\boldsymbol{r}_i$ and R_i denote the position and the effective radius of each star, respectively. At the initial stage ($t = 0$), the surface density is set to be

$$\Sigma_0 = 0.505 + 0.495 \tanh \left(\frac{r - r_{\mathrm{in}}}{H} \right) , \tag{5}$$

where r_{in} and H denote the radius of the disk inner edge and the width of the transition region. The initial velocity is set to be

$$\boldsymbol{v}_0 = \Omega \begin{pmatrix} -y \\ x \end{pmatrix} , \tag{6}$$

where

$$\Omega = \left[\frac{G\,(M_1 + M_2)}{a^3} \min \left(1,\, \frac{a^3}{r^2} \right) - \frac{{c_{\mathrm{s}}}^2}{\Sigma_0 r} \frac{d\Sigma_0}{dr} \right]^{1/2} . \tag{7}$$

The density and velocity are kept at the initial values in the region $r \geq r_{\mathrm{out}}$.

The hydrodynamical equations were integrated in the rotating frame of which angular velocity was the mean angular velocity of the binary. The computation region was covered with the Cartesian grid having 2400^2 to 3456^2 cells. We adopted the numerical scheme of Roe which captures shock waves without numerical oscillations. We used Monotone Upsream-centerd Schemes for Conservation Laws (MUSCL) to achieve accuracy in time and space. The time step was taken to be twice longer in the region $r \leq r_{\mathrm{out}}/2$ than in the outer region. This dual time step reduced the numerical viscosity and hence improved the accuracy significantly.

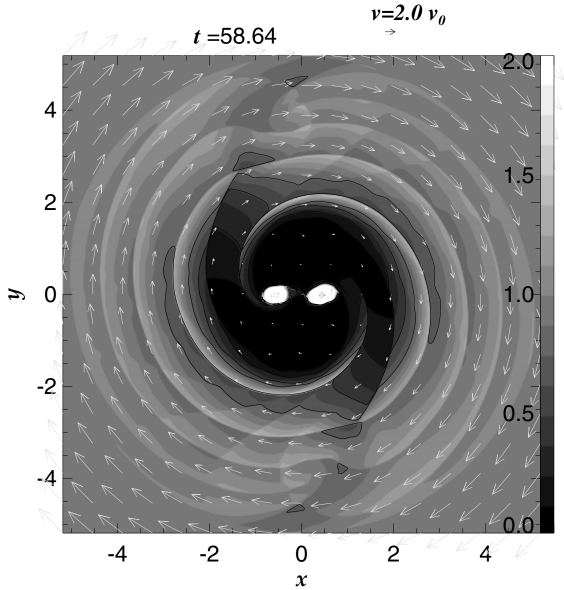

Fig. 1. The surface density distribution at the moment $t = 58.64$ for the model with $c_{\mathrm{s}} = 0.2$, $q = 0.8$, $e = 0.0$, $r_{\mathrm{in}} = 1.75$, and $r_{\mathrm{out}} = 5.175$ is shown. The arrows denote the velocity in the corotating frame

3 Results

3.1 Typical Model

Figure 1 shows the surface density distribution at $t = 58.64$ for the model with $c_{\mathrm{s}} = 0.2$, $q = 0.8$, $e = 0.0$, $r_{\mathrm{in}} = 1.75$, and $r_{\mathrm{out}} = 5.175$. The brightness denotes the surface density in the linear scale in the surface density range $\Sigma \leq 2$. The circum-primary and circum-secondary disks have much higher surface densities. Although they are surrounded by a very low surface density region, the gas accretes from the circum-binary disk through the gap. The circum-binary disk has tightly wound spiral shock waves. While a pair of the spiral waves corotates with the binary, the other pair rotates more slowly. When the inner tail of the latter shock waves transit the L_2 point, the accretion through the L_2 point increases.

Figure 2 is the enlargement of the central part of Fig. 1. The circum-primary disk (right) has a higher surface density than the circum-secondary one (left). As shown by the arrows, the gas flows into the secondary lobe through the L_2 point and into the primary lobe after circulating half around the secondary.

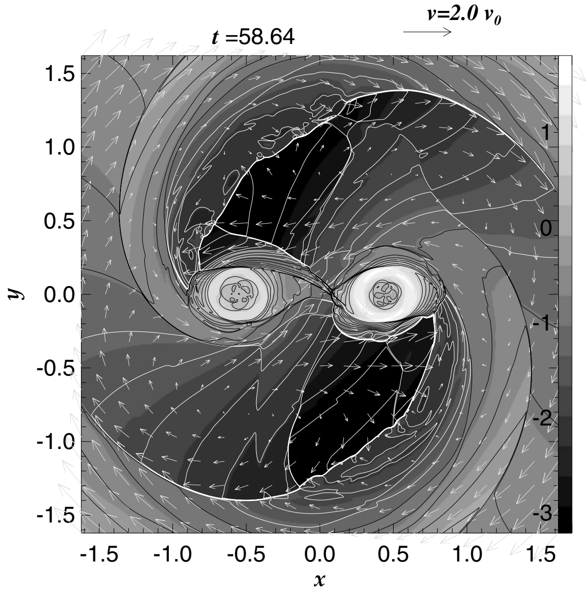

Fig. 2. The surface density distribution at the moment $t = 58.64$ for the model with $c_\mathrm{s} = 0.2$, $q = 0.8$, $e = 0.0$, $r_\mathrm{in} = 1.75$, and $r_\mathrm{out} = 5.175$ is shown. The arrows denote the velocity in the corotating frame

Figure 3 shows the mass of the circum-primary disk, M_{1d}, and that of the circum-secondary one, M_{2d}, as a function of time. The former is defined as the mass contained in the circle the center of which coincides with the primary and with a radius equal to the distance from the primary to L_1 point. The mass of the circum-secondary disk is defined similarly. The circum-primary disk is heavier than the circum-secindary disk, in contradiction with the earlier numerical simulations [1, 2].

Figure 4 shows the accretion rate of the circum-primary disk, $\dot{M}_\mathrm{1d}$, oscillating with a large amplitude. The dashed curve denotes the average accretion rate, $\langle \dot{M}_\mathrm{1d} \rangle$, which is obtained by fitting the 8th order polynomial to $\dot{M}_\mathrm{1d}$. The average accretion rate has a peak around $t = 28$ and decreases gradually. The average accretion rate of the circum-secondary disk is much lower than that of the circum-primary disk in the period $t \geq 40$, as shown in Fig. 3. We can evaluate the radial velocity in the circum-binary disk,

$$\langle v_r \rangle = - \frac{\dot{M}_\mathrm{1d} + \dot{M}_\mathrm{2d}}{2\pi \Sigma r} \, , \tag{8}$$

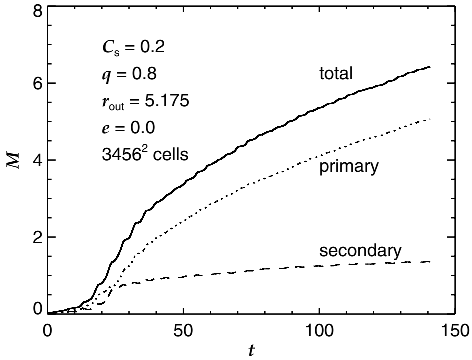

Fig. 3. The masses of the circum-primary (dashed) and circum-secondary (dotted) disks are shown as a function of the time for the model with $c_s = 0.2$, $q = 0.8$, and $e = 0$. The solid curve denotes the sum of the disk masses

$$\langle v_r \rangle = -4.0 \times 10^{-3} \left(\frac{\dot{M}_1 + \dot{M}_2}{0.05} \right) \left(\frac{r}{2\,a} \right)^{-1} , \tag{9}$$

from the average accretion rates. The evaluated radial velocity is much smaller than both the rotation velocity, v_φ, and the sound speed, c_s. It is even smaller than ${c_s}^2/v_\varphi$. This indicates that high accuracy is necessary for evaluating the accretion rate from the disk.

We computed the power spectrum of $\dot{M}_{1d} - \langle \dot{M}_{1d} \rangle$ to evaluate the oscillation frequency of the accretion rate. The power spectrum has a main peak around $2\pi\nu \simeq 0.75\,\Omega_*$, where Ω_* denotes the angular velocity of the binary. Suppose that the oscillation frequency coincides with the synodic frequency between Ω_* and Ω_{sh}, where Ω_{sh} denotes the pattern angular velocity of the shock wave. Then we have $\Omega_{sh} \simeq 0.25\,\Omega_*$, since $2\pi\nu = 0.75\,(\Omega_* - \Omega_{sh})$. This implies that the shock wave corotates with the circum-binary disk at $r \approx 2.5\,a$ and is likely to be excited by some kind of 1:4 resonance. Remember that the Lindblad resonance has the angular velocity of $\Omega_*/2$ and takes place at $r = 1.59a$. Thus the Lindblad resonance is not responsible for the excitation of the shock wave.

3.2 Dependences on Model Parameters

We have made more than 10 models by changing the spatial resolution and the model parameters q, r_{in}, r_{out}, and c_s. We have confirmed that the accretion rate on the circum-secondary disk is larger than that of the circum-primary disk when the spatial resolution is not sufficiently high [3]. The gas accretes directly onto the circum-secondary disk after inflowing through the L_2 point when the spatial resolution is low. The direct accretion onto the circum-secondary disk is due to numerical viscosity. We think that the discrepancy

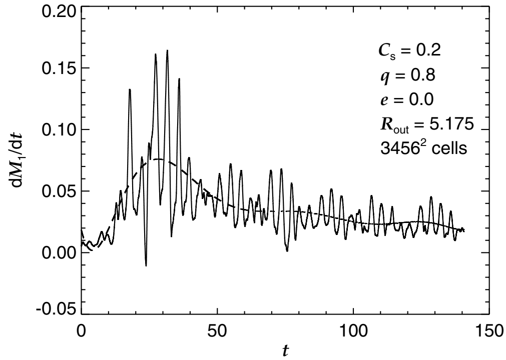

Fig. 4. The accretion rate on the circum-primary disk is shown as a function of the time for the model with $c_s = 0.2$, $q = 0.8$, and $e = 0$. The dashed curve denotes the average accretion rate

between the earlier simulations [1, 2] and ours is due to their low spatial resolution.

Qualitative features of our models depend little on the parameters q, $r_{\rm in}$, $r_{\rm out}$, and $c_{\rm s}$. The differences between the models are mainly quantitative. When $r_{\rm in}$ is larger, the start of accretion is delayed. The delay is evaluated to be $\Delta t = 25\,\Delta r_{\rm in}$ by comparing models with $r_{\rm in} = 1.75$, 2.1, and 2.5. This means that the disk's inner edge moves inward at $v_{\rm in} = -0.04$ – mush faster than $\langle v_r \rangle$ evaluated from the accretion rate. Thus the accretion from the circum-binary disk is mainly due to the angular momentum redistribution within the disk. The angular momentum redistribution is ascribed to spiral shock waves which are excited by resonance with the binary orbital motion.

When the binary orbit is eccentric, the power spectrum of the accretion rate has a peak at the rotation period, $\nu = 1$. The accretion rate changes not purely periodically but semi-regularly. The peak accretion rate differs from cycle to cycle. Again, the accretion rate of the circum-primary disk dominates over that of the circum-secondary disk.

References

1. P. Artymowicz, S. H. Lubow: ApJ **467**, L77 (1996)
2. M. R. Bate, I. A. Bonnell: MNRAS **285**, 33 (1997)
3. Y. Ochi, K. Sugimoto, T. Hanawa: ApJ **623**, 922 (2005)

The Nearest Pre-Main Sequence Multiple Stars

C.A. Grady

Eureka Scientific and Exploration of the Universe Division, Goddard Space Flight Center, Greenbelt, MD 20771, USA cgrady@echelle.gsfc.nasa.gov

Summary. Protoplanetary disks are where planets form, and where the pre-biotic materials which produce life-bearing worlds are assembled or produced. We need to understand them, how they interact with their central stars, and their evolution both to reconstruct the Solar System's history, and to account for the observed diversity of exo-planetary systems. Our knowledge of these systems, in terms of their disks, gas content, dust mineralogy, and accretion is most complete for the nearby PMS A stars, the Herbig Ae stars. Previously, many of the nearby Herbig Ae stars were thought to be single stars: a new generation of high angular resolution and high contrast imagery has revealed a number of binary, and multiple star systems, with a wide range of signatures of dynamical interaction with the primary star. Our current understanding of these systems is reviewed.

1 Introduction

The first 20-30 Myr in the evolution of a planetary system appear to be crucial in establishing the architecture of the system. The nearest debris disks in the β Pictoris moving group, β Pic and AU Mic at 12 Myr have centrally cleared debris disks with dynamical signatures of the presence of as yet unseen planetary mass bodies (Wahhaj et al. 2003 [50]; Liu et al. 2004 [30]), and no protoplanetary disks older than $\approx$ 10 Myr are currently known. In our own Solar System, the meteoritic and impact data indicate that the first 20-30 Myr spans the era of planetesimal formation, central clearing of the inner disk, and the formation of the terrestrial planet embryos (Jacobsen & Yin 2003 [24]; Kleine et al. 2003 [26]).

The PMS and young planetary systems which are currently easiest to study are nearby systems with large disks which are well-illuminated by their central stars, favoring systems around stars which are more massive, and hence luminous than the Sun. Similarly, prior to the launch of *Spitzer*, our knowledge of the dust mineralogy of the inner disks was far more complete for disks associated with A stars than for young, Solar analogs. Line of sight absorption studies also favor A and B stars since these rely, particularly at UV and FUV wavelenghts where many of the atomic and ionic transitions of cosmically abundant elements are concentrated, on the availability of a bright, rotationally washed-out, photospheric spectrum as a background continuum.

The result is that currently we know the most about protoplanetary and debris disks associated with 1.5-2.5 $M_{\odot}$ stars within 150 pc of the Sun.

2 Finding the Binary and Multiple Systems Associated with the A Stars

While our knowledge of the disks, dust mineralogy, and the circumstellar gas is most complete for young, nearby, lightly reddened A stars, our knowledge of whether these objects are single or multiple systems is much less complete than either for low-mass stars, where the presence of even planetary mass companions can be easily detected from the ground (Chauvin et al. 2005 [9]), or for bright, massive stars which provide abundant photons for bispeckle analysis or for interferometry. In the optical, these stars are typically bright, with 8.5≤V≤3.1. The immediate consequence is that in conventional, broad-band optical surveys such as the DSS, or even the Supercosmos Hα survey, the light of the A star swamps a region between 5-30" from the star (Fig. 1). Near-IR surveys, such as 2MASS are a bit better since the contrast between a late-type star and the A star is more favorable, but are typically unable to detect stellar sources closer than 5" from the primary. Moving to wavelengths where late-type stars are still conspicuous, and older A stars are not observed to be bright, such as in the x-ray (Simon et al. 1995 [40] has proven to be a more promising technique. X-ray surveys such as the ROSAT All-Sky Survey (RASS) were sufficiently deep to detect single, low-mass stars out to 50 pc, and multiple systems at larger distances, while deeper, pointed observations can sample the entire region within 150 pc of the Sun, albeit at low spatial resolution (≈15"). Such surveys have revealed a hitherto unexpected wealth of young stellar associations and moving groups (see review by Zuckerman & Song 2004 [59]) which are securely dated to 5-50 Myr. Deeper, and higher resolution imagery, such as can be provided by *Chandra* are needed to sample activity from brown dwarfs in this age range (Tsuboi et al. 2003 [47]).

Both the HR 4796 A/B/C and HD 141569 A/B/C (Weinberger et al. 1999 [53], 2000 citeWeinb00) systems were detected in the RASS (de la Reza & Pinzón 2004 [12]). Higher angular resolution *Chandra* imagery of HD 141569 (Feigelson et al. 2003 [15]) indicates that 2 of the 3 expected sources were detected, with L_x in the range expected for young M stars. Feigelson et al. (2003) [15] identify these sources with the A star and an unknown companion, but Stelzer (2005, priv. comm.) notes that the x-ray sources are more correctly associated with the 2 M stars. Similarly, archival *Chandra* imagery containing HR 4796 A detects the M stars, but not the A star, providing an upper limit to the x-ray luminosity of the A star of 10^{26} erg s^{-1}, some 3 orders of magnitude below the level typical of accreting Herbig Ae stars (Hamaguchi et al. 2005 [23]).

The disks in these systems indicate the presence of sculpting by the companions. HD 141569 A has distinct rings in the scattered light imagery of the

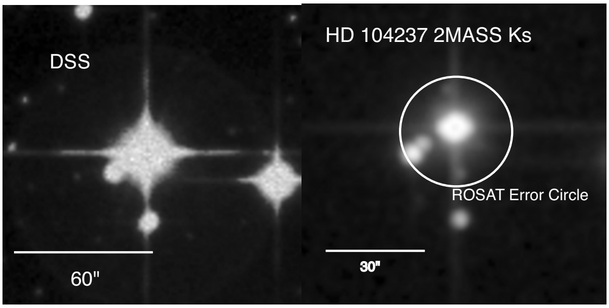

Fig. 1. Optically bright Herbig Ae stars present a challenging environment for the detection of low-mass stellar companions. Left: In the DSS, light from HD 104237 swamps the region within 12" of the star, with only one companion visible. Right: At Ks, as seen by 2MASS, the 15" and 10" companions are visible

disk, and tidal tails reminiscent of interacting galaxies extend to the M star companions (Clampin et al. 2003 [11]; Mouillet et al. 2001 [33]; Augereau et al. 2001 [3]). Some of the structure in the HD 141569 A disk has been linked to the M-star companions (Augereau & Papaloizou et al. 2004 [4]). HR 4796 A's disk is a distinct ring at 70 AU (Augereau et al. 1999 [2]; Schneider et al. 1999 [38]; Koerner et al. 1998 [27]; Jayawardhana et al. 1998 [25]) consistent with truncation of the disk by the companions. No tails are visible in the HR 4796 system, but Ardila et al. (2005) [1] note that such features should be ephemeral. In both cases there appears to be central clearing of the disks, which has prompted speculation that there are additional, potentially planetary mass bodies in the inner disk (Wyatt et al. 1999 [57]; Ardila et al. 2005 [1]).

Single A stars at d=100 pc are below the RASS detection limit, but multiple systems are still detectable, and deeper, pointed observations can reach 10^{29} erg s^{-1} (Hamaguchi et al. 2005 [23]; Zinnecker & Preibisch 1994 [58]). *Chandra*, with its greater sensitivity and 1" resolution, can reach upper limits of L_x=10^{26} erg s^{-1}, a factor of 100 below the RASS upper limits for nearby associations. *Chandra* has demonstrated that younger, and actively accreting A stars do indeed appear to be x-ray sources, or to have x-ray sources associated with the A star at the 1" resolution of *Chandra* (Feigelson et al. 2003 [15], Skinner et al. 2004 [42]; Swartz et al. 2005 [45]). These x-ray detections include the optically brightest Herbig Ae star, DX Cha (HD 104237).

3 HD 104237

Long considered the prototype for an "isolated" Herbig Ae star, HD 104237 (d=115 pc, van den Ancker et al. 1997 [49]) is among the few Herbig Ae stars detected in the RASS, and is sufficiently bright and hard to permit higher energy x-ray observations with ASCA (Skinner & Yamaguchi et al. 1996 [41]). *Chandra* not only detected a source coincident with the A star, but a string of sources spanning 20" (Feigelson et al. 2003 [15]; Skinner et al. 2004 [42]; Fig. 2). Subsequent optical and IR imagery reveal the presence of 3 T Tauri stars at 1.2-15" from the A star, two of which have IR excesses in their own right. The hottest member of the association, an extremely late A star, or early F star with UV excess, is actively accreting, and drives a bipolar microjet (Grady et al. 2004 [19]). Subsequently, Böhm et al. (2004) [6] find that this object is itself a spectroscopic binary, with the companion a likely K star.

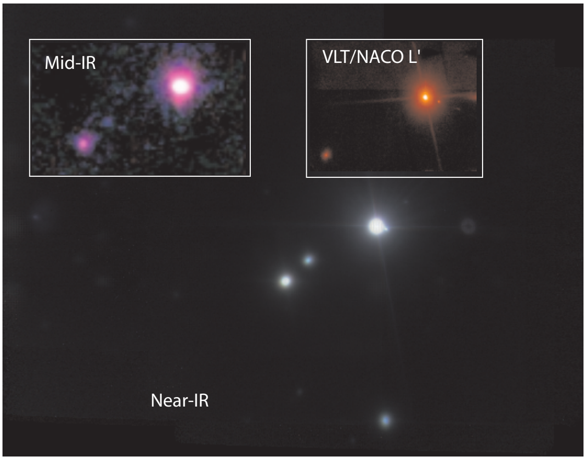

Fig. 2. The optically brightest Herbig Ae star, HD 104237, is revealed as the brightest member of a small aggregate of T Tauri stars. The presence of a circumstellar excess is visible in a color-composite image (J-H-K) made with the VLT/NACO while the presence of mid-IR excesses can be seen with two of the T Tauri companions at L′ (upper right) and L′-M-N (ESO 3.6m and TIMMI II (upper left)

The disk around the Herbig Ae star is not directly detected in HST coronagraphic imagery, although thermal emission and solid-state features are conspicuous in mid-IR spectroscopy (Meeus et al. 2001 [32]; van Boekel et al. 2005 [48]). An upper limit to the disk size is provided by the closest point where the counterjet, which is seen in projection behind the disk, can be detected. For HD 104237, this is 0.6" (70 AU). The disk non-detection from the HST/STIS coronagraph suggests that the disk is somewhat smaller, with r$\leq$0.5" (58 AU). The disk size limit is somewhat larger than the 0.3 $\times$ the projected separation between HD 104237 A and B, suggesting that the projected separation of the two stars is a lower bound to the true separation.

4 HD 169142

First identified as a Vega-like system in the late 1980s (Walker & Wolstencroft 1988 [51]), HD 169142 differs from typical debris disk systems in having a conspicuous PAH emission spectrum (Sylvester et al. 1996 [46]; Meeus et al. 2001 [32]). Molecular gas is present in the disk, with CO at a level intermediate between debris disks and the accreting Herbig Ae stars (Dent et al. 2005 [13]). The disk has been imaged via differential polarimetric imaging (Kuhn et al. 2001 [28]) at H, coronagraphically from the ground at Ks (Boccaletti et al. 2004 [5]), and at F110W with HST/NICMOS. In all cases the disk presents as face-on nebulosity (i$\leq$20°) with a surface brightness intermediate between bright nebulosity such as that seen in HD 141569 (Weinberger et al. 1999 [53]; Augereau et al. 2001 [3]; Clampin et al. 2003 [11]) and fainter disks like HD 163296 (Grady et al. 2000 [17]). While Kuhn et al. (2001) [28] report patchy structure in the disk, there is no hint of such features in the NICMOS imagery; instead the disk presents as a featureless structure out to 1.1” from the star with surface brightness dropping slowly with increasing distance from the star. The PAH emission seen by Sylvester et al. (1996) and Meeus et al. (2001) [32], is spatially extended to at least 0.2” from the star (20 AU) (Habart et al. 2005 [22]). In combination with the appearance of the IR spectral energy distribution (SED), these data all indicate the presence of a flared disk with a flare angle which is intermediate between systems like HD 100546 (Grady et al. 2001 [18]; 2005a [20]) and geometrically flat systems like HD 163296.

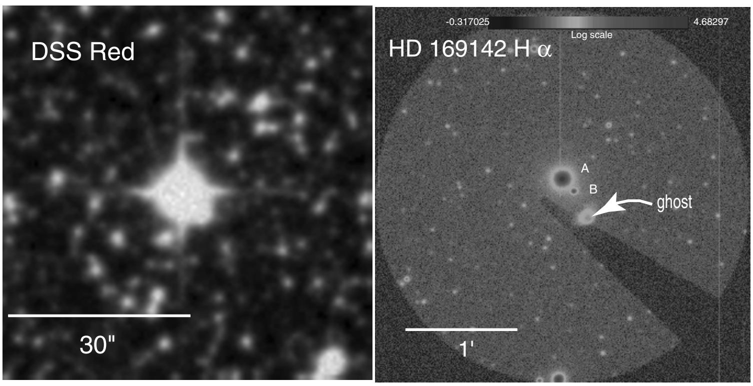

Fig. 3. While the presence of an 8” companion to HD 169142 is at best marginally resolved in DSS red imagery, both stars are conspicuous in narrow-band imagery obtained with the Goddard Fabry-Perot on the Apache Point Observatory 3.5m

A ROSAT source (2RXP J182429.1 -294659) is located within 14” of the Herbig Ae star. At the spatial resolution and positional accuracy of ROSAT, this source has a high probability of being associated with the Herbig Ae star. However, at d=145 pc, the A star alone cannot account for the x-ray emission. When scaled to a count rate at d=115 pc, the observed count rate of 0.0645 c/s is comparable to that of the HD 104237 aggregate, and is consistent with the presence of 3-5 objects similar to those seen in the HD 104237 aggregate. 2MASS imagery reveals a source 7-8" to the SW of the Herbig Ae star (Fig. 3) which partially confused with the Herbig Ae star. Higher angular resolution data obtained with the Goddard Fabry-Perot on the Apache Point Observatory 3.5m demonstrates the presence of Hα sources at the Herbig Ae star and at the 7.7" object. Low resolution spectra obtained with the Apache Point observatory Dual Imaging Spectrograph indicate a type of M2.5Ve for the 7.7" source (Fig. 4). This object has apparently been co-moving with the Herbig Ae star since the mid-80s, excluding a foreground Main Sequence M star. Second epoch high angular resolution imagery will be needed to demonstrate that the 7.7" object shares the proper motion of the Herbig Ae star against the numerous background stars, but, as noted for HD 141569 A, the probability of finding a T Tauri star and a Herbig Ae star in this proximity at this distance and having them not associated is neglibly small.

Is this the only nearby late-type object which can be associated with the Herbig Ae star? Detection of point sources near brighter objects is facilitated in NICMOS imagery by differencing data obtained at two spacecraft roll angles, such as are routinely obtained for all NICMOS coronagraphic observations (Lowrance et al. 2000 [31]). When applied to HD 169142, the 7.7" object is seen in both images (Fig. 5). There are numerous fainter objects in the NICMOS imagery, but none are seen closer than 2" to the Herbig Ae primary. However, careful inspection of the NICMOS data further reveals that the 7.7" source is resolved into a 112 mas pair, with a 0.7 magnitude

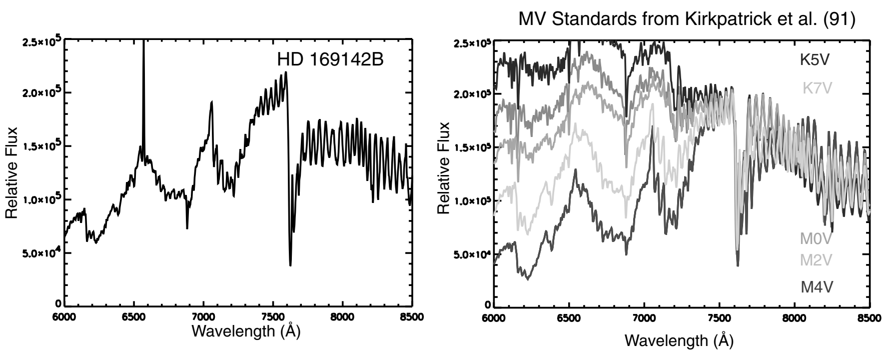

Fig. 4. The 8" source has both the Hα emission and an M2.5V spectral type expected for a young, late-type companion to a Herbig Ae star, as seen in low resolution spectra obtained with the Apache Point Observatory 3.5 m and Dual Imaging Spectrograph

difference at F110W (Fig. 6). Tiny-Tim fits to the two sources do not account for all of the NIR light, suggesting that there is either a third source in the vicinity of the M stars (associated or background) or circumstellar material. Combining the NICMOS data, converted to J, an assumed distance of 145 pc, and a stellar T_{eff} consistent with the optical spectrum yields an estimated age for the M stars of 8±2-3 Myr.

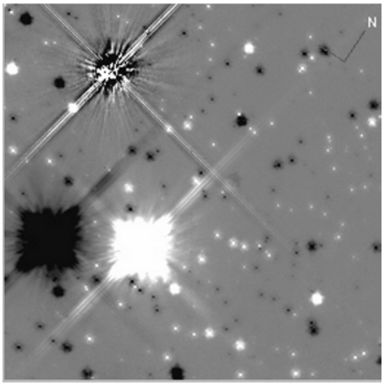

Fig. 5. Roll-differenced HST imagery affords an efficient way of removing the stellar point spread function and any circularly-symmetric nebulosity (e.g. face-on disks), to reveal point sources in the immediate vicinity. NICMOS coronagraphic imagery is sufficiently deep to detect J=19.5 sources within a few arcseconds of the occulted primary. Associated, stellar companions have conspicuous diffraction spikes, while brown dwarfs and background objects can be significantly fainter. The NICMOS data provide no indication of a companion within $0.3 \leq r \leq 2''$ of HD 169142

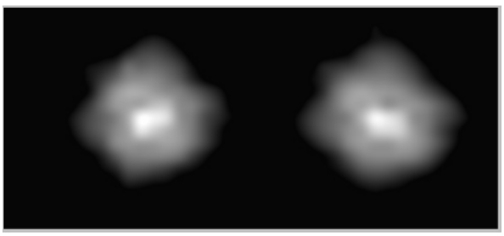

Fig. 6. The 7.7” companion to HD 169142 is resoved by HST/NICMOS into two sources, seen here at two different spacecraft roll angles

Central Clearing of the Disk: Clearing the center of the disk is an expected consequence of planetary system formation, but can also mark the dynamical effects of a stellar or substellar companion (Augereau & Papaloizou 2004 [4]) or an encounter with an unbound companion (Quillen et al. 2005 [35]). The low fractional IR luminosity of this system (0.08, Dunkin et al. 1997 [14]), and deficit of thermal emission from warm grains, detectable either as an excess at $\lambda \leq 8\ \mu$m, or as emission in the 10μm silicate band suggested a deficit of small grains near the star. While the star does exhibit emission lines indicative of the presence of stellar activity, such as the Hα and He I emission noted by Dunkin et al. (1997) [14], and the Lyα, O I, C II and C IV seen in IUE spectra, the star does not exhibit any detectable UV excess longward of 1600 Å when compared to UV spectral type standard stars. This is in marked contrast to the actively accreting Herbig Ae stars such as MWC 480 (Stecklum et al. 2005 [44]), HD 163296, and HD 104237 (Grady et al. 2004 [19]), all of which have distinct excess light at these wavelengths. Moreover, narrow band Hα observations do not reveal any HH knots such as are seen in GFP data for HD 163296 (Wassell et al. 2005 [52]). This suggests a deficit of gas in the immediate vicinity of the Herbig Ae star. Habart et al. (2005) [22] have resolved the 3.3μ PAH emission in HD 169142. After a rapid increase in strength with decreasing radius from the star in to ≈25 AU, the PAH emission profile flattens out at smaller radii. The mid-IR PAH features are transiently excited by the absorption of a FUV photon, which in this system would be most likely a Lyα photon, and should exhibit an r^{-2} dependence for a constant number density of PAHs with radius. A roll-over in the profile is similar to the behavior of the fluorescent H_2 emission in HD 100546 (Grady et al. 2005a [20]). The combination of a deficit of PAH emission near the star, the absence of warm dust features, and the low current accretion rate, all indicate the probable presence of an additional body in the inner portion of this disk. Follow-on HST/ACS and *Chandra* imaging may prove useful in establishing the nature of any such close companion, however, given the estimated age, a planetary mass companion cannot be excluded.

5 Binarity and Multiplicity

Not all of the optically visible, bright Herbig Ae stars are members of multiple systems or single stars. The HST coronagraphic surveys of Herbig Ae stars were initially selected based on the presence of an optically detected star with minimal foreground extinction and overall proximity to us. The STIS sample included only two binary/multiple systems, HR 5999 and the HD 104237 aggregate (Grady et al. 2005b [21]). NICMOS coronagraphic imagery is now available for additional Herbig Ae stars with low-mass companions, including HD 169142 and HD 150193. None of these stars show diffuse nebulosity similar to the envelope surrounding HD 100546, a single star. The disks are not detected by STIS for either HD 104237 or HR 5999, suggesting a small outer radius. The presence of counterjet emission in Lyman α at r≥0.6" in HD 104237 provides further support for interpretation of these disks as being tidally truncated by the 1-2" companions. HD 169142, with

2 M star companions at 8” from the primary, has a remarkably crisp-edged disk, extending only 1.6” from the Herbig Ae star (Raman et al. 2005 [36]), which may make this system another case for tidal truncation of the disk. The situation for HD 150193 is less clear, and may represent a case where the projected primary-secondary distance is not the true distance. The presence of either wide (HR 5999) or close companions (HD 104237, Böhm et al. 2004 [6]) does not appear to affect the frequency of microjets: they are seen equally frequently in the single star systems as in the binary/multiples, at least through 7 Myr.

At this time, there is a sufficiently large sample of coronagraphically imaged Herbig Ae stars that we can begin to say something about how these systems are similar to or differ from star formation in denser aggregates. The available data include 16 fields, with three multiple systems (HD 104237, HD 141569, and HD 169142), two binaries (HD 150193 and HR 5999) and the rest apparently single objects at the resolution of HST. The 31% binary/multiple star frequency in this sample is comparable both to that of that seen in G-K stars in the Solar neighborhood and the Pleiades (Bouvier et al. 1997 [8]), or in dense star forming regions (Padgett et al. 1997 [34], Ratzka et al. (2005 [37]). Additional nearby Herbig Ae stars are known, and some (Fig. 7) are binaries, so the 31% frequency is clearly a lower bound to the true binary fraction, which is likely closer to the Tau-Aur level.

How does the binary/multiple frequency compare with nearby, young stellar associations? Here we can estimate the binary frequency among the A stars using the x-ray detections: the x-ray sources at 8-20 Myr are those with late-type companions, which may be either physical companions or co-moving objects. de la Reza & Pinzón (2004) [12] used the RASS to survey nearby, stellar associations through t=50 Myr. For the youngest associations in the sample, they find an x-ray detection rate for the A star from the RASS of 33% which is very similar to what we observe. The RASS data are incomplete for substellar objects, but *Chandra* with its combination of superior spatial resolution and greater sensitivity can extend such surveys into the sub-stellar regime. When known brown dwarf companions are included (Lowrance et al. 2000 [31]; Tsuboi et al. 2003 [47]) the detection rate increases to 40%, which is comparable to the binary/multiple rate in Tau-Aur (Ghez et al. 1993 [16]; Leinert et al. 1993 [29]; Simon et al. 1995 [40]).

6 Significance of the PMS Multiple Stars:

As noted by Simon et al. (2000 [39]), PMS binary and multiple stars provide the most direct measure of stellar masses, and are crucial in calibrating stellar evolution models, provided the stars are well-resolved. Isolated PMS stars, even those with the best available parallax data are much harder to date and to place into context. These difficulties increase with increasing stellar mass,

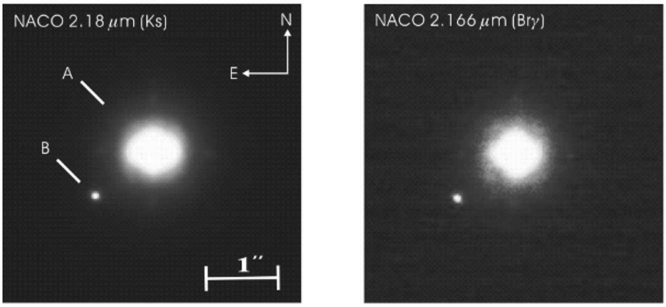

Fig. 7. The newly identified candidate M star companion to HD 100453 (Chen et al. 2005 [10])

and luminosity, since the PMS lifetimes shorten. If low-mass physical or co-moving companions can be independently dated using the parallax data for the primary and spectral type and photometry data for the companions, the aggregate can be located in the H-R diagram. The next step is to compare the HR diagram with evolutionary model calculations. This yields a relative dating sequence, if the same model or group of models is used to estimate the ages of several binary/multiple systems, with internal errors as small as 2-3 Myr. This process has been done for the lone A star in the TW Hya association, HR 4796 A/B/C, yielding an age estimate of 8±2 Myr (Stauffer 1995 [43]), which is consistent with the dating of other confirmed TW Hya association members. In the case of HD 141596 A/B/C, Weinberger et al. (2000) [54] found an age of 5±3 Myr, in contrast to the estimate of t≥5 Myr based on the A star alone (van den Ancker et al. 1997 [49]). This suggests that the age estimates for other, truly isolated, Herbig Ae stars are uncertain by at least 5 Myr, which is sufficient, in a population with ages which are almost certainly under 10 Myr, to wash out any evolutionary trends.

While different evolutionary models yield slightly different age estimates, the availability of a relative age sequence allows us to make some important inferences about these systems. First, there does not appear to be a simple age-evolution pattern: some systems are largely centrally cleared by 2-5 Myr, while others are still actively accreting at 5 Myr, and producing microjets (Grady et al. 2004 [19]; Swartz et al. 2005 [45]). This is similar age spread in clearing seen in T Tauri stars, and suggests that the evolution of the disk is not strongly coupled to the stellar mass, at least over 0.1-2.5 $M_{\odot}$. If the clearing is associated with planetary mass bodies, rather than brown dwarfs, the available data suggest that giant planets capable of sculpting their host disks can form within a few Myr, a time frame which is intermediate between planet formation-as-mini star models (Boss 2003 [7]) or those which require formation of a 10-15 Earth Mass core and subsequent accretion of a gaseous envelope (Wuchterl et al. 2000 [56]). Rather than representing anomalously gas-rich debris disk systems associated with Main Sequence stars, the disks around HD 141569 A and HD 169142 A appear to have been caught in a potentially short-lived transitional phase, suggesting that the gas lifetime of the disk is shorter than that of the the dust disk.

The nearest PMS multiple systems, particularly those where the companions retain circumstellar material are critical laboratories for probing the chemistry and physics of planetesimal formation. Mid-IR observations of such companions will enable comparative mineralogical studies of the dust, where the only variables are the stellar mass and radiation field. Astrometric studies of the systems with evidence for central clearing will enable the earliest detection of resonances associated with forming giant planets, and may shed light onto planetary migration. High angular resolution imaging, such as will be provided by JWST, and large ground-based telescopes will allow us to probe compositional gradients in protoplanetary and young planetary disks. Finally, with TPF/C it may prove possible to directly image young planets.

Acknowledgements

This study combined data obtained with the HST/STIS coronagraph obtained under HST-GO-7065, HST-GO-8065, HST-GO-8474, and NICMOS coronagraphic imagery obtained under HST-GO-10177.

References

1. Ardilla, D.R., Lubow, S.H., Golimowski, D.A. Astrophys. J. **627**, 986, (2005).
2. Augereau, J.C., Lagrange, A.M., Mouillet, D., Ménard, F. Astron. & Astrophys. **350**, L51, (1999).
3. Augereau, J.C., Lagrange, A.M., Mouillet, D., and Ménard, F., Astron. & Astrophys. **365**, 78, (2001).
4. Augereau, J.C. and Papaloizou, J.C.B. Astron. & Astrophys. **414**, 1153, (2004).
5. Boccaletti, A., Riaud, P., Boudoz, P., et al. PASP, **116**, 1061, (2004).
6. Bohm, T., Catala, C., Balona, L., and Carter, B. Astron. & Astrophys. **427**, 907 (2004).
7. Boss, A., Astrophys. J. **599** 577, (2003).
8. Bouvier, J., Rigaut, F., Nadeau, D, Astron. & Astrophys. **323**, 139 (2005).
9. Chavin, G., Lagrange, A.-M, Dumas, C. et al. Astron. & Astrophys. **438** L25, (2005).
10. Chen, X.P., Henning, T., van Boekel, R., and Grady, C.A. Astron. & Astrophys. (submitted), (2005).
11. Clampin, M., Krist, J.E., Ardila, D.R., et al. Astron. J. **126**, 385 (2003).
12. de la Reza, R., and Pinzón, G., Astron. J., **128** 1812 (2004).
13. Dent, W.R.F., Greaves, J.S., Coulson, I.M. MNRAS **359**, 663 (2005).
14. Dunkin, S.K., Barlow, M.J., Ryan, S.G. MNRAS, **290**, 165 (1997).
15. Feigelson, E.D., Lawson, W.A., Garmire, G.P. Astrophys. J. **599** 1207 (2003).

16. Ghez, A.M., Neugebauer, G., Matthews, K. Astron. J. **106**, 2005 (1993).
17. Grady, C.A., Devine, D., Woodgate, B., et al., Astrophys. J. **544** 895 (2000).
18. Grady, C.A., Polomski, E.F., Henning, Th., et al. Astron. J. **122** 3396 (2001).
19. Grady, C.A., Woodgate, B., Torres, C.A.O., et cal. Astrophys. J. **608** 809, (2004).
20. Grady, C.A. Woodgate, B., Heap, S.R., Astrophys. J. **620** 470, (2005a).
21. Grady, C.A., Woodgate, B.E., Bowers, C.W. Astrophys. J. **630** 958, (2005b).
22. Habart, E.. Natta, A., Testi, L., and Carbillet, M., astro-ph 053105 (2005).
23. Hamaguchi, K., Yamauchi, S., Koyama, K., Astrophys. J. **618** 360, (2005).
24. Jacobsen, S.B. and Yin Q., LPI, **34** 1913 (2003).
25. Jayawardhana, R., Fisher, S., Hartmann, L., et al. Astrophys. J. **503**, L79 (1998).
26. Kleine, T., Mezger,K., Münker, C., Meteoritics & Planetary Science **38**, Supplement 5212 (2003).
27. Koerner, D.W., Ressler, M.E., Werner, M.W., Backman, D.E. Astrophys. J. **503**, L83. (1998).
28. Kuhn, J.R., Potter, D., Parise, B., Astrophys. J. **553**, L189, (2001).
29. Leinert, Ch. Zinnecker, H., and Weitzel, N., Astron. & Astrophys. **278**, 129 (1993).
30. Liu, M.C., Science **305**, 1442 (2004).
31. Lowrance, P.J., Schneider, G., Kirkpatrick, J.D., et al. Astrophys. J. **541** 390 (2000).
32. Meeus, G., Waters, L.B.F.M., Bouwman, J. et al. Astron. & Astrophys. **365**, 476, (2001).
33. Mouillet, D., Lagrange, A.M., Augereau, J.C., and Ménard, F. Astron. & Astrophys. **372** L61, (2001).
34. Padgett, D., Strom, S.E., Ghez, A., Astrophys. J. **477**, 705 (1997).
35. Quillen, A.C., Varniére, P., Minchev, I., Frank, A. Astronomical J. **129**, 2481 (2005).
36. Raman, A., Lisanti, M., Wilner, D.J., Qi, C., Hogerheijde, M. 2005, astro-ph/0512478
37. Ratzka, T., Köhler, R., and Leinert, Ch. Astron., & Astrophys. **437**, 611, (2005).
38. Schneider, G. Smith, B.A., Becklin, E.E., et al. Astrophys. J. **513**, L127, (1999).
39. Simon, M., Dutrey, A., and Guilloteau, S., Astrophys. J. **545**, 1034, (2000).
40. Simon, T., Drake, S.A., and Kim, P.D. Pub. Astron. Soc. Pacific **107**, 1034 (1995).
41. Skinner, S. & Yamaguchi S., Astrophys. J. **471**, 987 (1996).
42. Skinner, S.L., Güdel, M., Audard, M., and Smith, K., Astrophys. J. **614**, 221 (2004).
43. Stauffer, J.R., Hartmann, L.W., Barrado y Navascues, D. Astrophys. J. **454** 910 (1995).
44. Stecklum, B., Grady, C.A., Bouret, J.-C., et al. Astron. & Astrophys. (submitted) (2005).
45. Swartz, D., Drake, J.J., Elsner, R.F. et al. Astrophys. J. **628**, 811 (2005).
46. Sylvester, R.J., Skinner, C.J., Barlow, M.J., and Mannings, V., MNRAS **279**, 915, (1996).
47. Tsuboi, Y., Maeda, Y., Feigelson, E.D. et al. Astrophys. J. **587**, L51 (2003).

48. van Boekel, R., Min, M., Waters, L.B.F.M. et al, Astron. & Astrophys. **437**, 189, (2005).
49. van den Ancker, M.E. , Thé, P.-S., Tjin A Djie, H.R.E., et al. Astron. & Astrophys. **324** L33 (1997).
50. Wahhaj, Z., Koerner, D.W., Ressler, M.E. et al. Astrophys. J. **584**, L27 (2003).
51. Walker, H.J., and Wolstencroft, R.D., Pub. A.S.P. **100**, 1509, (1988).
52. Wassell, E.J., Grady, C.A. Woodgate, B.E., et al. Astronomical J. (submitted).
53. Weinberger, A.J., Becklin, E.E., Schneider, G. et al. Astrophys. J. **525**, L53, (1999).
54. Weinberger, A.J., Rich, R.M., Becklin, E.E., et al. Astrophys. J. **544**, 937, (2000).
55. Woitas, J., Leinert, Ch., and Köhler, R., Astron. & Astrophys. **376**, 982 (2001).
56. Wuchterl, G., Guillllot, T., and Lissaur, J.J. Giant Planet Formation in *Protostars and Planets IV*, ed. by Mannings, V., Boss, A.P., and Russell, S.S. (University of Arizona Press, Tucson 2000), pp 1081-1110.
57. Wyatt, M.C., Dermott, S.F., Telesco, C.M., et al. Astrophys. J. **527**, 918, (1999).
58. Zinnecker, H. and Preibisch, T. Astron. & Astrophys. **292**, 152 (1994).
59. Zuckerman, B., and Song, I. Young Stars Near the Sun. In: *Annual Reviews of Astronomy & Astrophysics*, **42**, 685, (2004).

A Study of the Young Quadruple System AO Vel with a ZAMS Eclipsing BpSi Primary and PMS Companions

J.F. González[1], S. Hubrig[2], N. Nesvacil[2,3] and P. North[4]

[1] Complejo Astronómico El Leoncito, Casilla 467, 5400 San Juan, Argentina
fgonzalez@casleo.gov.ar
[2] European Southern Observatory, Casilla 19001, Santiago 19, Chile
shubrig@eso.org, nnesvaci@eso.org
[3] Department of Astronomy, University of Vienna, Türkenschanzstrasse 17, 1180 Vienna, Austria
[4] Ecole Polytechnique Fédérale de Lausanne (EPFL), Laboratoire d'Astrophysique, Observatoire, CH-1290 Sauverny, Switzerland
Pierre.North@obs.unige.ch

Summary. Using recent spectroscopic observations we discovered that the triple system AO Vel with an eclipsing BpSi primary is in fact a remarkable quadruple system formed by two double-lined spectroscopic binaries with ZAMS and PMS companions. For the first time, direct determinations of the radius and the mass have been obtained for a BpSi star.

1 Observations and RV Measurements

We obtained five spectra of AO Vel with FEROS at the 2.2m telescope at La Silla (R = 48,000), and 6 additional spectra with the 2.1m telescope of the CASLEO and the echelle spectrograph REOSC (R=13,000). The spectral line profiles exhibit a variable and complex structure indicating four spectral companions identified here as A, B, C, and D. In order to obtain separate spectra for all four components of the system and to measure their radial velocities (RVs), we applied the iterative method described in [3], which was adapted here for multiple systems. RV curves are shown in Fig. 1.

2 Spectral Analysis

For each component in the system, we calculated synthetic spectra using the SYNTH code [7], the VALD database [5] and ATLAS9 model atmospheres [6]. Comparing a variety of syntheses with different $T_{\rm eff}$ to our observations we determined the parameters that produced the best fits (Table 1). In order to reproduce the line intensities of the peculiar star A the abundances of He and Mg were decreased by 1.45 and 1.04 dex, respectively, while the Si abundance had to be increased by 0.5 dex relative to solar composition.

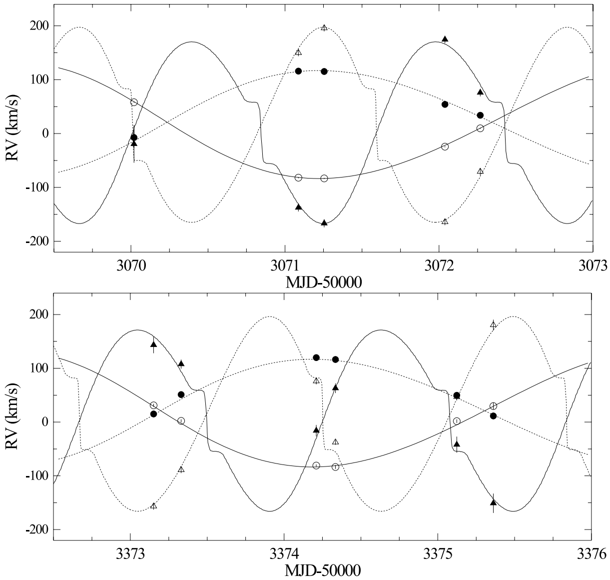

Fig. 1. Radial velocity curves for La Silla (up) and CASLEO (bottom) spectra. Filled and open symbols correspond to the primary and secondary component of each binary, respectively

Table 1. Atmospheric parameters derived from comparison with synthetic spectra.

Star	$T_{\rm eff}$ [K]	$\log g$	$v \sin i$ [$\rm km\,s^{-1}$]
A	13700 (adopted)	4.3	65
B	12500 ± 250 K	4.3 ± 0.1	73
C	10500 ± 500 K	4.1 ± 0.2	40
D	10000 ± 500 K	4.2 ± 0.2	18

3 Orbital Analysis

Spectroscopic orbits for the two binaries A+B and C+D were calculated using the 11 RV measurements of each star. In the case of the system A+B, we fitted the RV curves using the Wilson & Devinney program [9,10] taking the inclination and relative radii from [2]. The resulting parameters are listed in Table 2. We recomputed the apsidal motion of the binary A+B and the wide orbit AB+CD from the analysis of the light-time effect over all the available times of minimum along with our spectroscopic observations. We calculated the orbital period of the eclipsing system to be $P_{AB} = 1.5846154 \pm 0.000002$ days. The value we found for the apsidal motion period (54.72 ± 0.45 yr) is indistinguishable from that found by previous works [2,11]. However, the orbit

AB+CD ($P_o = 41.0 \pm 0.2$ yr, $a_{o,1} \sin i_o = 11.15 \pm 0.07$ AU, $e_o = 0.291 \pm 0.005$) is essentially different.

Table 2. Spectroscopic orbits and stellar parameters of binary systems C+D and A+B.

Parameter	Units	Value
P_{CD}	days	4.15008 ± 0.00016
T_{CD}(periastron)	MJD	53074.059 ± 0.060
$V\gamma_{CD}$	$\mathrm{km\,s^{-1}}$	21.2 ± 0.7
ω_{CD}	deg	60 ± 6
e_{CD}		0.047 ± 0.015
$M_C \sin^3 i_{CD}$	$M_\odot$	1.94 ± 0.07
$M_D \sin^3 i_{CD}$	$M_\odot$	1.77 ± 0.08
$V\gamma_{AB}$	$\mathrm{km\,s^{-1}}$	8.9 ± 2.3
M_A	$M_\odot$	3.63 ± 0.18
M_B	$M_\odot$	3.38 ± 0.18
R_A	$R_\odot$	2.34 ± 0.08
R_B	$R_\odot$	2.11 ± 0.08

4 Physical Parameters

The masses and radii calculated for the stellar components of the eclipsing binary are located near the ZAMS in the mass-radius diagram (Fig. 2). A lower limit to the masses of stars C and D can be obtained from the outer orbit between the two systems and the mass of the binary A+B, using the expression

$$\frac{(1+q_o)^2}{q_o^3} = (a_{o,1} \sin i_o)^{-3} \cdot P_o^2 \cdot M_{A+B} \cdot \sin^3 i_o,$$

where M_{A+B}, $(a_{o,1} \sin i_o)$, and P_o are known parameters. From the condition $i_o \leq 90°$ we obtain $M_C \geq 2.55 \pm 0.09$ M$_\odot$ and $M_D \geq 2.34 \pm 0.10$ M$_\odot$. Using the spectroscopic temperatures and the luminosity difference between the two binary systems, and assuming that the four stars are coeval, we found that the age of the system is about $10^{6.6}$-$10^{6.8}$ yr in the pre-main sequence grid of Bernasconi [1]. The fact that components C and D are still pre-main sequence stars, implies that stars A and B are just on the ZAMS. Specifically, the post-main sequence evolutionary age of the peculiar star A is only 1-2% of their main-sequence lifetime.

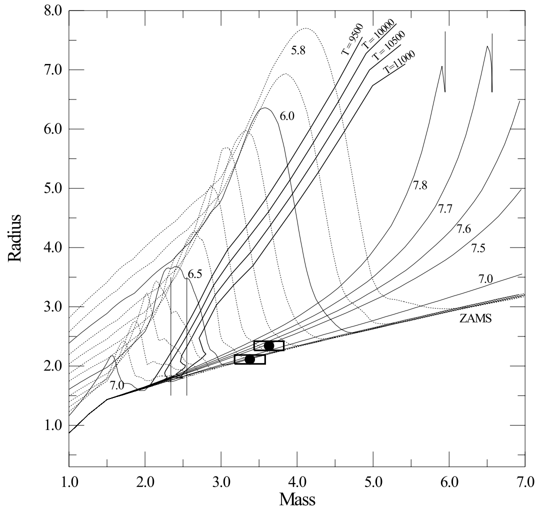

Fig. 2. Mass-radius diagram. Filled circles with error boxes are stars A and B belonging to the eclipsing system. Minimum masses for stars C and D are marked with vertical bars. Main sequence [8] (continuous lines) and pre-main sequence [1] (dotted lines) isochrones are plotted and labeled with log(age). Thick lines are isotherms interpolated for pre-main-sequence models

5 Conclusions

- AO Vel, the known triple system with an eclipsing BpSi primary, is in fact a remarkable quadruple system with ZAMS and PMS companions.
- It is formed by two spectroscopic binaries that move in a wide eccentric orbit (e=0.29) with a period of 41 yr.
- Absolute masses and radii are derived for stars A and B, and a lower limit to the masses of stars C and D has been established.
- The analysis of the stellar parameters reveals the extreme youth of all companions confirming our previous results that contrary to peculiar stars with masses below 3 $M_\odot$, stars of higher mass seem to fill the whole width of the main-sequence band in the H-R diagram [4].

References

1. Bernasconi, P. A.: A&AS, 120, 57 (1996)
2. Clausen, J. V., Giménez, A., & van Houten, C. J.: A&AS, 109, 425 (1995)
3. González, J. F., & Levato, H.: A&A, submitted (2005)
4. Hubrig, S., North, P., & Szeifert, T.: "Evolution of Magnetic Fields in Stars Across the Upper Main Sequence: Results from Recent Measurements with FORS 1 at the VLT," in *Astronomical Polarimetry: current status and future directions*, edited by A. Adamson, ASP Conf. Series, vol. 343, in press (2005).

5. Kupka F., Piskunov N., Ryabchikova T.A., Stempels H.C., Weiss W.W.: A&AS 138, 119 (1999)
6. Kurucz R.L.: CDROM13, SAO Cambridge (1993)
7. Piskunov N. E.: in “Stellar magnetism”, eds. Yu.V.Glagolevskij & I.I. Romanyuk, Nauka, St. Petersburg, 92 (1992)
8. Schaller, G., Schaerer, D., Meynet, G., & Maeder, A.: A&AS, 96, 269 (1992)
9. Wilson, R. E., & Devinney, E. J.: ApJ, 166, 605 (1971)
10. Wilson R. E.: ApJ, 356, 613 (1990)
11. Wolf, M., & Zejda, M.: A&A, 437, 545 (2005)

Multiplicity of Massive Stars

Hans Zinnecker

Astrophysikalisches Institut Potsdam, An der Sternwarte 16, D-14482 Potsdam, Germany, hzinnecker@aip.de

Summary. We review the multiplicity of massive stars by compiling the abstracts of the most relevant papers in the field. We start by discussing the massive stars in the Orion Trapezium Cluster and in other Galactic young clusters and OB associations, and end with the R136 cluster in the LMC. The multiplicity of field O-stars and runaway OB stars is also reviewed. The results of both visual and spectroscopic surveys are presented, as well as data for eclipsing systems. Among the latter, we find the most massive known binary system WR20a, with two $\sim 80\,\mathrm{M}_\odot$ components in a 3 day orbit. Some 80 % of the wide visual binaries in stellar associations are in fact hierarchical triple systems, where typically the more massive of the binary components is itself a spectroscopic or even eclipsing binary pair. The multiplicity (number of companions) of massive star primaries is significantly higher than for low-mass solar-type primaries or for young low-mass T Tauri stars. There is also a striking preponderance of very close nearly equal mass binary systems (the origin of which has recently been explained in an accretion scenario). Finally, we offer a new idea as to the origin of massive Trapezium systems, frequently found in the centers of dense young clusters.

1 The Origin of the Orion Trapezium system

Let us begin by discussing the origin of the massive stars in the center of the Orion Nebula Cluster, i.e. the well-known Trapezium system Θ^1 Ori. Numerical SPH simulations of supersonic gravo-turbulent fragmentation of a protocluster cloud ($1000\,\mathrm{M}_\odot$) suggest that a collapsing cloud develops a few subclusters (star+gas systems) which subsequently merge into a single cluster entity. Each subcluster carries one most massive star (likely multiple), thus the merging of subclusters results in a central Trapezium-type system, as observed in the core of the Orion Nebula cluster (see Fig. 1).

Figure 1 shows the stellar cluster forming through hierarchical fragmentation of a turbulent molecular cloud. Each panel shows a region of 1 parsec per side. The logarithm of the column density is plotted from a minimum of 0.025 (black) to a maximum of $250\,\mathrm{g\,cm}^{-2}$ (white). Stars are indicated by the white dots. The four panels A–D capture the evolution of the $1000\,\mathrm{M}_\odot$ system at times of 1.0, 1.4, 1.8 and 2.4 initial free-fall times, where the free-fall time for the cloud is $\mathrm{t}_{ff} = 2 \times 10^5$ years. The turbulence causes shocks

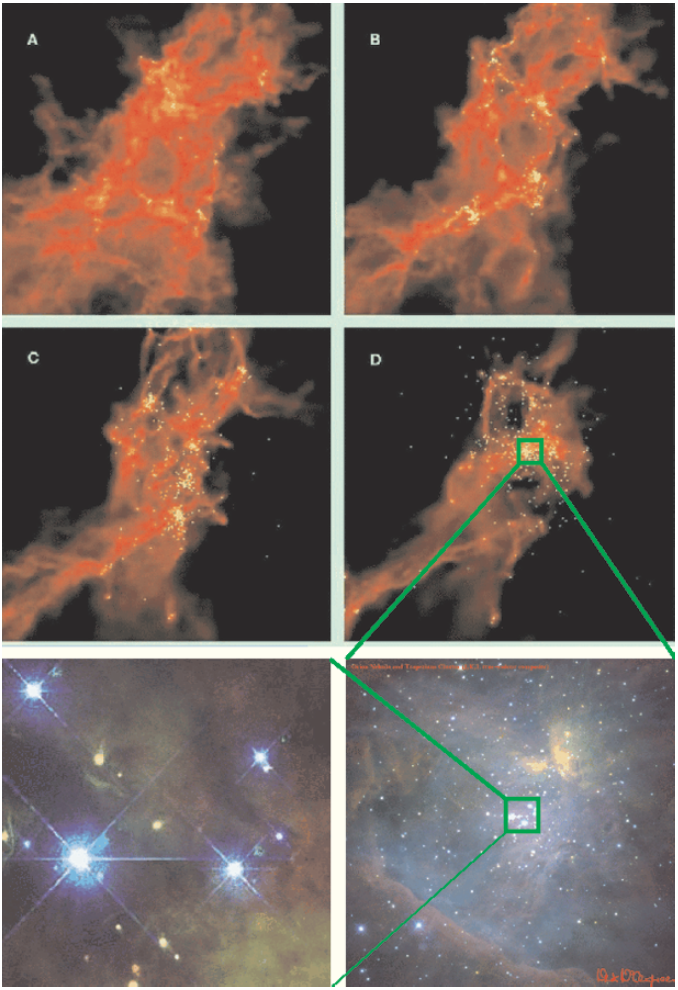

Fig. 1. Panels A, B, C, D: SPH simulations of star cluster formation by Bonnell, Bate, & Vine (2003); bottom right: Orion Trapezium cluster IRTF infrared JKL image (courtesy McCaughrean & Rayner); bottom left: Orion Trapezium system HST/WFPC2 nb-optical image (Bally et al. 1998)

to form in the molecular cloud, dissipating kinetic energy and producing filamentary structures which fragment to form dense cores and individual stars (panel A). The stars sink towards local potential minima and hence form subclusters (panel B). These subclusters evolve by accreting more stars and gas, ejecting stars, and by merging with other subclusters (panel C). There is one massive star per subcluster. The final state of the simulation is a single, centrally condensed cluster with little substructure but with 4 massive stars, one from each subcluster (Trapezium-system) (panel D). The cluster contains more than 400 stars and has a gas fraction of approximately 16%.

2 Relevant Papers

"Binary Stars in the Orion Trapezium Cluster Core"

M. G. Petr, V. Coudé Du Foresto et al. 1998

Abstract. We have obtained high angular resolution (0.13" FWHM) near-infrared images of the central $\sim$ 40" $\times$ 40" of the Trapezium cluster, using a speckle holography technique that we describe in detail. A search for close binary systems was made in K_s (2.16 μm) and H (1.65 μm) mosaic images. We show that the massive Trapezium star Θ^1 Ori A has a nearby companion separated by $\sim$0.2" ($\sim$90 AU). The location of this companion is coincident, within the positional uncertainties, with a nonthermal and variable VLA radio source, which was previously associated with Θ^1 Ori A itself. We give H photometry for 32 stars, K_s photometry for 43 stars, and present a color-magnitude diagram for the Trapezium core.

"Bispectrum Speckle Interferometry of the Orion Trapezium Stars: Detection of a Close (33 mas) Companion of Θ^1 Ori C"

G. Weigelt, Y. Balega et al. 1999

Abstract. We present bispectrum speckle interferometry observations with the SAO 6 m telescope of the four brightest stars in the Orion Trapezium. Diffraction-limited images with an unprecedented resolution λ / D of 57 mas and 76 mas were obtained in the H- and K-band, respectively. The H and K images of Θ^1 Ori C (the star responsible for the proplyds) show for the first time that Θ^1 Ori C is a close binary with a separation of only $\sim$33 mas (H-band observation). The sub-arcsecond companions of Θ^1 Ori A and Θ^1 Ori B reported by Petr et al. (1998) are confirmed. We use the magnitudes and colors of the companions to derive information about their stellar properties from the HR-diagram. In addition we briefly discuss the multiplicity of the Trapezium stars. Considering both, the visual and the spectroscopic companions of the 4 Trapezium stars, there are at least 7 companions, i.e. at least 1.75 companions per primary on average. This number is clearly higher than that found for the low-mass stars in the Orion Nebula cluster as well as in the field population. This suggests that a different mechanism is at work in the formation of high-mass multiple systems in the dense Trapezium cluster than for low-mass stars.

"Multiplicity of the Massive Stars in the Orion Nebula Cluster"

T. Preibisch, Y. Balega et al. 1999

Abstract. We present bispectrum speckle interferometry observations of 13 bright Orion Nebula cluster member stars of spectral type O or B. Diffraction-limited images with a resolution λ / D of 75 mas in the K'-band were obtained with the SAO 6 m telescope. In our speckle images we find 8 visual companions in total. Using the flux ratios of the resolved systems to estimate the masses of the companions, we find that the systems generally have mass ratios below 1 / 2. The distribution of mass ratios seems to be consistent with a companion mass function similar to the field IMF. Considering both, the visual and the spectroscopic companions of the 13 target stars, the total number of companions is at least 14. Extrapolation with correction for the unresolved systems suggests that there are at least 1.5 companions per primary star on average. This number is clearly higher than the mean number of ~ 0.5 companions per primary star found for the low-mass stars in the Orion Nebula cluster as well as in the field population. This suggests that a different mechanism is at work in the formation of high-mass multiple systems in the dense Orion Nebula cluster than for low-mass stars (see also IAU-Symp. 200, p. 69).

"Orbital Motion of the Massive Multiple Stars in the Orion Trapezium"

D. Schertl, Y. Y. Balega et al. 2003

Abstract. We present bispectrum speckle interferometry of the multiple Orion Trapezium stars Θ^1 Ori A, Θ^1 Ori B, and Θ^1 Ori C obtained with the SAO 6 m telescope in Russia over a period of 5.5 years (epochs 1995-2001). Our diffraction-limited images have a resolution λ / D of 42 mas (J-band), 57 mas (H-band) and 76 mas (K-band). We clearly detect motion of the companions relative to their primary stars in the systems Θ^1 Ori A1-2 (mean separation $\rho \sim 220$ mas, change in position angle $\Delta \mathrm{PA} = 6°$), Θ^1 Ori B2-3 ($\rho \sim 205$ mas, $\Delta \mathrm{PA} = 8°$), and Θ^1 Ori C1-2 ($\rho \sim 37$ mas, $\Delta \mathrm{PA} = 18°$); Fig. 2. In our K-band image of Θ^1 Ori B we resolve a fourth visual component, confirming its discovery by Simon et al. . We determine the J, H, and K magnitudes of the system components and estimate the stellar masses of the companions in the HR-diagram. The companions Θ^1 Ori C2 and Θ^1 Ori B2 show clear evidence of near-infrared excess in the color-color diagram. The companions Θ^1 Ori A2 and Θ^1 Ori B3 show much stronger extinction than their primary stars, providing evidence of the presence of circumstellar material around the companions.

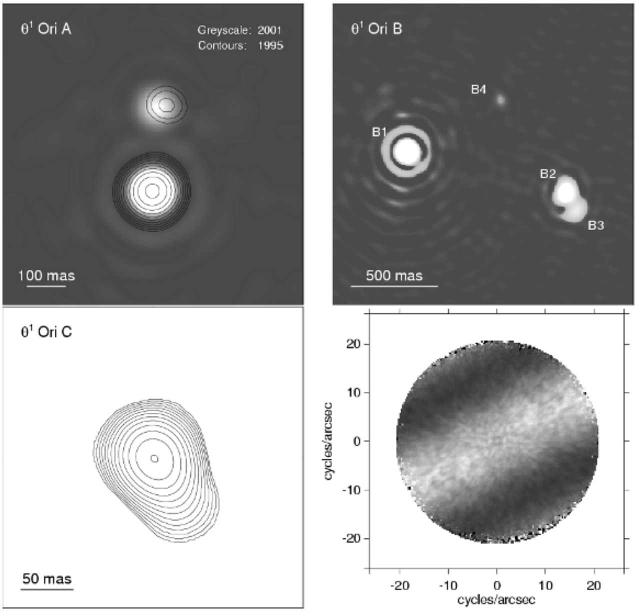

Fig. 2. Upper left: bispectrum speckle K-band images of Θ^1Ori A. The greyscale image was reconstructed from the 2001 data, the contour image from the 1995 data. The orbital motion of the companion can be easily seen. Upper right: bispectrum speckle K-band image of Θ^1Ori B (2001 data). The faint fourth component is seen near the center of the upper half of the image. Note that Θ^1Ori B1 (BM Ori) is itself an eclipsing spectroscopic binary (Popper & Plavec 1976). Lower left: contour representation of our J-band bispectrum speckle image of Θ^1Ori C (2001 data). Lower right: reconstructed power spectrum of Θ^1Ori C (J band, 2001 data) (Schertl, Balega et al. 2003)

"The Origin of Runaway Stars"

R. Hoogerwerf, J. H. J. de Bruijne, & P. T. de Zeeuw 2000

Abstract. Milliarcsecond astrometry provided by Hipparcos and by radio observations makes it possible to retrace the orbits of some of the nearest runaway stars and pulsars to determine their site of origin. The orbits of the runaways AE Aurigae and μ Columbae and of the eccentric binary ι Orionis intersected each other $\sim$2.5 Myr ago in the nascent Trapezium cluster, confirming that these runaways were formed in a binary-binary encounter. The path of the runaway star ξ Ophiuchi intersected that of the nearby pulsar PSR J1932+1059, $\sim$1 Myr ago, in the young stellar group Upper Scorpius. We propose that this neutron star is the remnant of a supernova that occurred in a binary system that also contained ξ Oph and deduce that the pulsar received a kick velocity of $\sim$350 km s^{-1} in the explosion. These two cases provide the first specific kinematic evidence that both mechanisms

proposed for the production of runaway stars, the dynamical ejection scenario and the binary-supernova scenario, operate in nature.

"Hubble Space Telescope NICMOS Imaging of W3 IRS 5: A Trapezium in the Making?"

S. T. Megeath, T. L. Wilson, & M. R. Corbin 2005

Abstract. We present Hubble Space Telescope NICMOS imaging of W3 IRS 5, a binary high-mass protostar. In addition to the two protostars, NICMOS images taken in the F222M and F160W filters show three new 2.22 μm sources with very red colors; these sources fall within a region 5600 AU in diameter and are coincident with an $\sim 100\,M_{\odot}$, dense molecular clump. Two additional point sources are found within 0.4" (800 AU) of one of the high-mass protostars; these may be stellar companions or unresolved emission knots from an outflow. We propose that these sources constitute a nascent Trapezium system in the center of the W3 IRS 5 cluster containing as many as five proto-OB stars. This would be the first identification of a Trapezium still deeply embedded in its natal gas.

"High-mass binaries in the Very Young Open Cluster NGC 6231. Implication for cluster and Star Formation"

B. Garcia & J. C. Mermilliod 2001

Abstract. New radial-velocity observations of 37 O- and B stars in the very young open cluster NGC 6231 confirm the high frequency of short-period spectroscopic binaries on the upper main sequence. Among the 14 O-type stars, covering all luminosity classes from dwarfs to supergiants, 8 are definitively double-lined systems and all periods but one are shorter than 7 days. Several additional binaries have been detected among the early B-type stars. NGC 6231 is an exceptional cluster to constrain the scenarios of cluster- and binary-star formation over a large range of stellar masses. We discuss the evidences, based on NGC 6231 and 21 other clusters, with a total of 120 O-type stars, for a clear dichotomy in the multiplicity rate and structure of very young open clusters containing O-type stars in function of the number of massive stars (for other cluster data, see IAU-Symp. 200, p. 191).

"Binary Systems and Stellar Mergers in Massive Star Formation"

I. A. Bonnell & M. R. Bate 2005

Abstract. We present a model for the formation of high-mass close binary systems in the context of forming massive stars through gas accretion in the

centres of stellar clusters. A low-mass wide binary evolves under mass accretion towards a high-mass close binary, attaining system masses of the order of $30-50\,M_\odot$ at separations of the order of 1 AU. The resulting high frequency of binary systems with two massive components is in agreement with observations. These systems are typically highly eccentric and may evolve to have periastron separations less than their stellar radii. Mergers of these binary systems are therefore likely and can lead to the formation of the most massive stars, circumventing the problem of radiation pressure stopping the accretion. The stellar density required to induce binary mergers is $\approx 10^6$ stars pc^{-3}, or ≈ 0.01 that required for direct stellar collisions.

"The Binary Population in OB Associations"

A. G. A. Brown 2001

Abstract. The OB associations in the solar vicinity contain a large fraction of all the bright O and B stars. Many studies of their multiplicity exist in the literature. As a first step, multiplicity data on the 3 subgroups of the nearby Sco OB2 association has been compiled (see Fig. 3).

"The Kinematical and Binary Properties of Association and Field O Stars"

D. R. Gies 1987

Abstract. A catalog of 195 Galactic O-type stars brighter than $V = 8.0$ mag has been compiled to compare the velocity distribution and binary frequency among cluster and association, field, and runaway stars. Both the field stars and runaway stars have a larger dispersion in peculiar radial velocity, a more positive mean peculiar radial velocity, and a wider z-distribution than stars found in clusters and associations, which is consistent with the ejection of field and runaway stars from their birthplaces in associations. Visual binaries are common among stars in clusters and associations, but their incidence is a factor of 2 lower among field stars, and they are absent in the runaway stars. Similarly, there is a deficiency of spectroscopic binaries among field stars, and especially the runaway stars, relative to the numbers found in clusters and associations. Many of these properties can be understood in terms of ejection through close gravitational interactions with binary stars during an early high number density epoch in the evolution of clusters.

"ICCD Speckle Observations of Binary Stars. XIX - an Astrometric/Spectroscopic Survey of O Stars"

B. D. Mason, D. R. Gies et al. 1998

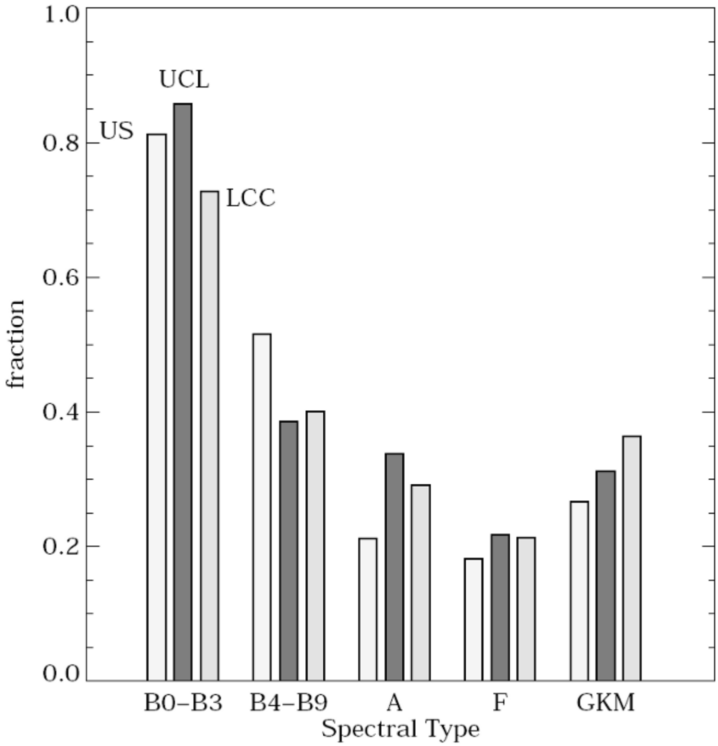

Fig. 3. The fraction of multiple systems vs. spectral type for the Hipparcos members of each of the 3 subgroups of Sco OB2 association. The fraction is incomplete beyond spectral type B9

Abstract. We present the results of a speckle interferometric survey made with the CHARA speckle camera and 4 m class telescopes of Galactic O-type stars with $V < 8$ mag. We can detect with the speckle camera binaries in the angular separation range $0.035 - 1.5$ arcsec with $\Delta m < 3$ mag, and we have discovered 15 binaries among 227 O-type systems. We combined our results on visual binaries with measurements of wider pairs from the Washington Double Star Catalog and fainter pairs from the Hipparcos Catalog, and we made a literature survey of the spectroscopic binaries among the sample. We then investigated the overall binary frequency of the sample and the orbital characteristics of the known binaries. Binaries are common among O stars in clusters and associations but less so among field and especially runaway stars. There are many triple systems among the speckle binaries, and we discuss their possible role in the ejection of stars from clusters. The period distribution of the binaries is bimodal in log P, but we suggest that binaries with periods of years and decades may eventually be found to fill the gap. The mass ratio distribution of the visual binaries increases toward lower mass ratios, but low mass ratio companions are rare among close, spectroscopic binaries. We present distributions of the eccentricity and longitude of periastron for spectroscopic binaries with elliptical orbits, and we find strong evidence of a bias in the longitude of periastron distribution.

"The O-type Binary 15 Monocerotis Nears Periastron"

D. R. Gies, B. D. Mason et al. 1997

Abstract. We present new radial velocity measurements for the massive binary 15 Monocerotis which indicate that the system is now very close to periastron (1996.9) in its 24 yr orbit. The velocity separation in the coming year may be large enough to permit an accurate estimate of mass ratio. We also present our first astrometric measurement of 15 Mon made with the Hubble Space Telescope Fine Guidance Sensors (FGS). The FGS transfer functions are consistent with an advanced orbital position close to periastron, and we present preliminary orbital elements for the combined spectroscopic and astrometric orbit. (PS. Derived component masses are 35 and 24 $M_\odot$)

"The Origin of Massive O-type Field Stars"

W. J. de Wit, L. Testi et al. 2005

Abstract. In two papers we try to confirm that all Galactic high-mass stars are formed in a cluster environment, by excluding that O-type stars found in the Galactic field actually formed there. In de Wit et al. (2004) we presented deep K-band imaging of 5 arcmin fields centred on 43 massive O-type field stars that revealed that the large majority of these objects are single objects. In this contribution we explore the possibility that the field O stars are dynamically ejected from young clusters, by investigating their peculiar space velocity distribution, their distance from the Galactic plane, and their spatial vicinity to known young stellar clusters. We (re-)identify 22 field O-type stars as candidate runaway OB-stars. The statistics show that $4 \pm 2\,\%$ of all O-type stars with $V < 8$ mag can be considered as formed outside a cluster environment. Most are spectroscopically single objects, some are visual binaries. The derived percentage for O-type stars that form isolated in the field based on our statistical analyses is in agreement with what is expected from calculations adopting a universal cluster richness distribution with power index of $\beta = 1.7$, assuming that the cluster richness distribution is continuous down to the smallest clusters containing one single star.

"Resolving OB Systems in the Carina Nebula with the Hubble Space Telescope Fine Guidance Sensor"

E. P. Nelan, N. R. Walborn et al. 2004

Abstract. We observed 23 OB stars in the Carina Nebula (NGC 3372) with the Hubble Space Telescope's Fine Guidance Sensor 1r (FGS1r) in its high angular resolution mode. Five of these OB stars are newly resolved binaries with projected separations ranging from 0.015" to 0.352" (37 to 880 AU at a distance of 2.5 kpc), and V-band magnitude differences ranging from 0.9 to 2.8. The most important astrophysical result is the unexpected resolution of the prototype O2 If* star HD 93129A as a 55 milliarcsecond (mas) double with a Δm_V of 0.9. This object has served as a spectroscopic benchmark for the analysis of the most massive hot stars and their winds on the prior assumption that it is a single star. This discovery supports the interpretation of recent radio and X-ray observations as evidence of colliding-wind phenomena in HD 93129A. Another interesting result is the determination of an upper limit of about 35 AU for the projected separation of the binary pairs in the hierarchical double spectroscopic binary HD 93206. The high incidence of resolved binaries provides motivation for a more thorough, statistically meaningful study of multiplicity among the most massive stars in the young ionizing clusters of the nebula to obtain a complete sample of the long-period systems that have evaded spectroscopic detection. However, considering that the nine spectroscopic binaries with accurate orbits in the Carina Nebula have orbital dimensions ≤ 1 AU, which at a distance of 2.5 kpc subtends an angle of only 0.4 mas, well below the $\simeq 10$ mas angular resolution of FGS1r, there remains a significant range of orbital periods and separations over which it is very difficult to detect multiplicity in the nebula with currently available instruments.

"V 3903 Sagittarii: a Massive Main-sequence (O7V+O9V) Detached Eclipsing Binary"

L. P. R. Vaz, N. C. S. Cunha et al. 1997

Abstract. We present for the first time an analysis based on *uvby* light curves, Hβ indices and on new spectroscopic data of the massive detached double-lined O-type eclipsing binary V 3903 Sgr. The *uvby* light curves are analysed with the WINK (initial solutions) and the Wilson-Devinney (WD, final solution) programs. Both codes were used in their extended versions, with stellar atmospheres and taking into account the geometric distortions and photometric effects caused by proximity of the components.

We conclude that V 3903 Sgr is one of the rare O-type detached systems where both components are still on the initial phases of the main sequence, with an age of either 1.6×10^6 yrs or 2.5×10^6 yrs (depending on the evolutionary model adopted) at a distance of ~ 1500 pc, the same as for the Lagoon Nebula (Messier8) complex, of which the system is probably a member. We determine the absolute dimensions: $M_A = 27.27 \pm 0.55$, $R_A = 8.088 \pm 0.086$, $M_B = 19.01 \pm 0.44$ and $R_B = 6.125 \pm 0.060$ (solar units). There is no evidence of mass transfer and the system is detached. The orbit

is circular, and both components show synchronous rotation, despite their early evolutionary stage. The absolute dimensions determined should be representative for normal single stars.

"WR 20a is an Eclipsing Binary: Accurate Determination of Parameters for an Extremely Massive Wolf-Rayet System"

A. Z. Bonanos, K. Z. Stanek et al. 2004

Abstract. We present a high-precision I-band light curve for the Wolf-Rayet binary WR 20a, obtained as a subproject of the Optical Gravitational Lensing Experiment. Rauw et al. have recently presented spectroscopy for this system, strongly suggesting extremely large minimum masses of 70.7 ± 4.0 and $68.8 \pm 3.8\ M_{\odot}$ for the component stars of the system, with the exact values depending strongly on the period of the system. We detect deep eclipses of about 0.4 mag in the light curve of WR 20a, confirming and refining the suspected period of $P = 3.686$ days and deriving an inclination angle of $i = 74.5\,d \pm 2.0\,d$. Using these photometric data and the radial velocity data of Rauw et al., we derive the masses for the two components of WR 20a to be 83.0 ± 5.0 and $82.0 \pm 5.0\,M_{\odot}$. Therefore, WR 20a is confirmed to consist of two extremely massive stars and to be the most massive binary known with an accurate mass determination. (PS. WR20a is actually a hydrogen-burning binary system)

"Speckle Masking Observation of the Central Object in the Giant H II Region NGC 3603"

K.-H. Hofmann & G. Weigelt 1986

Abstract. The first reconstruction of a true diffraction-limited image of the central object HD 97950 AB in NGC 3603 is reported. The image has been reconstructed by a four-dimensional version of speckle masking (triple correlation processing). Speckle masking is a solution of the phase problem in speckle interferometry. The reconstructed image shows that HD 97950 AB consists of 4 stars (V-magnitudes 11.7, 11.7, 11.7, and 12.2; separations relative to Al: 0.78, 0.37 and 0.34 arcsec).

"R136a in the 30 Doradus Nebula Resolved by Holographic Speckle Interferometry"

G. Weigelt & G. Baier 1985

Abstract. Digital speckle interferometry observations of R136, the luminous central object in the 30 Doradus nebula have been performed. It was possible to reconstruct a diffraction-limited true image of R136a by using R136b and

R136c as the deconvolution keys (holographic speckle interferometry). The reconstructed image shows for the first time that R136a is a dense star cluster consisting of 8 stars within a diameter of 1 arcsec (at wavelength approximately 710 nm). The dominating objects are three stars of almost identical magnitudes with separations of 0.10 and 0.48 arcsec. The reconstructed image has a resolution of 0.09 arcsec.

"The ionising Cluster of 30 Doradus. IV. Stellar Kinematics"

G. Bosch, F. Selman et al. 2001

Abstract. On the basis of multislit spectroscopy of 180 stars in the ionising cluster of 30 Doradus we present reliable radial velocities for 55 stars. We calculate a radial velocity dispersion of $\sim 35\,\mathrm{km\,s^{-1}}$ for the cluster and we analyse the possible influence of spectroscopic binaries in this rather large velocity dispersion. We use numerical simulations to show that the observations are consistent with the hypothesis that all the stars in the cluster are binaries, and the total mass of the cluster is $\sim 5 \times 10^5\,\mathrm{M}_\odot$. A simple test shows only marginal evidence for dynamical mass segregation which if present is most likely not due to dynamical relaxation.

"Orbits of Four Very Massive Binaries in the R136 Cluster"

P. Massey, L. R. Penny, & J. Vukovich 2002

Abstract. We present radial velocity and photometry for four early-type, massive, double-lined spectroscopic binaries in the R136 cluster. Three of these systems are eclipsing, allowing orbital inclinations to be determined. One of these systems, R136-38 (O3 V + O6 V), has one of the highest masses ever measured for the primary, $57\,\mathrm{M}_\odot$. Comparison of our masses with those derived from standard evolutionary tracks shows excellent agreement. We also identify five other light variables in the R136 cluster that are worthy of follow-up study. (PS. R145 ...)

"Forty Eclipsing Binaries in the Small Magellanic Cloud: Fundamental Parameters and Cloud Distance"

R. W. Hilditch, I. D. Howarth, & T. J. Harries 2005

Abstract. We have conducted a programme to determine the fundamental parameters of a substantial number of eclipsing binaries of spectral types O and B in the Small Magellanic Cloud (SMC). New spectroscopic data, obtained with the two-degree-field (2dF) multi-object spectrograph on the 3.9-m Anglo-Australian Telescope, have been used in conjunction with photometry from the Optical Gravitational Lens Experiment (OGLE-II) data

base of SMC eclipsing binaries. Previously we reported results for 10 systems; in this second and concluding paper we present spectral types, masses, radii, temperatures, surface gravities and luminosities for the components of a further 40 binaries. The uncertainties are typically $\pm 10\,\%$ on masses, $\pm 4\,\%$ on radii and ± 0.07 on $\log \mathrm{L}$. The full sample of 50 OB-type eclipsing systems is the largest single set of fundamental parameters determined for high-mass binaries in any galaxy. We find that 21 of the systems studied are in detached configurations, 28 are in semidetached post-mass-transfer states, and one is a contact binary.

The overall properties of the detached systems are consistent with theoretical models for the evolution of single stars with SMC metal abundances ($\mathrm{Z} \simeq 0.004$); in particular, observed and evolutionary masses are in excellent agreement. Although there are no directly applicable published models, the overall properties of the semidetached systems are consistent with them being in the slow phase of mass transfer in case A. About 40 % of these semidetached systems show photometric evidence of orbital-phase-dependent absorption by a gas stream falling from the inner Lagrangian point on the secondary star towards the primary star. This sample demonstrates that case-A mass transfer is a common occurrence amongst high-mass binaries with initial orbital periods $\mathrm{P} \leq 5\,\mathrm{d}$, and that this slow phase has a comparable duration to the detached phase preceding it.

Each system provides a primary distance indicator. We find a mean distance modulus to the SMC of $18.91 \pm 0.03 \pm 0.1$ (internal and external uncertainties; $\mathrm{D} = 60.6 \pm 1.0 \pm 2.8\,\mathrm{kpc}$). This value represents one of the most precise available determinations of the distance to the SMC.

"High Intrinsic Binarity Rate for Massive Stars: Multi-epoch Radial Velocity Survey of O-stars in Ultracompact HII Regions"

D. Apai, A. Bik et al. 2006

Abstract. We present here the first multi-epoch radial velocity study of very young massive stars using near-infrared spectra obtained by the ISAAC/VLT instrument aiming to measure their intrinsic binarity rate. Our 28 targets are associated to known ultracompact HII regions ensuring that dynamic evolution of the clusters did not influence the binarity rate. We identify two stars with about 90 km/s velocity differences between the two epochs proving the presence of close massive binaries. In addition, we show that the radial velocity dispersion of the full sample is about 35 km/s, significantly larger than our accuracy ($\sim 25\,\mathrm{km/s}$). Simple Monte Carlo models are used to test different binarity fractions and mass ratios and we conclude that "a substantial number" of the young massive stars are formed as binaries. Implications to previously proposed formation scenarios are discussed.

Final Note

A summary table of masses and other parameters of massive binary systems is provided by Gies (2001), while Zinnecker (2003) reviews the formation of massive binaries (see also Zinnecker & Bate 2002).

Acknowledgment

I would like to thank the SOC for their invitation to present this review and U. Hanschur (AIP) for technical assistance.

References

1. D. Apai, A. Bik et al.: in prep. (2006)
2. J. Bally, R. S. Sutherland et al.: AJ **116**, 293 (1998)
3. A. Z. Bonanos, K. Z. Stanek et al.: ApJ **611**, L33 (2004)
4. I. A. Bonnell, M. R. Bate, & St. G. Vine: MNRAS **343**, 413 (2003)
5. I. A. Bonnell & M. R. Bate: MNRAS **362**, 915 (2005)
6. G. Bosch, F. Selman et al.: A&A **380**, 137 (2001)
7. A. G. A. Brown: Astron. Nachr. **322**, 43 (2001)
8. W. J. de Wit, L. Testi et al.: A&A **425**, 937 (2004)
9. W. J. de Wit, L. Testi et al.: A&A **437**, 247 (2005)
10. G. Duchêne, T. Simon et al.: A&A **379**, 147 (2001)
11. B. Garcia & J. C. Mermilliod: A&A **368**, 122 (2001)
12. D. R. Gies: ApJS **64**, 545 (1987)
13. D. R. Gies, B. D. Mason et al.: ApJ **475**, L49 (1997)
14. D. R. Gies: Masses and other parameters of massive binaries. In: *A Massive Star Odyssey: From Main Sequence to Supernova, Proceedings of IAU-Symp. 212*, ed by K. van der Hucht, A. Herrero, & C. Esteban (San Francisco: Astronomical Society of the Pacific 2003) p. 91
15. R. W. Hilditch, I. D. Howarth, & T. J. Harries: MNRAS **357**, 304 (2005)
16. K.-H. Hofmann & G. Weigelt: A&A **167**, L15 (1986)
17. R. Hoogerwerf, J. H. J. de Bruijne, & P. T. de Zeeuw: ApJ **544**, L133 (2000)
18. B. D. Mason, D. R. Gies et al.: AJ **115**, 821 (1998)
19. P. Massey, L. R. Penny, & J. Vukovich: ApJ **565**, 982 (2002)
20. S. T. Megeath, T. L. Wilson, & M. R. Corbin: ApJ **622**, L141 (2005)
21. A. F. J. Moffat, L. Drissen, & M. M. Shara: ApJ **436**, 183 (1994)
22. E. P. Nelan, N. R. Walborn et al.: AJ **128**, 323 (2004)
23. M. G. Petr, V. Coudé Du Foresto et al.: ApJ **500**, 825 (1998)
24. D. M. Popper & M. Plavec: ApJ **205**, 462 (1976)
25. T. Preibisch, Y. Balega et al.: New Astronomy **4**, 531 (1999)
26. D. Schertl, Y. Y. Balega et al.: A&A **402**, 267 (2003)
27. L. P. R. Vaz, N. C. S. Cunha et al.: A&A **327**, 1094 (1997)
28. G. Weigelt & G. Baier: A&A **150**, L18 (1985)
29. G. Weigelt, Y. Balega et al.: A&A **347**, L15 (1999)

30. H. Zinnecker & M. R. Bate: Multiplicity of Massive Stars – a Clue to their Origin? In: *Hot Star Workshop III: The Earliest Stages of Massive Star Birth. ASP Conference Proceedings* vol. 267, ed by P. A. Crowther (San Francisco, Astronomical Society of the Pacific 2002) p. 209
31. H. Zinnecker: Formation of massive binaries. In: *A Massive Star Odyssey: From Main Sequence to Supernova, Proceedings of IAU-Symp. 212*, ed by K. van der Hucht, A. Herrero, & C. Esteban (San Francisco: Astronomical Society of the Pacific 2003) p. 80

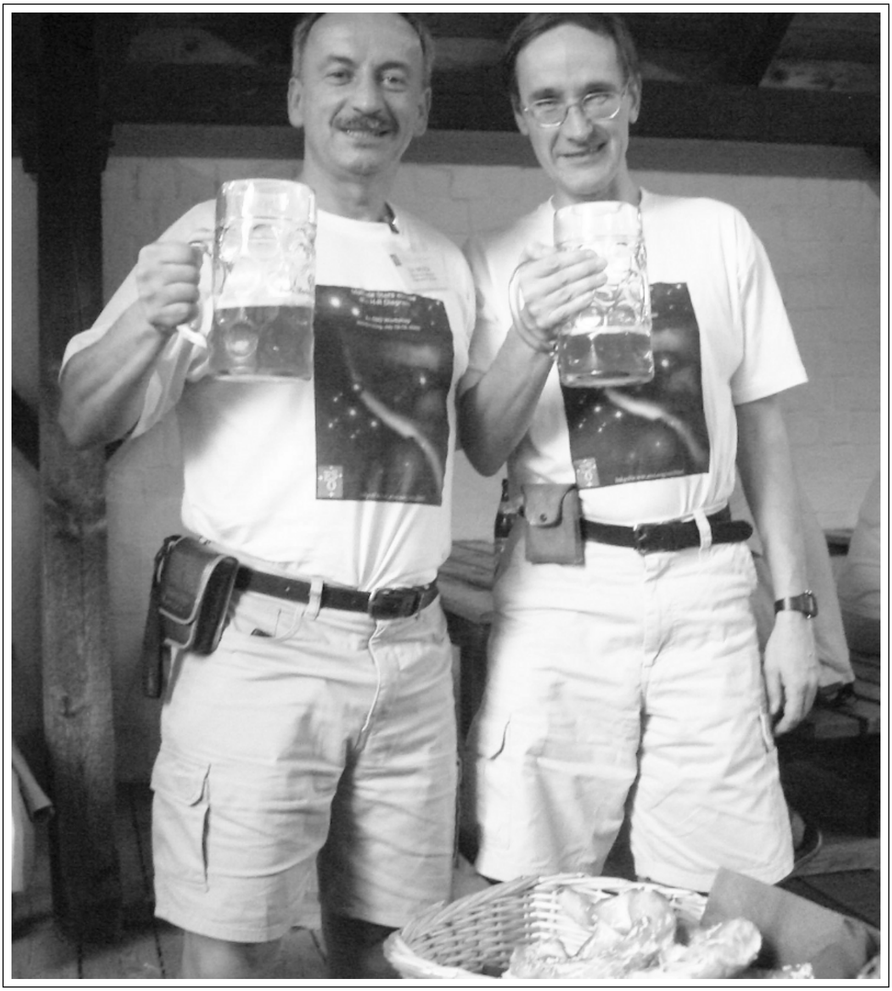

Yuri Balega (left), Andrei Tokovinin (right)

The Triple System θ^1 Orionis A in the Heart of the Orion Trapezium Cluster

Monika G. Petr-Gotzens[1] and Maria Massi[2]

[1] European Southern Observatory, Karl-Schwarzschild Str. 2, D-85748 Garching, Germany mpetr@eso.org
[2] Max-Planck-Institut für Radioastronomie, Auf dem Hügel 69, 53121 Bonn, Germany mmassi@mpifr-bonn.mpg.de

Summary. Almost two decades ago, strong non-thermal variable radio-emission had been detected from θ^1 Orionis A, the third most luminous OB star in the Orion Trapezium Cluster. The source of the emission, has been a puzzling issue since then. Now, it is established that θ^1 Orionis A is a close triple stellar system and that the radio emission originates from the visual companion θ^1 Orionis A2. In this contribution we re-analyse available radio data combined with near-infrared observations in order to constrain the nature of θ^1 Orionis A2. Stringent constraints on the size of the non-thermal radio emission imply the presence of very large magnetic structures. Conceivable scenarii are a) θ^1 Orionis A2 is a single young intermediate-mass star with strong magnetic interactions between the star and its circumstellar disk, b) θ^1 Orionis A2 is a binary and radio flaring originates from interactions between the magnetic structures of both stars.

1 Introduction

At the center of the famous Orion Nebula Cluster one finds a group of luminous OB stars, which is called the Orion Trapezium. The probably most interesting source among this well studied stars is θ^1 Orionis A (HD 37020), the third most luminous of the Trapezium stars. The spectral classification of θ^1 Orionis A (hereafter θ^1A) is B0.5V [1].

A distinguishing feature detected towards θ^1A is its strong, non-thermal, variable radio-emission that had been found by Churchwell et al. [2]. During repeatedly observed flaring events at 2cm and 6cm wavelengths the source has temporarily been the brightest radio source in the whole Orion Nebula Cluster [3,4]! Several attempts to explain the origin of the unexpectedly high non-thermal radio emission have been made, including interaction of stellar winds, chaotic wind emission, and a rapidly rotating magnetic star [3–5]. However, the observations never fully fit with any model predictions, and the nature of the emission remained a puzzling issue. As θ^1A is a close triple stellar system, it has also been difficult to identify which component of the system actually is the radio emitter.

In this contribution we review and re-analyse available radio data in combination with near-infrared observations, and we discuss some scenarii for the enigmatic radio emission from the θ^1A system.

2 Review of Available Data and Facts of θ^1 Ori A

2.1 Multiplicity

For quite some time θ^1A had been thought to be an early type single star, until Lohsen [6] discovered a very close eclipsing companion in 1973. An orbital period of P = 65.4325d has first been derived by [7], and later confirmed and refined by other authors [8,9]. Furthermore, the mass and evolutionary state of the eclipsing companion was investigated through spectroscopic monitoring, leading [10] to conclude that the eclipsing companion is a T Tauri star of $\sim 2.4\mathrm{M}_\odot$.

Then, in the late 1990s even another, third component was discovered with high angular resolution speckle techniques [11, 12]. This speckle companion is separated from θ^1A by $0.2''$ ($\sim 90\,$AU), and we will refer to it as θ^1A2 in the following. At times when the existence of the speckle companion was still unknown, most attempts that have been put forward to explain the nature of the radio-emission [4,5], involved the close-by eclipsing companion. However, no model did fully satisfactorily fit with the observations. When the speckle companion, θ^1A2, was detected it was obvious to check if θ^1A2 might be the source of the strong radio emission. Positional uncertainties present in the radio data, however, prevented a unique identification. Nevertheless, based on some qualitative arguments and on a positional coincidence at least within 1σ, Petr et al. [11] speculated that θ^1A2 is the radio emitting star.

2.2 Radio Observations

The first detection of θ^1Ori A as a radio source [13] and, moreover, as a highly variable strong emitter at 2cm and 6cm wavelengths [2] triggered intensive radio observing campaigns during the following years. Using mainly VLA and VLBI observations, it was confirmed that θ^1Ori A is associated with a high brightness temperature ($T_B \geq 4 \times 10^7\,$K) and strong variability, indicating a non-thermal emission [3, 4]. The radio spectral index of θ^1Ori A was on average flat, which allows us to consider in Figure 1 data from 2cm and 6cm observations alltogether. In this Figure 1 we display radio measurements of θ^1Ori A taken over a period of almost 11 years. The plot visualizes the absolute fluxes and the range of the variability, which is of a factor of $\sim$30 between the strongest flare and the quiescent level. Felli et al. [5] also pointed out that the time scale of the variability is similar or smaller than their sampling interval of 10–20 days.

More recent radio observations carried out at $\lambda = 6$cm with MERLIN and global VLBI providing sub-mas astrometry have finally solved the positional uncertainty of the θ^1Ori A radio source: Garrington et al. [14] indisputable associated the radio emission source with the speckle companion θ^1A2; no emission was detected from θ^1A1, the primary OB star (including the eclipsing lower mass TTauri-type companion). Thanks to the improved uv-coverage

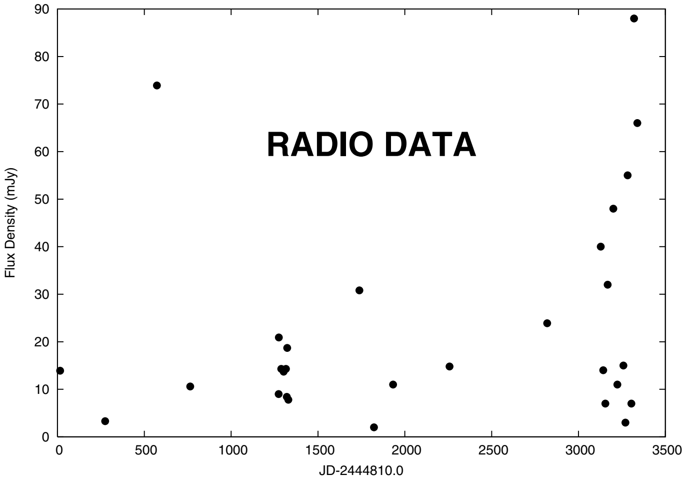

Fig. 1. Radio flux measurements of the source θ^1Ori A as reported in [4, 5] versus date

and sensitivity of the present global VLBI network, these authors were also able to reconstruct a 6cm VLBI image and to determine a source size of $\sim$ 1mas from visibility fitting. The size is roughly consistent with the previously determined size of $\sim$ 1.3mas by [4]. At the distance of the Orion Nebula cluster 1mas corresponds to 0.45 AU or $\sim 90 R_\odot$, which means a huge emitting source size, and a very important information for constraining the nature of the emission.

2.3 Infrared Observations

In order to investigate the stellar characteristics of the radio emitter θ^1A2 we searched the literature for various photometric measurements. Near-infrared system magnitudes (i.e. photometry for the triple θ^1A as a whole) have been collected [11, 15–18] +2MASS magnitudes. Whenever speckle imaging or adaptive optics techniques were used, we could extract individual near-infrared photometry for both, θ^1A2 and θ^1A1. We also added our own observations obtained with ESO's adaptive optics system ADONIS and from speckle measurements [11].

Surprisingly, we find that the system brightness at J, H, or K-band, as reported by the various authors, shows a large discrepancy (up to $\sim 0.5^{\mathrm{m}}$ at J, $\sim 0.6^{\mathrm{m}}$ at H, $\sim 0.8^{\mathrm{m}}$ at K), which is larger than the typically quoted individual uncertainties. Either the photometry is complicated due to the large crowding in the Trapezium or the source is variable. On the other hand, the brightness ratio of θ^1A1/θ^1A2 is rather consistent across different authors. As there is no good reason why a specific measurement from a certain group of authors should be prefered, we translate the range of photometric results to an uncertainty in the near-infrared colours and magnitudes of θ^1A2. Consequently, the possible space for the radio emitter θ^1A2 in the colour-colour diagram (Fig. 2) and colour-magnitude diagram allows for a number of valid interpretations of its stellar nature.

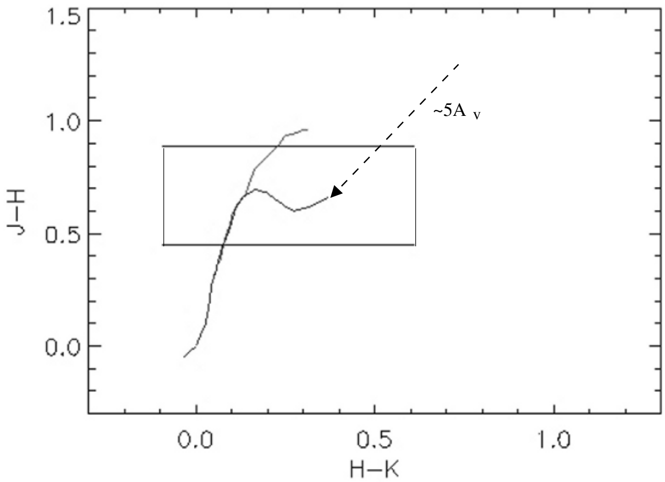

Fig. 2. Near-infrared colour-colour diagram for the star θ^1Ori A2. The box outlines the possible space for θ^1Ori A2 in this diagram. The box is large, because of the large differences in JHK-photometry reported by different authors

From the colour-colour diagram we deduce that θ^1Ori A2 might either be a slightly extincted late-type dwarf or a highly extincted ($A_V > 3$mag) early type star (see also [19]). However, the observed J-band luminosity of θ^1Ori A2 indicates that it is too luminous to be consistent with a young late-type, i.e. low-mass star. Comparing the possible positions of θ^1Ori A2 in the colour-magnitude diagram (shown elsewhere) with pre-main sequence evolutionary tracks by Palla & Stahler [20], we find that θ^1Ori A2 is at least a moderately massive, probably pre-main sequence star with $M_\star > 3.5M_\odot$. On the other hand, from the photometric information alone, we cannot exclude that θ^1Ori A2 might even be a cool giant, as proposed by [21], although we consider this option less likely.

3 The Possible Nature of θ^1 Ori A2

In case θ^1Ori A2 is a late-type giant, it would be difficult to explain its evolutionary stage within the 1 Myr old population of the Trapezium Cluster.

In fact, any K or M-giant would be much brighter at JHK than observed, if placed at the distance of the Orion Trapezium Cluster. However, the probability that θ^1Ori A2 is really physically related to θ^1Ori A1 is quite high, disproving suspicions that θ^1Ori A2 is an unrelated object: Given the separation of only $\sim 0.2''$ between θ^1Ori A1 and A2 the probability of the pair being not a chance projection is 99.6%. Furthermore, observations taken over 10 years have shown slight (orbital?) motion of θ^1Ori A2 (Figure 3). Intrinsic JHK luminosities of a G-type giant, on the other hand, seem to be compliant with a distance of ~450pc and the observed JHK brightnesses, but no strong radio continuum emission, like observed for θ^1Ori A2, would be expected.

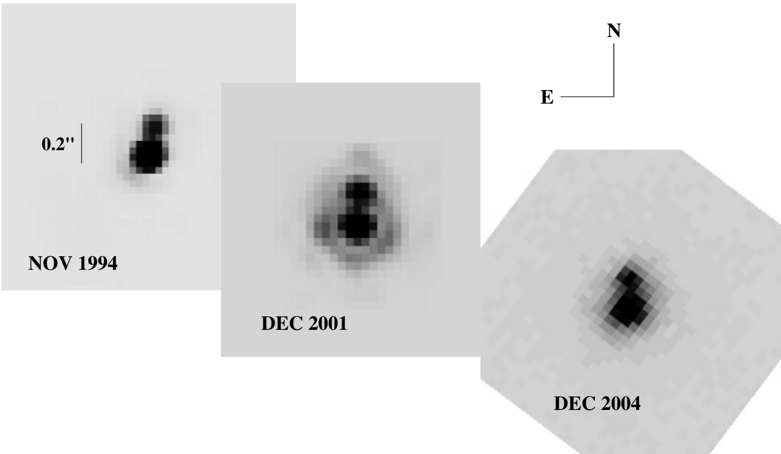

Fig. 3. Orbital motion of θ^1Ori A2 (northern component) around θ^1Ori A1 (southern component). All images show observations in the K-band around 2.2μm. The first image was obtained with the MAGIC camera at Calar Alto observatory via speckle mode. The second image was taken with the adaptive optics system ADONIS on the ESO/3.6m tel. at La Silla Observatory and the third, most recent, observation shows an ESO VLT/NACO acquisition image

We also exclude that θ^1Ori A2 is an ordinary intermediate-mass Herbig Ae/Be star, since those stars clearly show thermal radio emission, as opposed to the observed non-thermal emission. A magnetic, chemically peculiar star, a class of objects that are often found to be non-thermal radio emitters [22], must be excluded as well, because in this case the radio emission is expected to occur close to the stellar photosphere, which contradicts the enormous size scales found in the VLBI observations. Furthermore, the dynamic range of the radio variability detected for magnetic chemically peculiar stars (up to a few mJy) is much smaller than what has been observed for θ^1Ori A2.

The huge size of the emitting region ($\sim 90R_\odot$) implies that the radio emission from θ^1Ori A2 must arise in "some" magnetic structures located far above the stellar photosphere. Such a structure may be that of a Helmet streamer which can be formed on top of stellar coronal loops and extending out to several tens of the stellar radius [23]. The interaction of the magnetic field confined in such a helmet structure with the magnetosphere of another close-by star can trigger strong radio flaring, as for example has been shown to be a plausible explanation for the non-thermal radio emission in the TTauri binary V773 Tau A [24]. Indeed, a very young ($< 10^6$ Myr) binary system, composed of a low-mass (0.6-2.0$M_\odot$) and an intermediate-mass (3-5$M_\odot$) star would be compliant with the near-infrared photometry of θ^1Ori A2. Possible combinations do certainly depend on the amount of interstellar extinction, which we varied between $A_V = 1 - 4$mag in order to find potential binary pairs. Evidence for the structure of a helmet streamer is further given by the elongation seen in the reconstructed 6cm image of [14].

An alternative single star scenario is that of radio flaring being caused by shearing, disruption and subsequent reconnection of the magnetic fields between a young, chemically peculiar/magnetic, intermediate-mass star and its circumstellar disk [25, 26]. Star-disk interactions are also often invoked to explain high x-ray emission, presumably caused by magnetic activity, from Herbig Ae/Be stars that have not shown to harbour lower mass companions [27]. Non-thermal radio emission is naturally expected. However, to date no apparently single Herbig Ae/Be star has been reported to be a non-thermal radio source (with the probable exception of EC95 [28]). This may, on the other hand, be due to the lack of systematic radio surveys among such stars, in particular among such sources in young stellar clusters.

References

1. Levato, H., Abt, H.A.: PASP **88**, 712 (1976)
2. Churchwell, E.B., Felli, M., Wood, D.O.S., Massi, M.: ApJ **321**, 516 (1987)
3. Felli, M., Massi, M., Churchwell, E.B.: A&A **217**, 179 (1989)
4. Felli, M., Massi, M., Catarzi, M.: A&A **248**, 453 (1991)
5. Felli, M., Taylor, G.B., Catarzi, M., et al.: A&AS **101**, 12 (1993)
6. Lohsen, E.: IBVS **988**, 1 (1975)
7. Baldwin, M., Mattei, J.: IAU Circ. **3004**, 1 (1976)
8. Bondar, N.I., Vitrichenko, É.A., Zakirov, M.M.: AstL **26**, 452 (2000)
9. Stickland, D.J., Lloyd, C.: The Observatory **120**, 141 (2000)
10. Bossi, M., Gaspani, A., Scardia, M., Tadini, M.: A&A **222**, 117 (1989)
11. Petr, M.G., Coud'e du Foresto, V., Beckwith, S.V.W., Richichi, A., McCaughrean, M.J.: ApJ **500**, 825 (1998)
12. Weigelt, G., Balega, Y.Y., Preibisch, T., Schertl, D. et al.: A&A **347**, L15 (1999)
13. Garay, G., Moran, J.M., Reid, M.J.: ApJ **314**, 535 (1987)
14. Garrington, S.T., van Langevelde, H.J., Campbell, R.M., Gunn, A.: MERLIN and global VLBI Observations of θ^1 Orionis A, In: *Proceedings of the 6th European VLBI Network Symposium*, June 2002 in Bonn, ed by E. Ros, R.W. Porcas, A.P. Lobanov, J.A. Zensus (publ. by MPIfR Bonn) p. 259 (2002)

15. McCaughrean, M.J., Stauffer, J.R.: AJ **108**, 1382 (1994)
16. Hillenbrand, L.A., Strom, S.E., Calvet, N. et al.: AJ **116**, 1816 (1998)
17. Simon, M., Close, L.M., Beck, T.L.: AJ **117**, 1375 (1999)
18. Vitrichenko, É.A.: AstL **25**, 179 (1999)
19. Schertl, D., Balega, Y.Y., Preibisch, T. Weigelt, G.: A&A **402**, 267 (2003)
20. Palla, F., Stahler, S.W.: ApJ **525**, 772 (1999)
21. Vitrichenko, É.A., Plachinda, S.I.: AstL **27**, 581 (2001)
22. Linsky, J.L., Drake, S.A., Bastian, T.S.: ApJ **393**, 341 (1992)
23. Endeve, E., Holzer, T.E., Leer, E.: ApJ **603**, 307 (2004)
24. Massi, M., Forbrich, J., Menten, K.M., Toricelli-Ciamponi, G., et al.: A&A, in press (2006)
25. Feigelson, E.D, Montmerle, T.: ARA&A **37**, 363 (1999)
26. Montmerle, T., Grosso, N., Tsuboi, Y., Koyama, K.: ApJ **532**, 1097 (2000)
27. Hamaguchi, K., Yamauchi, S., Koyama, K.: ApJ **618**, 360 (2005)
28. Smith, K., Güdel, M., Benz, A.O.: A&A **349**, 475 (1999)

In front: Monika Petr-Gotzens, Roger Griffin, Christian Hummel, during the conference dinner in the Garchinger Beergarden

The Primordial Binary Population in OB Associations

Thijs Kouwenhoven

Astronomical Institute 'Anton Pannekoek', University of Amsterdam, Kruislaan 403, 1098 SJ Amsterdam, The Netherlands kouwenho@science.uva.nl

Summary. We describe our method to find the primordial binary population in the Sco OB2 association. We present the results of our ADONIS and VLT/NACO near-infrared adaptive optics binarity surveys of A and late-B stars in Sco OB2. We combine these results with literature data on visual, spectroscopic, and astrometric binary stars. With our observations we remove part of the selection effects present in the combined dataset. Using simulated observations the remaining biases can be removed in order to derive the true binary population. Detailed N-body simulations, including stellar and binary evolution are required to derive constraints on the binary population which was present just after the natal gas has been removed from Sco OB2, i.e., the primordial binary population.

1 Introduction

Over the last decade observations of star forming regions and young stellar clusters have shown that most, possibly even all stars form in binaries or higher-order multiple systems. For our understanding of the star and cluster formation process it is important to characterize the properties of binary stars as a function of, e.g., the mass of the primary star and environment. Ideally, one would like to know all properties of binary and multiple systems just after the stars have formed. Unfortunately, performing a binarity study in star forming regions poses severe observational difficulties due to the large amount of interstellar gas and dust. However, shortly after the first massive stars are formed, their stellar winds rapidly remove the gas and dust from the star-forming region. From this point in time, accretion ceases almost completely and the binary stars do not interact with the gas anymore. After the gas has been removed the dynamical evolution of the binary population is expected to become much less important.

The primordial binary population (PBP) is *the population of binaries as established just after the gas has been removed from the forming system, i.e., when the stars can no longer accrete gas from their surroundings* [1]. The evolution of stars and dynamics of the newly born stellar population is influenced by the presence of gas, but when the gas is removed, the binary population is only affected by stellar evolution and pure N-body dynamics. The PBP is also a natural boundary for simulations of the formation of star clusters and binary stars. Hydrodynamical simulations of a contracting gas cloud, e.g. [2], result in the primordial binary population when the gas is removed by accretion, stellar winds, or supernova explosions. Pure N-body simulations, e.g. [3], can be used to study the subsequent evolution of the star cluster and binary population.

OB associations are well suited for studying the PBP. They are young ($5 - 50$ Myr) and low-density ($< 0.1 M_\odot \mathrm{pc}^{-3}$) aggregates of stars. Their youth implies that only a handful of the most massive systems have changed due to stellar evolution. The effects of dynamical evolution are expected to be limited due to the young age and low stellar density of the association. Moreover, in contrast to, e.g. the Taurus T association, OB associations cover the full range of stellar masses.

Scorpius OB2 is the closest young OB association and the prime candidate for studying the binary population. The proximity of Sco OB2 ($118 - 145$ pc) facilitates observations. The young age ($5 - 20$ Myr) suggests that dynamical evolution has not significantly altered the binary population since the moment of gas removal. Sco OB2 consists of three subgroups: Upper Scorpius (US), Upper Centaurus Lupus (UCL), and Lower Centaurus Crux (LCC). The three subgroups are located at a distance of 145 pc, 140 pc, and 118 pc, and have an age of 5 Myr, $15 - 22$ Myr, and $17 - 23$ Myr, respectively. The membership and stellar content of the association was established by [4] using *Hipparcos* parallaxes and proper motions. The structure of the Sco OB2 complex is likely the result of sequential star formation. The LCC and UCL subgroups are the oldest, and may have triggered star formation in US, which in turn may have triggered star formation in the star forming region ρ Oph [5, 6]. By studying the properties of the binary population in the three different subgroups in Sco OB2, one can establish whether the binary population has evolved as a function of time.

Our ultimate goal is to derive the PBP in Sco OB2. Our strategy is to (i) collect data on binarity in Sco OB2 using observations and literature data, (ii) correct for the selection effects introduced by the different observing techniques, and (iii) use inverse dynamical population synthesis, e.g. [7], to derive the PBP.

2 The Observed Binary Population

Brown [8] performed an extensive literature search on binarity in Sco OB2, including visual, spectroscopic, and astrometric binaries. A drastic decline is seen in binary fraction going from early-type to late-type stars, which may very well be due to observational selection effects (Figure 1). This selection effect has at least partially been removed by the B-star adaptive-optics binarity survey of [9]. Anticipating on to finding many new companion stars, we performed a near-infrared adaptive optics survey amongst A and late-B stars in Sco OB2. Near-infrared observations are preferred over optical observations, because of the much smaller luminosity contrast between a massive primary

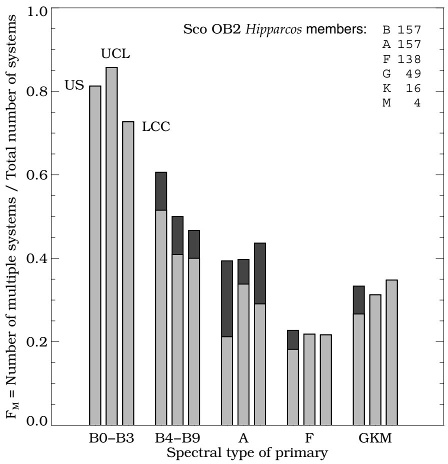

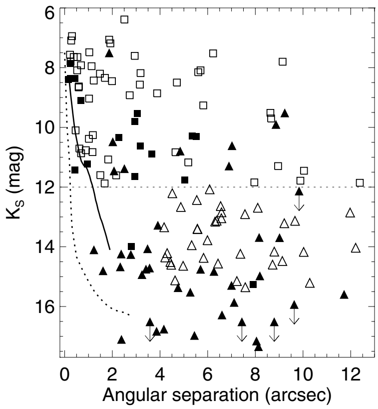

Fig. 1. *Left:* The fraction of stellar systems which is multiple versus the spectral type of the primary, for the three subgroups of Sco OB2. The light and dark gray parts of the bars correspond to literature data and the new data presented, respectively. The spectral types of the companion stars (not included in this plot) are always later than those of the primary stars. Apparently, the multiplicity is a function of spectral type, but this conclusion may well be premature when observational biases are not properly taken into account. *Right:* The results of our ADONIS and VLT/NACO binarity surveys amongst A and late-B members of Sco OB2, showing the confirmed and candidate companions (closed and open squares), as well as the confirmed and candidate background stars (closed and open triangles). The solid and dotted curves are estimates for the detection limit of the ADONIS and NACO surveys, respectively. Only one brown dwarf companion ($K_S > 12$ mag) is found between $1''$ and $4''$ in the sample of 199 Sco OB2 members, which provides supporting evidence for the existence of a brown dwarf desert for A and late-B stars in Sco OB2

and a low-mass companion. With adaptive optics observations we bridge the gap between the known close spectroscopic binaries and wide visual binaries.

We carried out a near-infrared adaptive optics survey among 199 A and late-B members of the Sco OB2 association [1]. In total 151 secondaries are detected, with angular separation $0.22'' \leq \rho \leq 12.4''$ and $6.4 \leq K_S \leq 15.4$ mag. Using a brightness criterion the secondaries are separated into 77 probable background stars and 74 candidate companions (of which 41 previously undocumented). We use 5 Myr and 20 Myr (for US and UCL/LCC, respectively) isochrones to derive masses and mass ratios. The mass ratio distribution follows $f(q) \propto q^{-0.33}$. Random pairing between primaries and companions is excluded (even if we would assume the background stars to be companions) in the observed primary mass and angular separation regime. No close ($\rho \leq 3.75''$) companions are found in the magnitude range $12 < K_S < 14$ mag, but several close probable background stars with $K_S > 14$ mag are found.

The non-detection of close companions with $12 \leq K_S \leq 14$ mag indicates the absence of close brown dwarf companions.

Seven close ($\rho < 3.75''$) candidate background stars with $K_S > 14$ mag were detected in the ADONIS survey. In order to find the nature of these objects, and to confirm the status of several doubtful candidate companions, we performed VLT/NACO JHK_S follow-up observations. The sample consists of 22 members of Sco OB2, including 7 next to which the close candidate background stars were found, the others with candidate companions. Our observations were sensitive to companions with $0.1'' < \rho < 12''$ and $K_S < 17$ mag. The multi-color observations allow us to place the secondaries in the color-magnitude diagram, and to compare their position to the isochrone. The seven close candidate background stars are indeed background stars. Six doubtful candidate companions found in the ADONIS survey turn out to be background stars. We confirm the status of the 18 candidate companions and 44 background stars. We find two brown dwarf companions of HIP81972, at an angular separation of $7.92''$ (1500 AU) and $2.97''$ (520 AU) with a mass of 32 M_J and 63 M_J, respectively. The 63 M_J companion is the only brown dwarf detected between $1'' \leq \rho \leq 4''$ (Figure 1). One cannot make a similar statement outside this angular separation range since brown dwarfs with $\rho < 1''$ are undetected in the wings of the primary PSF, and for $\rho > 4''$ the status of many background stars is only statistically confirmed. For a semi-major axis distribution of the form $f(a) \propto a^{-1}$, about 12% of the companions (thus also 12% of the brown dwarf companions, assuming that companion mass and a are independent) are expected to have $1'' \leq \rho \leq 4''$.

In our survey among 199 A and late-B stars in Sco OB2 we find only *one* brown dwarf companion in the angular separation range $1'' - 4''$, although we should have detected brown dwarfs around all stars in this range, if present. This implies a virtual absence of $0.007\ M_\odot < M < 0.1\ M_\odot$ ($7\ M_J < M < 105 M_J$) companions of A and late-B stars with semi-major axes of $\sim 150 - 550$ AU. The brown dwarf companion fraction for $\sim 150 - 550$ AU is $0.5 \pm 0.5\%$, which is much smaller than the stellar companion fraction of $14 \pm 3\%$ in this range. *Our results provide supporting evidence for the existance of a brown dwarf desert for A and late-B stars.*

We combine the results of our ADONIS and NACO surveys with all available literature data on binarity in Sco OB2, including visual, spectroscopic, and astrometric binaries. The *observed* binary fraction shows a clear correlation with the spectral type of the primary (Figure 1), but our results indicate that this trend is at least partially due to selection effects. The observed companion star fraction $F_M \equiv (B + 2T + \ldots)/(S + B + T + \ldots)$ slightly decreases with the age of the subgroups, with a value of 0.61 for US, 0.52 for UCL, and 0.45 for LCC. The overall observed companion star fraction of Sco OB2 is 0.52.

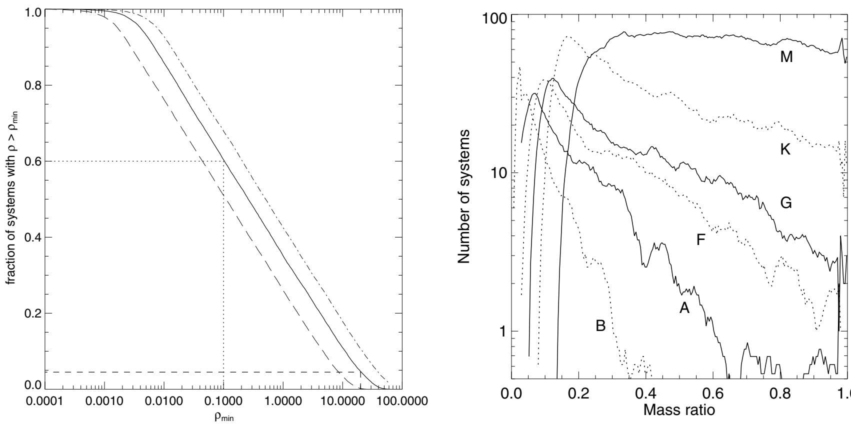

Fig. 2. *Left:* The fraction of binary systems with angular separation $\rho > \rho_{\rm min}$ as a function of $\rho_{\rm min}$. An association with 25,000 binaries at a distance of 145 pc (solid curve) is used. The association has a thermal eccentricity distribution and a semi-major axis distribution of the form $f(\log a)$ = constant between $10^2\ R_\odot$ and $10^6\ R_\odot$, where the limits correspond to the distances at which Roche lobe overflow and Galactic tidal forces become important. In our ADONIS and NACO surveys we can measure angular separations between $\sim 0.1''$ (dotted line) and $\sim 20''$ (dashed line), and hence about 55% of the companion stars. The observable fraction of binary systems varies slowly with distance, as is illustrated for the models with a distance much closer (75 pc, dash-dotted curve) or farther (350 pc, long-dashed curve) than that of Sco OB2 . *Right:* The mass ratio distribution resulting from random pairing between primary and companion star from the Preibisch mass function, split up by primary spectral type. The mass range of the stars is $0.08\ M_\odot \leq M \leq 20\ M_\odot$. This figure clearly illustrates the danger of comparing mass ratio distributions resulting from binarity surveys of different primary spectral types

3 The True Binary Population

Our binarity dataset contains measurements obtained with a wide range of techniques and instruments, each with their specific observational biases. In order to interpret Figure 1 correctly, and to get the *true* (i.e., not *observed*) binary parameters in Sco OB2 (or any other population of binaries), it is of crucial importance to understand all selection effects. It is impossible to observe the complete binary parameter space in Sco OB2 due to observational and time constraints, but it is possible to estimate the true binary population using simulations. We use sophisticated simulation techniques to characterize the selection effects and to find the true binary population of Sco OB2.

The most prominent observational selection effects are the constraints on angular separation ρ. With our surveys we are sensitive to $\sim 0.1'' < \rho \sim 20''$, and can only detect companions within this range. Even though these constraints seem rather strict, we are still able to detect $50 - 55\%$ of the companion stars in our surveys (Figure 2).

Another important selection effect results from the properties of the surveyed sample. For example, the observed mass ratio distribution depends strongly on the spectral type of the primaries on the sample, even when other selection effects are ignored. The same intrinsic pairing function (e.g., random pairing) can result in different mass ratio distributions for surveys of stars with different spectral types (Figure 2). For the comparison between mass ratio distributions resulting from different samples (e.g., binarity survey among solar-type stars by [10] and our early-type binarity survey), one has to carefully study the sample selection effect.

We will investigate the selection effects resulting from observational constraints, sample selection, and background star contamination using detailed simulated observations. We will perform this analysis for visual, spectroscopic, and astrometric binarity surveys, which will give us the true binary population.

The next step will be to derive the primordial binary population from the true binary population. We will use the STARLAB package [3], which uses state-of-the-art N-body simulations, stellar evolution, and binary evolution. Using inverse dynamical population synthesis, e.g. [7], we will find the primordial binary population that corresponds most to the true binary population.

Acknowledgments

The author wishes to thank Anthony Brown, Lex Kaper, Simon Portegies Zwart, and Hans Zinnecker for their crucial roles in making this project possible. The author also thanks the Leids Kerkhoven Bosscha Fonds for providing financial support for participation in this workshop.

References

1. Kouwenhoven, M. B. N., Brown, A. G. A., Zinnecker, H., Kaper, L., Portegies Zwart, S. F.: A&A **430**, 137 (2005)
2. Bate, M. R., Bonnell, I. A., Bromm, V.: MNRAS **339**, 577 (2003)
3. Portegies Zwart, S. F., et al.: MNRAS **321**, 199 (2001)
4. de Zeeuw, P. T., et al.: AJ **117**, 354 (1999)
5. de Geus, E. J.: A&A **262**, 258 (1992)
6. Preibisch, T., Zinnecker, H.: AJ **117**, 2381 (1999)
7. Kroupa, P.: MNRAS **277**, 1491 (1995)
8. Brown, A. G. A.: AN **322**, 43 (2001)
9. Shatsky, N., Tokovinin, A.: A&A **382**, 92 (2002)
10. Duquennoy, A., Mayor, M.: A&A **248**, 485 (1991)

Multiplicity of Early-type Stars in the Field: Progress Report

N. Huélamo[1], G. Chauvin[1], C. Foellmi[1], M. Hartung[1], X. Haubois[1], V. V. Ivanov[1], C. Melo[1], D. Nürnberger[1] and M. Sterzik[1]

European Southern Observatory, Alonso de Cordova 3107, Santiago, Chile
nhuelamo@eso.org

1 Introduction

The multiplicity of early-type stars is still not well established. Several works have tried to derive the binary fraction of early-type stars in young clusters and OB associations (e.g. Preibisch et al. 2000, Shatsky & Tokovinin 2002, Kouwenhoven et al. 2005). The main result from these studies is that the multiplicity of early-type stars is different for individual star forming regions, i.e., it seems to depend on the star forming environment. However, the statistical basis is still not solid enough to understand the environmental effects on the binary fraction, mass ratio and separations of multiple systems with early-type primaries.

The age of stellar systems can also affect their multiplicity: older systems are expected to have undergone more dynamical interactions than younger ones resulting in a smaller binary fraction. Again, this has not been statistically confirmed with the study of large enough samples. Moreover, the multiplicity of early-type stars in the field has never been determined. To fill in this gap, we have started a project to derive the multiplicity of a volume-limited sample of early-type field stars. The idea is to look for companions through a common proper motion search.

This is an on-going project. In this paper we present preliminary results from the first epoch observations.

2 Sample Selection

The sample under study contains early-type (B- and A-type) field stars which have been selected according to the following criteria:

- Stars from the HIPPARCOS Catalogue with DEC $\leq$0 and any RA.
- The apparent color $B-V$ $\leq$0.2 mag. This is a conservative criterion met by all unreddened BA-type stars as well as a small number of contaminating later-type stars. To exclude the later-type stars, we have cross-correlated this preliminary sample with the SIMBAD database, and retained only stars classified as BA dwarfs.

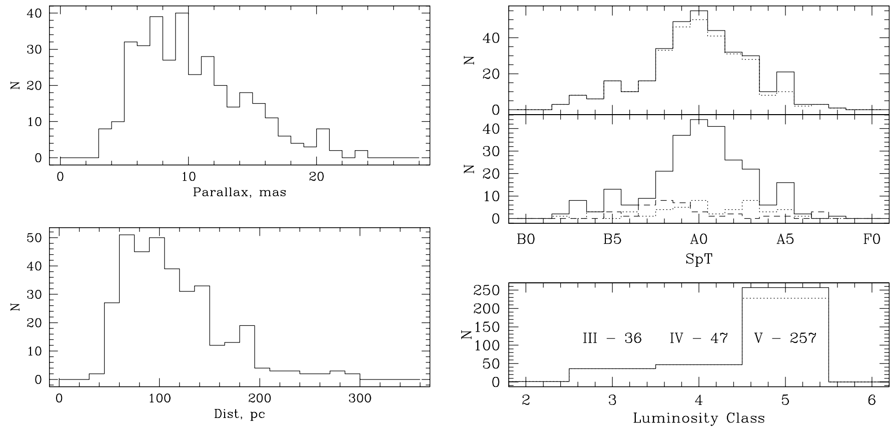

Fig. 1. Main properties of the sample of early-type field stars. The distributions of parallax, distance, spectral type and luminosity class are displayed. The spectral type distribution is plotted (i) for the whole sample and (ii) for different luminosity classes: MS stars (solid line), subgiants (dotted line) and giants (dashed line)

– The apparent V-magnitudes range between V=5-6, so they are suitable reference stars for the adaptive optics system at the Very Large Telescope (VLT), even under poor atmospheric conditions.
– The stars are within 300 pc from the Sun. The limit was chosen to ensure that we probe the local volume. The distances to individual stars were taken from the HIPPARCOS catalog.
– The sample contains only field stars. In order to discriminate between the field and clusters stars, we excluded from our list all members of OB-associations listed by de Zeeuw et al. (1999) and sources that belong to nearby associations (d<100 pc) like TW Hydrae.
– All stars in the sample show proper motions larger than 27 mas/yr. In this way, we will be able to confirm or reject any companion candidate as physical or background object, taking second-epoch data one or two years after the first-epoch observations.

The final sample contains 307 early-type stars in the field. The main properties are summarized in Figure 1.

3 Observations

The observations are performed with NAOS-CONICA (NACO), the adaptive optics facility at the VLT. All the targets are observed with the S27 objective, which provides a total field of view of $27''$x$27''$ (plate scale of 27 mas/pix). The observations are taken in the K-band and, depending on the brightness of the target, we use two different setups: the brightest objects are observed with a broad-band (K_s) plus a neutral density (ND) filter, while the faintest ones are observed with an intermediate-band filter (IB 2.18). The total exposure time on-source is $\sim$ 5 minutes. Some of the obtained NACO images are displayed in Figure 2.

The predicted detection limit for a companion to an early-type star with $K = 6$ mag and d = 200 pc is displayed in Figure 3. The figure shows the K-band magnitude difference between the primary and a companion versus their separation in arcseconds. In this example, the $5\,\sigma$ detection limit refers to a five minutes exposure with the K_s+ ND filters.

Table 1. Preliminary results from the analyzed data

	Number of sources	**Fraction (%)**
Total	307	100
Observed	180	59
Analyzed	143	46
Single[1]	75	52
Binary and Multiple Candidates[1]	68	48

Note: [1] Derived from the 143 analyzed sources

4 Current Status

- We have already obtained first epoch observations of 180 (out of 307) targets. The data of 143 sources have been already processed: 75 are single and 68 are candidates for double or multiple systems. These preliminary results are summarized in Table 1.
- First epoch observations of the remaining targets (127) are scheduled for the upcoming semester (October 2005 - March 2006).

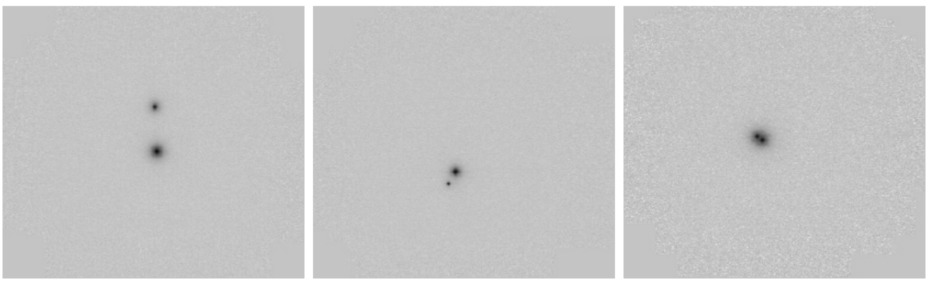

Fig. 2. NACO images of early-type field stars with companion candidates. The images have been taken in the K-band with the S27 objective (plate scale of $0.027''$/pix) which provides a field-of-view of $27''$ x $27''$

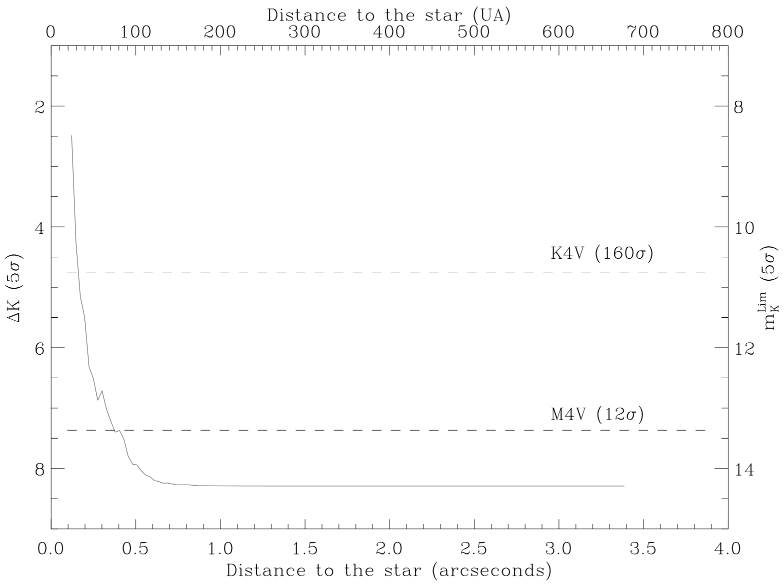

Fig. 3. Detection limit calculation for a five minutes exposure with the K_S + *ND* filters. The primary is a $K = 6$ mag B-type star at a distance of 200 pc. The difference in magnitudes (K-band) between the early-type star and a companion is plotted versus their separation in arcseconds. Two horizontal lines indicate the magnitude difference between the primary and two companions of spectral type K4 and M4. They would be detected at a $5\,\sigma$ level at separations of $0.2''$ and $0.4''$, respectively

References

1. de Zeeuw, P.T., Hoogerwerf, R., de Bruijne, J.H.J. et al., 1999: AJ 117, 354
2. Kouwenhoven, M. B. N.; Brown, A. G. A.; Zinnecker, H.; Kaper, L.; Portegies Zwart, S. F., 2005: A&A 430, 137
3. Preibisch, T., Hofmann, K.H., Schertl, D., et al., 2000: Birth and Evolution of Binary Stars, Poster Proceedings of IAU Symposium No. 200, ed. by Bo Reipurth and Hans Zinnecker, p. 106
4. Shatsky & Tokovinin, A., 2002: A&A 382, 92

Search for Low-mass Companions to X-ray Emitting A-type Stars

B. Stelzer[1,2], G. Micela[2], N. Huélamo[3] and M. Hünsch[4]

[1] Università di Palermo, Italy
[2] INAF – Osservatorio Astronomico di Palermo, Italy
[3] European Southern Observatory, Chile
[4] Universität Kiel, Germany
stelzer@astropa.unipa.it

Summary. There is no obvious theory that would explain X-ray emission from main-sequence A-type stars. Therefore, the X-ray emission identified with these stars on basis of low spatial resolution X-ray observations is usually attributed to magnetic activity from unknown late-type companion stars. We systematically study the literature and public 2 MASS data in search for binaries among A stars. This way, we identify new candidate counterparts for the X-ray sources in at least 60 % of the A-type stars claimed to be detected in the *ROSAT* All-Sky Survey. There is marginal evidence that this fraction decreases from early to late A spectral type, possibly indicating the onset of intrinsic X-ray emission for the latest A stars which may have deep enough convection zones to support magnetic activity.

1 The Mysterious X-ray Emission from A Stars

For stars on the main-sequence two mechanisms are known to be responsible for the observed X-ray emission: In O- and early B-type stars the X-rays are produced by instabilities arising in their strong radiatively driven stellar winds [3,4], and in late-type stars a solar-like magnetic dynamo is thought to heat and confine hot coronal plasma, which is a tracer of stellar activity [5].

No X-ray emission is expected from stars whose spectral types are late B and early A, because they do not drive strong enough winds nor do they possess convective zones necessary to sustain a magnetic dynamo. Nevertheless, X-ray detections of these stars have been repeatedly reported throughout the literature (see Stelzer et al. 2003 [9]). In absence of a theoretical explanation, the X-ray emission of main-sequence late B-type and early A-type stars is commonly attributed to unresolved late-type companions. Many A and B stars are known or suspected binaries. But the connection between their multiplicity and their X-ray properties has never been investigated systematically.

In this contribution we examine the sample of A stars in the solar neighborhood detected in X-rays during the *ROSAT* All-Sky Survey (RASS). The aim is to search for alternative counterparts to the X-ray sources, either bound companions to the A stars or unrelated nearby objects.

2 Search for New Counterparts

The sample studied here is composed of all 248 X-ray sources identified with an A-type star in the RASS (see Hünsch et al. 1998 [2]; hereafter H98). The optical identifications of the X-ray sources in H98 are based on a cross-correlation between A, F, G, and K stars from the Bright Star Catalog [1] and RASS X-ray sources, using a 90″ cut radius ($\Delta_{\rm ox}$). We investigate the reliability of these identifications by examining the sky region near the A stars and the X-ray sources with the aim to uncover other objects that may replace the A stars as counterparts to the X-ray sources. To this end we use different approaches: A literature search for known spectroscopic and visual binaries among the A-type stars identified with a RASS source (Sect. 2.1), analysis of 2 MASS archival data (Sect. 2.2).

2.1 Known Binaries among X-ray Emitting A stars

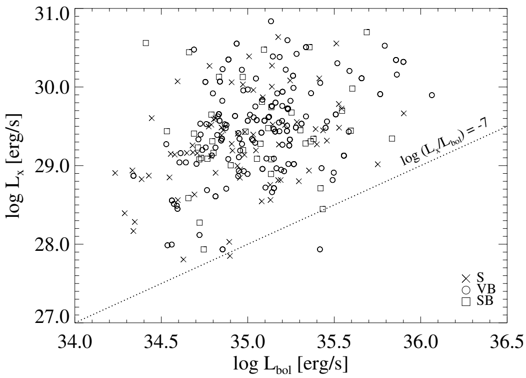

Fig. 1. $\log L_{\rm x} - \log L_{\rm bol}$ diagram for A stars identified with X-ray sources detected in the RASS; data from H98. The dotted line marks the empirical $\log(L_{\rm x}/L_{\rm bol})$ relation for O-type stars. The large spread observed for the A-type stars and their location above this line, show that they are not wind-driven X-ray sources

Fig. 1 shows the A star sample from H98 in a $\log L_{\rm x} - \log L_{\rm bol}$ diagram. Bolometric luminosities were computed from the V band magnitudes, X-ray luminosities adopted from H98. Spectroscopic binaries (SB), visual binaries (VB), and supposedly single stars (S) are marked with different plotting symbols. There are 72 ($\sim 29\,\%$) A-type stars in the total sample of 248 that are not known to be multiples so far: 42 are spectroscopic binaries, 87 are visual binaries, 47 binaries have both spectroscopic and visual components.

2.2 2-MASS Objects Near X-ray Emitting A Stars

In a search for alternative counterparts to the RASS X-ray sources assigned previously to A stars we are exploring the 2 MASS archive, using the following selection criteria for candidate IR counterparts:

– Separation to X-ray position $< 90''$, corresponding to the X-ray/opt. identification radius Δ_{ox} applied by H98. This way we ensure that the A-type stars are among the 2 MASS counterparts.
– Object with photometry quality flag 'A', 'B' or 'C' in all three bands JHK, or object identified with an original A star X-ray counterpart from H98.

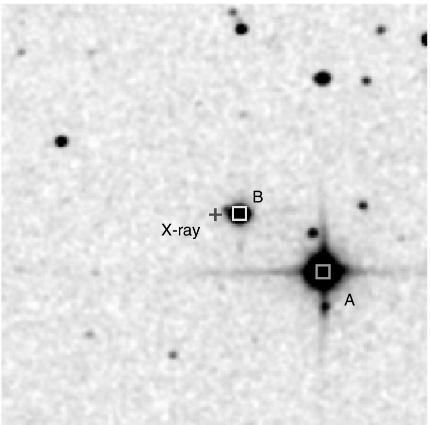

Fig. 2. $180'' \times 180''$ 2 MASS K band image of HR 1490 centered on the RASS X-ray position (marked with a cross). The A star itself (brightest object in the field) and the known visual companion are labeled 'A' and 'B', respectively. Clearly the X-ray source must be identified with the known visual companion at a separation $10.3''$; whereas the A star originally identified as counterpart is separated from the X-ray position by $52''$

An example of the results is shown and discussed in Fig. 2. In total, among 248 examined 2 MASS fields within $90''$ of an A star there are: 41 fields with one 2 MASS source closer to the X-ray position than the A star, and 45 fields with more than one 2 MASS source closer to the X-ray position than the A star. For almost all fields with offsets $\Delta_{ox} > 40''$ in H98 there is at least one other 2 MASS source closer to the X-ray position than the A star. This suggests that the excessively large opt./X-ray identification radius applied by H98 yielded mostly spurious identifications beyond $40''$.

3 Assigning New Counterparts to the X-ray Sources

We tentatively assign new counterparts to the X-ray sources using two different approaches:

1. We exclude the A star as X-ray emitter whenever there is another object within $40''$ of the X-ray position, i.e. either a visual companion, or another 2 MASS object, or a spectroscopic companion. This way the original sample of 248 A star X-ray emitters reduces to 28 X-ray sources without known alternative counterpart, i.e. for a fraction of $\sim 90\,\%$ a new object has been identified that may be responsible for the X-ray emission.

2. We consider as counterpart always the object which is closest to the X-ray position, i.e. either a visual companion, or a spectroscopic companion, or another 2 MASS object. This leaves a total of 91 out of 248 X-ray sources associated with an A star, i.e. a fraction of $\sim$ 60 % have possible new counterparts.

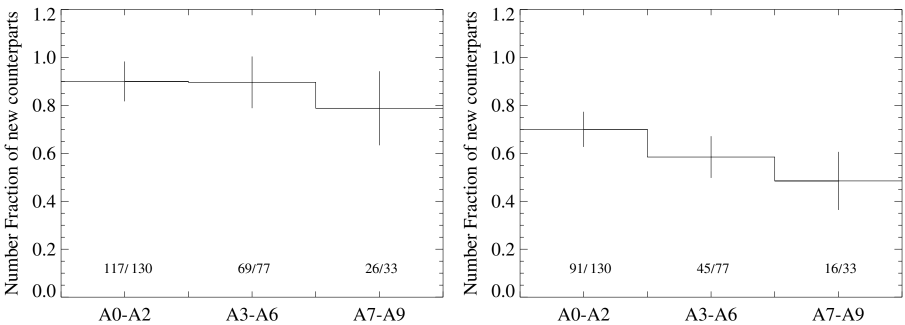

Fig. 3. Fraction of objects where a counterpart not identical with a single A star was identified among known companions or 2 MASS objects: *left* - objects other than the A star within 40″ of X-ray position, *right* - closest optical/IR objects to X-ray source (for details see text in Sect. 3). Eight stars classified Ap or Am are omitted

Finally, we examine the fraction of new counterparts as a function of spectral type (Fig. 3). A slight, but at most marginally significant, decrease in the fraction of new counterparts is suggested for the latest spectral types. If real, this effect could indicate the onset of intrinsic emission from A stars. The minimum depth of a convective envelope able to support magnetic activity is not well established. Based on previous observations the onset of significant dynamo action has been placed somewhere between spectral type A7 and F4 [6, 7].

Outlook: The question whether A stars are intrinsic X-ray emitters or not is being pursued also by (1) X-ray imaging with high spatial resolution to pinpoint the position of the X-ray source, (2) spectroscopy of the candidate counterparts to establish if they are late-type (active) stars, (3) IR imaging with high spatial resolution using adaptive optics searching for additional close visual counterparts (see Stelzer et al. 2005 [8]).

References

1. Hoffleit D. E. & Warren W. H. jr., 1991: The Bright Star Catalogue, 5th Rev. (ed.), Yale Univ. Obs., New Haven

2. Hünsch M., Schmitt J. H. M. M., Voges W., 1998: A&AS 132, 15 (H98)
3. Lucy L. B. & White R. L. 1980: ApJ 241, 300
4. Owocki S. P. & Cohen D. H., 1999: ApJ 520, 833
5. Parker E. N., 1955: ApJ 122, 293
6. Schmitt J. H. M. M., Golub L., Harnden F. R. Jr, et al., 1985: ApJ 290, 307
7. Schmitt J. H. M. M., 1997: A&A 318, 215
8. Stelzer B., Huélamo N., Hubrig S., et al., 2005, In: Proc. 13th Cambridge Workshop on Cool Stars, Stellar Systems, and the Sun, Eds. F. Favata, G. A. J. Hussain & B. Battrick, ESA-SP 560, 213
9. Stelzer B., Huélamo N., Hubrig S., et al., 2003, A&A 407, 1067

ESO ASTROPHYSICS SYMPOSIA
European Southern Observatory

Series Editor: Bruno Leibundgut

A. Weiss, T.G. Abel, V. Hill (Eds.),
The First Stars
Proceedings, 1999. XIII, 355 pages. 2000.

A. Fitzsimmons, D. Jewitt, R.M. West (Eds.),
Minor Bodies in the Outer Solar System
Proceedings, 1998. XV, 192 pages. 2000.

L. Kaper, E.P.J. van den Heuvel, P.A. Woudt (Eds.),
Black Holes in Binaries and Galactic Nuclei: Diagnostics, Demography and Formation
Proceedings, 1999. XXIII, 378 pages. 2001.

G. Setti, J.-P. Swings (Eds.)
Quasars, AGNs and Related Research Across 2000
Proceedings, 2000. XVII, 220 pages. 2001.

A.J. Banday, S. Zaroubi, M. Bartelmann (Eds.),
Mining the Sky
Proceedings, 2000. XV, 705 pages. 2001.

E. Costa, F. Frontera, J. Hjorth (Eds.),
Gamma-Ray Bursts in the Afterglow Era
Proceedings, 2000. XIX, 459 pages. 2001.

S. Cristiani, A. Renzini, R.E. Williams (Eds.),
Deep Fields
Proceedings, 2000. XXVI, 379 pages. 2001.

J.F. Alves, M.J. McCaughrean (Eds.),
The Origins of Stars and Planets: The VLT View
Proceedings, 2001. XXVII, 515 pages. 2002.

J. Bergeron, G. Monnet (Eds.),
Scientific Drivers for ESO Future VLT/VLTI Instrumentation
Proceedings, 2001. XVII, 356 pages. 2002.

M. Gilfanov, R. Sunyaev, E. Churazov (Eds.),
Lighthouses of the Universe: The Most Luminous Celestial Objects and Their Use for Cosmology
Proceedings, 2001. XIV, 618 pages. 2002.

R. Bender, A. Renzini (Eds.),
The Mass of Galaxies at Low and High Redshift
Proceedings, 2001. XXII, 363 pages. 2003.

W. Hillebrandt, B. Leibundgut (Eds.),
From Twilight to Highlight: The Physics of Supernovae
Proceedings, 2002. XVII, 414 pages. 2003.

P.A. Shaver, L. DiLella, A. Giménez (Eds.),
Astronomy, Cosmology and Fundamental Physics
Proceedings, 2002. XXI, 501 pages. 2003.

M. Kissler-Patig (Ed.),
Extragalactic Globular Cluster Systems
Proceedings, 2002. XVI, 356 pages. 2003.

P.J. Quinn, K.M. Górski (Eds.),
Toward an International Virtual Observatory
Proceedings, 2002. XXVII, 341 pages. 2004.

W. Brander, M. Kasper (Eds.),
Science with Adaptive Optics
Proceedings, 2003. XX, 387 pages. 2005.

A. Merloni, S. Nayakshin, R.A. Sunyaev (Eds.),
Growing Black Holes: Accretion in a Cosmological Context
Proceedings, 2004. XIV, 506 pages. 2005.

L. Stanghellini, J.R. Walsh, N.G. Douglas (Eds.)
Planetary Nebulae Beyond the Milky Way
Proceedings, 2004. XVI, 372 pages. 2006.

S. Randich, L. Pasquini (Eds.)
Chemical Abundances and Mixing in Stars in the Milky Way and its Satellites
Proceedings, 2004. XXIV, 411 pages. 2006.

A.P. Lobanov, J.A. Zensus, C. Cesarsky, P.J. Diamond (Eds.)
Exploring the Cosmic Frontier
Astrophysical Instruments for the 21st Century.
XXVI, 270 pages. 2006.

I. Saviane, V.D. Ivanov, J. Borissova (Eds.)
Groups of Galaxies in the Nearby Universe
Proceedings, 2005. XX, 390 pages. 2007.

G.W. Pratt, P. Schuecker, H. Boehringer (Eds.)
Heating versus Cooling in Galaxies and Clusters of Galaxies
Proceedings, 2006. XIV, 468 pages. 2007.

M. Kissler-Patig, R.J. Walsh, M.M. Roth (Eds.)
Science Perspectives for 3D Spectroscopy
Proceedings of the ESO Workshop held in Garching, Germany, 10-14 October 2005
Proceedings, 2006. XVIII, 402 pages. 2007.

S. Hubrig, M. Petr-Gotzens, A. Tokovinin (Eds.)
Multiple Stars Across the H-R Diagram
Proceedings of the ESO Workshop held in Garching, Germany, 12-15 July 2005
Proceedings, 2006. XIV, 304 pages. 2007.